Functional Analysis of Membrane associated Organophosphate Hydrolase (OPH) Complex in *Sphingobium fuliginis* ATCC 27551

Thesis submitted for the degree of Doctor of Philosophy in Animal Biology

By Ramurthy Gudla (12LAPH02)

Supervisor **Prof. S. Dayananda**



Department of Animal Biology School of Life Sciences University of Hyderabad Hyderabad – 500 046 INDIA 2018



University of Hyderabad (A Central University established in 1974 by an act of parliament) HYDERABAD – 500 046, INDIA

CERTIFICATE

This is to certify that this thesis entitled "Functional Analysis of Membrane associated Organophosphate Hydrolase (OPH) Complex in *Sphingobium fuliginis* ATCC 27551" submitted by Mr. Ramurthy Gudla, bearing registration number 12LAPH02 in partial fulfillment of the requirements for award of Doctor of Philosophy in the Department of Animal Biology, School of Life Sciences is a bonafide work carried out by him, under my supervision and guidance.

This thesis is free from plagiarism and has not been submitted previously in part or in full to this or any other University or Institution for award of any degree or diploma. Publications.

- 1. J. Biol. Chem. **290**, 29920–30 (2015) (PMID: 26453310)
- 2. Genome Biol Evol. 275; 77-81 (2016) (PMID: 28175269)
- 3. Proc Indian Natn Sci Acad. **83**; 865-875 (2017) (DOI: 10.16943/ptinsa/2017/49140)

Further, the student has passed the following courses towards fulfillment of coursework requirement for Ph.D.

S. No.	CourseCode	Name	Credits	Pass/Fail
1	AS 801	Seminar	1	Pass
2	AS 802	Research Ethics &	2	Pass
		Management		
3	AS 803	Biostatistics	2	Pass
4	AS 804	Analytical Techniques	3	Pass
5	AS 805	Lab Work	4	Pass



University of Hyderabad (A Central University established in 1974 by an act of parliament) HYDERABAD – 500 046, INDIA

DECLARATION

This is to declare that the work embodied in this thesis entitled "Functional Analysis of Membrane associated Organophosphate Hydrolase (OPH) Complex in *Sphingobium fuliginis* ATCC 27551" has been carried out by me under the supervision of Prof. S. Dayananda, Department of Animal Biology, School of Life Sciences. The work presented in this thesis is a bonafide research work and has not been submitted for any degree or diploma in any other University or Institute. A report on plagiarism statistics from the University Librarian is enclosed.

Ramurthy Gudla (12LAPH02)

Prof. S. Dayananda (Research supervisor)

Date:

Acknowledgements

At this moment of accomplishment, firstly I express my deep gratitude to my supervisor, **Prof. Dayananda Siddavattam**, for introducing me to this exciting field of molecular biology. His dedicated help, suggestions, inspiration, encouragement and continuous support throughout my Ph.D is greatly appreciated. I am really glad to be associated with him as my mentor in my life.

I am grateful to Prof. K.V.A Ramaiah, Dean, School of Life Sciences, and former Deans Prof. Reddanna, Prof. A.S Raghavendra, Prof. M. Ramanadham, and Prof. R.P. Sharma for providing all the facilities in the school.

I thank Prof. Anita jagota. Head, Dept. of Animal Biology, and former Head Prof. Jagan Pongubala, and Prof. B. Senthil kumaran for providing the necessary facilities in the department to carry out my research work.

I thank my doctoral committee members Prof. Aparna Dutta Gupta, and Dr. Sreenivasulu Kurukuti for their critical comments and valuable suggestions.

I would like to extend my sincere thanks to Prof. Manjula sritharan and Prof. H.N Nagarajaram for their guidance in iron uptake study and in silico work.

I specially thank Dr. Manjula Reddy, Principal Scientist, CCMB for providing Keio collections strains.

I am thankful to Dr. Gourishankar, Principal Scientist, CDFD for allowing me conducting transduction experiments in his laboratory

I also extend my acknowledgements to late Prof. P. S. Sastry for his intellectual interactions and constant motivation.

I wish to acknowledge the help and suggestions of all faculty members in the School of Life Sciences, during different stages of my work.

I would like to thank all the lab members of Prof. Manjula sritharan, Prof. Prof. Aparna Dutta Gupta, Prof. Apparao podile and Dr. Kota Arun Kumar for their timely help when required.

I am thankful to Guru Prasad for helping me in bioinformatics work.

I am thankful to Dr. Devi prasanna, Dr. Toshi, Dr. Swetha kamireddy, Dr. Sujana, Dr. Santosh, Dr. Sunil parthasarathy, Dr. Ashok Madikonda, Venkateshwar Reddy and Uday for their encouragement and support during my entire Ph. D duration.

Huge thanks to my lab mates Harshita, Hari, Aparna, Annapoorni, Ganeshwari, Akbar, Tanu and Dr. Devyani for the help and enjoyable company.

I specially thank Dr. Rajesh Kamindla for his guidance and encouragement.

Special thanks to Krishna and Rajendra Prasad for technical help in the lab.

Special thanks to my friends Dr. Paparao, Dr. Vinod chouhan, Elsin, Bantu, Shanmuka, and all friends from school of life sciences for their support and happy stay in University of Hyderabad.

I am thankful to Mrs. Monika, Mrs. Kalpana for their help in Ultracentrifugation at proteiomics Facility.

I thank DBT, ICMR, UGC, UPE-II, UGC-SAP and DBT-CREBB for providing financial support to lab and for the infrastructural facility of the school.

I specially thank CSIR for JRF and SRF. The financial assistance from Aurobindo pharma and Biological E limited is greatly acknowledged.

I wish to express my deepest gratitude and reverence to my parents, who have sacrificed every comfort of their life to give a better life for me and for their epitome of patience in allowing me to choose the career of my interest.

I wish to thank my sister, my brother, brother In-law and friends for their support and encouragement throughout my doctoral studies.

Especially I would like to thank and dedicate my thesis to my parents and my better half "Ravali" for all their hardships to bring me till this stage.

I thank Almighty for giving me strength, support, patience and courage.

Ramurthy Gudla

Contents

Abbreviations	i
List of tables	ii-iii
List of figures	iii-v
1. Introduction	1-11
1.1 Chemistry of Organophosphate Compounds	1
1.2. Bacterial Phosphotriesterases	2
1.2.1. Organophosphorus Acid Anhydrolase (OPAA)	2
1.2.2. Methyl parathion hydrolase (MPH)	3
1.2.3. Organophosphate hydrolase (OPH)	4
1.3. Structural comparison of OPH and MPH	5
1.4. Evolution of OPH	6
1.5. OPH is a Tat substrate	7
1.6. Tat translocation pathway	9
1.7. OPH is a Lipoprotein	10
1.8. Objectives	11
2. General Materials and Methods	12-31
2. 1. Growth Media	15
2. 2. Preparation of iron free media & solutions	15
2. 3. Preparation of Antibiotic & chemical stock solutions	16
2. 4. DNA Manipulations: Preparation of solutions and buffers	17
2. 4. 1. Agarose gel electrophoresis	18
2. 4. 2. Isolation of Plasmid by Alkaline Lysis method	18
2. 4. 3. DNA Quantification	19
2. 4. 4. Polymerase Chain Reaction (PCR)	19
2. 4. 5. Site-Directed Mutagenesis	20
2. 4. 6. Molecular Cloning	20
2.5. Gene transfer methods	21-22
2.6. Protein Methods	22
2. 6. 1. Solutions for SDS-Polyacrylamide Gel electrophoresis	22
2. 6. 2. Solutions for Protein Estimation	24
2. 6. 3. Solutions for Western Blotting	24

2. 6. 4. Protein estimation by Bradford's assay	25
2. 6. 5. Protein Precipitation	25
2. 6. 6. Poly Acrylamide Gel Electrophoresis	25
2. 6. 7. Semi-Dry Western Blotting	26
2. 7. Subcellular fractionation	27
2. 8. Enzyme assays and preparation of reagents	28
2. 8. 1. Reagents for Glucose-6-phosphate dehydrogenase assay	28
2. 8. 2. Reagents for Nitrate reductase assay	28
$2.8.3.$ Reagents for β -galactosidase assay	28
2. 8. 4. Reagents for Methyl parathion activity	29
2.8.5. Glucose-6-phosphate dehydrogenase (G6PD) -Cytoplasmic	
marker	29
2. 8. 6. Nitrate reductase -Membrane Enzyme	30
2. 8. 7. β -galactosidase activity	30
2. 8. 8. Parathion Hydrolase Assay	31
Chapter I: Identification of proteins co-purified with OPH	32-49
3.1. Objective specific methodology	32
3.1.1. Immuno-purification of membrane associated OPH complex	32
3.1.2. Generation of Affinity column with anti-OPH antibodies.	32
3.1.3. Enrichment of OPH antibodies:	32
3.1.4. Preparation of Protein A/G-Anti-OPH antibody column	33
3.1.5. Isolation of Membrane	34
3.1.6. Membrane Solubilization:	35
3.1.7. Blue Native –PAGE (BN-PAGE)	35
3.1.8. Tricine SDS-PAGE	36
3.1.9. Identification of interacting partners by Mass Spectrometry	36
3.2. Results and Discussion	37
3.2.1. Purified OPH complex from membrane of Sphingobium	
fuliginis	37
3.2.2. The 85kDa OPH associated protein is TonB dependent	40
receptor (TonR)	40
3.2.3. The 36kDa OPH associated protein is energy transducing	41
component TonB	41
3.2.4. The 25kDa OPH associated protein is energy transducing	42

component ExbB

3.2.5. The 17kDa OPH associated protein is outer membrane porin	43
(OmpW)	
3.2.6. The 14kDa OPH associated protein is energy transducing	44
component ExbD	
3.2.7. OPH associated proteins are TonB dependent transport	46
components	10
4. Chapter II. Interactions between OPH and Ton complex	50-86
4.1 Objective Specific Methodology	50
4.1.1. Construction of opd variant to code for OPH ^{CAviTag}	55
4.1.2. Pulldown strategy	56
4.1.3. Requirement for compatible expression vector to co-express	57
OPH interacting partners	37
4.1.4. Reciprocal pulldown Assays	62
4.1.5. Analysis of protein-protein interaction with Bacterial two-	6.4
hybrid system	64
4.1.6. ExbD-OPH interactions	64
4.1.7. TonB-OPH interactions	64
4.1.8. ExbD-OPH interactions: in silico predictions	65
4.1.9. Generation of OPH variants and validation of OPH/ExbD	
interactions	66
4.2. Expression and detection of OPH variants	67
4.3. Results and Discussion	68
4.3.1. Biotinylation of OPH	68
4.3.2. Expression of Ton complex in <i>E. coli</i> Arctic express with N-	60
terminal His-tag	69
4.3.3. The $TonB^{N6xHis}$ and $ExbD^{N6xHis}$ are found in soluble fractions	69
4.3.4. The ExbB ^{N6xHis} is not stable	70
4.3.5. ExbB is stable in presence of ExbD	71
4.3.6. OPH interacts with TonB	72
4.3.7. OPH interacts with ExbD	74
4.3.8. ExbB/ExbD and OPH form complex	77
4.3.9. <i>In silico</i> predictions on OPH-ExbD interactions	78
4.4. OPH interacts with ExbD through 91 and 96 arginine residues	82

4.4.1. The TonR ^{N6xHis} goes in to inclusion bodies	84
5. Chapter III. Reconstitution of sfTonBDT system in GS027	87-110
5.1. Objective specific Methodology	87
5.1.1 Reconstruction of S. fuliginis TonB dependent Signal	89
Transduction system in <i>E. coli</i>	09
5.1.2. Generation of TonBDT negative strains of <i>E. coli</i>	89
5.1.3. Generation of <i>ExbD</i> mutant:	90
5.1.4. Transduction	90
5.1.5. E. coli exbD, tonB double mutant	91
5.1.6. Construction of compatible expression systems to	92
Reconstitute SfTonBDT in E. coli	92
5.1.7. Construction of expression vector with <i>oriV</i> of p15A	92
incompatible group)2
5.1.8. Construction of pGS6	93
5.1.9. Construction of pGS25	94
5.2. Expression and subcellular localization of sfTonBDT components in	95
GS027	73
5.2.1. Expression and subcellular localization of TonR ^{C6xHis}	95
5.2.2. Expression and subcellular localization of	95
ExbBNFLAG/ExbDCMyc	75
5.2.3. Expression and subcellular localization of TonB ^{C6xHis}	95
5.2.4. Expression and subcellular localization of OPHCAviTag	96
5.2.5. Co-expression of OPH ^{CAviTag} and TonB ^{C6xHis} and	96
subcellular localization of OPH ^{CAviTag}	70
5.2.6. Co-expression of OPH ^{CAviTag} and ExbB ^{NFLAG} /ExbD ^{CMyc} and	96
subcellular localization of OPH ^{CAviTag}	,,,
5.2.6. Co-expression of OPH ^{CAviTag} and ExbB ^{NFLAG} /ExbD ^{CMyc} and	96
subcellular localization of OPH ^{CAviTag}	,,,
5.2.7. Verification of <i>E. coli</i> GS027 for TonBDT null phenotype	96
5.2.8. Reconstitution of $_{Sf}$ TonBDT without OPH in $E.\ coli$ GS027	96
5.2.9. Reconstitution of $_{Sf}$ TonBDT with OPH in $E.\ coli$ GS027	97
5.3. Results and Discussion	97
5.3.1. Construction of TonB dependent transport deficient Arctic	97
express cells (<i>E. coli</i> GS027)	

5.3.2. The $TonR^{C6xHis}$ is found in the membrane of GS027 cells.	99
5.3.3. The $ExbB^{NFLAG}$ and $ExbD^{CMyc}$ are found in the membrane	101
5.3.4. TonB ^{C6xHis} is found in the membrane	102
5.3.5. Expression and subcellular localization of Ton complex.	103
5.3.6. OPH targets membrane in presence of TonB, ExbB/ExbD	104
5.3.7. Reconstitution of SfTonBDT system in E. coli GS027	107
6. Chapter IV. Role of OPH in iron transport	111-117
6.1. Objective specific methodology	111
6.1.1. Growth of reconstitution of E. coli GS027 (sfTonBDT) under	111
iron limiting conditions	111
6.2. Determination of OPH influence on transport of ferric enterobactin	112
6.2.1. Preparation of ⁵⁵ Fe-enterobactin complex	112
6.2.2. ⁵⁵ Fe-enterobactin uptake assay	112
6.3. Results & Discussion	113
6.3.1. OPH enhances the growth of GS027 (sfTonBDT) cells under iron limiting conditions	113
6.3.2. OPH dependent increase in iron uptake	115
7. Conclusions	118
8. References	119-127
9. Publications	
10. Anti-plagiarism Certificate	

Abbreviations

Amp : ampicillin

ATCC : American type culture collection

°C : degrees Celsius

Cm : chloramphenicol

DDM : n-dodecyl-β-D maltoside

dNTP : deoxynucleoside triphosphate

DSS : disuccinimidyl suberate

Gm : Gentamycin

gm : gram h : hour

IPTG : Isopropyl β -D-1-thiogalactopyranoside

Km : Kanamycin

kb : kilobase pairs (1000 bp)

kDa : Kilo Dalton

 $\begin{array}{ll} \mu & : micro \\ M & : molar \end{array}$

MP : Methyl Parathion

MPH : Methyl Parathion Hydrolase

ONPG : O-nitrophenyl-β-D galacatopyranoside

OP : Organophosphate

OPAA : Organophosphate acid anhydrase

OPH : Organophosphate hydrolase

PCR : Polymerase Chain Reaction
PMF : Proton Motive Force

PTE : Phosphotriesterase

Sec : Secretory

sfTonBDT : Sphingobium fuliginis TonB dependent Transport System

SRP : Signal Recognition Particle

Tat : Twin Arginine Translocase

TonBDT : TonB dependent transporter

List of Tables

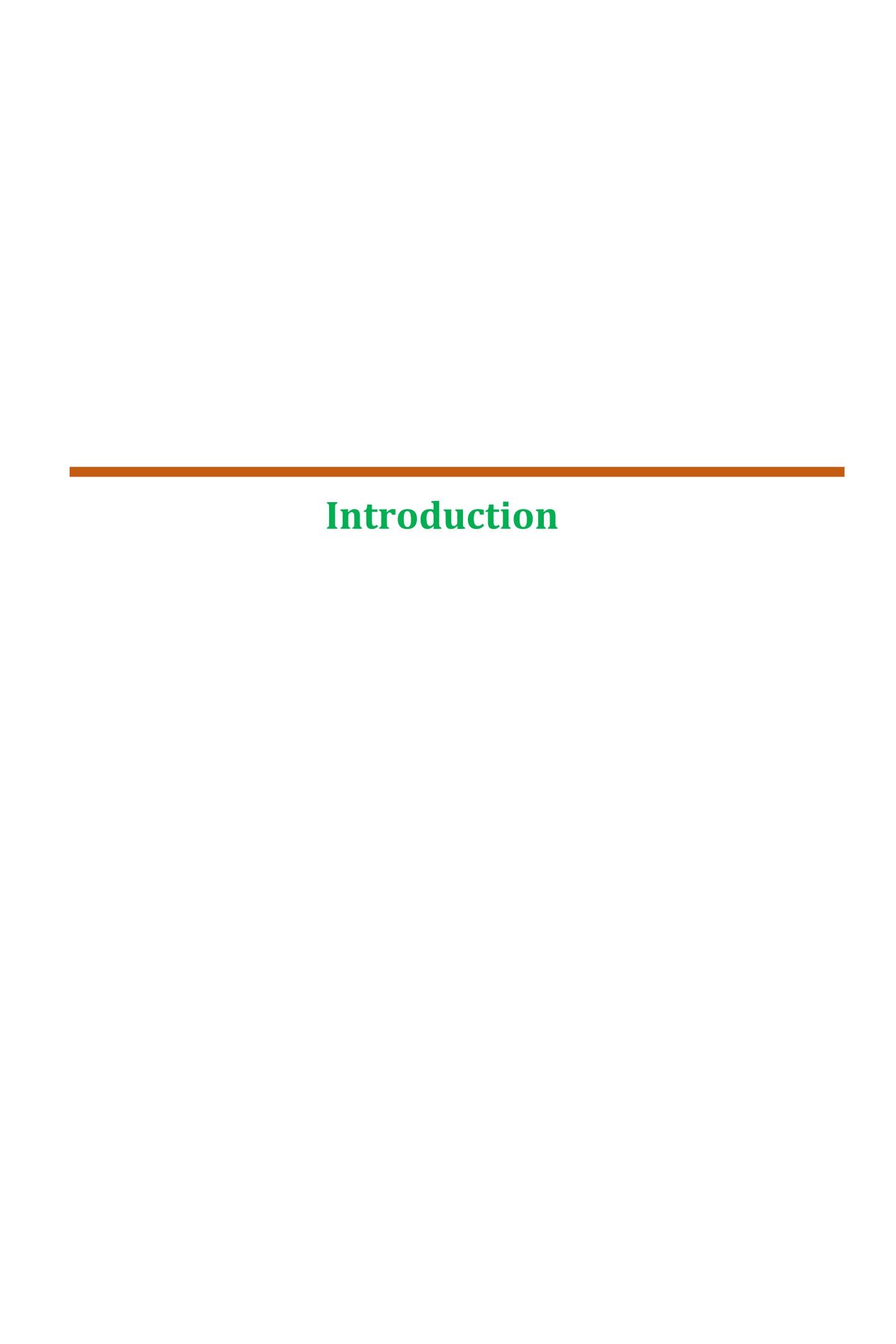
	Page No.
Table 2. A: Antibiotics	12
Table 2. B: Chemicals	12
Table 2. C: Restriction enzymes and DNA modifying enzymes	14
Table 2. D: Standard PCR programme for Thermocycler	20
Table 2. E: Composition of the resolving gel for SDS-PAGE	26
Table 2. F: Composition of the stacking gel for SDS-PAGE	26
Table 4. A: Primers used in chapter II	50
Table 4. B: Plasmids used in chapter II	53
Table 4. C: Strains used in chapter II	55
Table 4. D: List of potential interactions between OPH and ExbD	
Interface residues	80
Table 5. A: Primers used chapter III	87
Table 5. B: Plasmids used in chapter III	88
Table 5. C: Strains used in chapter III	89

List of Figures

	Page No.
Fig. 1. 1. General structure of OP compounds	1
Fig. 1. 2. Phylogenetic tree of bacterial phosphotriesterases (PTEs)	2
Fig. 1. 3. Crystal structure of Methyl parathion hydrolase (MPH)	4
Fig. 1. 4. Crystal structure of Organophosphate hydrolase (OPH)	5
Fig. 1. 5. Structural comparison between OPH and MPH	6
Fig. 1. 6. Active site comparison of OPH and MPH	6
Fig. 1. 7. Structural basis for natural lactonase and promiscuous	
phosphotriesterase activity	7
Fig. 1. 8. General Tat signal sequence	8
Fig. 1. 9. Schematic diagram represents the Tat translocation pathway	9
Fig. 1. 10. Shows mature form of OPH is linked to Diacylglycerol	11
Fig. 3. 1. Enrichment of anti-OPH antibodies	33
Fig. 3. 2. Generation of anti-OPH antibody column	34
Fig. 3. 3. Shows the activities of glucose-6-phosphate dehydrogenase and	
nitrate reductase in the cytosolic and membrane fractions of	
Sphingobium fuliginis	37
Fig. 3. 4. Immuno-purified OPH complex analysed on BN-PAGE and Tricine-PAGE	38
Fig. 3. 5. Resolution of OPH associated proteins	39
Fig. 3. 6. Identification of 85kDa OPH associated protein	41
Fig. 3. 7. Identification of 36kDa OPH associated protein	42
Fig. 3. 8. Identification of 25kDa OPH associated protein	43
Fig. 3. 9. Identification of 17kDa OPH associated protein	44
Fig. 3. 10. Identification of 14kDa OPH associated protein	45
Fig. 3. 11. Identification of 52kDa OPH associated protein	46
Fig. 3. 12. The identified OPH associated proteins	46
Fig. 3. 13. Schematic diagram of TonB dependent transport system	48
Fig. 4. 1. Construction of pAVB400	56
Fig. 4. 2. Expression of biotinylated OPH in <i>E. coli</i> Arctic express	57
Fig. 4. 3. Construction of expression vector pGS2N	58
Fig. 4. 4. Construction of pGS20	59
Fig. 4. 5. Construction of pGS16	60
Fig. 4. 6. Construction of nGS19	60

Fig. 4. 7. Construction of pGS17	61
Fig. 4. 8. Construction of pGS23	62
Fig. 4. 9. Schematic representation of pulldown assays performed to detect	
interactions between OPH and TonB dependent transport components.	63
Fig. 4. 10. Alignment of templates to ExbD used for homology modelling of ExbD	65
Fig. 4. 11. Expression and stability of OPH ^{CAviTag}	68
Fig. 4. 12. Expression and subsequent detection of TonBN6xHis and ExbDN6xHis	70
Fig. 4. 13. Expression and subsequent detection of ExbBN6xHis	71
Fig. 4. 14. Expression and subsequent detection of ExbBNFLAG and ExbDCMyc	71-72
Fig. 4. 15. Pulldown assays for OPH-TonB interactions	73
Fig. 4. 16. Bacterial Two hybrid assay for OPH-TonB interactions	74
Fig. 4. 17. Pulldown assays for OPH-ExbD interactions	75
Fig. 4. 18. Bacterial Two hybrid assay for OPH-ExbD interactions	76
Fig. 4. 19. Interactions between OPH ^{CAviTag} and ExbB ^{NFLAG} /ExbD ^{CMyc} complex	77
Fig. 4. 20. Homology model of ExbD	78
Fig. 4. 21. Shows Ramachandran and Errat plot for homology model of ExbD	78
Fig. 4. 22. Shows Circos plot representing top 100 coevolving residues of OPH	
and ExbD	79
Fig. 4. 23. Shows protein-protein docking of OPH and ExbD	81
Fig. 4. 24. Shows the chromatogram of the wild type opd and opd variants	82
Fig. 4. 25. Shows Stability and activity of OPH variants	83
Fig. 4. 26. Shows pulldown assay for interactions between OPH variants and	
ExbD ^{N6xHis}	84
Fig. 4. 27. Shows expression and subsequent detection of TonR ^{N6xHis}	85
Fig. 5. 1. Construction of expression vector pGS2C	92-93
Fig. 5. 2. Construction of pGS24	93
Fig. 5. 3. Construction of pGS6	94
Fig. 5. 4. Construction of pGS25	95
Fig. 5. 5. Generation of km sensitive <i>E. coli</i> ($\Delta exbD$)	98
Fig. 5. 6. Generation of <i>E. coli</i> GS027	98
Fig. 5. 7. Expression of TonR ^{C6xHis} in GS027 (pGS25) cells	99
Fig. 5. 8. Membrane localization of TonR ^{C6xHis} in GS027 cells	100
Fig. 5. 9. Membrane localization of ExbB ^{NFLAG} and ExbD ^{CMyc} in GS027 cells	101
Fig. 5. 10. Expression of TonB ^{C6xHis} in GS027 (pGS25) cells	102

Fig. 5. 11. Membrane localization of TonB ^{C6xHis} in GS027 cells	103
Fig. 5. 12. Expression of ExbBNFLAG/ExbDCMyc and TonBC6xHis in GS027 cells	103
Fig. 5. 13. Subcellular localization of ExbBNFLAG/ExbDCMyc and TonBC6xHis in GS027	
cells	104
Fig. 5. 14. Subcellular localization of OPH ^{CAviTag} in GS027 (pGS24) cells	105
Fig. 5. 15. Membrane localization of OPHCAviTag in GS027 (pGS23) cells	106
Fig. 5. 16. Shows growth of <i>E. coli</i> GS027 in iron limiting minimal media	107
Fig. 5.17. Reconstitution of <i>sf</i> TonBDT system in GS027	108
Fig. 6. 1. Schematic diagram showing labelling of enterobactin with 55 Fe $^{+3}$ and	
purification of 55 Fe-enterobactin complex	112
Fig. 6. 2. Shows Growth of reconstitution of <i>E. coli</i> GS027 (s/TonBDT) under iron	
limiting conditions	114
Fig. 6. 3. Shows uptake of 55Fe by wildtype, E. coli GS027, GS027 (pGS6+pGS25)	
and GS027(pGS6+pGS25+pOPHV400) cells	115
Fig. 6. 4. Shows proposed role of OPH as part of Ton complex	117



1. Introduction

1.1. Chemistry of Organophosphate Compounds.

Organophosphates (OPs) are ester or thiol derivatives of phosphoric, phosphonic or phosphoramidic acid. Their general formula is shown in fig.1.1. Where, the R_1 and R_2 are the aryl or alkyl groups, which can be directly attached to a phosphorus atom (phosphinates) as an ester bond or via oxygen (phosphates) or a sulphur atom (phosphothionates). In some cases, R_1 is directly bonded with phosphorus and R_2 with an oxygen or sulfur atom (phosphonates or thio phosphonates, respectively). In all the OP compounds, the X group is diverse and may belong to a wide range of aliphatic, aromatic, heterocyclic or halide groups. The X group, also binding to the phosphorus atom through an oxygen or sulphur atom is called 'leaving group', because, it is released from the phosphorus atom on hydrolysis of the ester bond (Sogorb & Vilanova 2002). A number of OP compounds were thus synthesized like parathion, methyl parathion, paraoxon etc.

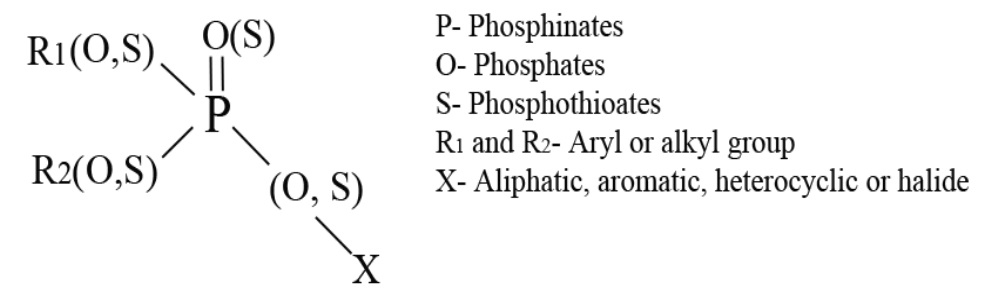


Fig. 1. 1. General structure of OP compounds.

Extensive use of OP compounds, contaminations of soil and water systems have been reported from all parts of the world (Singh *et al.*, 2008). The OP compounds possess very high mammalian toxicity and therefore early detection and subsequent decontamination and detoxification of the polluted environment is essential. Additionally, about 200,000 tons of extremely toxic OP chemical warfare agents are stock piled in various countries and they need to be destroyed following the directions of Chemical Weapons Convention (CWC) (Anonymous, 1993; Chemical Weapons Convention Signature Analysis). Chemical and physical methods of decontamination do not provide a complete solution. These approaches convert compounds from toxic into less toxic states, which in some cases can accumulate in the environment and still be toxic to a range of organisms (Timmis & Piper 1999). Several soil bacteria have been isolated and characterized which can degrade OP compounds in the environment and use these as a source of phosphorus or carbon or both (Sethunathan & Yoshida 1973). The bacterial strains degrading OP compounds contain an esterase that

specifically hydrolyse triester linkage found in a wide range of OP compounds and nerve agents. Since these esterases hydrolyse third ester linkage of OP compounds, the OP degrading esterases are designated as phosphotriesterases (PTEs) (Fig. 1. 2).

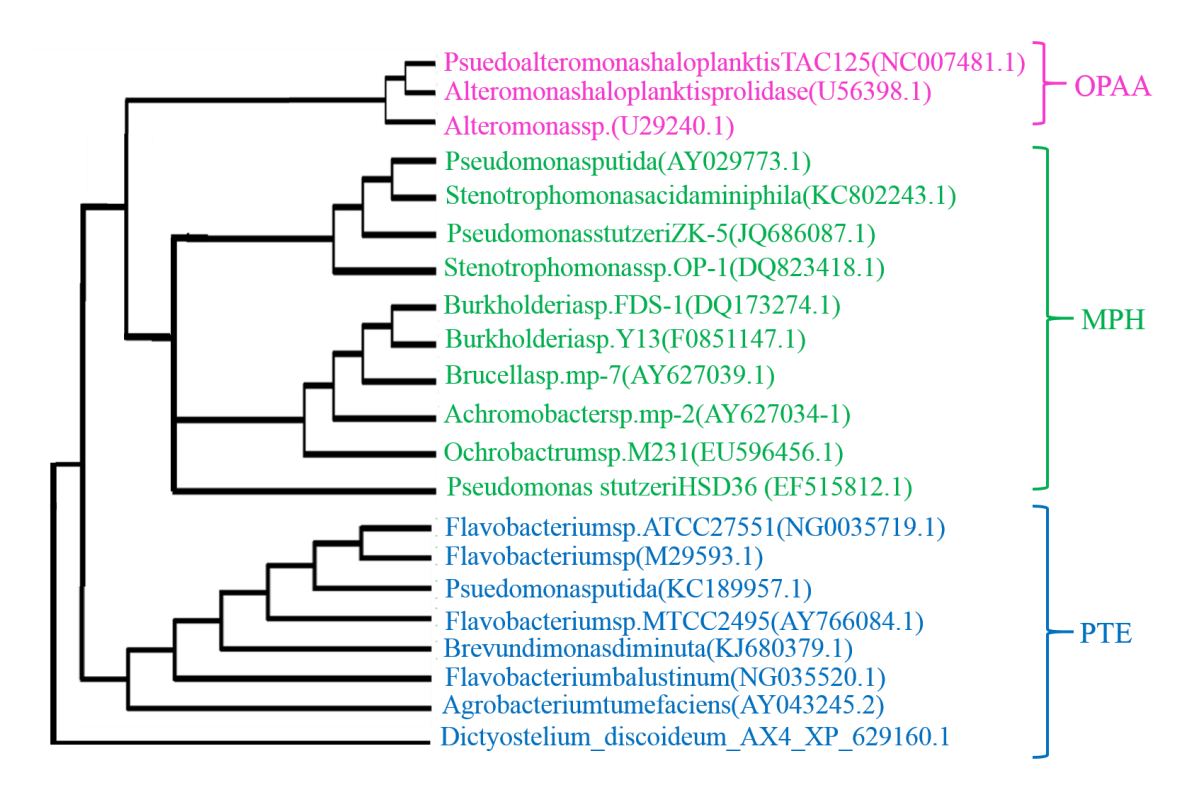


Fig. 1. 2. Phylogenetic tree of bacterial phosphotriesterases (PTEs). The homologues of *opaA* (OPAA) *mpd* (MPH) and *opd* (OPH), coding sequences available in NCBI database were used to construct phylogenetic tree using online tool 'interactive tree of life' (www.itol.embl.de) (Parthasarathy *et al.*, 2017).

1.2. Bacterial Phosphotriesterases

The bacterial PTEs isolated till date are grouped into three major classes based on their structural similarity. They are homologues of Organophosphate Hydrolase (OPH), Methyl Parathion Hydrolase (MPH) and Organophosphate Acid Anhydrolase (OPAA) (Singh *et al.*, 2008; Parthasarathy *et al.*, 2017).

1.2.1. Organophosphorus Acid Anhydrolase (OPAA)

Organophosphorus acid anhydrolase (OPAA) are found in both prokaryotes and eukaryotes. They are first reported in squids (Hoskin & Roush 1982), followed by protozoans (Landis *et al.*, 1987) and bacteria (Attaway *et al.*, 1987). A highly active form of the enzyme was isolated from *Alteromonas sp.* JD6.5 (Defrank *et al.*, 1991; Cheng *et al.*, 1993). It is a monomeric protein with a molecular mass of 60kDa and possesses high activity against a range of organophosphorus compounds including fluoride-containing G-

type nerve agents such as sarin, cyclosarin, tabun, and soman (Zheng et al., 2005). However the catalytic efficiency of OPAA against P-O bond containing OP compounds is less when compared with the P-F bond containing OPs. OPAA belonging to the di-peptidase family and catalyze the di-peptide linkage with a proline residue at the C-terminus (Cheng et al., 1991). Therefore the OPAA is renamed as prolidase. The OPs are fortuitous substrates for prolidases.

1.2.2. Methyl parathion hydrolase (MPH)

The second group of PTEs are methyl parathion hydrolases. They were isolated from Plesiomonas sp. M6 (Zhongli et al., 2001), Pseudomonas sp. WBC-3 (Dong et al., 2005), and Pseudomonas sp., A3 (Zhongli et al., 2002), the soil bacteria collected from different regions of the China. Among these methyl parathione hydrolase purified from Pseudomonas strain is a well characterized enzyme (Zhongli et al., 2001; Liu et al., 2004). It hydrolyses a wide range of OP compounds such as methyl parathion, DDVP, chlorpyrifos, malathion, fenitrothion (Yang et al., 2008). It hydrolyses methyl parathion with a catalytic efficiency as high as k_{cat}/K_m of 10^6 M⁻¹ s⁻¹ (T.K. Ng et al., 2015). MPH retains significant arylesterase and lactonase activities (Baier et al., 2014, 2015). MPH possess promiscuous catalyzes esterase/lipase, lactonase, and phosphodiesterase in addition to its native phosphotriesterase activity (Baier et al., 2015). However methyl parathion is the ideal substrate for methyl parathion hydrolase purified from Pseudomonas sp. WBC-3 (Dong et al., 2005), which can degrade chlorpyrifos, ethyl parathion, and sumithion (Chu et al., 2003). The MPH of Burkholderia sp. FDS-1 can degrade parathion, methyl parathion and sumithion, but not chlorpyrifos, methamidophos, phoxim and triazophos (Zhang et al., 2006). The crystal structure of MPH was determined for MPH purified from *Pseudomonas* sp. WBC-3 (PDB code 1P9E) to 2.4A° resolution (Dong et al., 2005). It is a dimer having bi-nuclear metal Zn^{+2} ions at the catalytic site, they are separated by 3.5A° and located between the inner β -sheets of the $\alpha\beta/\beta\alpha$ sandwich and coordinated to the protein via the side chains of four histidine residues (His55, His57, His201, and His230) and Asp301 (Fig. 1. 3). The two metals are bridged via a carbamylate group from Lys169 and a nucleophile hydroxide ion. The monomer structure of MPH can be described as an $\alpha\beta/\beta\alpha$ sandwich typical of the metallo hydrolase/oxidoreductase fold (Dong et al., 2005). The MPH crystal structure confirms it as a member of the metallo-β-lactamase family with significant conservation of the metal coordinating residues in the binuclear metal center.

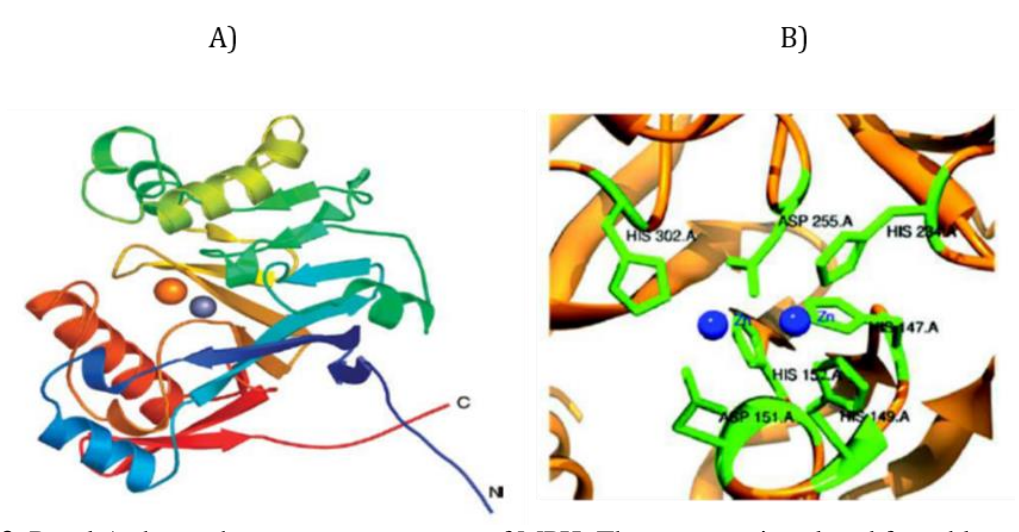


Fig. 1. 3. Panel A shows the monomer structure of MPH. The structure is colored from blue at the N terminus to red at the C terminus. The two metal ions are shown as silver (Zn) and gold (Cd) spheres (Dong *et al.*, 2005). Panel B shows the active site residues found in methyl parathion hydrolase of *Pseudomonas* sp. WBC3 are highlighted in green color. The zinc ions found in bimetallic center of the active site are shown in blue color. The crystal structures are taken from Dong *et al.*, 2005, and the data is published elsewhere (Dong *et al.*, 2005).

1.2.3. Organophosphate hydrolase (OPH)

These groups of enzymes are implicated in the hydrolysis of a wide range of organophosphate compounds such as parathion, methyl parathion and fenusulfothion and organophosphate chemical warfare agents like sarin, soman with high catalytic efficiency. They have wide range substrate specificities that contain different chemical bonds containing P-O, P-F, P-CN and P-S bonds with different efficiency. They show maximum activity against P-O linkage. The purified form of the OPH shows more specificity towards P-O bond with a highest catalytic rate of K_{cat}/K_m 4x10⁷ M⁻¹ S⁻¹ identified for paraxon (Ghanem & Raushel 2005) and shows less specificity for P-S bond with a catalytic efficiency of K_{cat}/K_m 6.2x10² M⁻¹ S⁻¹ for VX (Efremenko et al., 2001). The opd gene encoding OPHs are identified from different soil microorganisms. The OPH characterized initially was purified from the Flavobacterium sp. ATCC 27551, a soil microorganism isolated from the paddy fields of Philippines (Sethunathan & Yoshida 1973), it has recently been reclassified as Sphingobium fuliginis ATCC 27551 (Kawahara et al., 2010). Identical opd genes were identified in Brevundimonas diminuta MG isolated from the agricultural soils of Texas, USA (Mulbry et al., 1986, 1987), Flavobacterium balustinum isolated from the agricultural soils of Ananthapur, India (Somara & Siddavattam 1995), and Agrobacterium tumifaciens C28 isolated from agricultural soils of Australia (Horne et al., 2002). In all these cases OPH encoded by opd is 89% -100% identical. Crystal structure is

available for OPH. It has homodimeric fold with a "TIM" barrel motif (β/α)₈. Its catalytic center possesses two Zn⁺² ions (Omburo *et al.*, 1992; Benning *et al.*, 1994 & 2001) ligated to the protein via direct interactions with 4 histidines and 1 aspartate (Fig. 1. 4). In addition, the two metal ions are bridged by a water molecule and a carbamoylated lysine residue (Vanhooke *et al.*, 1996). It is suggested that the reaction mechanism proceeds via the bridging water molecule (or hydroxide) attacking the phosphorus center of the bound substrate (Benning *et al.*, 1994).

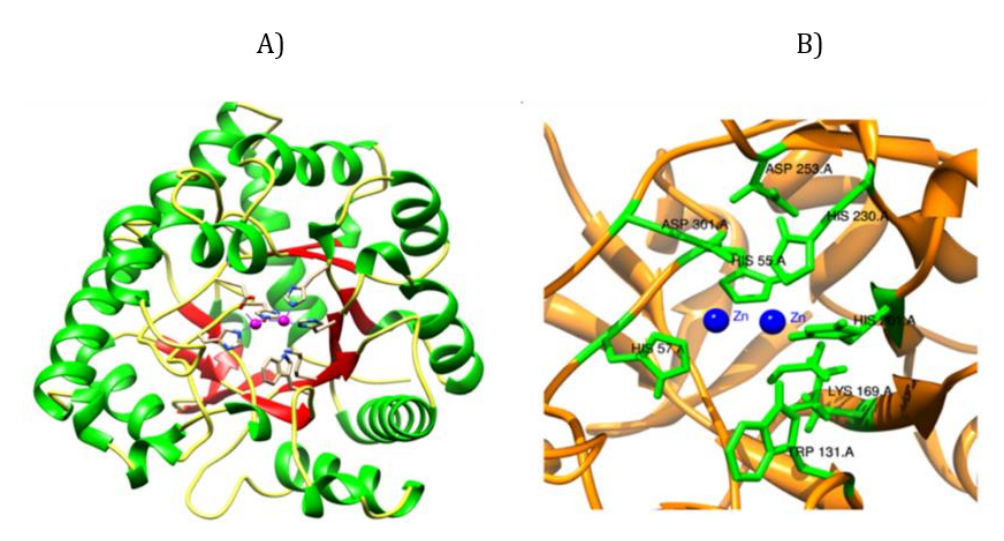


Fig. 1. 4. Panel A shows the crystal structure of OPH. Panel B shows the location of two zinc ions at the active site of OPH. The crystal structures are taken from Benning *et al.*, 1994 and the results are published elsewhere (Benning *et al.*, 1994).

1.3. Structural comparison of OPH and MPH

The physiological substrates are not known for MPH and OPH homologues. Which catalyze identical substrates despite of having no structural similarity (Fig. 1. 5). Since they act on similar substrates, they are proposed to have evolved to degrade OP compounds (Elias & Tawfik 2012). Except in the active site region there exists no structural similarity between MPH and OPH (Fig. 1. 5) (Dong *et al.*, 2005). Both of them contain a similar bi-nuclear zinc center. The 2 metals are separated by 3.4 A^0 and coordinated to the protein via the side chains of 4 histidine residues (His55, His57, His201, and His230) and Asp301 (Benning *et al.*, 2001). The 2 metals are bridged *via* a carbamylate group from Lys169 and a nucleophile hydroxide ion (Fig. 1. 6). Such type of functional convergence from a structurally independent enzymes is considered as symbol for convergent molecular evolution (Tawfik *et al.*, 2006). MPH belongs to the protein family of β -lactamases, the enzymes hydrolyse β -lactam-derived antibiotics (Tian *et al.*, 2008). The MPH homologues share high structural similarity with β -lactamases (Fig. 1. 4) (Dong *et al.*, 2005; Parthasarathy *et al.*, 2017).

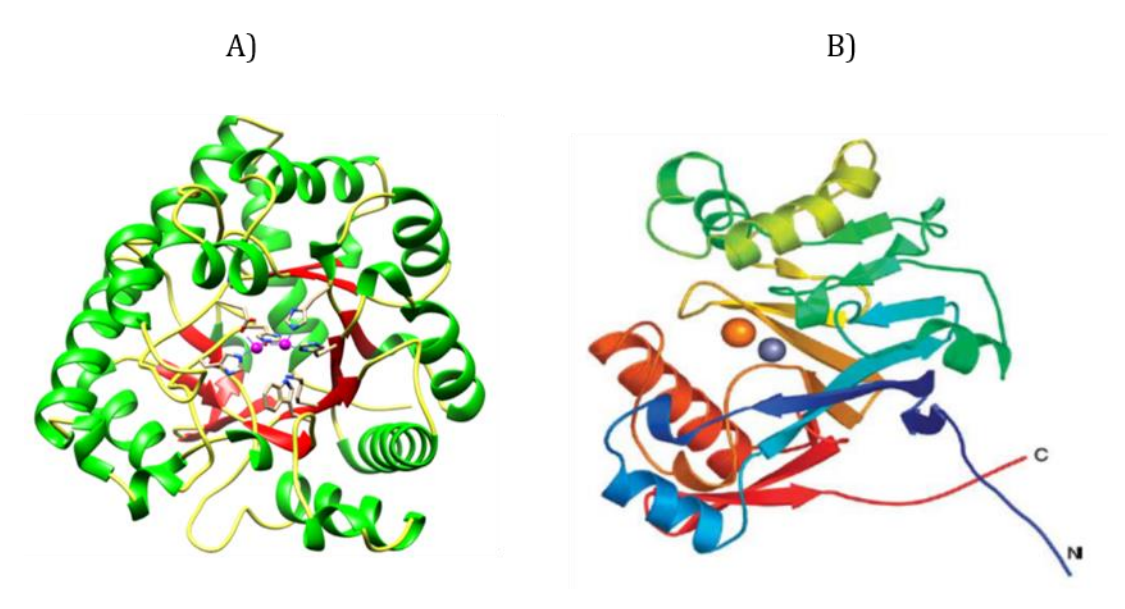


Fig. 1. 5. Structural comparison between OPH and MPH. Panel A shows OPH structure, panel B shows MPH structure. The figures taken and modified from Benning *et al.*, 1994 and Dong *et al.*, 2005 and the results are reviewed elsewhere (Parthasarathy *et al.*, 20017).

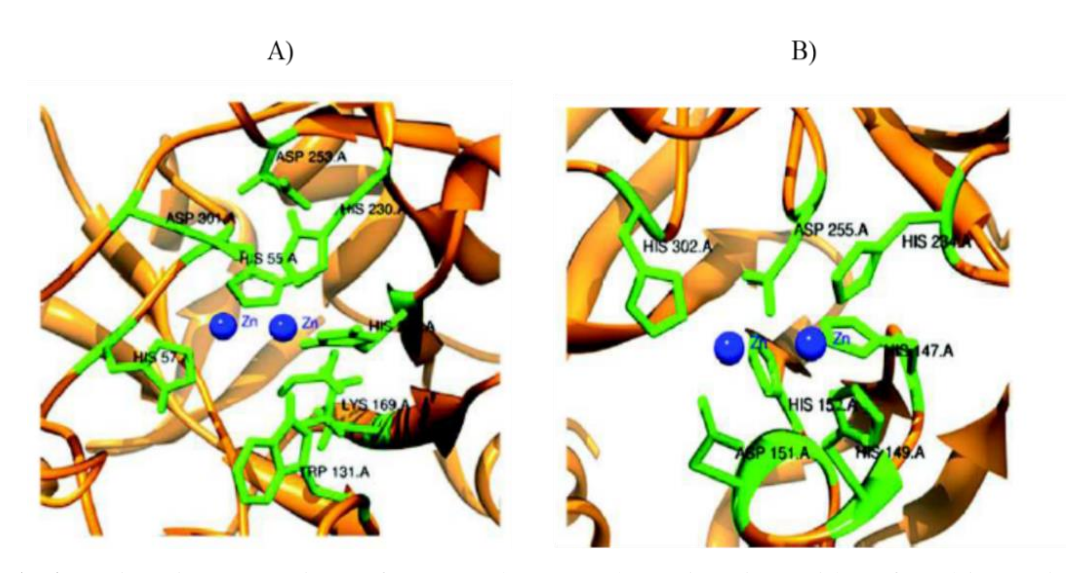


Fig. 1. 6. Active site comparison of OPH and MPH. The active site residues found in *B. diminuta* phosphotriesterase (A) and methyl parathion hydrolase of *Pseudomonas* sp. WBC-3 (B) are highlighted in green color. The zinc ions are found in bimetallic center of the active are shown in blue color. The figures taken from Benning *et al.*, 1994 & Dong *et al.*, 2005 and the results are published elsewhere (Parthasarathy *et al.*, 2017).

1.4. Evolution of OPH

Promiscuous enzymatic activity serves as a starting point for acquiring a new function through gene duplication (Harper *et al.*, 1988; Benning *et al.*, 1994; Lai *et al.*, 1995; Kolakowski *et al.*, 1997 & Rastogi *et al.*, 1997). In fact, these promiscuous activities are considered to be the vestiges of the function of their corresponding ancestral protein (Lai *et al.*, 1995 & Kolakowski *et al.*, 1997). The phosphotriesterases have been shown to have

phosphodiesterase, carboxyl esterase, and lactonase activities (McDaniel *et al.*, 1988; Defrank *et al.*, 1993 & Cheng *et al.*, 1997). In general, family members that have diverged from a common ancestor often share promiscuous activities (Poelarends *et al.*, 2005; Roodveldt *et al.*, 2005b; Yew *et al.*, 2005 & Elias *et al.*, 2008). The N-acyl homoserine lactonases hydrolyses Quorum sensing molecules which were involved in bacterial communication. The N-acyl homoserine lactonases and OPH are structurally similar and the N-acyl homoserine lactonase shows phosphotriesterase activity and OPH shows promiscuous lactonase activity (Afriat *et al.*, 2006). Considering structural and functional similarities, the lactonases are considered as progenitors of organophosphate hydrolases (Fig. 1. 7).

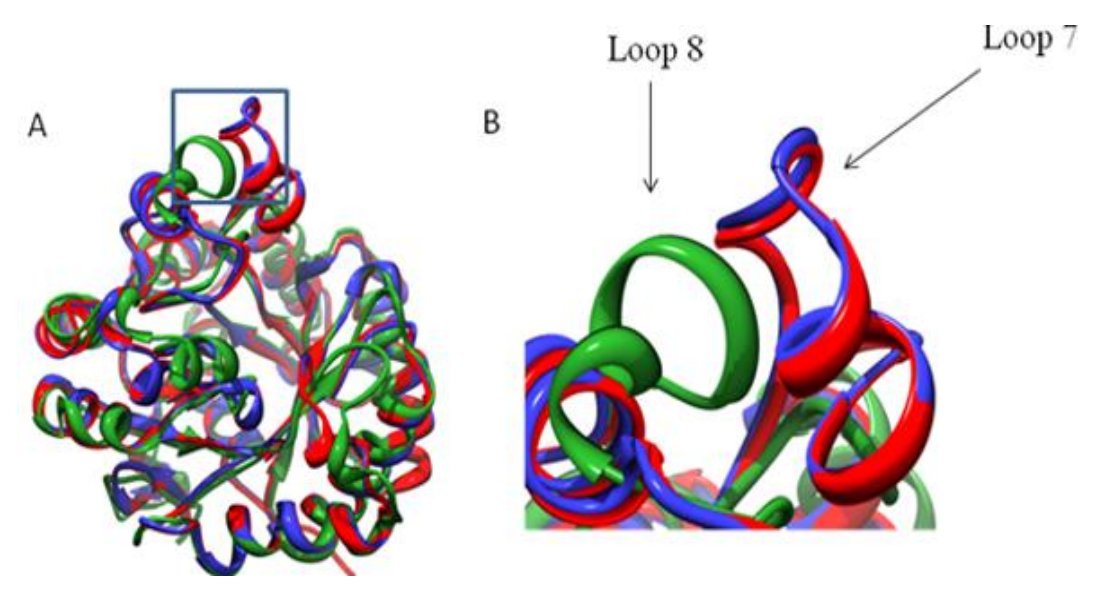


Fig. 1. 7. Structural basis for natural lactonase and promiscuous phosphotriesterase activity. Superimposition of PTEs of *Brevundimonas diminuta* (red) and *A. radiobacter* (blue) with the phosphotriesterase like lactonases PLLs, (green) of *S. solfataricus* (SsoPox), Absence of 15 residue long loop 7 in SsoPox, is shown with arrow mark. The crystal structures obtained from Protein data bank (www.pdb.org) were superimposed using UCSF chimera and the images were traced using persistence of Vision RaytracerVersion 3.6 (www.povray.org). The proposed structural comparison is reviewed by *Parthasarathy et al.*, 2017. The figures are taken from Zhang *et al.*, 2015; Parthasarathy *et al.*, 2017.

1.5. OPH is a Tat substrate

As stated in the aforementioned sections, the OPH is a homo-dimeric metalloprotein. It consists of two identical subunits, each having 360 amino acids. It contains a signal peptide of 23 amino acids and it is unique in a number of ways. It contains Twin Arginine Transport (TAT) motif with a consensus sequence of MQTRRVVLK, along with a lipobox (LAGC) motif and an invariant cysteine residue at the junction of signal peptide cleavage site (Gorla

et al., 2009; Parthasarathy et al., 2016). The twin arginine motif is essential to gain recognition for an alternate protein transport system evolved to target/translocate prefolded proteins across the membrane. The transport pathway otherwise known as Twin Arginine Translocation (Tat) pathway is initially identified in plants (Weiner et al., 1998 & Sargent et al., 1998), especially in nuclear genome encoded proteins destined to target thylakoid membrane. Signal peptides control the entry of virtually all proteins to the secretory pathway, both in eukaryotes and prokaryotes (Gierasch, 1989; von Heijne, 1990; Rapoport, 1992). The signal peptide of secretory proteins function as both the targeting and recognition signal and ranges in length from 18 to about 30 amino acid residues. It is composed of three domain: the positively charged amino terminus (N region); The H domain, and C domain.

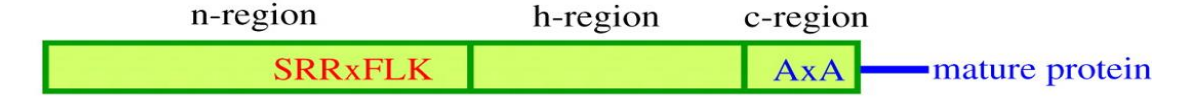


Fig. 1. 8. General Tat signal sequence (Adapted from Julia et al., 2012).

The TAT-substrates contain positively charged N-region contains a consensus signature sequence with conserved twin arginine residues (S/T-R-R-X-F-L-K) (Julia et al., 2012). Substitutions to the twin arginines of the Tat motif, even with similarly charged lysines hamper transport process. The signal recognition particle (SRP) specifically interacts with Tat motif before taking the prefolded proteins to Tat-specific translocases (Keenan et al., 2001). The H domain is the hydrophobic core of a signal sequence and varies in length from 7 to 15 amino acids. The total hydrophobicity of the H region determines the efficiency of translocation and the translocation efficiency increases with the length and hydrOphobicity of the H region (Chou & Kendall, 1990). The leader peptidase cleavage site (C domain) is the only part of the signal sequence that demands some primary sequence specificity. Two types of leader peptidases are known, type I, serving ordinary preproteins, and type II, cleaving the leaders of lipoproteins. Lipoproteins depend on type II leader peptidases, the type II peptidase substrates show substrate differences only at the -3 and +1 positions (Sankaran & Wu, 1994). Precursors of lipoproteins contain larger hydrophobic amino acid residues at the -3 position, with a preference for leucine (Fekkes & Driessen, 1999). At the +1 position, a cysteine is always present and has to undergo modification prior to processing.

1.6. Tat translocation pathway

The Tat pathway is protein secretion/export pathway present in plants, bacteria and archea. In contrast to the Sec-pathway which translocates proteins in an unfolded manner, the Tat pathway translocates fully folded proteins. It generally involves translocation of proteins that (i) requires a large cofactors for activity (Berks, 1996: Palmer et al., 2005;), (ii) that acquire folded confirmation while they are still in cytoplasm (Berks et al., 2003) (iii) unfavorable extracellular environment, such as high temperature, salt concentration, etc. for folding (iv) the fail to fold in a relatively more oxidizing environment prevailing in periplasmic space of Gram-negative bacteria and (v) multi-subunit protein complexes (Berks et al., 2003; Parthasarathy et al., 2016). Tat pathway has evolved through unique protein translocases and chaperones to translocate prefolded proteins across the hydrophobic phospholipid bilayer, without damaging its integrity. The mechanism of Tat translocation pathway is well studied in E. coli. In E. coli, the Tat translocase is made of three proteins TatA, TatB and TatC. These three proteins are coded by an operon consisting of four open reading frames (ORFs) tatA, tatB, tatC and tatD (Strauch and Georgiou, 2007). Although tatABC are shown essential, deletion of tatD had no influence on transport of Tat-substrates (Sargent et al., 1998).

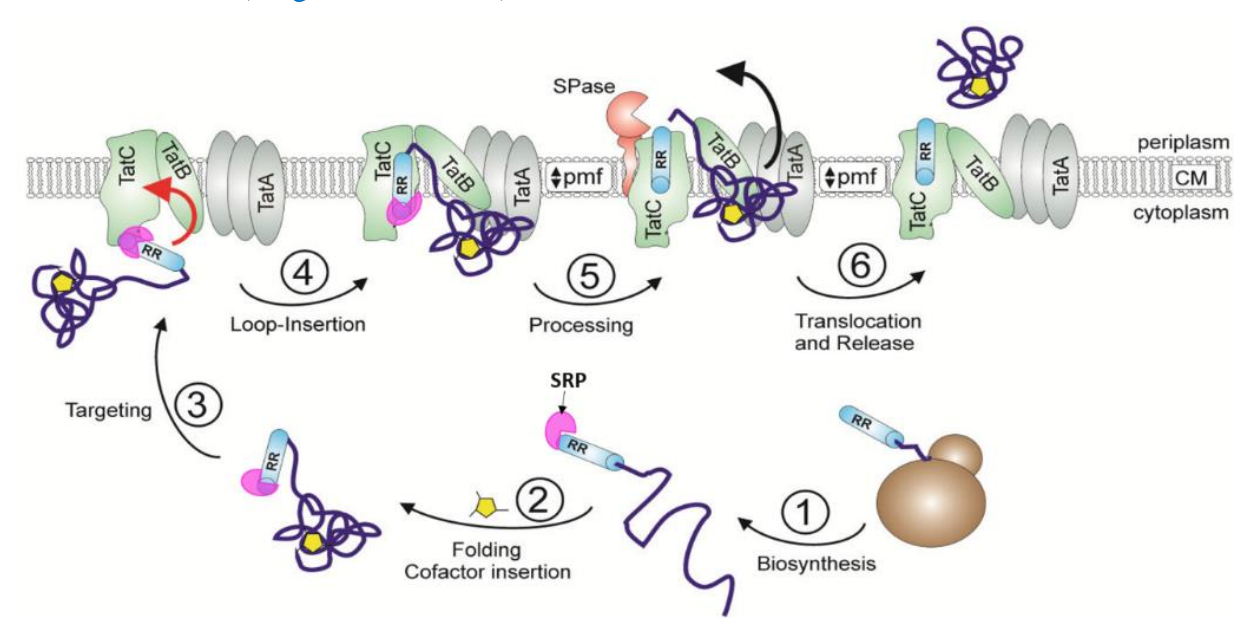


Fig. 1. 9. Schematic diagram represents the Tat translocation pathway (Adapted from the web page of Prof. Freudl).

In addition to the *tat* operon, the *tatA* paralogue, *tatE* is found elsewhere in the chromosome. TatE, due to its homology to TatA complements TatA functions. TatA and TatB have considerable sequence similarity and are associated in the membrane (Leeuw *et*

al., 2001). The TatA is the most abundant protein of all Tat-translocases and is assessed to be present at around 20 times more than TatB and TatC (Jack et al., 2001; Sargent et al., 2001). TatA is a 9.6kDa polypeptide with 89 amino acids and contains N-terminal hydrophobic α -helix region followed by a short hinge region and a longer amphipathic α helix region (Hu et al., 2010). The TatA forms tetrameric homo oligomers in the cytoplasmic membrane generating an intramolecular pore. TatB having 171 amino acids with a molecular mass of 18.5kDa and TatC contains 258 amino acids with a molecular mass of 29kDa. As predicted by its secondary structure, this protein traverses the membrane six times, possessing an N-in C-in topology (Punginelli et al., 2007) and it forms an initial complex which recognizes the Tat substrates (Eijlander et al., 2009). The details of translocation process are presented in fig. 1. 9. Upon recognition of the cognate substrate by the chaperone or the SRP, the SRP bound to the RR motif is recognized by the TatC protein. The TatB and TatC then form an initial association with many copies of each of the constituent subunits (Orriss et al., 2007). This TatBC complex is the membrane binding site for Tat substrates which then recruits TatA to form the active translocation site. TatA forms homo-oligomeric ring-like structures that constitute the protein translocating channels of the Tat system (Fig. 1. 9). The proton motive force generated due to pH gradient across the membrane appears to facilitate the transport of prefolded proteins (Delisa et al., 2002). As a result of a series of co-ordinated events, the prefolded proteins successfully translocate to the cell exterior (Delisa et al., 2003; Lee et al., 2006).

1.7. OPH is a Lipoprotein

OPH contains an invariant cysteine residue at the junction of signal peptidase II cleavage site. The invariant cysteine residue is linked to diacylglycerol containing myristic and oleic fatty acids (Parthasarathy *et al.*, 2016). OPH anchors to the inner membrane through a diacyl glycerol moiety (Fig. 2). As revealed by PEG-Mal (methoxypolyethylene glycol maleimide) labelling experiments OPH is exposed to the periplasmic space of the inner membrane (Parthasarathy *et al.*, 2017). Recently our laboratory has shown existence of OPH as 292kDa membrane associated protein complex (Parthasarathy *et al.*, 2016). However there exists no information on OPH interacting partners and their physiological role. The research work to be described in the thesis is formulated with the following objectives to provide answers to some of the aforementioned problems pertaining to OPH biology.

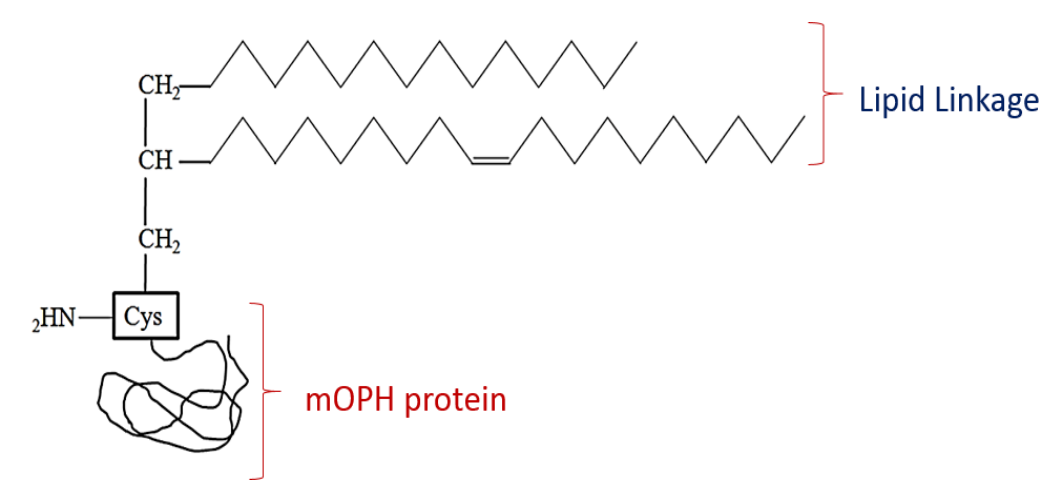
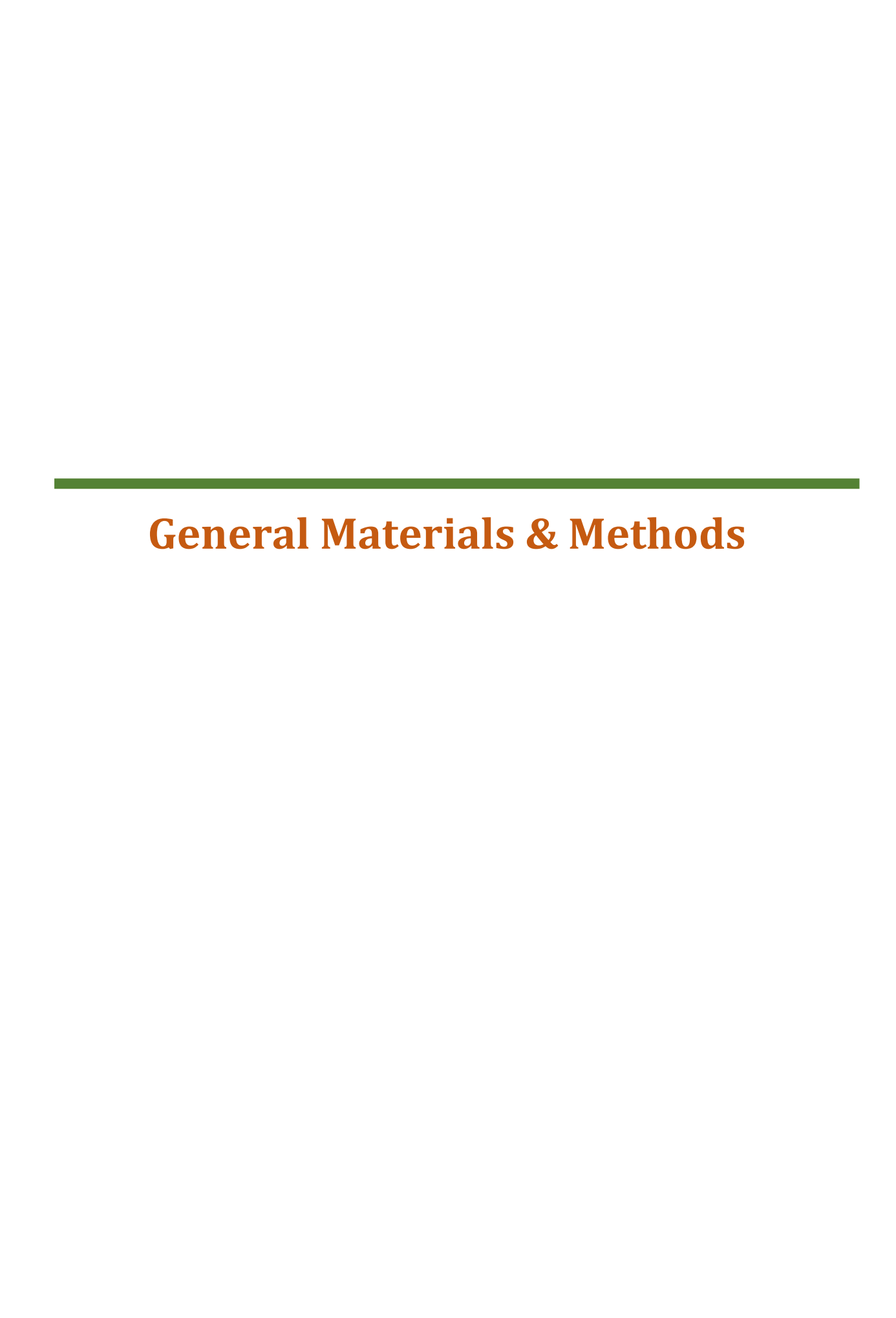


Fig. 1. 10. Shows mature form of OPH is linked to Diacylglycerol (Parthasarathy et al., 2017).

1.8. Objectives

- 1. To identify OPH interacting proteins.
- 2. To establish inter protein interactions.
- 3. To reconstitute *Sphingobium fuliginis* TonB dependent transport (TonBDT) system in *E. coli*.
- 4. To elucidate the physiological role of OPH complex in *Sphingobium fuliginis*.



2. General Materials & Methods

Table 2. A: Antibiotics

Name of the antibiotic	Name of the supplier
Ampicillin sodium salt	HIMEDIA
Chloramphenicol	HIMEDIA
Gentamycin	HIMEDIA
Kanamycin Sulfate	HIMEDIA
PolymyxinB	HIMEDIA
Streptomycin	HIMEDIA
Tetracycline hydrochloride	HIMEDIA

Table 2. B: Chemicals

Name of the Chemical	Name of the supplier
Absolute alcohol	Hayman's
Acetic Acid (Glacial)	SRL
Acetone	SRL
Acetonitrile	SRL
Acrylamide	Sigma Aldrich
Agar agar	Himedia
Ammonium chloride	SRL
Ammonium persulphate	SRL
Ammonium nitrate	SRL
Bovine serum albumin	Himedia
Bis- Tris	Amersco
Bromophenol blue	SRL
Butanol	SRL
Calcium chloride	SRL
Glucose	Himedia
Glycerol	SRL

Hydrochloric acid L-Arginine SRL Isopropanol Isopropyl thiogalactopyranoside (IPTG) G-biosciences Lithium Chloride SRL Methyl parathion Sigma Aldrich Methyl viologen Sigma Aldrich Magnesium sulphate SRL Methanol NADP (Nicotinamide Adenine Dinucleotide Phosphate) Nickle Chloride Nickle Chloride N,N'-Methylene diamine dihydrochloride Sigma Aldrich N,N'-Methylene bis acrylamide GE Healthcare Peptone Himedia Phenol (water saturated) Phosphoric acid Merck β-mercaptoethanol ONPG (O-nitrophenyl-β-D-galactopyranoside) SRL Potassium chloride SRL Potassium chloride Qualigens	Glycine	SRL
Isopropanol Isopropyl thiogalactopyranoside (IPTG) G-biosciences Lithium Chloride SRL Methyl parathion Sigma Aldrich Methyl viologen Sigma Aldrich Magnesium sulphate SRL Methanol SRL MADP (Nicotinamide Adenine Dinucleotide Phosphate) Sigma Aldrich Nickle Chloride SRL N-(1-Napthyl) ethylene diamine dihydrochloride Sigma Aldrich N,N'-Methylene bis acrylamide GE Healthcare Peptone Himedia Phenol (water saturated) Phosphoric acid Merck β-mercaptoethanol ONPG (O-nitrophenyl-β-D-galactopyranoside) Sigma Aldrich SRL Phenol Saturated SRL	Hydrochloric acid	SRL
Isopropyl thiogalactopyranoside (IPTG) Lithium Chloride SRL Methyl parathion Sigma Aldrich Methyl viologen Magnesium sulphate SRL Methanol NADP (Nicotinamide Adenine Dinucleotide Phosphate) Nickle Chloride Nickle Chloride N-(1-Napthyl) ethylene diamine dihydrochloride N,N'-Methylene bis acrylamide Peptone Himedia Phenol (water saturated) Phosphoric acid Merck β-mercaptoethanol ONPG (O-nitrophenyl-β-D-galactopyranoside) SRL SRL Sigma Aldrich Merck Sigma Aldrich SRL SRL SRL SRL SRL SRL SRL SR	L-Arginine	SRL
Lithium Chloride Methyl parathion Sigma Aldrich Methyl viologen Sigma Aldrich Magnesium sulphate SRL Methanol NADP (Nicotinamide Adenine Dinucleotide Phosphate) Nickle Chloride N-(1-Napthyl) ethylene diamine dihydrochloride N,N'-Methylene bis acrylamide GE Healthcare Peptone Himedia Phenol (water saturated) Phosphoric acid β-mercaptoethanol ONPG (O-nitrophenyl-β-D-galactopyranoside) Sigma Aldrich SRL Sigma Aldrich SRL Merck Sigma Aldrich Sigma Aldrich Sigma Aldrich	Isopropanol	SRL
Methyl parathion Sigma Aldrich Methyl viologen Sigma Aldrich Magnesium sulphate SRL Methanol SRL NADP (Nicotinamide Adenine Dinucleotide Phosphate) Sigma Aldrich Nickle Chloride SRL N-(1-Napthyl) ethylene diamine dihydrochloride Sigma Aldrich N,N'-Methylene bis acrylamide GE Healthcare Peptone Himedia Phenol (water saturated) SRL Phosphoric acid Merck β-mercaptoethanol Sigma Aldrich ONPG (O-nitrophenyl-β-D-galactopyranoside) Sigma Aldrich Phenol Saturated SRL	Isopropyl thiogalactopyranoside (IPTG)	G-biosciences
Methyl viologen Sigma Aldrich Magnesium sulphate SRL Methanol SRL NADP (Nicotinamide Adenine Dinucleotide Phosphate) Sigma Aldrich Nickle Chloride SRL N-(1-Napthyl) ethylene diamine dihydrochloride Sigma Aldrich N,N'-Methylene bis acrylamide GE Healthcare Peptone Himedia Phenol (water saturated) SRL Phosphoric acid Merck β-mercaptoethanol Sigma Aldrich ONPG (O-nitrophenyl-β-D-galactopyranoside) Sigma Aldrich Phenol Saturated SRL	Lithium Chloride	SRL
Magnesium sulphate SRL Methanol SRL NADP (Nicotinamide Adenine Dinucleotide Phosphate) Sigma Aldrich Nickle Chloride SRL N-(1-Napthyl) ethylene diamine dihydrochloride Sigma Aldrich N,N'-Methylene bis acrylamide GE Healthcare Peptone Himedia Phenol (water saturated) SRL Phosphoric acid Merck β-mercaptoethanol Sigma Aldrich ONPG (O-nitrophenyl-β-D-galactopyranoside) Sigma Aldrich Phenol Saturated SRL	Methyl parathion	Sigma Aldrich
Methanol SRL NADP (Nicotinamide Adenine Dinucleotide Phosphate) Sigma Aldrich Nickle Chloride SRL N-(1-Napthyl) ethylene diamine dihydrochloride Sigma Aldrich N,N'-Methylene bis acrylamide GE Healthcare Peptone Himedia Phenol (water saturated) SRL Phosphoric acid Merck β-mercaptoethanol Sigma Aldrich ONPG (O-nitrophenyl-β-D-galactopyranoside) Sigma Aldrich Phenol Saturated SRL	Methyl viologen	Sigma Aldrich
NADP (Nicotinamide Adenine Dinucleotide Phosphate) Nickle Chloride SRL N-(1-Napthyl) ethylene diamine dihydrochloride N,N'-Methylene bis acrylamide Peptone Himedia Phenol (water saturated) Phosphoric acid β-mercaptoethanol ONPG (O-nitrophenyl-β-D-galactopyranoside) Sigma Aldrich SRL	Magnesium sulphate	SRL
Nickle Chloride SRL N-(1-Napthyl) ethylene diamine dihydrochloride Sigma Aldrich N,N'-Methylene bis acrylamide GE Healthcare Peptone Himedia Phenol (water saturated) SRL Phosphoric acid Merck β-mercaptoethanol Sigma Aldrich ONPG (O-nitrophenyl-β-D-galactopyranoside) Sigma Aldrich Phenol Saturated SRL	Methanol	SRL
N-(1-Napthyl) ethylene diamine dihydrochloride N,N'-Methylene bis acrylamide Peptone Phenol (water saturated) Phosphoric acid β-mercaptoethanol ONPG (O-nitrophenyl-β-D-galactopyranoside) Sigma Aldrich Phenol Saturated Sigma Aldrich SRL	NADP (Nicotinamide Adenine Dinucleotide Phosphate)	Sigma Aldrich
N,N'-Methylene bis acrylamide Peptone Himedia Phenol (water saturated) Phosphoric acid β-mercaptoethanol ONPG (O-nitrophenyl-β-D-galactopyranoside) SRL Sigma Aldrich Sigma Aldrich Sigma Aldrich Sigma Aldrich Sigma Aldrich	Nickle Chloride	SRL
Peptone Himedia Phenol (water saturated) SRL Phosphoric acid Merck β-mercaptoethanol Sigma Aldrich ONPG (O-nitrophenyl-β-D-galactopyranoside) Sigma Aldrich Phenol Saturated SRL	N-(1-Napthyl) ethylene diamine dihydrochloride	Sigma Aldrich
Phenol (water saturated) Phosphoric acid Phosphoric acid β-mercaptoethanol ONPG (O-nitrophenyl-β-D-galactopyranoside) Sigma Aldrich Phenol Saturated SRL	N,N'-Methylene bis acrylamide	GE Healthcare
Phosphoric acid Merck β-mercaptoethanol Sigma Aldrich ONPG (O-nitrophenyl-β-D-galactopyranoside) Sigma Aldrich Phenol Saturated SRL	Peptone	Himedia
β-mercaptoethanol Sigma Aldrich ONPG (O-nitrophenyl-β-D-galactopyranoside) Sigma Aldrich Phenol Saturated SRL	Phenol (water saturated)	SRL
ONPG (O-nitrophenyl-β-D-galactopyranoside) Sigma Aldrich Phenol Saturated SRL	Phosphoric acid	Merck
Phenol Saturated SRL	β-mercaptoethanol	Sigma Aldrich
	ONPG (O-nitrophenyl-β-D-galactopyranoside)	Sigma Aldrich
Potassium chloride Qualigens	Phenol Saturated	SRL
	Potassium chloride	Qualigens
Potassium dihydrogen ortho phosphate Merck	Potassium dihydrogen ortho phosphate	Merck
PMSF GE Healthcare	PMSF	GE Healthcare
Protease inhibitor cocktail Sigma Aldrich	Protease inhibitor cocktail	Sigma Aldrich
SERVA blue G Serva	SERVA blue G	Serva
Sodium citrate SRL	Sodium citrate	SRL
Sodium chloride SRL	Sodium chloride	SRL
Sodium dodecyl sulfate SRL	Sodium dodecyl sulfate	SRL
Sodium hydrogen orthophosphate SRL	Sodium hydrogen orthophosphate	SRL

Sodium hydroxide	SRL
Sucrose	SRL
RNase A	Bangalore GeneI
Tetra ethyl methylene diamine (TEMED)	Sigma Aldrich
Tris-base	Merck
Tricine	Amersco
Triton X-100	Sigma Aldrich
Tryptone	Himedia
Tween 20	Amersco
X-gal	SRL
Yeast extract	Himedia

Table 2. C: Restriction enzymes and DNA modifying enzymes

Name of the enzyme	Name of the supplier
BamHI	Thermo Fisher Scientific, India.
BglII	Thermo Fisher Scientific, India.
EcoRI	Thermo Fisher Scientific, India.
HindIII	Thermo Fisher Scientific, India.
KpnI	Thermo Fisher Scientific, India.
NdeI	Thermo Fisher Scientific, India.
NotI	Thermo Fisher Scientific, India.
PstI	Thermo Fisher Scientific, India.
SacI	Thermo Fisher Scientific, India.
SalI	Thermo Fisher Scientific, India.
SmaI	Thermo Fisher Scientific, India.
XhoI	Thermo Fisher Scientific, India.
CIAP	Thermo Fisher Scientific, India.
T4 DNA Ligase	Thermo Fisher Scientific, India.
PfuDNA polymerase	Thermo Fisher Scientific, India.

Phusion® High-Fidelity DNA polymerase	New England Biolabs, Gurgaon, India.
TaqDNA polymerase	Thermo Fisher Scientific, India.
DNase	Sigma Aldrich, India.
RNase A	Thermo Fisher Scientific, India.
HyperLadder 1kb DNA Ladder	Bioline, Indore, India.
Unstained Protein Ladder, 10-200kDa,	Genetix, India.

2. 1. Growth Media

The following growth media were prepared and used for the propagation of bacteria. The media were stringently autoclaved for 20 min at 121°C. For preparation of solid media 2gm of agar was added to 100ml of broth and sterilized. Whenever required, appropriate concentrations of antibiotic and chemical stocks were added after cooling the medium to 40-50°C.

Luria-Bertani (LB) medium

To prepare LB medium, 10gm of peptone, 5gm of yeast extract and 10gm of Sodium chloride were dissolved in 1000ml of double-distilled water. The pH of the LB medium was adjusted to 7.0 with 2N NaOH (approx. 0.5ml) and sterilized by autoclaving for 20 mins at 121°C.

Terrific broth (TB) medium

To prepare TB medium, 12gm of tryptone, 24gm of yeast extract, 3.12gm of KH₂PO₄, 12.5gm of K₂HPO₄ and glycerol 4ml were dissolved in 1000ml of double-distilled water and sterilized by autoclaving at 121°C for 20 mins.

2. 2. Preparation of iron Free Media and solutions

Minimal salts media and component solutions were made iron free by passing through chelex 100 resin (Bio-Rad).

Minimal salts medium for E. coli.

Minimal salts medium was prepared by dissolving 1.2gm of KH₂PO₄, 4.8gm of K₂HPO₄ in 1000ml of double-distilled water. This medium was autoclaved at 15psi (1.05kg/cm²) on liquid cycle for 20 minutes. After sterilization the solution was allowed to cool to room temperature and sterile stock solutions of 10% of MgSO₄.7H₂O, 20% of CaNO₃4H₂O, 1% of FeSO₄ and 50% Glucose were added to obtain a final concentration of

0.2gm of MgSO₄.7H₂O (2ml from stock), 0.04gm of CaNO₃4H₂O (200 μ l from stock) 0.001gm of Fe SO₄ (1ml from stock 1% FeSO₄) and 2ml of 50% Glucose to 1000ml of above solution to get complete minimal salts medium.

Preparation of high iron solution.

1% of FeSO₄ stock solution was prepared by dissolving of 1gm of FeSO₄.7H₂O (Merck) in 100ml of milliQ water and sterilized by autoclaving. 100 μ l of this solution added to 100ml of culture medium gives a final concentration of 10 μ g Fe/ml.

Preparation of low iron solution.

 $2\mu g$ Fe/ml of stock solution was prepared by adding $20\mu l$ of high iron solution from stock (1% FeSO₄) in to 20ml of milliQ water to gives $2\mu g/ml$ concentration and sterilized by autoclaving 1ml of this solution added to 100ml of culture medium gives a final concentration of $0.02\mu g$ Fe/ml.

Preparation of iron-free glassware.

All glassware was made iron-free by first soaking in 2% methanolic KOH for overnight. They were rinsed 3 to 4 times with MilliQ water and then soaked for two days in 6N HCl, and the glassware washed with milliQ water and sterilized by autoclaving for 20 mins at 15psi (1.05 kg/cm²) on liquid cycle.

2. 3. Preparation of Antibiotic & Chemical stock solutions.

Ampicillin: Stock solution of Ampicillin was prepared by dissolving 1gm of ampicillin in 10ml of sterile milliQ water and filtered through 0.2μM syringe filter. This stock solution was distributed into 1ml aliquots and stored at -20°C. When required 10μl of stock solution was added to 10ml of medium to get a final concentration of 100μg/ ml of medium.

Chloramphenicol: Stock solution of Chloramphenicol was prepared by dissolving 300mg of chloramphenicol in 10ml of 70% ethanol (v/v) and filtered through 0.2 μ M syringe filter. This stock solution was distributed into 1ml aliquots and stored at -20°C. When required 10 μ l of stock solution was added to 10ml of medium to get a final concentration of 30 μ g/ml of medium.

Gentamycin: Stock solution of gentamycin was prepared by dissolving 200mg of gentamycin sulfate in 10ml of milliQ water and sterilized by filtration. The stock solution was stored in 1ml aliquots at -20°C after filter sterilization. When required 10μl of gentamycin stock solution was added to 10ml of medium to get a final concentration of 20μg/ml of medium.

Kanamycin: Stock solution of kanamycin was prepared by dissolving 300mg of kanamycin sulfate in 10ml of milliQ water and sterilized by filtration. The stock solution was stored in 1ml aliquots at -20°C. When required 10μl of kanamycin stock solution was added to 10ml of medium to get a final concentration of 30μg/ml of medium.

Polymyxin B: Stock solution of polymyxin B was prepared by dissolving 100mg of polymyxin B in 10ml of milliQ water. The stock solution was stored at -20°C in 1ml aliquots after filter sterilization. When required 10μl of polymyxin B stock solution was added to 10ml of medium t0 get a final concentration of 10μg/ml of medium.

Streptomycin: Stock solution of streptomycin was prepared by dissolving 200mg of streptomycin in 10ml of milliQ water. The stock solution was stored in 1ml aliquots at -20°C after filter sterilization. When required 10µl of streptomycin stock solution was added to 10ml of medium to get a final concentration of 20µg/ml of medium.

Tetracycline: Tetracycline stock solution was prepared by dissolving 200mg of tetracycline in 10ml of 70% ethanol (v/v) and filtered through $0.2\mu M$ syringe filter. This stock solution was distributed into 1ml aliquots and stored at-20°C. When required 10 μ l of stock solution was added to 10ml of medium to get a final concentration of $20\mu g/ml$ of medium.

IPTG: Isopropyl-β-D-thio-galactoside: IPTG stock (1M) solution was prepared by dissolving 238mg of IPTG in 1ml of autoclaved milliQ water and stored at -20°C. When required the stock solution was thawed on ice and 100μl of stock solution was added to the 100ml of cooled medium (45°C) to get 1mM working concentrations of IPTG.

X-Gal: 5-bromo-4-chloro-indolyl-β-D-galactopyranoside: X-gal stock (4%) solution was prepared by dissolving 40mg of X-gal in 1 ml of N, N' –dimethylf0rmamide. When required, 100μl of stock solution of 4% (w/v) X-gal was added to 100ml of medium after cooling it to 45°C.

2.4. DNA manipulation: Preparation of solutions and buffers.

2.4.1. Agarose gel electrophoresis

Gel electrophoresis was used for separation of DNA fragments. The phosphateribose backbone of nucleic acids is negatively charged and DNA fragments migrate through the matrix of an agarose gel after applying voltage to the gel. The electrophoretic mobility of DNA fragments is dependent on the size and structure of the DNA. Therefore, the migration distance of a DNA fragment after a given time is proportional to the negative logarithm of the base length. PCR amplicons and plasmid DNA ranging from 0.5-12kb were separated in small horizontal agarose gels containing 0.8-2% (w/v) agarose in TAE buffer and 0.5μg ml⁻¹ ethidium bromide. Nucleic acid samples were mixed with 6x DNA loading dye and filled into the wells of an agarose gel immersed in 1x TAE buffer. The fragments were separated in 1x TAE buffer for about 20 minutes at electric field strength of about 100V. Ethidium bromide is a fluorescent dye that intercalates between bases of double stranded DNA and RNA and emits orange colour light after exposure to UV light at 302nm. Thus, the positions of the DNA fragments in the agarose gel were visualized by exposure with UV light and the results were documented by capturing image using UVItech gel documentation system. The size of the DNA fragments was determined bands on mobility of DNA standard (1kb ladder; Fermentas) that was loaded to adjacent wells of the samples.

TAE buffer: A stock solution of 50x TAE (Tris-Acetate- EDTA) buffer was prepared by mixing 242gm of Tris base, 100ml of 0.5M EDTA (pH 8.0) and 57.1ml of glacial acetic acid to 900ml of double distilled water, after complete dissolution of the contents the volume of the solution was made up to 1000ml with double distilled water. When required, appropriate volume of stock (50x TAE) was taken and diluted to get 1x TAE.

6x Gel loading buffer: 12.5mg of bromophenol blue, 12.5mg of xylene cyanol FF and 7.5gm of Ficoll (Type 400; Pharmacia) were dissolved in 75ml of milliQ water and finally made up to 100ml and stored at room temperature.

Ethidium bromide stock solution (EtBr): 10mg of ethidium bromide was mixed with 1ml of sterile water and kept for vortex amber color eppendorf tube. This solution was further diluted to get a final working stock solution of 1mg/ml. While preparing agarose gel 5μl of working stock solution was added to 100ml of gel solution to get a final concentration of 0.05μg/ml (Sambrook *et al.*, 1989).

2.4.2. Isolation of Plasmids.

Isolation of plasmid DNA by Alkaline Lysis method was described by Birnboim & Doly 1979. A single colony containing desired plasmid was inoculated into 3ml LB medium substituted with required antibiotic and was incubated for 12h at 37°C with shaking. Bacterial cells were collected from 1ml of overnight culture by centrifugation at 13,000 rpm for 1 minute. The cell pellet was resuspended in 100µl of ice-cold solution-I (TEGL) (50mM glucose; 10mM EDTA, pH 8.0; 25mM Tris-Cl, pH 8.0) by vigorous vortexing. The above bacterial suspension was mixed with 200µl of solution-II (freshly prepared) (equal

volume of 1% SDS, 0.2N NaOH) and samples were incubated on ice for 4 to 5 min before adding 150μl of ice-cold solution-III (3M Sodium acetate, pH 4.8). The contents were then thoroughly mixed by inverting the tube 3-4 times. Then tube was kept on ice for 3-5 minutes. The contents were centrifuged at 13,000 rpm for 10 minutes. The supernatant was then transferred into a fresh tube and extracted with equal volumes of phenol: chloroform and later with chloroform and isoamyl alcohol (24:1). The clear aqueous phase was transferred to a fresh tube and the plasmid DNA was precipitated by adding 1/10th volumes of 3M sodium acetate, pH 4.8 and 2 volumes of ethanol and tubes were incubated at -80°C for 20 minutes. The plasmid was collected by centrifugation at 13000rpm for 20 min. The traces of salts in the plasmid were removed by washing with cold 70% ethanol. The plasmid was further dried and redissolved in 30μl of TE.

2.4.3. DNA Quantification

Nucleic acid concentration was quantified spectrophotometrically using a Nano Drop ND-1000 system (Thermo Scientific). 1.5µl of sample were pipetted on the sample pedestal and the absorbance peak of nucleic acid in the sample was measured at 260nm. The software calculated the nucleic acid concentration according to the Beer-Lambert Law with an extinction coefficient of $0.020(ng/\mu l)^{-1}cm^{-1}$ and $0.030~(ng/\mu l)^{-1}cm^{-1}$ for double stranded and single stranded DNA, respectively. Protein contamination in the sample was estimated by measuring the ratio of absorbance at 260 and 280nm with a 260/280 ratio of approximately 1.8 considered as pure for DNA. In addition, the nucleic acid purity can be further determined by measuring the ratio of absorbance at 260nm and 230nm, which typically results in values between 1.8 and 2.2 for nucleic acid samples without contaminants.

2.4.4. Polymerase Chain Reaction (PCR)

PCR amplification reactions were carried out in a 25μl volume containing 2.5mM MgCl₂, dNTP mix containing 200μM each of dATP, dCTP, dGTP and dTTP mix (Thermo Fisher Scientific), 10 picomoles of each forward and reverse primers, 1.0 Unit of *Taq* polymerase or *pfu* DNA polymerase, 10-20ng of plasmid or genomic DNA was used as template. Amplifications were carried out in the thermal cycler (Bio-Rad) by adjusting the PCR programme as per the amplicon size and Tm of the primers. Amplification products were analyzed on 0.8% agarose gel electrophoresis.

Table 2. D. Standard PCR programme for Thermocycler

Step	Temperature	Time	Cycles
Denaturation	94°C	4 min	1
Denaturation	94°C	30 sec	
Annealing	50°C-60°C	30 sec	30
Elongation	72°C	1 min /kb	
Final Elongation	72°C	5 min	1
Hold	12°C	Infinite	-

2. 4. 5. Site-Directed Mutagenesis.

Q5[®] Site-Directed Mutagenesis Kit (cat no Eo554S) (New England Biolabs, USA) protocol was performed to introduce amino acid substitutions in a gene. Initially the region to be mutated was selected and overlapping primers were generated by introducing desired mutations in the primer sequence. The plasmid containing the gene of interest was used as template and the PCR was performed using appropriate primers having mutation at required place. The plasmid DNA template was isolated from a strain with an intact *dam* methylation system (usually DH5α) and performed PCR by following instructions protocols and the PCR products were treated with KLD enzyme mix provided by kit and resulting PCR product was transformed into competent cells of *E. coli* strain. The plasmids were extracted from the strains and the sequence was checked by sequencing for correct introduction of the mutation at the desired position.

2. 4. 6. Molecular Cloning

Restriction Digestion

Restriction endonuclease enzymes are of bacterial origin and cleave double stranded DNA at specific recognition sites by hydrolysis of the phosphodiester bonds at the DNA backbone. The cleavage site is close or within the recognition sequence, which is usually palindromic, and has a length of 4-8bp. Restriction digest reactions were carried out in a volume of 20µl with restriction endonuclease enzymes at a concentration of 1 unit per 1µg of DNA. The restriction digest reaction mixture was incubated in general at 37°C or at the specific temperatures required for particular enzymes as detailed by the manufacturer's

literature. Incubation time of reactions containing vector DNA did not exceed 2 hours, whereas PCR products were digested overnight if the restriction sites were close to the end of a DNA fragment.

Restriction enzymes were removed from vector DNA and DNA fragments either by gel extraction or precipitation by 3M sodium acetate pH 4.8 and ethanol solution. The Vector DNA for cloning was dephosphorylated with alkaline phosphatase (Fermentas) after digestion with restriction endonuclease enzymes to prevent self-ligation of the linearised vector. Alkaline phosphatase hydrolyzes 5'-monophosphate groups from DNA and RNA and also 5'-diphosphate and 5'-triphosphate groups from RNA. Thus, the vector DNA cannot ligate with itself or form concatemers as 5'-terminal phosphate groups are required for ligation. Dephosphorylation of vector DNA was performed in the manufacturer's buffer in 20µl final volume with 2 units of alkaline phosphatase at 37°C for 1 hour.

DNA Ligation.

DNA fragments were inserted into linearised vectors for cloning by joining the compatible ends of the double-stranded DNA with T4 DNA ligase (Thermo scientific). T4 DNA ligase catalyzes the formation of phosphodiester bonds between neighbouring 3'-hydroxyl and 5'-phosphate ends in double-stranded DNA and also repairs single-stranded nicks in double-stranded DNA.

About 100ng of total DNA with a molar vector:insert ratio of 1:3 were used in one reaction. The following equation was used to calculate the appropriate amounts of DNA.

$$mass_{insert}[ng] = \frac{mass_{vector}[ng] \times size_{insert}[bp]}{size_{vector}[bp]} \times 3$$

2. 5. Gene transfer methods

2. 5. 1. Preparation of Ultra-competent cells

A single colony of *E coli* DH5α was taken from 12-18 hr old plate, inoculated into 10 ml of LB broth and incubated at 37°C with vigorous shaking at 200 rpm. Around 2.5ml of this culture was inoculated into 250ml of LB broth and incubated at 18-22°C for 20 hr with moderate shaking. The culture was allowed to grow till the culture density reaches to 0.5 when measured at 600 nm. Cells from these cultures was harvested by centrifuging at 5500 rpm for 10 min at 4°C and washed with 80ml of sterile ice cold Inoue transformation buffer (55mM MnCl₂.4H₂O, 15mM CaCl₂.2H₂O, 250mM KCl, 10mM PIPES, pH 6.7).

Finally the cell pellet was resuspended in 20ml of ice cold Inoue transformation buffer along with 1.5ml of DMSO and kept on ice for 10 minutes. Working quickly, the cell suspension was distributed into 100µl aliquots in chilled sterile micro-centrifuge tubes and immediately snap-freezed in a bath of liquid nitrogen and stored at -80°C until further use.

2. 5. 2. Transformation

The frozen competent cells were thawed by placing them on ice bath. The ligation mixture/plasmid of interest was added and incubated on ice for 30 minutes. After 30 minutes, the cells were subjected to heat shock at 42°C for exactly 1 min 30 sec and immediately chilled on ice for 2 min. Further, 750µl of LB broth was added and incubated at 37°C for 45 min. The cells were collected by centrifugation and resuspended in 70µl of LB broth and plated on required selective LB media. When needed 2% X-gal and 1mM IPTG was added along with required antibiotic. The plates were then incubated at 37°C for more than 12h for colonies to appear.

2. 5. 3. Electroporation

Electro-competent cells were prepared by taking 10ml of mid log phase culture and harvested at 6500 rpm at 4°C for 5min and washed two to three times with cold 10% glycerol and finally resuspend the cells in 100μl of 10% glycerol. About 1 to 2μg of DNA was added to 100μl of electro-competent cells. The suspension was mixed by flicking the tube. The cells/DNA mixture was placed in a pre-chilled cuvette, between the electrodes and a pulse of 2.5 kV was applied for 4.5 sec using Genepulser (Bio-Rad, USA). Following the pulse, immediately 1 ml of SOC medium was added to the cells (SOC: 2% tryptone, 0.5% yeast extract, 1mM NaCl, 2.5mM KCl, 1mM MgCl₂, 10mM MgSO₄, 20mM glucose). The cells mixed in the broth were taken in a 1.5ml tube and incubated at 37°C for 1 hour with constant shaking. After the incubation period, the cells were diluted appropriately in SOC medium and plated on LB agar plates containing appropriate antibiotics.

2. 6. Protein Methods

2. 6. 1. Solutions for SDS-Polyacrylamide Gel electrophoresis

Acrylamide mix Solution: A 30% stock solution of Acrylamide was prepared by mixing 30 g of acrylamide and 0.8gm of N, N'- methylene-bis-acrylamide in 70ml of MilliQ water for overnight, till the contents were dissolved completely and finally made up to 100ml and stored at 4°C.

Resolving gel buffer: 18.17gm of Tris base was dissolved in 80ml of milliQ water and pH of the solution was adjusted to 8.8 by adding 3ml of conc. HCl. Finally the volume of the buffer solution was made up to 100ml using deionized water, autoclaved for 20 minutes at 15psi (1.05kg/cm2) on liquid cycle. To the above solution 0.3% of SDS was added and stored at room temperature. When required the stock was added to the gel components to get a final concentration of 390mM Tris-HCl, pH 8.8.

Stacking gel buffer for SDS-PAGE: 12.14gm of Tris base was dissolved in 80ml of milliQ water and the pH of the solution was adjusted to 6.8 by adding 4.2ml of conc. HCl and finally the volume of the buffer was made up to 100ml with milliQ water. This solution was autoclaved. To the above solution 0.4% of SDS was added and stored at room temperature. When required the stock was added to the gel components to get a final concentration of 130mM Tris-HCl, pH 6.8.

Tris glycine electrophoresis buffer (pH 8.3): 10x stock solution of Tris glycine buffer was prepared by mixing 30gm of Tris base, 140gm of Glycine (electrophoresis grade) and 10gm of SDS in 1litre of double distilled water and stored at room temperature. For running SDS-PAGE, 1x Tris glycine buffer containing 25mM Tris base, 250mM Glycine, and 0.1% SDS was used.

2x SDS gel loading buffer: 2x stock solution of SDS loading buffer was prepared by mixing 1ml of 1M Tris-Cl pH 6.8, 2gm SDS, 10mg of bromophenol blue and 10ml of glycerol in 25ml of milliQ water and kept at 45°C for 10 min for complete solubilization of SDS. To this reagent 0.699ml of β -Mercaptoethanol was added and finally made up to 50ml with milliQ water. 10ml aliquots of this buffer were distributed and stored at -20°C. For running protein samples on SDS-PAGE, equal volume of this buffer was added to the protein sample, boiled for 5 min and loaded on to the gel.

Staining solution: 0.25gm of coomassie brilliant blue R-250 was dissolved in 50ml of methanol. To this solution 15ml of acetic acid was added and finally made up to 100ml using double distilled water. The contents were filtered and stored at room temperature in dark brown color bottle until further use.

Destaining solution: 30ml of methanol is mixed with 10ml of glacial acetic acid before making up the volume to 100ml using double distilled water. The prepared solution used once to destain the PAGE gels. Gels can be stored in 7% acetic acid solution.

Colloidal coomassie Staining:

Fixative: To fix the gel 40ml of ethanol, 10ml of acetic acid and 50ml of double distilled water were mixed and used immediately.

Dye stock solution: 18.81ml of *ortho*-phosphoric acid and 100g of ammonium sulphate were completely dissolved in 800ml of water, to this 1gm of coomassie brilliant blue G-250 was added while stirring and made up to 1litre and kept for stirring for 24h.

Dye working solution: To 4 parts of stock solution 1 part of methanol was added while stirring and used immediately.

De-staining solution: 1% (v/v) acetic acid was used for destaining 2D gels.

2. 6. 2. Solutions for Protein Estimation

Standard BSA: A 10mg/ml stock solution of BSA (Bovine serum albumin) was prepared by dissolving 10mg of BSA in 0.17M NaCl. This solution was store at -20°C. When required 1mg/ml BSA working solution was prepared and used for the construction of standard graph.

Bradford's reagent: To prepare Bradford's reagent 10mg of coomassie brilliant blue G-250 powder was dissolved in 50ml of 95% ethanol, to this 10ml of 85% (w/v) *ortho*-phosphoric acid was added. After complete solubilization of the dye the solution was made up to 100ml with milliQ water. Finally the reagent was filtered and stored in amber colour bottle at 4°C for 3 months.

2. 6. 3. Solutions for Western Blotting

Towbin buffer (protein transfer buffer): 3.03gm of Tris-base and 14.4gm of glycine was dissolved in 500ml of distilled water. To this 200ml of methanol was added and final volume was made up to 1000ml with double distilled water.

TBST Buffer: (washing buffer): 20ml of 1M Tris-HCI (pH 7.6), 8gm of sodium chloride and 1 ml of Tween-20 were dissolved in 800ml of double distilled water and finally made up to 1litre.

Blocking Reagent: 10% solution of skimmed milk powder prepared in TBST was used for blocking PVDF membrane.

Membrane stripping solution: Membrane stripping solution was prepared by dissolving 1.5gm of glycine, 0.1gm of SDS and 1ml of tween 20 in 100ml of double distilled water. The solution pH was adjusted to 2.2 with 6N HCI.

Ponceau S reagent: 100mg of ponceau salt was dissolved in 100ml of 5% acetic acid.

2. 6. 4. Protein estimation by Bradford's assay

Protein standard graph was prepared using 2, 4, 6, 8, 10 µg's of BSA in 10µl of solution and adding 990µl of Bradford's reagent. The mixture was incubated in dark for 10 minutes. OD at 595nm was read and a standard graph was prepared. The amount of protein in sample was assayed as described earlier and the protein concentration was estimated with appropriate blanks.

2. 6. 5. Protein Precipitation

The protein sample was mixed with two times the sample volume of methanol, one sample volume of chloroform and three times the sample volume of deionized, ultrapure water. The precipitated sample was spun down at 13000 rpm for 5 min and the upper layer was discarded. The sample was washed with three sample volumes of methanol and spun down at 13000 rpm for 5 min. The supernatant was carefully removed and the pellet was dried in air. The protein pellet was finally resuspended in 2x Laemmli buffer or any other buffer of choice.

2. 6. 6. Poly Acrylamide Gel Electrophoresis

SDS-PAGE

The protein samples were separated by SDS-Polyacrylamide gel electrophoresis following the procedures of Laemmli (1970). SDS-PAGE gels were prepared using Mini-PROTEAN II System (Bio-Rad) by clamping the spacer plate and the short plate into the casting frame and fitting the whole assembly into the casting stand. The resolving gel was prepared and poured between the two glass plates to approximately 2 cm below the top edge of the short plate. The resolving gel was covered with water saturated *n*-Butanol and left to polymerise. After polymerisation of the resolving gel butanol was removed by repeated washing and the traces of water were removed by wiping with filter paper and the stacking gel was poured on top of the resolving gel to the top edge of the short plate. A required size of a comb was inserted immediately to create wells in the stacking gel and it was allowed to polymerize for 10 minutes. After 10 minutes the comb was removed and the wells were washed with

double distilled water. The polymerised gels between the glass plates were placed into the buffer tank with the electrode assembly and the buffer tank was filled with SDS-PAGE running buffer. The protein samples were mixed with equal volumes of 2x sample loading buffer and kept in a boiling water bath for 5 minutes. The contents were then briefly centrifuged before loading the sample into the wells. The electrophoresis was performed at 100 volts till the tracking dye reached the anode end of the gel. The gel was removed from the glass plates and the protein bands were stained with staining solution for 30 min to 1h. The gel was then destained by using destaining solution.

Table 2. E: Composition of the resolving gel for SDS-PAGE

Solution	12.5% for 5 ml	15% for 5 ml
H ₂ O	1.7 ml	1.25 ml
Resolving Buffer (pH 8.8)	1.25 ml	1.25 ml
Acrylamide mix (30%)	2 ml	2.5 ml
APS (10%)	50 μl	50 μl
TEMED	5 μl	5 μl

Table 2. F: Composition of the stacking gel for SDS-PAGE

Solutions	7.5% for 2.5 ml
H ₂ O	1.25 ml
Stacking gel Buffer (pH 6.8)	0.625 ml
Acrylamide mix (30%)	0.625 ml
APS (10%)	25 μl
TEMED	2.5 μl

2. 6. 7. Semi-Dry Western Blotting

After protein samples were separated by SDS-PAGE, the gel was soaked in Towbin buffer for 5 minutes. Meanwhile, PVDF membrane (Amersham Hybond-ECL, GE healthcare) and four filter papers were cut to the size of the gel and soaked separately in Towbin buffer for 10 min. Two layers of filter paper were placed on the positive electrode

of the transfer apparatus and the transfer membrane and the gel were sandwiched between two additional layers of filter paper on top. The transfer membrane was facing the negative electrode at the bottom of the transfer apparatus, while the gel was placed on top. The apparatus was assembled according to the instructions by the manufacturer and the transfer was performed at 18V for 40 minutes in the transfer apparatus.

After transfer of the proteins, the membrane was blocked in 10% skimmed milk suspension in TBST at room temperature for an hour, or at 4°C overnight, with shaking at 60 rpm. After blocking, the membrane was incubated with the primary antibody solution at the appropriate dilution for 1h at room temperature with gentle shaking. The membrane was washed 3 times with TBST for 10 minutes and, if appropriate, incubated with the secondary antibody at the correct dilution for 1 hour with shaking. The membrane was finally washed three to five times with TBST.

The secondary antibody was conjugated to horse radish peroxidase (HRP), which catalyses the oxidation of luminol in presence of H₂O₂ resulting in a chemiluminescence reaction which is enhanced by *p*-coumaric acid. This was used to detect antibody-coupled HRP, which was indirectly bound to the target protein on the membrane. Immunoreactive protein bands were detected using ECL Western Blotting detection reagent and chemiluminescent bands were exposed to hybond imaging film (GE healthcare), which was developed in the dark room or the chemiluminescence was captured using Kodak image station.

2. 7. Subcellular fractionation

Arctic express cells were transformed with expression plasmid coding for a gene of interest. These cells were grown in 50ml LB containing appropriate antibiotics at 37°C till mid log phase with shaking 180 rpm. Cells were induced with 1mM IPTG and incubated at 18°C for 12h. The cells were harvested by centrifugation at 6500 rpm for 10 min. Cells were harvested from the culture medium and washed once in 20mM Tris-Cl pH 8.0. Finally the cells were resuspended as 1gm in 7 ml 20 mM Tris pH 8.0, 150 mM NaCl and 5% glycerol containing 1 mM PMSF and lysed by sonication. Cell debries and unbroken cells from the lysate were removed by centrifuging at 15000 rpm for 30 min. The clear supernatant obtained was then subjected to ultra-centrifugation for 40,000 rpm for 1h 20 min (Optima™ MAX-XP tabletop ultracentrifuge, Beckman coulter). Membrane fraction obtained in the pellet fraction was separated and resuspended in the same volume of 20mM

Tris-Cl pH 8.0 buffer. The purity of the membrane was assessed by assaying marker enzymes assay.

2. 8. Enzyme Assays and Preparation of reagents

2. 8. 1. Reagents for Glucose-6-phosphate dehydrogenase assay

Glycylglycine buffer (250mM, pH 7.4): Glycylglycine buffer was prepared by dissolving 3.03 gm of Glycylglycine free base in 70ml of deionized water and the pH of the solution was adjusted to 7.4 with 1M NaOH and finally the volume was made up to 100ml with deionized water. The solution was stored at RT until further use.

D-Glucose-6-Phosphate Solution (60mM): D-Glucose-6-Phosphate solution was prepared by dissolving 0.04gm of D-glucose-6-phosphate in 2ml of milliQ water and stored at -20°C until further use.

NADP solution (20mM): NADP solution was prepared by dissolving 297mg of Nicotinamide Adenine Dinucleotide Phosphate in 20ml of milliQ water and the solution was kept at -20°C until further use.

Magnesium Chloride (**300mM**): 0.121gm of Magnesium Chloride was dissolved in 2ml of deionized water and stored at 4°C until further use.

2. 8. 2. Reagents for Nitrate reductase assay

Methyl viologen: Methyl viologen solution was prepared by dissolving 50mg of sodium hydrosulfite in 10ml of 0.01M NaOH and 4% sulfanilamide containing 25% HCl. The contents were mixed with 0.08% N-(1-Napthyl) ethylene diamine dihydrochloride. The solution can be stored at 4°C until further use.

0.1M potassium nitrate: 1.01gm of potassium nitrate was dissolved in few ml of double distilled water and the volume of the contents were made up to 100ml with double distilled water to get 0.1M of potassium nitrate.

0.1M phosphate buffer (pH 7.2): 1.74gm of K₂HPO₄ and 13.6gm KH₂PO₄ of were dissolved in 700ml of double distilled water and the pH of the buffer was adjusted to 7.2 with acetic acid, and final volume was made up to 100ml with milliQ water.

2. 8. 3. Reagents for β-galactosidase assay

Z buffer: Solution prepared by dissolving 40mM Na₂HPO4, 60mM NaH₂PO4, 10mM KCl, 1mM MgSO₄ and 50mM β -mercaptoethanol pH 7.0. This solution stored at 4°C until further use.

Substrate solution: ONPG (*ortho*-Nitrophenyl β-galactoside) solution: About 400mg of ONPG was dissolved in 100ml of phosphate buffer prepared by dissolving (Na₂HPO₄.7H₂O (1.61gm) and NaH₂PO₄.H₂O (0.55gm) in 90ml milliQ water (pH 7.0). This solution transferred to an amber colour bottle and stored at 4° C until further use.

Stop solution: 1M sodium carbonate was prepared by dissolving 12.4gm of sodium carbonate in 100ml of milliQ water. The solution was stored at room temperature.

2. 8. 4. Reagents for Methyl parathion activity

CHES buffer: 200mM CHES, pH 9.0 was prepared by adding 4.15gm CHES to 80ml double distilled water & the pH was adjusted to 9.0 with NaOH. The solution was made up to 100ml total volume with double distilled water and autoclaved.

Substrate solution: Stock solution of methyl parathion was prepared by dissolving 26.3mg in 1ml of methanol to get 0.1M concentration and the stock solution was stored at 4° C until further use. Whenever needed for parathion hydrolase enzyme assay 200 μ M of methyl parathion was used from the stock solution.

Assay Buffer: Contains 20mM CHES, pH 9.0 and 50µM CoCl₂.

2. 8. 5. Glucose-6-phosphate dehydrogenase (G6PD) - Cytoplasmic marker

Glucose-6-phosphate dehydrogenase was used as a cytoplasmic marker enzyme. Subcellular fractions were assayed for G6PD activity by monitoring glucose-6-phosphate dependent reduction of NADP at 340nm. The assay was performed at 37°C in Tris buffer (50mM Tris–HCl pH 7.5) containing 250mM NADP⁺. The reaction was initiated by addition of 12.5mM glucose-6-phosphate (Sargent *et al.*, 1998). The specific activity was calculated using the formulae given below.

Activity =
$$\frac{(\Delta A_{340} \text{ nm/min Test} - \Delta A_{340} \text{ nm/min Blank}) (3) (df)}{(6.22) (0.1)}$$

Where.

3 = Total volume (in milliliters) of assay

df = Dilution factor

6.22 = Milli molar extinction coefficient of β-NADPH at 340nm

0.1 = Volume (in milliliters) of enzyme used

2. 8. 6. Nitrate reductase -Membrane Enzyme

The assay of nitrate reductase was done by following the method described by Michael & Showe, 1968. The assay was initiated by pre-incubating the subcellular fractions for 5 min at 37°C in a 2.4ml volume of the reaction mixture containing 0.1M phosphate buffer (pH 7.2), 0.1M potassium nitrate, and 10⁻⁴M methyl viologen. Before starting the reaction, 50mg of sodium hydrosulfite was dissolved by mixing gently in a 10ml of 0.01M NaOH solution and the reaction was started by adding 0.1ml of sodium hydroxide solution to the reaction mixture. After 10 minutes, the reaction was stopped by shaking the tube to oxidize the remaining hydrosulfite and reduced methyl viologen. To determine nitrite, 0.75ml of sulfanilamide solution prepared by mixing two parts of 4% sulfanilamide in 25% HCl solution with one part of 0.08% N-(1-Napthyl) ethylene diamine dihydrochloride was added to 2.5ml reaction mixture. After 10 min, the absorbance of the reaction mixture was read at 540nm. One unit of enzyme is defined as the amount of enzyme required to convert 1μmole of nitrate to nitrite in 10min. Specific activity is defined as enzyme units per microgram of protein. The specific activity of nitrate reductase was calculated using the following formulae.

$$\textbf{Activity} = \frac{ \text{(OD of the Test at A}_{540} \text{ nm) x df x 1000} }{ \text{mg of protein from subcellular fraction x time in minutes (10 min) x OD of }$$

mg of protein from subcellular fraction x time in minutes (10 min) x OD of the standard (A_{540} nm/ μ mol).

2. 8. 7. β-galactosidase activity

The β -galactosidase activity was performed by following the protocol described by Miller, 1972. About 500µl of culture was withdrawn from the 10ml culture flask and cells were harvested by centrifuging at 6000 rpm for 10 minutes. Then supernatant was carefully discarded and bacterial cell pellet was resuspended in same volume of chilled Z buffer. The cells were permeabilized by adding 100µl of choloroform, 50µl of 0.1% SDS and mix the cells by vortex and kept at 28°C for 5 min After brief incubation at 28°C, the volume of the above reaction mixture was made up to 1ml using Z-buffer. In order to initiate the reaction 0.2ml of ONPG (4mg/ml) was added to the cell suspension. The samples were incubated at 28°C until the faint yellow color is developed. The reaction was stopped by adding 0.5ml of 1M Na₂CO₃. The time length of incubation was recorded. The reaction mixture was then centrifuged at 13000 rpm for 1 min and 1ml of clear supernatant was taken to check the

absorbance at 420nm and 550nm. The β -galactosidase activity was measured by monitoring the release of *ortho*-nitrophenol (yellow color) from substrate ONPG. The β -galactosidase activity levels were calculated using the formula given below and the specific activity was represented as Miller units.

Miller Units =
$$1\underline{000x [(OD_{420}-1.75xOD_{550})]}$$

 $TxVxOD_{600}$

Where,

T = time elapsed between ONPG added and addition of Na₂CO₃ solution in minutes

V = volume of the culture added to the reaction mixture

A600 = OD of the culture at 600nm

A420 = OD of the reaction mixture at 420nm

2. 8. 8. Parathion Hydrolase Assay

A spectrophotometric assay was adapted to determine organophosphate hydrolase (OPH) activity. The reaction was carried out in the eppendorf tubes containing 200 μ M of methyl parathion in 1ml of 20mM CHES buffer (pH 9.0). The reaction was started by adding one of the components such as crude extract or cytoplasmic and membrane fractions as source of OPH. The tubes were incubated at 37 0 C for 30 minutes. An increase in the absorbance at 410nm due to formation of p-nitrophenol was determined (Chaudhry *et al.*, 1988). The concentration of p-nitrophenol formed in the reaction was determined using the extinction coefficient of PNP (17500/M/cm). The specific activity of the enzyme was expressed as micromoles of PNP produced per milligram of OPH protein per minute. The specific activity of the enzyme was calculated using the formula given below.

Specific activity = Enzyme activity/mg of protein /min

Identification of proteins co-purified with OPH

3. 1. Objective specific methodology

3. 1. 1. Immuno-purification of membrane associated OPH complex

Affinity purification of membrane associated OPH complex was performed by two independent methods. One of them was by using metal-ion affinity purification and the strategy followed was described elsewhere (Parthasarathy *et al.*, 2016). In order to gain accuracy in composition of OPH associated proteins an independent method was developed using anti-OPH antibodies.

3. 1. 2. Generation of Affinity column with anti-OPH antibodies.

3. 1. 3. Enrichment of OPH antibodies

Initially antibodies were generated against purified OPH using New Zealand white rabbits following standard procedures (Cooper & Patterson, 2008). The serum containing polyclonal antibodies against recombinant OPH was used to purify OPH-specific antibodies. Before proceeding for purification OPH specific antibodies, pure OPH protein (10mg) used as ligand was dissolved in 2ml coupling buffer, 0.1M NaHCO₃ pH 8.3 containing 0.5M NaCl. After dissolving OPH protein in coupling buffer about 500 μ l of CNBr-activated SepharoseTM 4B (GE Healthcare) was added and the contents were kept at room temperature for 1h with head to head rotation to complete coupling process of OPH to CNBr-activated Sepharose. The contents were then transferred into a column (i.d x H: 0.7 × 2.5 cm) and washed with 5 column volumes of coupling buffer to remove unbound OPH. After washing the column, the coupled OPH-CNBr Sepharose was incubated with 0.1M Tris-HCl buffer, pH 8.0 for 2h to block any remaining active groups of CNBr Sepharose. The column was then washed 4 times with alternatively with one column volumes of 0.1M sodium acetate buffer pH 4.0, 0.5M NaCl followed by 0.1M Tris-HCl pH 8.0, 0.5M NaCl. The OPH-Sepharose column thus prepared was used to purify OPH-specific antibodies.

The OPH antisera was passed through the OPH-coupled Sepharose column at a flow rate of 0.5 ml per minute. The flow-through was collected and reloaded onto the column to ensure complete binding of OPH-specific antibodies to the column. The nonspecific antibodies and serum proteins were removed by washing the column with three column volumes of wash buffer (20mM Tris-HCl, pH 7.6). The bound anti-OPH antibodies were eluted (0.1M glycine-HCl, pH 2.5) as 1ml fractions into pre-chilled tubes containing 50µl of 2M Tris-HCl, pH 9.0 to ensure quick neutralization of the eluate. The antibody fractions were then

pooled and dialyzed against coupling buffer (10mM sodium phosphate, pH 7.2, 150mM NaCl).

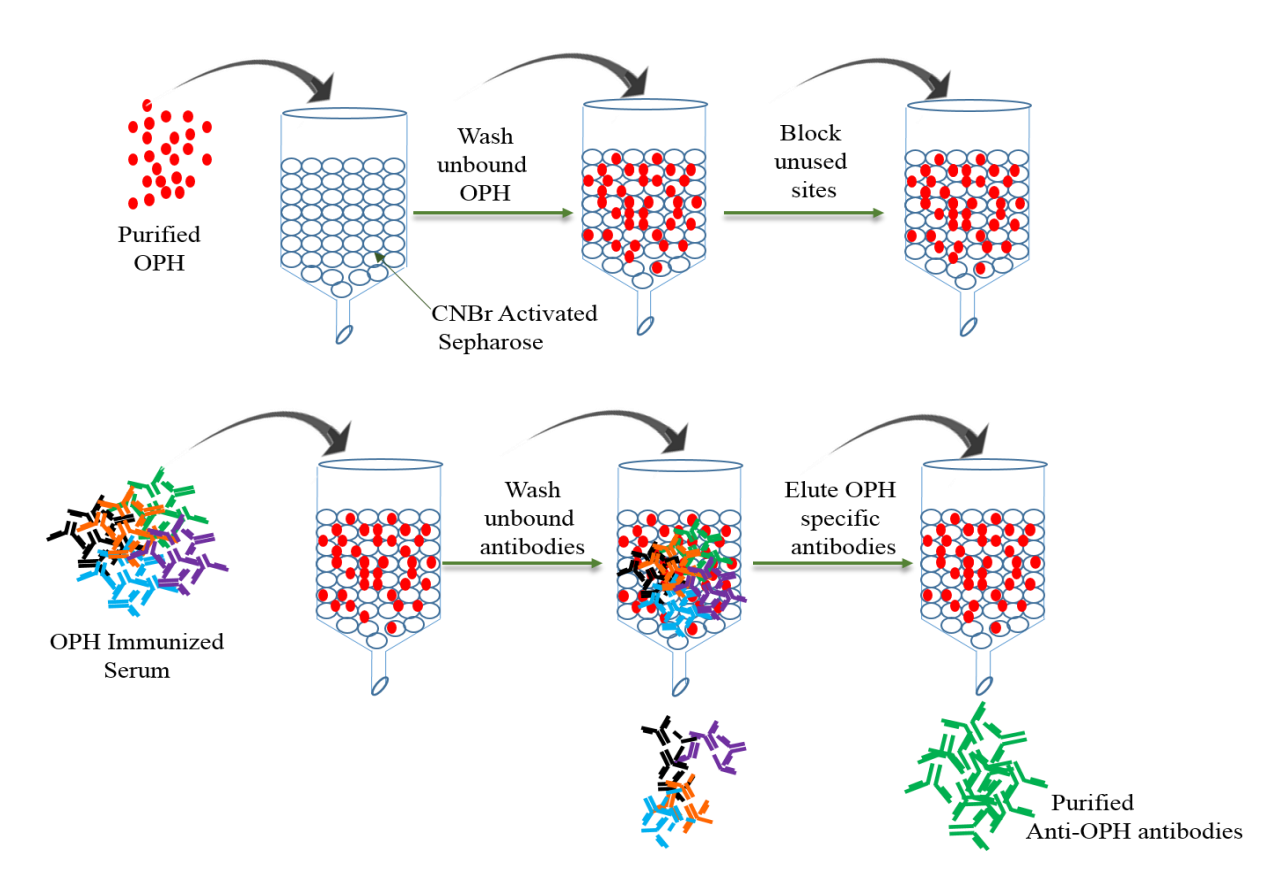


Fig. 3. 1. Schematic diagram showing enrichment of anti-OPH antibodies.

3. 1. 4. Preparation of Protein A/G-Anti-OPH antibody column:

While generation anti-OPH antibody column approximately 1.5mg of purified anti-OPH antibodies were mixed with 750µl of protein A/G-agarose plus beads (Thermo Scientific) and equilibrated with coupling buffer (10mM Sodium phosphate, pH 7.2, 150mM NaCl). The contents were kept for 1hour at 4°C with gentle shaking and applied on to a column. The unbound antibodies were removed by washing the column with three column volumes of coupling buffer. The anti-OPH antibodies bound to protein A/G-agarose beads were covalently linked by adding one column void volume of cross-linking buffer containing 10mM Sodium phosphate, pH 7.2, 150mM NaCl and 2.5mM disuccinimidyl suberate (DSS). The column was left for one hour at room temperature to complete cross-reaction and the excess DSS were quenched by washing the column with 25mM Tris-HCl, pH 7.6. The OPH-antibody cross-linked protein-A/G agarose beads were then taken into a clean tube and suspended in 1 ml of pre-chilled binding buffer (20mM Tris-HCl, pH 7.6, 150mM

NaCl, 2% glycerol). The generated anti-OPH antibody column stored at 4°C until further use.

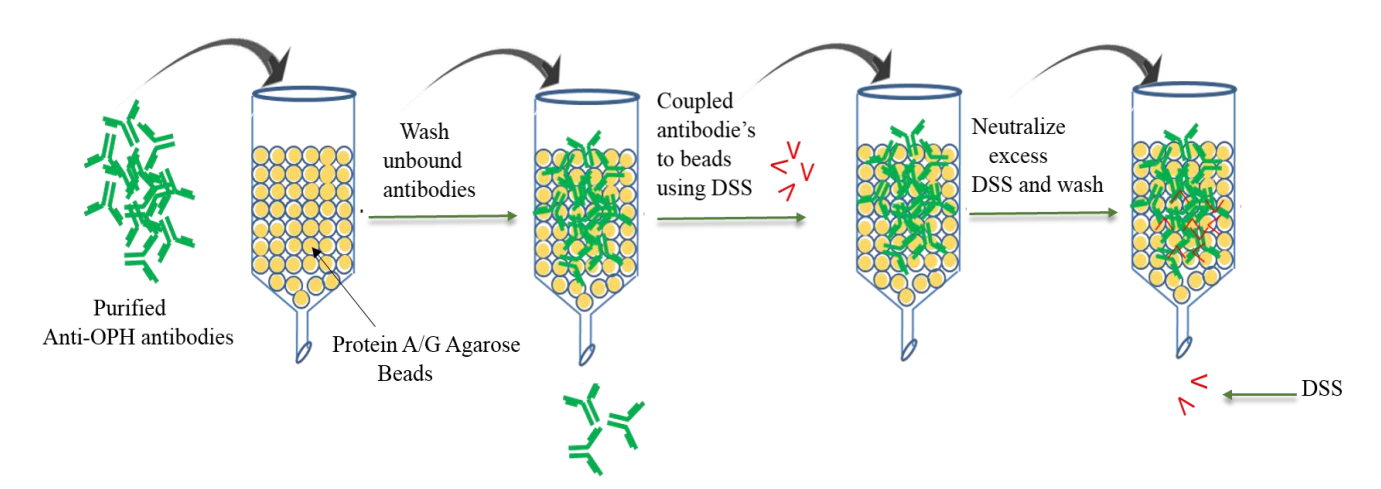


Fig. 3. 2. Diagrammatic representation of various events involved in generation of anti-OPH antibody affinity column.

3. 1. 5. Isolation of Membrane

Sphingobium fuliginis ATCC 27551 was grown in 2 litre LB broth containing PolymyxinB (10µg/ml) at 30°C with vigorous shaking till the culture density was reached to mid log phase (0.5 OD). Cells were harvested from the culture medium and washed once in 20mM Sodium phosphate buffer (SPB) pH 7.4. Finally, 1gm of cell pellet was resuspended in 10ml of 20mM of SPB pH 7.4 having 5% glycerol and 150mM NaCl. Formaldehyde (250µl) solution was added to the cell suspension and incubated at RT with a head to head rotation for 10-20 min to establish crosslinking among closely associated proteins (Sutherland et al., 2008). After incubation the reaction was stopped by adding 3ml of 1M glycine. After crosslinking the cell suspension was centrifuged at 6500 rpm for 10 min to remove excess amount of cross linker and glycine and the cell pellet was washed twice with 10ml of 20mM sodium phosphate buffer pH 7.4 having 150mM NaCl, 5% glycerol. Finally, the pellet was resuspended in 20mM sodium phosphate buffer pH 7.4 having 150mM NaCl, 5% glycerol. The contents were mixed with PMSF (1mM) (phenylmethylsulfonyl fluoride) and protease inhibitor cocktail (250µl/1gm cell pellet). The cells were lysed by sonication (10 cycles of 20 sec ON and 40 sec OFF) the cell debris and unbroken cells were removed by centrifuging the cell lysate at 15,000 rpm for 30 minutes. The clear supernatant obtained was then subjected to ultracentrifugation at 40,000 rpm for 1 hour 20 min to sediment membrane. The obtained membrane fraction was washed with 10ml of 20mM SPB pH 7. 4 having 150mM NaCl, 5% glycerol to remove cytoplasmic contaminants.

Finally the marker enzyme assays were performed to check the purity of the obtained membrane and cytoplasmic fractions. Described in general methods section. Glucose-6-phosphate dehydrogenase (G6PD) and nitrate reductase were used as cytoplasmic and membrane marker enzymes and measured their activity to ascertain their purity.

3. 1. 6. Membrane Solubilization

The obtained membrane pellet was suspended in 10ml of 20mM sodium phosphate buffer pH 7. 4. (150mM NaCl, 5% glycerol). After suspension the amount of protein present in membrane fraction was estimated and the isolated membrane was dissolved by adding DDM (n-dodecyl β-D-maltoside) to a final concentration of 10mg of DDM/5mg of protein. Membrane proteins were solubilized by incubating the contents at 4°C for 1hr with a constant rotation. The solubilized membrane fraction was centrifuged 40,000 rpm for 1 hour to remove lipids and protein aggregates. The clear supernatant containing dissolved membrane proteins were taken for further purification. The protein concentration and OPH activity were assayed both in the pellet and supernatant fractions and the process was repeated till the complete OPH activity is found in supernatant fraction. The obtained solubilized membrane fraction (5mg/ml) was incubated with anti-OPH antibodies coupled A/G agarose beads and left overnight with head-to-head rotation at 4°C. After incubation the contents were centrifuged at 3000g to sediment anti-OPH protein A/G agarose beads. The beads were washed 3-4 times with 20mM SPB pH 7.4, (150mM NaCl, 5% glycerol) and the bound OPH was eluted by 1ml of 0.1M glycine-HCl pH 2.2. The eluted OPH was immediately neutralized by adding 100µl of 100mM Tris-HCl pH 9.0. The eluted fractions were concentrated by using amicon centrifugal filter unit (10kDa cut off) (Merck, India) and analysed on BN-PAGE and the purified OPH complex was precipitated by adding 250µl of ice cold (1:0.5) methanol/chloroform and proteins were analysed on Tricine SDS-PAGE.

3. 1. 7. Blue Native –PAGE (BN-PAGE)

Blue Native PAGE was performed to further ascertain the molecular weight of the complex. The OPH complex was purified by using the protocol described earlier. Blue Native PAGE (BN-PAGE) was performed to separate proteins under non denaturing conditions (Schagger *et al.*, 1991, 1994 & Schagger, 2001). BN-PAGE gels 4-16% precast gels (Native PAGE Bis-Tris gel system) were procured from Life technologies. The gels were assembled as per manufacturer's instructions and were placed into the buffer tank with the electrode assembly and the buffer tank was filled initially with cathode buffer B. Prior to

loading, protein samples were mixed with the BN-PAGE sample buffer. The protein samples were loaded into the wells of the stacking gel and a molecular weight standard (HMW Native Marker Kit, GE healthcare) was loaded into wells next to the samples. Electrophoresis was performed in accordance with the described protocol i.e., 100V for 0.5h, 200v for 0.5h, the cathode buffer B (50mM Tricine, 15mM Bis-Tris pH 7.0, 0.02% Serva blue) was removed and replaced with a fresh cathode buffer B10 (50mM Tricine, 15mM Bis-Tris pH 7.0, 0.002% Serva blue) and set at 250V for 0.5h. Finally the cathode buffer B10 was removed and replaced with fresh cathode buffer (50mM Tricine, 15mM Bis-Tris pH 7.0) and electrophoresis was performed by setting voltage at 300V for 0.5h. The gels were initially destained to remove the excess SERVA Blue G dye and later were stained using the colloidal coomassie staining protocol. The gel image was scanned and the molecular weight of the complex was calculated by using the Firereader V4 image analysis software, UVItech ltd, Cambridge.

3. 1. 8. Tricine SDS-PAGE

Tricine-SDS PAGE was performed according to the protocol described elsewhere (Schagger *et al.*, 2006). A gradient Tricine-SDS PAGE containing 10% to 16% resolving gel and 4% stacking gel was prepared by using stock solution containing 48% of acrylamide, 1.5% bis-acrylamide in 3x gel buffer (3M Tris HCl, 0.3% SDS, pH 8.45) glycerol (10%) was used in preparation of resolving gel. After polymerization, the gels were placed into the buffer tank with the electrode assembly and filled initially with cathode buffer containing 100mM Tris-HCl, 100mM Tricine, and 0.1% SDS, pH 8.25. The protein samples were loaded into the wells of the stacking gel along with a molecular weight marker. After loading the samples, the tank was filled with anode buffer containing 100mM Tris-HCl, pH 8.9. The whole electrophoretic setup was maintained at 4°C and running conditions were maintained at a voltage of 50V. The gel was fixed using 50% methanol, 10% acetic acid; stained and visualized using Proteo Silver, silver stain kit (Sigma-Aldrich, India).

3. 1. 9. Identification of interacting partners by Mass Spectrometry

After visualizing the proteins with silver stain, enriched protein bands were carefully excised manually by using sterile scalpel blade from the gel and the gel pieces were destained with a solution of 1% K₃ [Fe (CN)₆] with 1.6% Na₂S₂O₃, dried with acetonitrile (ACN) and reduced with dithiothreitol (DTT) in 25mM NH₄HCO₃ for 1h at 50°C, alkylated using a 55mM iodoacetamide in 25mM NH₄HCO₃ for 45min at room temperature. The gel

pieces were dehydrated with ACN, rehydrated with a minimum volume of 50mM NH₄HCO₃ containing Trypsin (10ng/μl), and digested at 37°C for 16h. The peptides were extracted twice with 50% (v/v) acetonitrile containing 1% (v/v) TFA. The obtained peptide mixture was dried using vacuum concentrator (Eppendorf) for 1 hr at room temperature. The tryptic peptides were dissolved in 2μl solution of 50% (v/v) ACN containing 1% (v/v) TFA and mixed with 2μl of 1% cyano-4-hydroxycinnamic acid (HCCA) dissolved in 50% ACN and 1% TFA and 1μl of it was applied on the MALDI target plate. Peptides were analysed using MALDI TOF / TOF Autoflex (Bruker Daltonics) in reflectron mode. MS/MS of selected peptides were performed by MALDI LIFT TOF/TOF and the spectra were calibrated by Pepmix (Bruker Daltonics).

3. 2. Results and Discussion

3. 2. 1. Purified OPH complex from membrane of Sphingobium fuliginis

The inner membrane of *Sphingobium fuliginis* was isolated and checked the purity of the membrane by performing marker enzyme assay as described in general methods section. The membrane fraction has showed higher nitrate reductase activity, and the activity of G-6-phosphate dehydrogenase (G6PD), which was used as cytoplasmic marker enzyme was found to be almost negligible (Fig. 3. 3). These marker enzyme assays revealed that the isolated membrane fraction was pure.

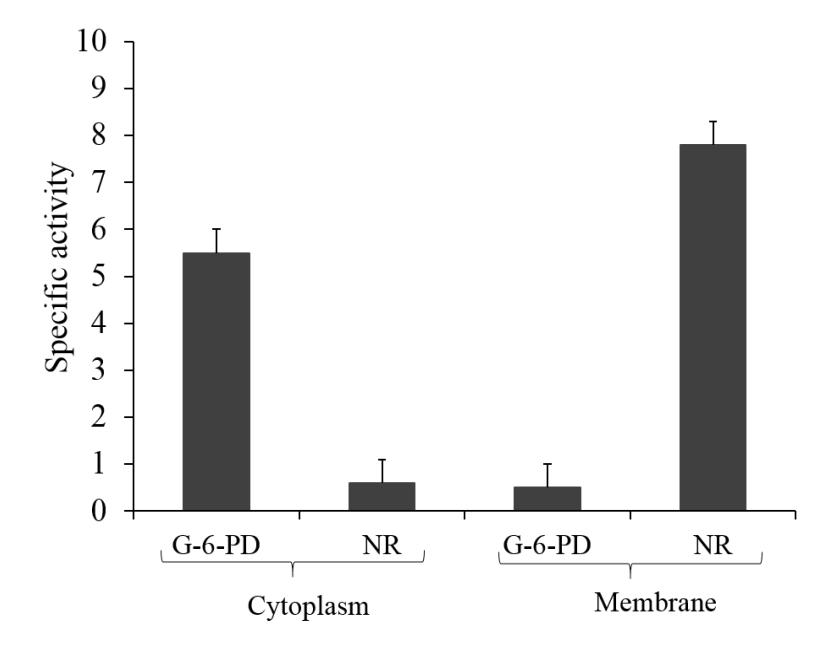


Fig. 3. 3. Shows the activities of glucose-6-phosphate dehydrogenase (G-6-PD) and nitrate reductase (NR) in the cytosolic and membrane fractions of *Sphingobium fuliginis*. The G-6-PD and NR were used as cytoplasmic and membrane specific enzymes respectively.

The isolated inner membrane of Sphingobium fuliginis was solubilized using various detergents. Though non-ionic detergents like Triton X-100, Triton X-114, solubilized most of the membrane associated OPH, the n-Dodecyl β-D-maltoside (DDM) facilitated release of nearly 80% of OPH from the membrane. While assessing the release of OPH, the total OPH activity was measured in units and it was taken as 100% OPH activity. Solubilization with different non-ionic detergents and subsequent measurement of OPH activity in supernatant, and pellet fraction was used to assess the release of OPH from the membrane. As stated before, n-Dodecyl β-D-maltoside (DDM) was shown to be the best detergent for solubilization of membrane to release OPH. After solubilization of membrane, the clear supernatant was passed through immuno-affinity anti-OPH antibody column at a flow rate of 0.5ml/min. The OPH activity was measured in the flowthrough. If OPH activity was found in the flowthrough, the process was repeated till the OPH activity was found negligible in the flowthrough. Finally the bound OPH complex was eluted and the concentrated OPH was analysed by BN-PAGE and denaturing Tricine-SDS-PAGE (Fig. 3. 4. Panel A & C). The membrane fraction obtained from the opd negative mutant of Sphingopyxis wildii was treated in similar manner and analysed on BN-PAGE (Fig. 3. 4. Panel B). As expected there was no band corresponding of OPH complex in BN-PAGE reflecting the results no OPH activity was found in elution fraction. The native PAGE gave single band showing that the affinity purified OPH was pure (Fig. 3. 4. Panel A).

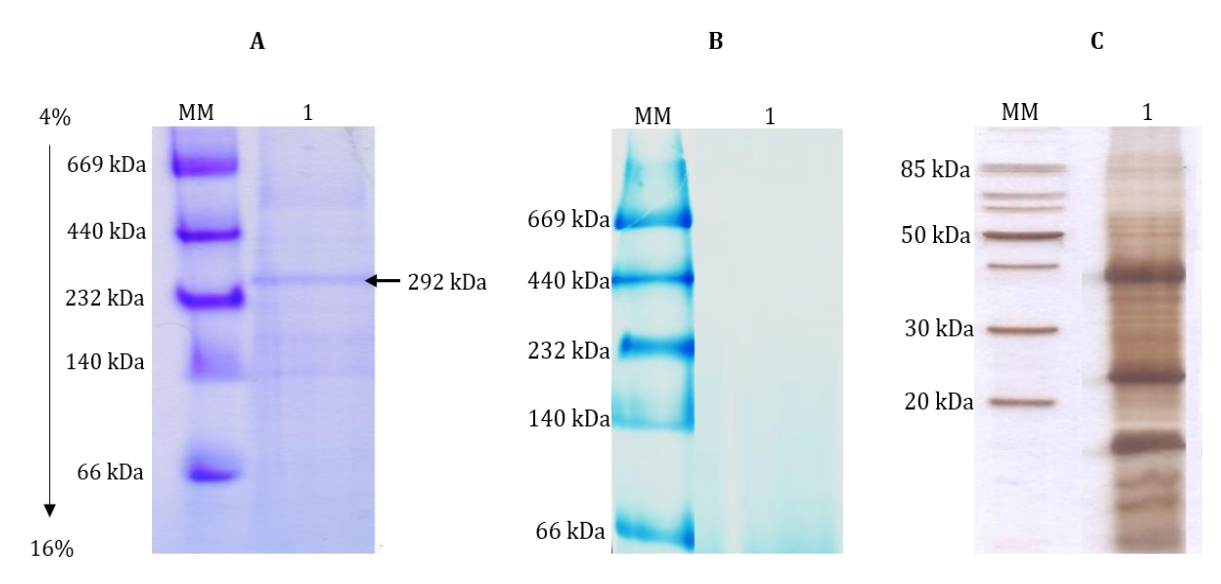


Fig. 3. 4. Panel A shows BN-PAGE analysis of immuno-purified OPH complex from *Sphingobium fuliginis*. The BN-PAGE profile of OPH complex purified from *opd* null mutant of *Sphingopyxis wildii* is shown in panel B. The Tricine-SDS PAGE profile of immuno-purified OPH complex is shown in panel C.

This size of native OPH complex as determined by BN-PAGE (4-16%) was approximately 292kDa (Fig. 3. 4. Panel A). The purified OPH complex was initially analysed on gradient Tricine-PAGE (10-16%) by running electrophoresis till bromophenol blue reached the bottom of gel (Fig. 3. 4. Panel C). A number of well resolved bands have separated on Tricine-PAGE (Fig. 3. 4. Panel C). However in these gels proteins with higher and lower molecular weights were not properly resolved (Fig. 3. 4. Panel C). Therefore electrophoresis was performed for longer duration (1hour 45 min at 150volts) to achieve clear resolution of higher molecular weight proteins (Fig. 3. 5. Panel A). Similarly a shorter electrophoretic separation was done (45 min at 150volts) to get proper resolution of lower molecular weight proteins (Fig. 3. 5. Panel B). The purified complex analysed on gradient Tricine-PAGE (10-16%) (1hour 45 min at 150volts) gave clear resolution of high molecular weight proteins and indicated existence of 85kDa, 52kDa, and 36kDa as part of OPH complex (Fig. 3. 5. Panel A). The lower molecular weight proteins were resolved for 45 min at 150 volts on 12. 5% Tricine-PAGE shown in fig. 3. 5. panel B, gave bands with a molecular mass of 25kDa, 17kDa, and 14kDa. The OPH complex was purified twice from the independently grown cultures. The pure OPH complex was then resolved on Tricine-PAGE to assess consistency in OPH associated proteins. Interestingly there was consistency with the OPH associated protein profile.

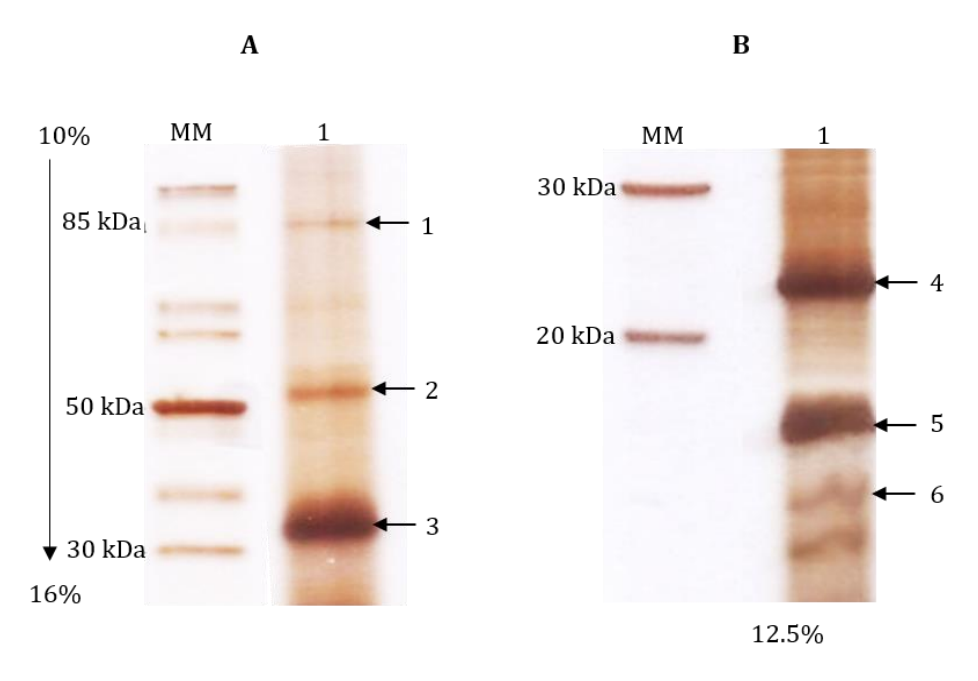


Fig. 3. 5. Resolution of OPH associated proteins. The Tricine-PAGE (10-16%) performed for 1hour 45 min and 45 min to resolve higher and lower molecular weight proteins respectively are shown in panels A and B. Lanes MM indicates molecular weight marker. The immuno-purified OPH complex is loaded in lane 1. The discrete protein bands obtained on Tricine-PAGE are shown with arrows.

The OPH associated proteins shown with arrows were carefully excised (Fig. 3. 5. Panel A & B) and used for tryptic digestion. The peptide mass profile of each band was determined by performing mass spectrometry as described in materials and methods section. Before establishing the identity of these proteins by comparing the peptide mass profile, a proteome database predicted from the total genome sequence of *Sphingobium fuliginis* was established. The predicted proteins were subjected to *in silico* tryptic digestion and an *in silico* peptide mass profile was generated for each one of the predicted protein of *Sphingobium fuliginis*. This database was then used to compare with the peptide mass fingerprint profile generated for each band identified on Tricine-PAGE. The selected fragments from each band was subjected to MS/MS analysis and the sequence generated from MS/MS analysis was aligned with the protein that matched with the mass fingerprint of OPH associated protein band.

3. 2. 2. The 85kDa OPH associated protein is TonB dependent receptor (TonR)

The peptide fingerprint of 85kDa protein (Fig. 3. 6. Panel-I) has perfectly match with the mass fingerprint pattern of TonB dependent receptor encoded by the genome of *Sphingobium fuliginis*. The Mascot score of 266 (Fig. 3. 6. Panel III) clearly indicate that the comparative data generated is beyond error zone. In order to gain further identity of the 85kDa OPH associated protein, the MS/MS analysis was done to the prominent peaks identified in the mass fingerprint profile (Fig. 3. 6. Panel IV). The sequence of the peptides generated through MS/MS analysis was then matched with the sequence of the protein, identified using peptide mass fingerprint. The peptide sequences have perfectly matched at the different positions of the TonB dependent receptor of the *Sphingobium fuliginis* ATCC 27551 (Fig. 3. 6. Panel V). Based on the peptide fingerprint pattern and sequence identity between TonB dependent receptor and the sequence generated for the selected peptides, the identity of 85kDa OPH associated protein was established as TonB dependent receptor (TonR) (Fig. 3. 6. Panel I)

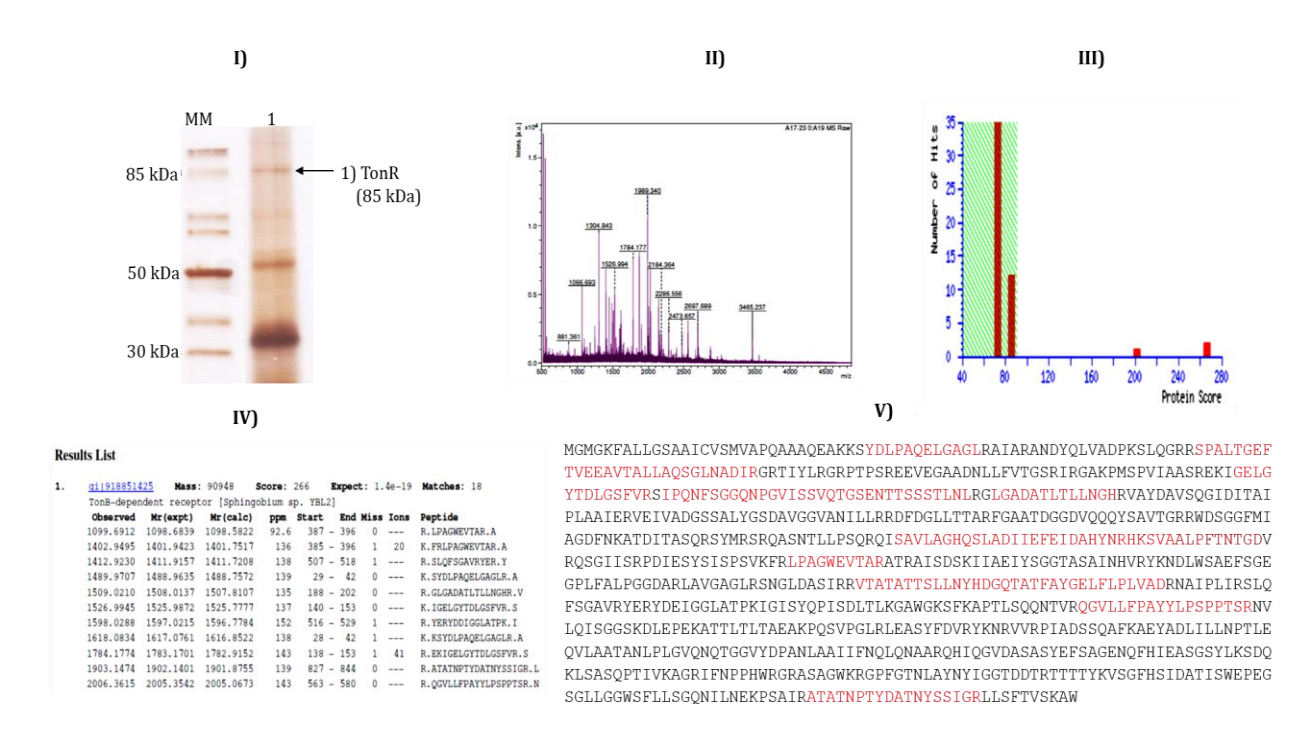


Fig. 3. 6. The 85kDa band selected for mass spectrometric analysis is shown in panel I. Tricine-PAGE profile of OPH associated proteins. The mass profile of tryptic digested peptide fragments and corresponding Mascot ID generated for 85kDa protein band is shown in panels II and III. The sequence of selected peptide generated through MS/MS analysis shown in panel IV. The sequence of TonR highlighted in red color indicate identity between the generated peptide sequences through MS/MS and the sequence of TonR predicted from the genome sequence of *Sphingobium fuliginis* ATCC 27551 (panel V).

3. 2. 3. The 36kDa OPH associated protein is energy transducing component TonB

The peptide fingerprint of 36kDa protein (Fig. 3. 7. Panel-I) has perfectly match with the mass fingerprint pattern of energy transducing component TonB encoded by the genome of *Sphingobium fuliginis*. The Mascot score of 729 (Fig. 3. 7. Panel III) clearly indicate that the comparative data generated is beyond error zone. In order to gain further identity of the 36kDa protein, the MS/MS analysis was done to the prominent peaks identified in the mass fingerprint profile (Fig. 3. 7. Panel IV). The sequence of the peptides generated through MS/MS analysis was then matched with the sequence of the protein, identified using peptide mass fingerprint. The peptide sequences have perfectly matched at the different positions of the energy transducing component TonB of the *Sphingobium fuliginis* ATCC 27551 (Fig. 3. 7. Panel V). Based on the peptide fingerprint pattern and sequence identity between TonB and the sequence generated for the selected peptides, the identity of 36kDa OPH associated protein was established as TonB (Fig. 3. 7. Panel I).

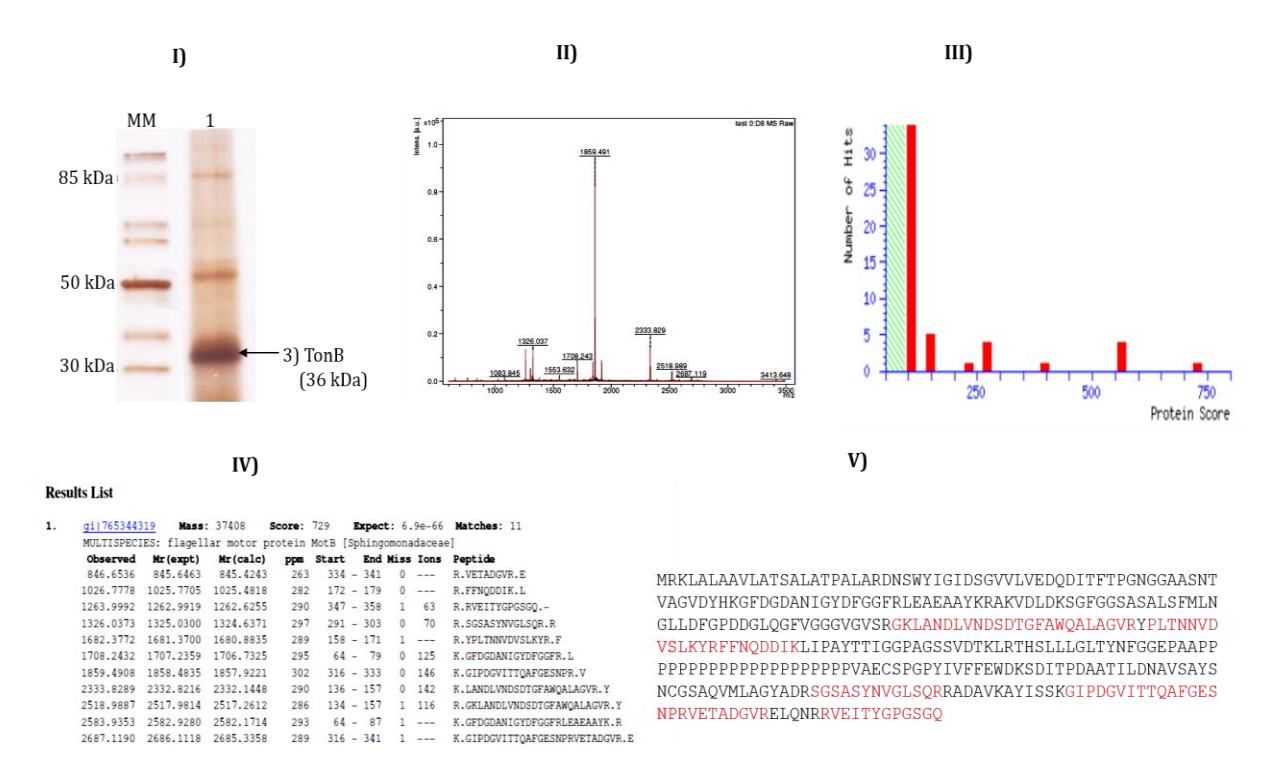


Fig. 3. 7. The 36kDa band selected for mass spectrometric analysis is shown in panel I. The mass profile of tryptic digested peptide fragments and corresponding Mascot ID generated for 36kDa protein band is shown in panels II and III. The sequence of selected peptide generated through MS/MS analysis shown in panel IV. The sequence of TonB highlighted in red color indicate identity between the generated peptide sequences through MS/MS and the sequence of TonB predicted from the genome sequence of *Sphingobium fuliginis* ATCC 27551 (panel V).

3. 2. 4. The 25kDa OPH associated protein is energy transducing component ExbB

The peptide fingerprint of 25kDa protein (Fig. 3. 8. Panel-I) has perfectly match with the mass fingerprint pattern of energy transducing component ExbB encoded by the genome of *Sphingobium fuliginis*. The Mascot score of 178 (Fig. 3. 8. Panel III) clearly indicate that the comparative data generated is beyond error zone. In order to gain further identity of the 25kDa protein, the MS/MS analysis was done to the prominent peaks identified in the mass fingerprint profile (Fig. 3. 8. Panel IV). The sequence of the peptides generated through MS/MS analysis was then matched with the sequence of the protein, identified using peptide mass fingerprint. The peptide sequences have perfectly matched at the different positions of the energy transducing component ExbB of the *Sphingobium fuliginis* ATCC 27551 (Fig. 3. 8. Panel V). Based on the peptide fingerprint pattern and sequence identity between TonB dependent receptor and the sequence generated for the selected peptides, the identity of 25kDa OPH associated protein was established as ExbB (Fig. 3. 8. Panel I).

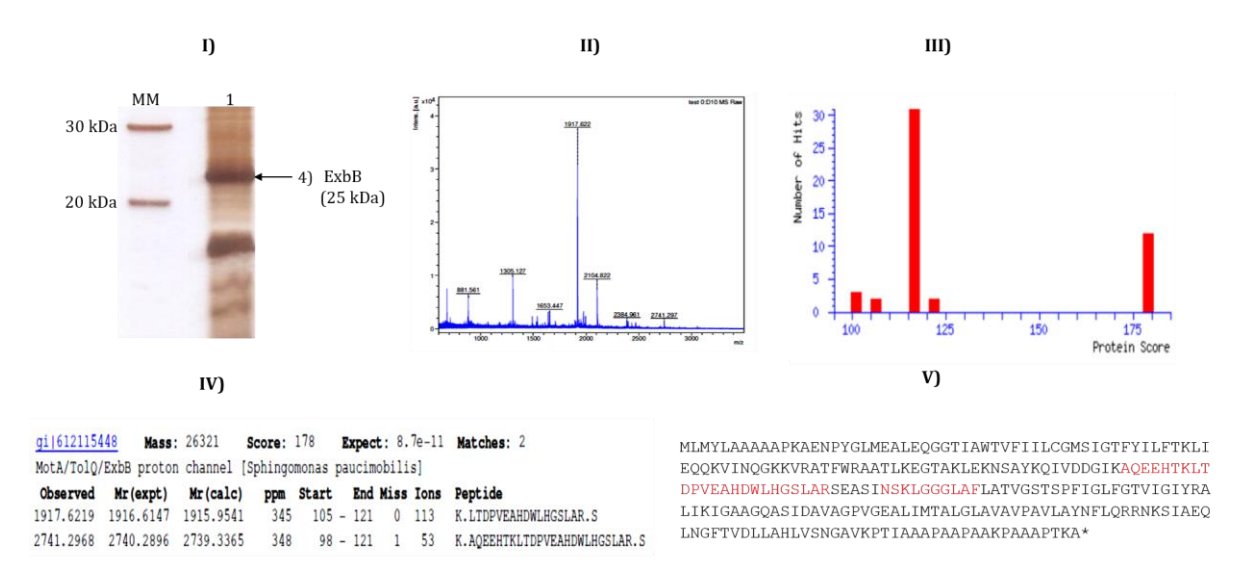


Fig. 3. 8. The 25kDa band selected for mass spectrometric analysis is shown in panel I. The mass profile of tryptic digested peptide fragments and corresponding Mascot ID generated for 25kDa protein band is shown in panels II and III. The sequence of selected peptide generated through MS/MS analysis shown in panel IV. The sequence of ExbB highlighted in red color indicate identity between the generated peptide sequences through MS/MS and the sequence of ExbB predicted from the genome sequence of *Sphingobium fuliginis* ATCC 27551 (panel V).

3. 2. 5. The 17kDa OPH associated protein is outer membrane porin (OmpW)

The peptide finger print of 17kDa protein (Fig. 3. 9. Panel-I) has perfectly match with the mass fingerprint pattern of outer membrane porin OmpW encoded by the genome of *Sphingobium fuliginis*. The Mascot score of 367 (Fig. 3. 9. Panel III) clearly indicate that the comparative data generated is beyond error zone. In order to gain further identity of the 17kDa protein, the MS/MS analysis was done to the prominent peaks identified in the mass fingerprint profile (Fig. 3. 9. Panel IV). The sequence of the peptides generated through MS/MS analysis was then matched with the sequence of the protein, identified using peptide mass fingerprint. The peptide sequences have perfectly matched at the different positions of the outer membrane porin OmpW of the *Sphingobium fuliginis* ATCC 27551 (Fig. 3. 9. Panel V). Based on the peptide fingerprint pattern and sequence identity between OmpW and the sequence generated for the selected peptides, the identity of 17kDa OPH associated protein was established as outer membrane porin OmpW (Fig. 3. 9. Panel-I).

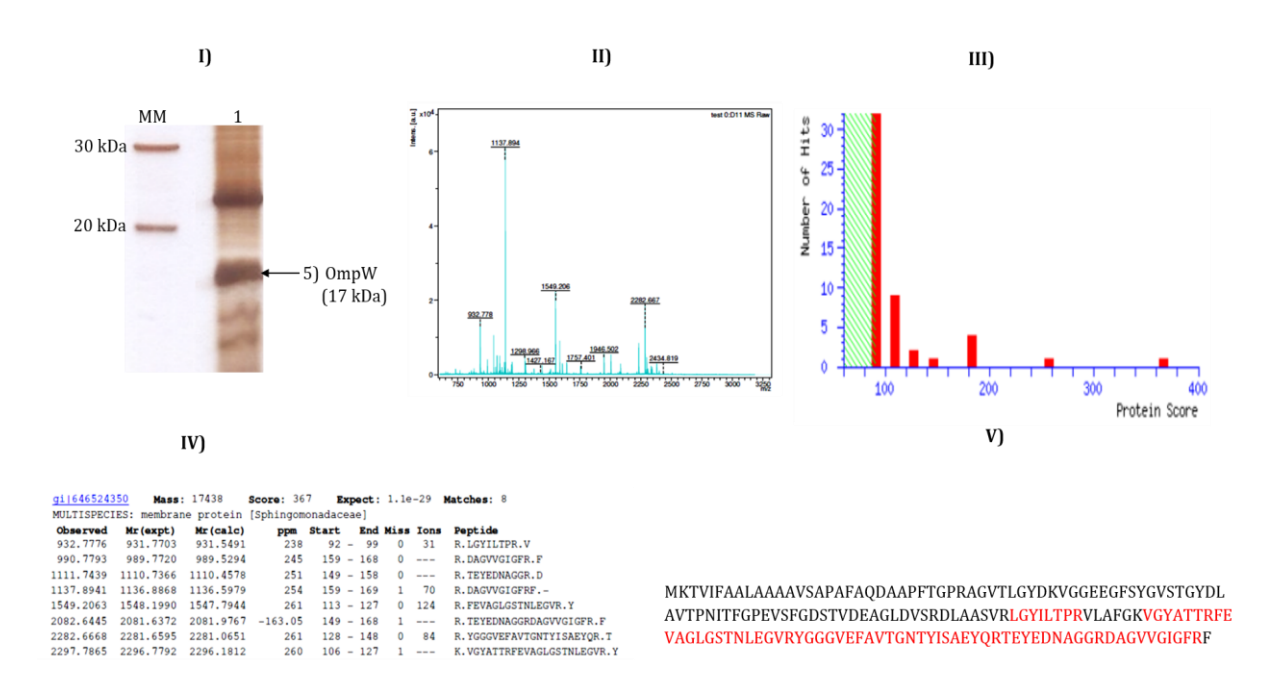


Fig. 3. 9. The 17kDa band selected for mass spectrometric analysis is shown in panel I. The mass profile of tryptic digested peptide fragments and corresponding Mascot ID generated for 17kDa protein band is shown in panels II and III. The sequence of selected peptide generated through MS/MS analysis shown in panel IV. The sequence of outer membrane porin OmpW highlighted in red color indicate identity between the generated peptide sequences through MS/MS and the sequence of OmpW predicted from the genome sequence of *Sphingobium fuliginis* ATCC 27551 (panel V).

3. 2. 6. The 14kDa OPH associated protein is energy transducing component ExbD

The peptide fingerprint of 14kDa protein (Fig. 3. 10. Panel I) has perfectly match with the mass fingerprint pattern of energy transducing component ExbD encoded by the genome of *Sphingobium fuliginis*. The Mascot score of 364 (Fig. 3. 10. Panel-III) clearly indicate that the comparative data generated is beyond error zone. In order to gain further identity of the 14kDa protein, the MS/MS analysis was done to the prominent peaks identified in the mass fingerprint profile (Fig. 3. 10. Panel IV). The sequence of the peptides generated through MS/MS analysis was then matched with the sequence of the protein, identified using peptide mass fingerprint. The peptide sequences have perfectly matched at the different positions of the energy transducing component ExbD of the *Sphingobium fuliginis* ATCC 27551 (Fig. 3. 10. Panel V). Based on the peptide fingerprint pattern and sequence identity between ExbD and the sequence generated for the selected peptides, the identity of 14kDa OPH associated protein was established as ExbD (Fig. 3. 10. Panel I)

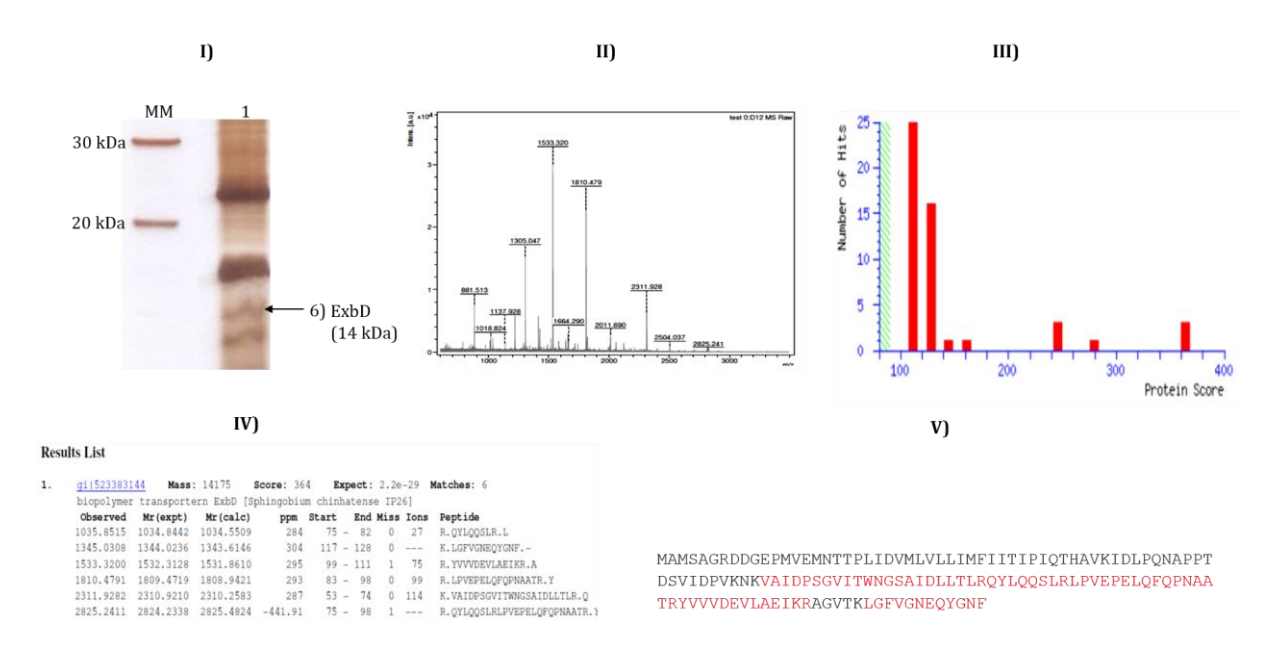


Fig. 3. 10. The 14kDa band selected for mass spectrometric analysis is shown in panel I The mass profile of tryptic digested peptide fragments and corresponding Mascot ID generated for 14kDa protein band is shown in panels II and III. The sequence of selected peptide generated through MS/MS analysis shown in panel IV. The sequence of ExbD highlighted in red color indicate identity between the generated peptide sequences through MS/MS and the sequence of ExbD predicted from the genome sequence of *Sphingobium fuliginis* ATCC 27551 (panel V).

The 52kDa protein peptide mass fingerprint profile didn't match with any of the protein found in the proteome database of *Sphingobium fuliginis*. Among the identified OPH associated proteins, no OPH was identified. Therefore, western blot was performed using anti-OPH antibody. Interestingly the 52kDa band whose mass profile didn't show any similarity with proteome of *Sphingobium fuliginis*, cross reacted with OPH antibody suggesting that the 52kDa band is OPH (Fig 3. 11). The mass of OPH as determined in SDS-PAGE was 35kDa. The band that cross reacts with OPH is 52kDa. There exists a 14kDa difference in the size of OPH. The reason for such size difference is not known. It may be due to the post translational modification of membrane associated OPH. Further experiments are in progress to detect such post translational modifications. Based on the results generated in the present study, the OPH associated proteins are TonB dependent receptor (TonR), Energy transducing component TonB, outer membrane porin OmpW, Energy transducing component ExbB and Energy transducing component ExbD. The identity of all OPH associated proteins are shown in fig 3. 12.

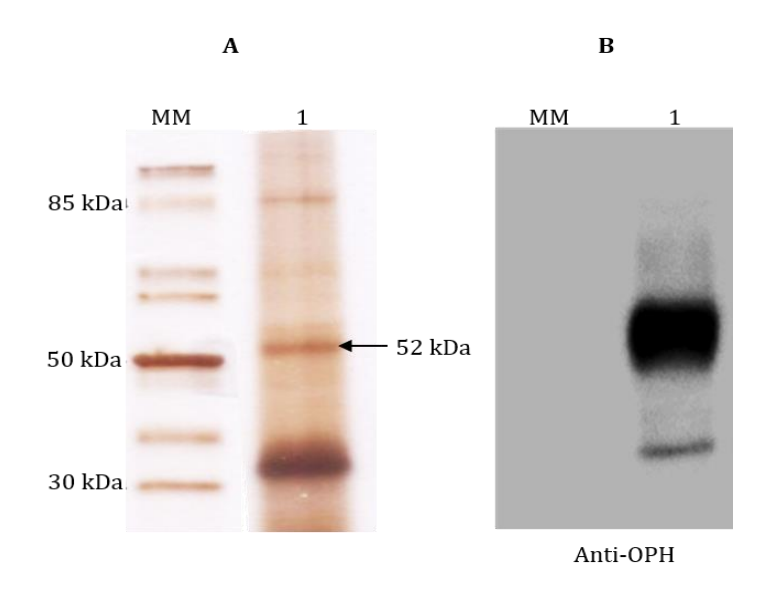


Fig. 3. 11. Identification of 52kDa OPH associated protein. The Tricine-PAGE profile of OPH associated protein and corresponding western blot are shown in panel A and panel B respectively. The 52kDa protein clearly cross reacts with anti-OPH antibodies.

3. 2. 7. OPH associated proteins are TonB dependent transport components

The identified OPH associated proteins were identified by mass spectrometry are TonB dependent receptor (TonR), energy transducing component TonB, outer membrane porin OmpW, energy transducing component ExbB and ExbD are shown in fig. 3. 12.

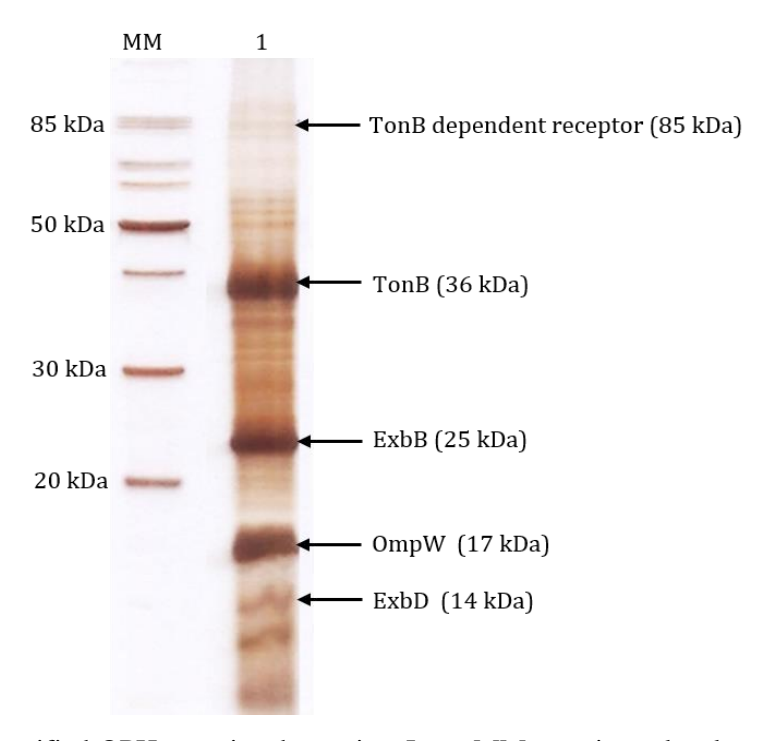


Fig. 3. 12. The identified OPH associated proteins. Lane MM protein molecular weight marker. The Tricine-PAGE profile of OPH associated proteins is shown in lane 1. The identity of each OPH associated protein band is shown with arrow.

The affinity purification system involving OPH specific antibodies appears to be highly specific as no OPH specific protein complex was found in the membrane samples purified from opd null mutants of Sphingopyxis wildii. Affinity purification of OPH associated complex showed a molecular mass of 292kDa. The TonB dependent transport (TonBDT) components, TonB dependent receptor (TonR), TonB, ExbB and ExbD are found to be OPH associated proteins. TonBDT system is an active transport mechanism existed in gram-negative bacteria to transport nutrients from across the outer membrane, of their molecular weight is greater than 600Da (Nikaido et al., 2003). The TonB dependent receptor (TonR) is an outer membrane receptor. The structural of TonR is unique in nature and it significantly differs from porins through which substrates are passed by diffusion. The TonR contain a C-terminal membrane spanning barrel domain contain 22 antiparallel βstrands (Krewulak et al., 2008). The barrel domain of TonR is much bigger than barrel domain found in outer membrane porins (Krewulak et al., 2008). The N-terminus of TonR forms a plug domain and it is responsible for binding substrates in a TonB independent manner. However release of substrate is dependent on TonB protein which transduces energy from cytoplasmic membrane. The TonB, ExbB and ExbD form a cytoplasmic membrane complex. The cellular ratio of TonB, ExbB and ExbD is 1:7:2 (Higgs et al., 2002). This complex transduces proton gradient of the cytoplasmic membrane to induce conformational change of the TonR protein bound to the substrates. Such conformational change facilitate the release of substrates in to cytoplasm. TonBDT system transports a number of nutrients, proteins, viruses. The heme, siderophores, vitamin B₁₂, colicins and naturally occurring antibiotics such as sideromycins are found to be substrates of TonB dependent transport system. (Braun 1999 & Killmann et al., 1995). In fact the phage T one (T1) does not infect E. coli that is deficient in either tonA or tonB genes. Therefore the unique outer membrane active transport system is named as TonB dependent transport system.

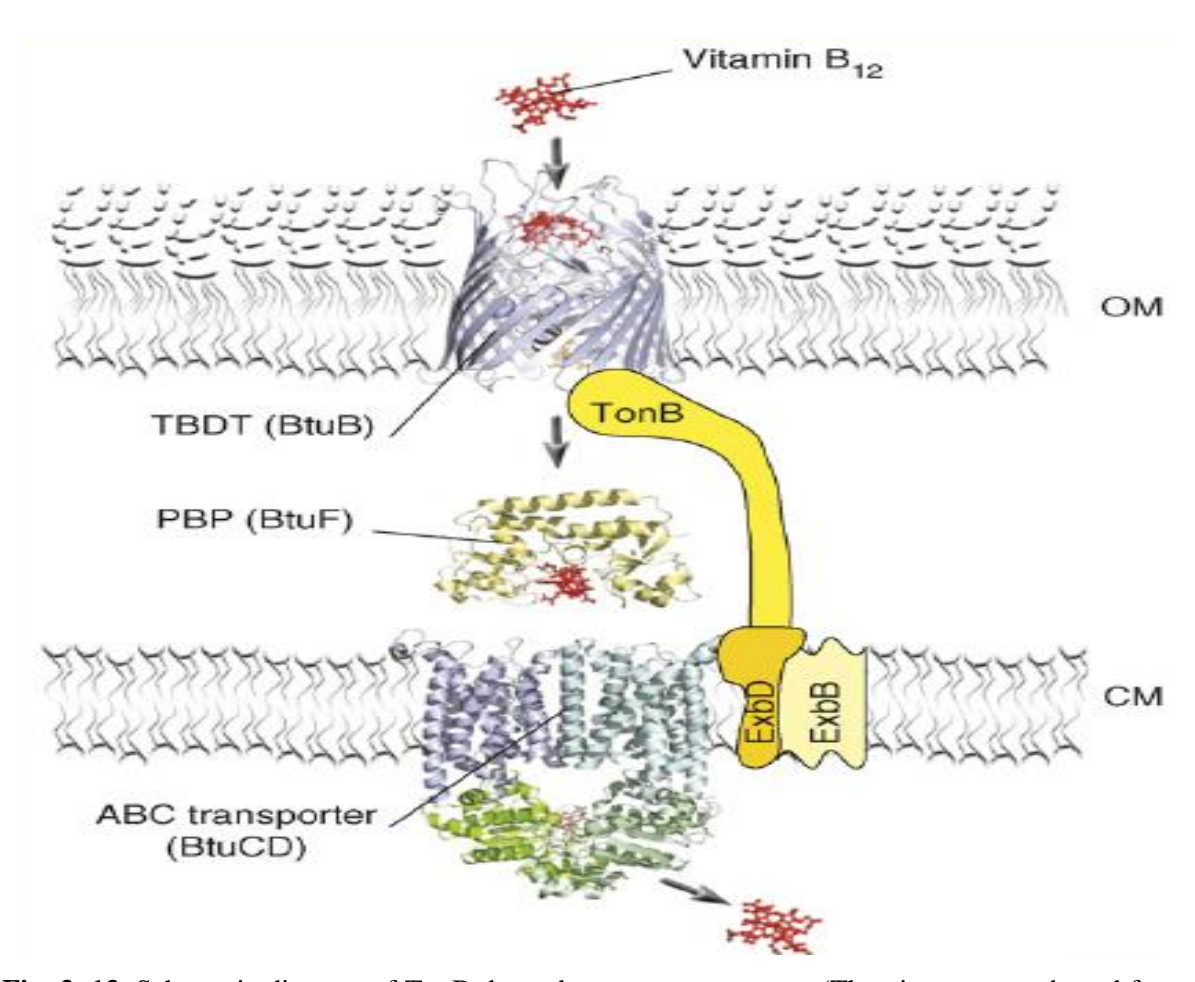


Fig. 3. 13. Schematic diagram of TonB dependent transport system. (The picture was adapted from Schauer *et al.*, 2008).

Since iron acquisition is an important physiological event, the tonB dependent transport system involving in iron acquisition process is very well characterized in *E. coli* and certain other gram-negative bacteria. The siderophore enterobactin after binding to ferric iron complexes with TonB dependent receptor by interacting with substrate binding domain identified as part of N-terminally located plug domain. The ferric-enterobactin binding to N-terminal plug domain is released into periplasm by using energy transduced from cytoplasmically located ExbB, ExbD and TonB complex. The ferric-enterobactin released into periplasm need to be hydrolysed to facilitate the release of iron bound strongly [3.03 E-05 K_D (M)] to the enterobactin. A periplasmically located esterase hydrolyses cyclic ferric-enterobactin to generate linear trimer of 2, 3-Dihydroxybenzoylserine or its dimer or monomeric form. Such hydrolysis of enterobactin facilitates release of iron from the ferric-enterobactin. The data generated in this chapter clearly indicates existence of OPH as part of TonB dependent transport components. The physiological relevance of such association is unknown. OPH is a known triesterase. It hydrolyses third ester linkage found in OP compounds such as insecticides and nerve agents (Singh & Walker, 2006; Yair *et al.*, 2008;

Singh, 2009). Considering its extraordinary catalytic efficiency the OPH is shown to have evolved from quorum quenching lactonases in response to OP insecticide residues accumulated in soil. In support of this proposition a weak lactonase activity was also identified in OPH. (Afriat et al., 2006). If this triesterase and lactonase activities of OPH are examined together with its association with TonB dependent receptor, it prompts to make the following observations. Since OP insecticides are more than 600Da, the *Sphingobium fuliginis* must be using TonBDT system for transport of OP insecticides into periplasmic space. Once transported in to periplasmic space, due to triesterase activity of periplasmically located OPH, it is hydrolysed to generate inorganic phosphate pool, to be transported into cytoplasm. Alternatively, it can also promote iron acquisition process by hydrolysing triserine lactone ring, due to its lactonase activity, to facilitate release of iron strongly bound to enterobactin. In order to gain better insights in to the aforementioned propositions further experiments were conducted and the inferences drawn were described in subsequent chapters of this dissertation.

Interactions between OPH and Ton complex

4.1. Objective specific methodology

In order to validate interactions among proteins found associated with OPH complex affinity pulldown assays were developed. While performing affinity pulldowns both OPH and its interacting proteins need to be expressed in *E. coli* as soluble proteins. If the expressed proteins have affinity tag they can be used for affinity pulldowns. In the present study the OPH is expressed with C-Terminal AviTag. The AviTag can be used to specifically pulldown using streptavidin magnetic beads. In the same way the interacting proteins were expressed with His-tag by cloning them in a compatible expression plasmid. The developed two plasmid system facilitated to perform reciprocal affinity pulldowns and to detect the interacting partners using tag-specific antibodies.

Table 4. A: Primers used in the present Study.

Primer Name	Sequence (5' -> 3')	Description
RG1 FP	AAT <u>GGATCC</u> ATGCGGAAGCTTGCCCTC	Forward primer used to amplify <i>tonB</i> from <i>S. fuliginis</i> . The <i>BamH</i> I site appended to facilitate cloning is underlined.
RG1 RP	AAT <u>AGATCT</u> TGGAAAATCTTACTGACCCG	Reverse primer used to amplify <i>tonB</i> from <i>S. fuliginis</i> . The <i>Bgl</i> II site appended to facilitate cloning is underlined.
RG2 FP	AAT <u>GGATCC</u> AACATGTTGATGTATCTCGCAG	Forward primer used to amplify <i>exbB</i> from <i>S. fuliginis</i> . The <i>BamH</i> I site appended to facilitate cloning is underlined.
RG2 RP	AAT <u>AGATCT</u> CTATCAGGCCTTGGTCGG	Reverse primer used to amplify <i>exbB</i> from <i>S. fuliginis</i> . The <i>Bgl</i> II site appended to facilitate cloning is underlined.
RG3 FP	AAT <u>GGATCC</u> TTTATGAAGACTGTGATTTTCGC	Forward primer used to amplify ompW from S. fuliginis. The appended BamHI site is underlined.
RG3 RP	AAT <u>AGATCT</u> TTAGAAGCGGAAACCGATACC	Reverse primer used to amplify <i>ompW</i> from <i>S. fuliginis</i> . The <i>Bgl</i> II site appended to facilitate cloning is underlined.
RG4 FP	ACT <u>GGATCC</u> ATCGCCATGGCAATGAGTGC	Forward primer used to amplify <i>exbD</i> from <i>S. fuliginis</i> . The <i>BamH</i> I site appended to facilitate cloning is underlined.
RG4 RP	AAT <u>AGATCT</u> CGGTTCTGACGGCCTTAGAA	Reverse primer used to amplify <i>exbD</i> from <i>S. fuliginis</i> . The <i>Bgl</i> II site appended to facilitate cloning is underlined.

DOC ED	7.7.0007.0007.0007.0007.7.0000000	E 1 ' 1, 1'C , D
RG5 FP	AAC <u>GGATCC</u> ATGGGTATGGGAAAGTTTGC	Forward primer used to amplify <i>tonR</i>
		from S. fuliginis. The BamHI site
		appended to facilitate cloning is
		underlined.
RG5 RP	CAA <u>AGATCT</u> AATGAGCATTACCAGGCCTT	Reverse primer used to amplify tonR
		from S. fuliginis. The BglII site
		appended to facilitate cloning is
		underlined.
RG6 FP	AAAGCGGCCGCCTCGATCCCGCGAAATTAATA	Forward primer used to amplify MCS
		of pRSETA vector. The NotI site
		appended to facilitate cloning is
		underlined.
RG6 RP	AAAGCGGCCGCCATTTCCCCGAAAAGTGCCA	Reverse primer used to amplify MCS
		of pRSETA vector. The <i>Not</i> I site
		appended to facilitate cloning is
		underlined.
RG7 FP	AAAGCGGCCGCGTGCCTCACTGATTAAGCATT	Forward primer used to amplify <i>oriV</i>
RO7 II		and kanamycin resistant gene of
		pACYC177. The <i>Not</i> I site appended
		to facilitate cloning is underlined.
RG7 RP	AAAGCGGCCGCAGTGTTACAACCAATTAACC	Reverse primer used to amplify <i>oriV</i>
KG/ KF	AAAGCGGCCGCAGTGTTACAACCAATTAACC	and kanamycin resistant gene of
		pACYC177. The <i>Not</i> I site appended
		to facilitate cloning is underlined.
	AAAGAATTCGAGAGGGAAGTCTTGAACATG GAC	Forward primer used to amplify
RG8 FP	TACAAAGACGATGACGACAAGATGTTGATGTAT	exbBD operon of S. fuliginis. The
	CTCGCAG	sequence specifying FLAG tag
		downstream of start codon is shown
		with bold case. The EcoRI site
		appended to facilitate cloning is
		underlined.
RG8 RP	AAAAGAGCTCTTACAGATCCTCTTCTGAGATGA	Reverse primer used to amplify
	GTTTTGTTCGAAATTGCCGTACTGTTC3'	exbBD operon of S. fuliginis. The
		sequence specifying Myc-tag at the
		C-terminus of ExbD is shown with
		bold case. The SacI site appended to
		facilitate cloning is underlined.
RG14 FP	AAA <u>CTGCAG</u> AAATGCAAACGAGAAGGGTTGT	Forward primer used to amplify opd
		from S. fuliginis to clone in pKT25
		and pUT18 vectors. The PstI site
		appended to facilitate cloning is
		underlined.
RG14 RP	AAAGGATCCTCATGACGCCCGCAAG	Reverse primer used to amplify opd
		from S. fuliginis to clone in pKT25
		and pUT18 vectors. The BamHI site
		appended to facilitate cloning is
		underlined.
RG15 FP	AAATCTAGAAATGGCAATGAGTGCCGGAAGA	Forward primer used to amplify <i>exbD</i>
		from S. fuliginis to clone in pKT25
		and pUT18 vectors. The <i>Xba</i> I site
		appended to facilitate cloning is
		underlined.
	1	unacimica.

RG15 RP	AAAGAATTCTTGAAATTGCCGTACTGTTCG	Reverse primer used to amplify <i>exbD</i>
KO15 KI	1 1 1 1 1 1 1 1 1 1 1 1 1 1 1 1 1 1 1 1	from S. fuliginis to clone in pKT25
		and pUT18 vectors. The <i>EcoRI</i> site
		appended to facilitate cloning is
		underlined.
RG16 RP	AGCCGCCGCGCGCGCGCAATCC	Primers used to generate OPH variant
		OPH ^{R91A/R96G} by performing site
RG17 FP	GGCGTGGGCACGATTGTCGATGTG	directed mutagenesis. The codons
ROI7 II		introduced to change OPH sequence
D G 10 D D		are underlined.
RG18 RP	AGCCGC <u>GAA</u> GGCGCGGCGCAATCC	RG17 FP and RG18 RP used to
		generate OPHR1F/R96G by performing
		site directed mutagenesis. The codons introduced to change OPH sequence
		are underlined.
RG19 FP	GGCGTG <u>TTC</u> ACGATTGTCGATGTG	RG16 RP and RG19 FP primer used to generate OPH ^{R91A/R96F} by
		performing site directed mutagenesis. The codons introduced to change
		OPH sequence are underlined.
RG20 FP	GCTATCCTCGAGGGCCTGAACCGCATCTTCGAG	Forward primer having AviTag
KG20 11	GCTCAGAAAATCGAA	specific sequence. The <i>Xho</i> I site
		appended to facilitate cloning is
		underlined.
RG20 RP	GCAGCTAAGCTTGCGGCCGCTTAGTGCCATTCG	Reverse Primer having AviTag
	ATTTTCTGAGCCTCG	specific sequence. The <i>Hind</i> III site
		appended to facilitate cloning is
		underlined.
RG21 FP	GCACA <u>CATATG</u> AAGGATAACACCGTGCCACTG	Forward primer used to amplify birA
		ligase from E. coli. The NdeI site
		appended to facilitate cloning is underlined.
RG21 RP	CTCCCCTCTCGAGTTTTTCTGCAC	Reverse primer used to amplify <i>birA</i>
KG21 KI		from E. coli. The XhoI site appended
		to facilitate cloning is underlined.
RG22 FP	AAATCTAGAAATGCGGAAGCTTGCCCTCG	Forward primer used to amplify <i>tonB</i>
		from S. fuliginis to clone in pKT25
		vector. The XbaI site appended to
		facilitate cloning is underlined.
RG22 RP	AAA <u>GGTACC</u> TTACTGACCCGAACCCGGACCG	Reverse primer used to amplify <i>tonB</i>
		from S. fuliginis to clone in pKT25
		vector. The <i>Kpn</i> I site appended to
RG23 FP		facilitate cloning is underlined.
KU23 FP	AAA <u>TCTAGA</u> AATGCGGAAGCTTGCCCTCGC	Forward primer used to amplify <i>tonB</i> from <i>S. fuliginis</i> to clone in pUT18
		vector. The <i>XbaI</i> site appended to
		facilitate cloning is underlined.
RG23 RP	AAAGGTACCAACTGACCCGAACCCGGACCGT	Reverse primer used to amplify <i>tonB</i>
1023 10	111111111111111111111111111111111111111	from S. fuliginis to clone in pUT18
		vector. The <i>Kpn</i> I site appended to
		facilitate cloning is underlined.
<u> </u>	l	

Table 4. B: Plasmids used in this study.

Plasmid	Description	Reference or
Name		Source
pMMB206	Cm ^r , low copy number, broad host range, expression vector.	Morales et al, 1991.
pACYC177	Km ^r , low copy number, broad host range vector.	Chang et al, 1978.
pRSETA	Amp ^r , The T7 promoter driven expression vector. Facilitates expression of cloned genes with N-terminal 6xHis-tag.	Invitrogen
pETDuet1	Amp ^r , The T7 promoter driven expression vector. Contains two multiple cloning sites. Facilitates coexpression of two proteins.	Novagen
pUT18	Amp ^r , High copy number vector, derivative of pUC19 containing a multiple cloning sequence at the 5' of the T18 fragment. (first 224 amino acids of the adenylate cyclase of <i>Bordetella pertussis</i>)	Karimova et al, 1998
pKT25	Km ^r , low copy number vector, derivative of pSU40 containing a multiple cloning sequence at the 3' of the T25 fragment (amino acids 225-399 of the adenylate cyclase of <i>B. pertussis</i>)	Karimova et al, 1998.
pSM5	Cm ^r , Expression plasmid. Codes preOPH ^{C6xHis} . Generated by cloning <i>opd</i> gene amplified from pPHYS 400 in pMMB206 as <i>EcoR</i> I and <i>Hind</i> III fragment.	Siddavattam et al, 2003.
pUCOPH	Amp ^r , <i>opd</i> cloned in pUC19 vector under the control of constitutive promoter.	Mulbry and Karns, 1989b
pOPHV400	Cm ^r , AviTag coding sequence inserted as <i>Xho</i> I and <i>Hind</i> III fragment inframe of <i>opd</i> gene of pSM5, codes for OPH ^{CAviTag}	Parthasarathy et al, 2016.
pBirA	Amp ^r , Expression plasmid. Generated by cloning <i>birA</i> ligase gene from <i>E. coli</i> amplified as <i>Nde</i> I and <i>Xho</i> I fragment at the second multiple cloning site of pETDuet1. Codes for BirA ligase.	Parthasarathy et al, 2016.
pAVB400	Amp ^r , pETDuet1 derived expression plasmid. Co-expresses OPH ^{CAviTag} and BirA ligase. Generated by cloning <i>opd</i> variant coding OPH ^{CAviTag} . The <i>opd</i> variant is amplified as <i>EcoR</i> I and <i>Hind</i> III fragment from pOPHV400 and cloned into pBirA.	Parthasarathy et al, 2016.
pGS2N	Km ^r , low copy number, broad host range expression vector, generated by ligating MCS of pRSETA to a fragment containing kanamycin resistant gene and <i>oriV</i> of pACYC177. When cloned it codes for a protein with N-terminal 6xHis-tag.	This Study
pGS ^{R91A/R96G}	Amp ^r , Expression plasmid. The pUCOPH derivative. Codes for OPH ^{R91A/R96G} .	This Study
pGS ^{R91F/R96G}	Amp ^r , Expression plasmid. The pUCOPH derivative. Codes for OPH ^{R91F/R96G} .	This Study
pGS ^{R91A/R96F}	Amp ^r , Expression plasmid. The pUCOPH derivative. Codes for OPH ^{R91A/R96F} .	This Study
pGS ^{R91F/R96F}	Amp ^r , Expression plasmid. The pUCOPH derivative. Codes for OPH ^{R91F/R96F} .	This Study

pGS16	Km ^r , Expression plasmid. Generated by cloning <i>tonB</i> gene amplified from <i>Sphingobium fuliginis</i> ATCC 27551 by using RG1 FP and RG1 RP as forward and reverse primers in pGS2N. Codes for TonB ^{N6xHis} .	This Study
pGS17	Km ^r , Expression plasmid. Generated by cloning <i>exbB</i> gene amplified from <i>Sphingobium fuliginis</i> ATCC 27551 by using RG2 FP and RG2 RP as forward and reverse primers in pGS2N. Codes for ExbB ^{N6xHis} .	This Study
pGS19	Km ^r , Expression plasmid. Generated by cloning <i>exbD</i> gene amplified from <i>Sphingobium fuliginis</i> ATCC 27551 by using RG4 FP and RG4 RP as forward and reverse primers in pGS2N. Codes for ExbD ^{N6xHis} .	This Study
pGS20	Km ^r , Expression plasmid. Generated by cloning <i>tonR</i> amplified from <i>Sphingobium fuliginis</i> ATCC 27551 by using RG5 FP and RG5 RP as forward and reverse primers in pGS2N. Codes for TonR ^{N6xHis} .	This Study
pGS21	Amp ^r , Cloning vector. Generated by ligating <i>exbBD</i> operon in pTZ vector. The <i>exbBD</i> operon was amplified from <i>Sphingobium fuliginis</i> ATCC 27551 by using RG8 FP and RG8 RP as forward and reverse primers.	This Study
pGS23	Amp ^r , Expression plasmid. Generated by ligating <i>exbBD</i> operon in one of the MCSs of pETDuet1. The <i>exbBD</i> operon was taken from pGS21 plasmid as <i>EcoR</i> I and <i>Sac</i> I. Codes for ExbB ^{NFLAG} /ExbD ^{CMyc} .	This Study
pGS26	Amp ^r , Expression plasmid. Generated by cloning complete <i>opd</i> gene inframe of the sequence coding T18 fragment of vector pUT18 as <i>Pst</i> I and <i>BamH</i> I.	This Study
pGS28	Km ^r , Expression plasmid. Generated by cloning complete <i>opd</i> gene inframe of the sequence coding T25 fragment of vector pKT25 as <i>Pst</i> I and <i>BamH</i> I.	This Study
pGS29	Km ^r , Expression plasmid. Generated by cloning complete <i>exbD</i> gene inframe of the sequence coding T18 fragment of vector pUT18 as <i>Xba</i> I and <i>EcoR</i> I.	This Study
pGS31	Km ^r , Expression plasmid. Generated by cloning complete <i>exbD</i> gene inframe of the sequence coding T25 fragment of vector pKT25 as <i>Xba</i> I and <i>Kpn</i> I.	This Study
pGS32	Km ^r , Expression plasmid. Generated by cloning complete <i>tonB</i> gene inframe of the sequence coding T25 fragment of vector pKT25 as <i>Xba</i> I and <i>Kpn</i> I.	This Study
pGS33	Amp ^r , Expression plasmid. Generated by cloning complete <i>tonB</i> gene inframe of the sequence coding T18 fragment of vector pUT18 as <i>Xba</i> I and <i>Kpn</i> I.	This Study

Table 4. C. Strains used in the present study.

Strains	Genotype or Phenotype	Reference or Source
E. coli DH5α	$\lambda supE44$, $\Delta lacU169$ ($\Delta 80$ lacZ $\Delta M15$) hsdR17 recA1 endA1 gyrA96 thi1 relA1	Hanahan <i>et al</i> , 1983
Arctic express	E. coli B F ompT hsdS (rB mB dcm Tet gal endA Hte (cpn10 cpn60 Gent)	Agilent Technologies
BTH101	Sm ^r , F cya-99 araD139 galE15 galK16 rpsL1 hsdR2 mcrA1 mcrB1	Roulland-Dussoix & Boyer 1969.
Sphingobium fuliginis ATCC 27551	Wild type strain, Sm ^r , PmB ^r , opd ⁺	Sethunathan & Yoshida 1973; Kawahara <i>et al</i> . 2010.

4.1.1. Construction of opd variant to code for OPH^{CAviTag}

a) Cloning of birA in second MCS of pETDuet1

The pETDuet1 vector contains two multiple cloning sites. The second MCS of pETDuet1 was used to clone *birA* gene. The *birA* gene, codes for BirA ligase, which ligates biotin at the conserved lysine residue of AviTag. The AviTag having biotin can be affinity purified using streptavidin magnetic beads. The *birA* ligase was amplified from the genomic DNA of *E. coli* as NdeI and XhoI fragment by using RG21 FP and RG21 RP and cloned at second MCS as NdeI-XhoI fragment (Fig. 4. 1. Panel A & B). The resulted plasmid is designed as pBirA. The plasmid pBirA codes BirA ligase.

b) Cloning of opd variant in pBirA

The *opd* variant coding OPH^{CAviTag} was generated by inserting an oligo coding AviTag inframe of *opd* gene by replacing its stop codon. Our lab has previously generated pSM5 which codes OPH^{C6xHis}. The description of the plasmid is given elsewhere (Siddavattam *et al.*, 2003). In pSM5 the His-coding sequence was introduced inframe as XhoI and HindIII fragment by replacing the stop codon of the gene. In the present study this His-coding sequence was replaced with AviTag coding sequence. Two complimentary oligos RG20 FP and RG20 RP appended with XhoI and *HindIII* respectively were annealed to generate AviTag coding sequence as XhoI and HindIII fragment. The plasmid pSM5 was digested with XhoI and HindIII to eliminate His-tag coding sequence and in its place AviTag coding sequence was ligated. The resulting plasmid named as pOPHV400 which encodes OPH with C-terminal AviTag. The *opd* variant coding OPH^{CAviTag} was digested with EcoRI and

HindIII fragment and ligated at one of the multiple cloning sites of pETDuet1 derived pBirA, digested with similar enzymes, the resulting plasmid named as pAVB400 (Fig. 4. 1. Panel C).

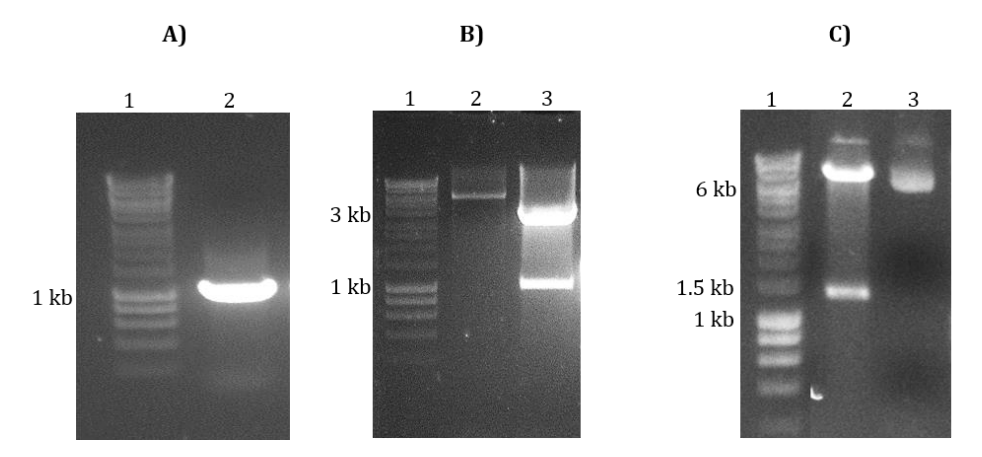


Fig. 4. 1. Construction of pAVB400. Panel A shows PCR amplification of *birA*. Lane 1 represents 1kb DNA ladder, PCR amplicon of *birA* (963bp) is shown in lane 2. Panel B shows confirmation of *birA* ligation in second MCS of pETDuet1. Lane 1 & 2 represents 1kb DNA ladder, and undigested plasmid. Release of *birA* due to digestion of recombinant plasmid pBirA with NdeI and XhoI is shown in lane 3. Panel C shows ligation of *opd* variant in first MCS of pBirA. Release of insert upon EcoRI and HindIII digestion of recombinant plasmid pAVB400 is shown in lane 2. Lane 3 represents undigested plasmid pAVB400.

4.1.2. Pulldown strategy:

Initially the pETDuet1 derivative pAVB400 was used to co-express both OPH variant OPH^{CAviTag} and BirA ligase. Ectopic expression of these two proteins facilitates ligation of biotin to Avi-tag found at the C-terminus of OPH without depending on chromosomally expressed *birA*. If the cells are grown in presence of biotin the ectopically expressed BirA is expected to optimally ligate biotin at the AviTag of over produced OPH^{CAviTag}. The strategy followed for the expression of biotinylated OPH is shown in fig 4. 2. Such addition of biotin to Avi-tag facilitates affinity pulldown of OPH^{CAviTag} using streptavidin magnetic beads. If OPH interacting proteins identified in previous chapter were co-expressed they can be pulled down along with OPH^{CAviTag} if there is an interaction between OPH and its interacting partners. In order to perform co-expression pulldown assays using *E. coli* as an expression host an expression plasmid compatible to pETDuet1 should be generated. The expression plasmid thus generated should also facilitate expression of proteins with detectable epitopes.

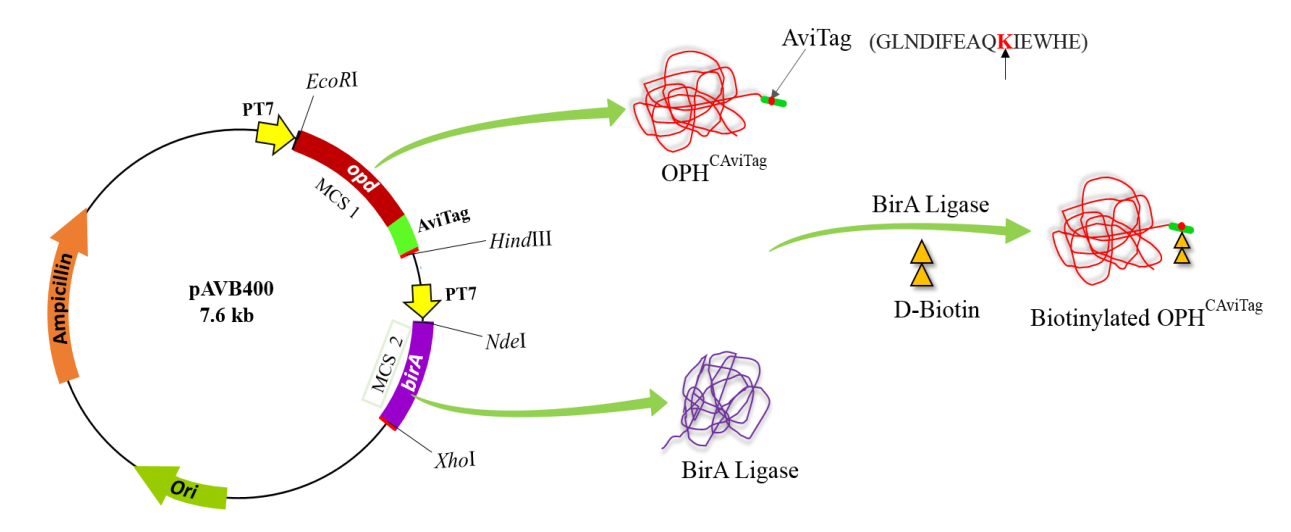


Fig 4. 2. Expression of biotinylated OPH in *E. coli* Arctic express. Ligation of D-biotin at the C-terminus of OPH^{CAviTag} by BirA ligase is shown.

4.1.3. Requirement for compatible expression vector to co-express OPH interacting partners:

The E. coli (pAVB400) strain codes OPH^{CAviTag}. Once expressed, the BirA ligase ligates biotin at the conserved lysine residue of OPHCAviTag. If OPH interacting partners are expressed in E. coli (pAVB400) their interactions can be studied by performing pulldown assays using streptavidin magnetic beads. The OPH contains 23 amino acids long signal peptide. The plasmid pAVB400 codes for precursor form of OPH. The precursor form of OPH remains as active soluble cytoplasmic protein in E. coli and it is not targeted to the membrane of E. coli cells (Gorla et al., 2009). If we need to study interactions between OPH and its interacting partners it is necessary to express OPH interacting partners as soluble cytoplasmic proteins. Therefore compatible expression vector has to be constructed to express OPH interacting proteins as soluble cytoplasmic proteins. However, the OPH interacting partners are membrane associated proteins. All of them have dedicated signal peptides to take them to the membrane. Therefore while expressing in E. coli strategies were developed to express them all with N-terminal His-tag. Addition of His-tag before signal peptide is expected to prevent their membrane targeting and thus expressed proteins remain in cytoplasm. Assuming that the OPH interacting proteins expressed with Nterminal His-tag remain in cytoplasm, an expression vector, compatible to pAVB400 was designed to co-express OPH interacting proteins with N-terminal His-tag.

Construction of pGS2N

The expression plasmid pAVB400 coding OPH^{CAviTag} is a derivative of pETDuet1, which is replicated using ColE1 replicative origin. Therefore a compatible expression vector is

constructed by using *oriV* sequence of pACYC177. Construction of expression vector pGS2N is illustrated in panel-I of fig 4. 3. While constructing pGS2N the replicative origin and kanamycin resistant gene was taken from pACYC177. The promoter and multiple cloning system were taken from expression vector pRSETA. The corresponding regions from these two plasmids were amplified as NotI fragments using primers sets RG6 FP, RG6 RP and RG7 FP, RG7 RP (Fig 4. 3. Panel-II A & B). The generated amplicons were digested with NotI and ligated following standard protocols. The resulting expression vector is designated as pGS2N (Fig 4. 3. Panel-II C). Since it contains pRSETA MCS the cloned genes are fused inframe to the vector specific His-tag coding sequences and the recombinant protein coded by pGS2N will have N-terminal 6xHis-tag.

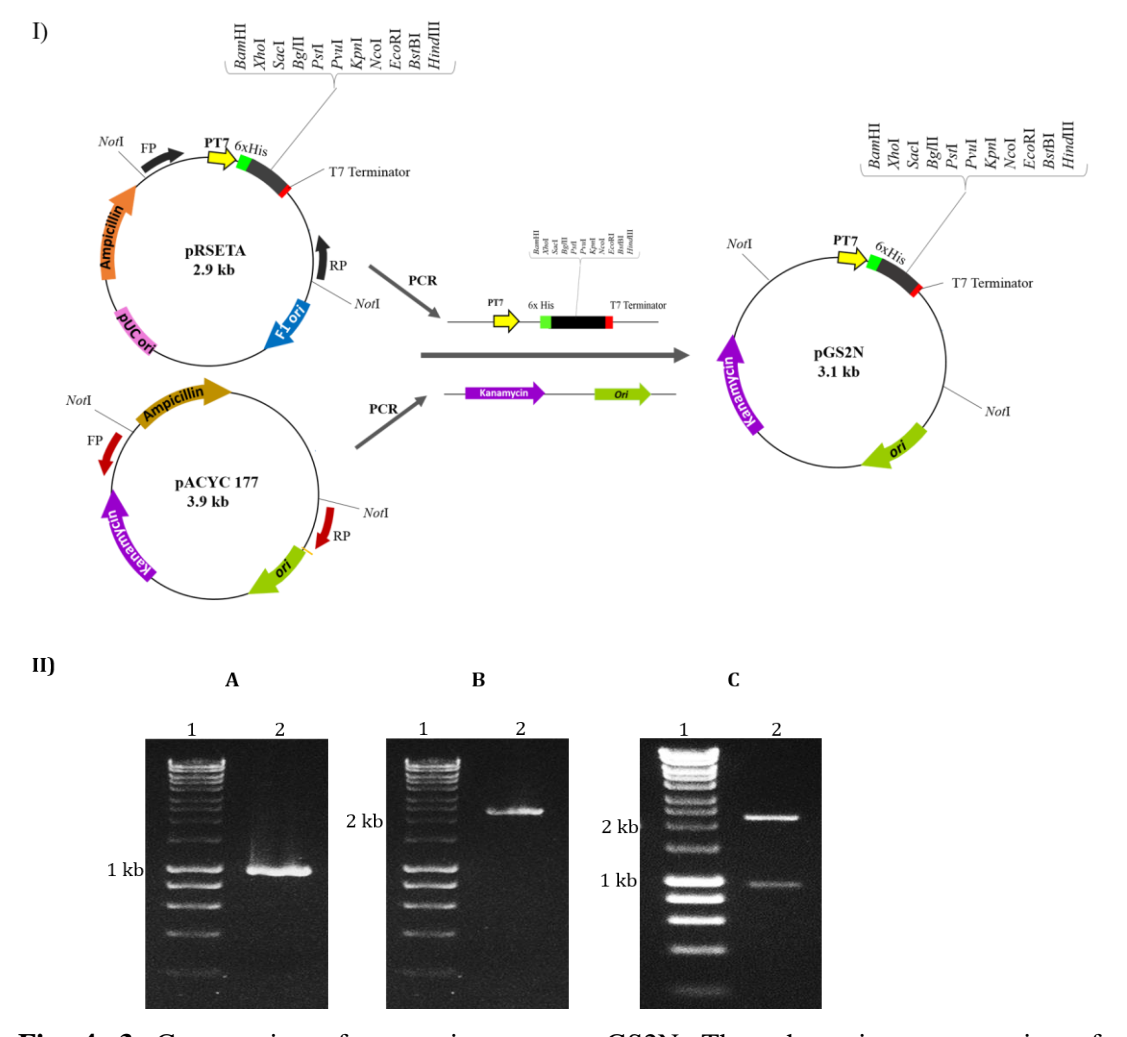


Fig. 4. 3. Construction of expression vector pGS2N. The schematic representation of pGS2N construction is shown in panel I. Panel II-A shows PCR amplification of MCS and T7 promoter region of pRSETA. Lanes 1 and 2 represent 1kb DNA ladder and PCR amplicon (931bp) containing MCS and T7 promoter region. Panel B shows PCR amplification of *oriV* and kanamycin resistance gene from pACYC177. Lanes 1 & 2 show PCR amplicon (2.2kb) containing *oriV* and kanamycin resistance gene and 1kb DNA ladder. Panel C shows ligation of MCS and T7 promoter of pRSETA to the *oriV* and kanamycin resistance gene of pACYC177. NotI digested pGS2N is shown in lane 2.

Construction of expression plasmid to express TonR^{N6xHis}

The gene coding *tonR* was amplified from *Sphingobium fuliginis* using its genomic DNA as template and RG5 FP and RG5 RP as forward and reverse primers (Fig. 4. 4. Panel A). Amplified product was digested with BamHI and BgIII and ligated to similarly digested pGS2N, the resulting recombinant expression plasmid designated as pGS20, codes for TonR^{N6xHis} (Fig. 4. 4. Panel B). The Arctic express (pGS20) cells were grown till mid log phase and the expression of TonR^{N6xHis} was induced by adding 1mM IPTG. Immediately after induction the cultures were shifted to an incubator shaker preset at 18°C. The expression of TonR^{N6xHis} was induced for further 12h before analysing the cultures to detect if TonR^{N6xHis} is produced as soluble cytoplasmic protein. The cells were lysed by sonication as described elsewhere and the lysate was centrifuged at 13,000 rpm for 20 min to separate cell lysate from debris and inclusion bodies. The clear lysate was taken to analyze on 10% SDS-PAGE and to detect TonR^{N6xHis} by performing western blots using anti-His antibodies.

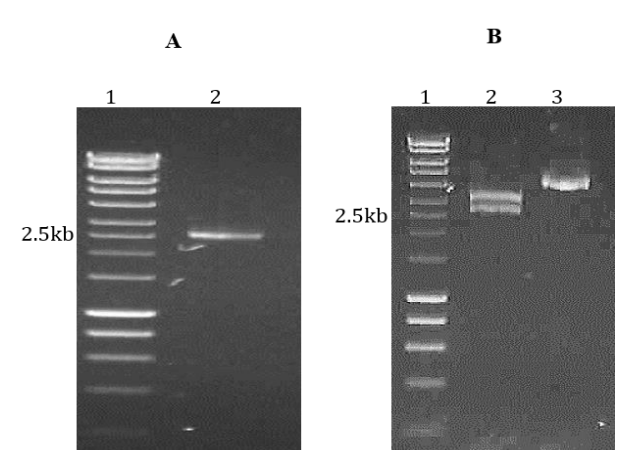


Fig. 4. 4. Construction of pGS20. Panel A shows PCR amplification of *tonR*. Lanes 1 & 2 show 1kb DNA ladder and PCR amplicon (2.5kb) of *tonR*. Panel B shows ligation in pGS2N. Lanes 1 & 2 show 1kb DNA ladder and release of insert containing *tonR* upon digestion of pGS20 with BamHI and BgIII. The undigested pGS20 is loaded in lane 3.

Construction of expression plasmid to express TonBN6xHis

The gene coding TonB protein (*tonB*) gene was amplified from *Sphingobium fuliginis* using its genomic DNA as template and primers RG1 FP and RG1 RP as forward and reverse primers (Fig. 4. 5. Panel A). Amplified product was digested with BamHI and BglII and ligated to similarly digested pGS2N, the resulting plasmid, designated as pGS16, codes for TonB^{N6xHis} (Fig. 4. 5. Panel B). The Arctic express (pGS16) cells were grown till mid log

phase and expression of TonB^{N6xHis} was determined by following protocols described above.

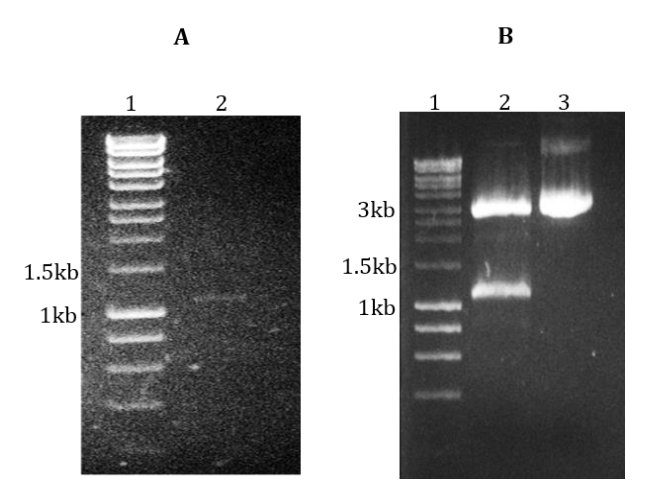


Fig. 4. 5. Construction of pGS16. Panel A shows PCR amplification of *tonB*. Lanes 1 & 2 show 1kb DNA ladder and PCR amplicon containing *tonB* (1.1kb). Panel B shows ligation of *tonB* in pGS2N. Lanes 1 & 2 show 1kb DNA ladder and release of insert containing *tonB* from pGS16 upon digestion with BamHI and BgIII. The undigested pGS16 is loaded in lane 3.

Construction of pGS19

The *exbD* gene coding energy transducing proton channel protein was amplified from *Sphingobium fuliginis* using its genomic DNA as template and RG4 FP and RG4 RP as forward and reverse primers (Fig. 4. 6. Panel A). Amplified product was digested with BamHI and BgIII and ligated to similarly digested pGS2N, the resulting plasmid designated as pGS19 (Fig. 4. 6. Panel B) codes for ExbD^{N6xHis}. The Arctic express (pGS19) cells were grown till mid log phase and expression of ExbB^{N6xHis} was determined following strategies described above.

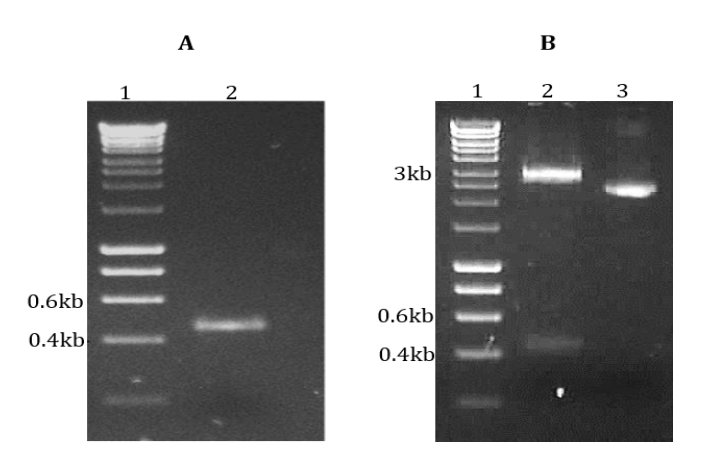


Fig. 4. 6. Construction of pGS19. Panel A shows PCR amplification of *exbD*. Lanes 1 & 2 show 1kb DNA ladder and PCR amplicon containing *exbD* (423bp). Panel B shows ligation of *exbD* in pGS2N. Lanes 1 & 2 show 1kb DNA ladder and release of insert containing *exbD* from pGS19 upon digestion with BamHI and BgIII. The undigested pGS19 is loaded in lane 3.

Construction of pGS17

The gene coding energy transducing proton channel protein (*exbB*) gene was amplified from *Sphingobium fuliginis* using its genomic DNA as template and primers RG2 FP and RG2 RP as forward and reverse primers (Fig. 4. 7. Panel A). Amplified product was digested with BamHI and BgIII and ligated to similarly digested pGS2N, the resulting plasmid named as pGS17 (Fig. 4. 7. Panel B) codes for ExbB^{N6xHis}. The Arctic express (pGS17) cells were grown till mid log phase and the expression of ExbB^{N6xHis} and the expression of ExbB^{N6xHis} determined strategies described above.

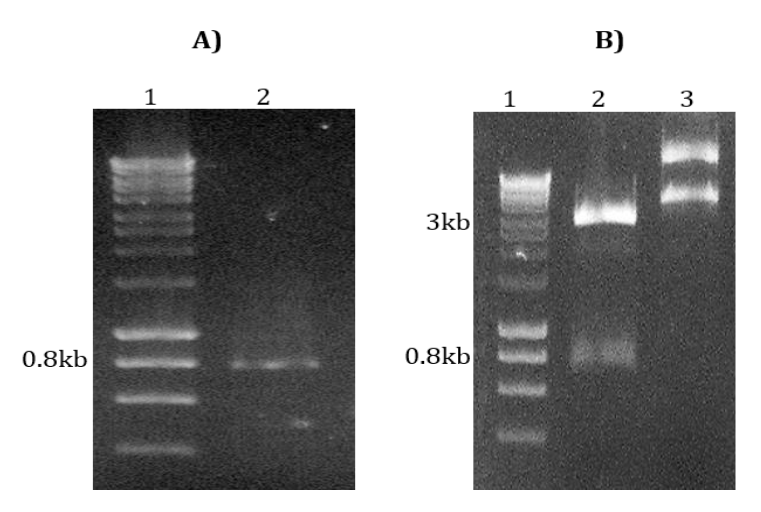


Fig. 4. 7. Construction of pGS17. Panel A shows PCR amplification of *exbB*. Lanes 1 & 2 show 1kb DNA ladder and PCR amplicon of *exbB* (762bp). Panel B shows ligation of *exbB* in pGS2N. Lanes 1 & 2 show 1kb DNA ladder and, release of insert containing *exbB* from pGS17 upon digestion with BamHI and BgIII. The undigested pGS17 is loaded in lane 3.

Construction of pGS23

ExbB is highly unstable in the absence of ExbD (Held *et al.*, 2002). The ExbB can't be expressed without co-expressing with ExbD. Therefore these two proteins were expressed together by cloning *exbBD* operon under the control of T7 promoter. While obtaining *exbBD* operon as PCR product, the primers were designed in such a way that the amplified *exbBD* operon codes for ExbB^{NFLAG} and ExbD^{CMyc}. This strategy helps to gain the stability of ExbB and to have independent detection of ExbB and ExbD using epitope specific antibodies. The *exbBD* operon of *S. fuliginis* ATCC 27551 was amplified by using forward primer RG8 FP. The primer is designed by taking the 5' region of *exbB* sequence. Upstream of the start codon of *exbB* the sequence specifying FLAG epitope (shown in bold case) was introduced inframe of *exbB* (Table 4. A). Similarly, in the reverse primer RG8 RP, the Myctag coding sequence was introduced by replacing the stop codon of *exbD* gene. The stop

codon is reintroduced after the *myc* specific codons. The amplicon containing *exbBD* was digested with EcoRI and SacI enzymes and ligated to pETDuet1 vector digested with similar enzymes (Fig. 4. 8. Panel A & B). The resulting recombinant plasmid was named as pGS23 (Fig. 4. 8. Panel C) and the expression plasmid pGS23 codes ExbB^{NFLAG} and ExbD^{CMyc}. The Arctic express (pGS23) cells were grown till mid log phase and the expression of ExbB^{NFLAG}/ ExbD^{CMyc} was determined following strategies described above.

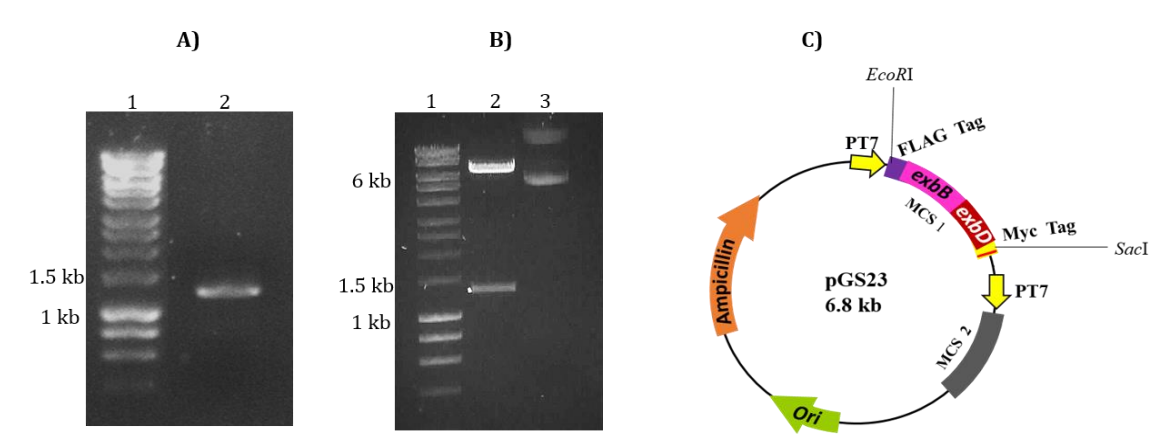


Fig. 4. 8. Construction of pGS23. Panel A shows PCR amplification of *exbBD* operon with FLAG and Myc tag coding sequences. Lanes 1 & 2 show 1kb DNA ladder and PCR amplicon containing *exbBD* operon (1.2kb). Panel B shows ligation of *exbBD* operon at the MCS 1 of pETDuet1 vector. Lanes 1 & 2 indicate 1kb DNA ladder and release of insert containing *exbBD* operon upon digestion of EcoRI and SacI. The undigested plasmid pGS23 is loaded in lane 3. Panel C shows diagrammatic representation of pGS23 plasmid.

4.1.4. Reciprocal pulldown Assays

The *E. coli* Arctic express (pAVB400) cells expressing OPH^{CAviTag} was independently transformed with the expression plasmids coding ExbD^{N6xHis} (pGS19) and TonB^{N6xHis} (pGS16). Similarly the *E. coli* Arctic express (pOPHV400) cells expressing OPH^{CAviTag} was co-transformed with the expression plasmid coding ExbB^{NFLAG} ExbD^{CMyc} (pGS23). These cultures were grown up to mid log phase in 10ml LB media and induced with 1mM IPTG along with 2μM D-Biotin (100μl from stock 1mM D-Biotin) and allowed to grow at 18°C for overnight. The cells were harvested at 6500 rpm for 10 min and cells were washed two times with wash buffer (PBS pH 7. 4, 150mM NaCl and 5% glycerol). The cell pellet obtained after washing was resuspended in 2ml of lysis buffer (PBS pH 7.4, 150mM NaCl, 5% glycerol, 1mM PMSF) and proteinase cocktail (10μl) was added before lysing the cells by sonication for 10 minutes (10 sec ON and 40 sec OFF for 5). The cell lysate was then subjected to centrifugation for 20 minutes at 13,000 rpm and the clear lysate (1ml) was divided in to two parts, one part of the lysate was mixed with streptavidin

magnetic beads (30µl slurry) (Dynabeads M-280 Streptavidin, Invitrogen) and the second part of the lysate was mixed with Ni-NTA magnetic beads (30µl slurry) (Thermo Fisher Scientific, India). The contents were kept at 4°C for overnight on head to head rotation and the magnetic beads were collected to the bottom of the tube with the help of magnet. The clear supernatant was taken into a clean eppendorf tube. The collected beads were washed 3 to 4 times with PBS pH 7.4 (150mM NaCl, 5% glycerol) and each wash fraction was collected into separate sterile eppendorf tube. The washed beads were resuspended in 50µl of 2x SDS-PAGE sample buffer and stored at -20°C until further use. Appropriate amounts of supernatant, wash fractions were taken into separate tubes and mixed with 2x SDS-PAGE sample buffer and boiled along with washed beads stored at -20°C for 5 min before analyzing all of them on 12.5% SDS PAGE. The separated proteins were detected by performing western blots using either OPH specific antibodies (to detect OPH^{CAviTag},) anti-FLAG antibodies (to detect ExbB^{NFLAG}), anti-myc antibodies (to detect ExbD^{CMyc}) and anti-His antibodies (to detect TonBN6xHis). Cell lysates prepared from E. coli cells expressing OPH^{CAviTag}, ExbB^{NFLAG} ExbD^{CMyc} and TonB^{N6xHis} independently were treated in a similar manner and used as controls.

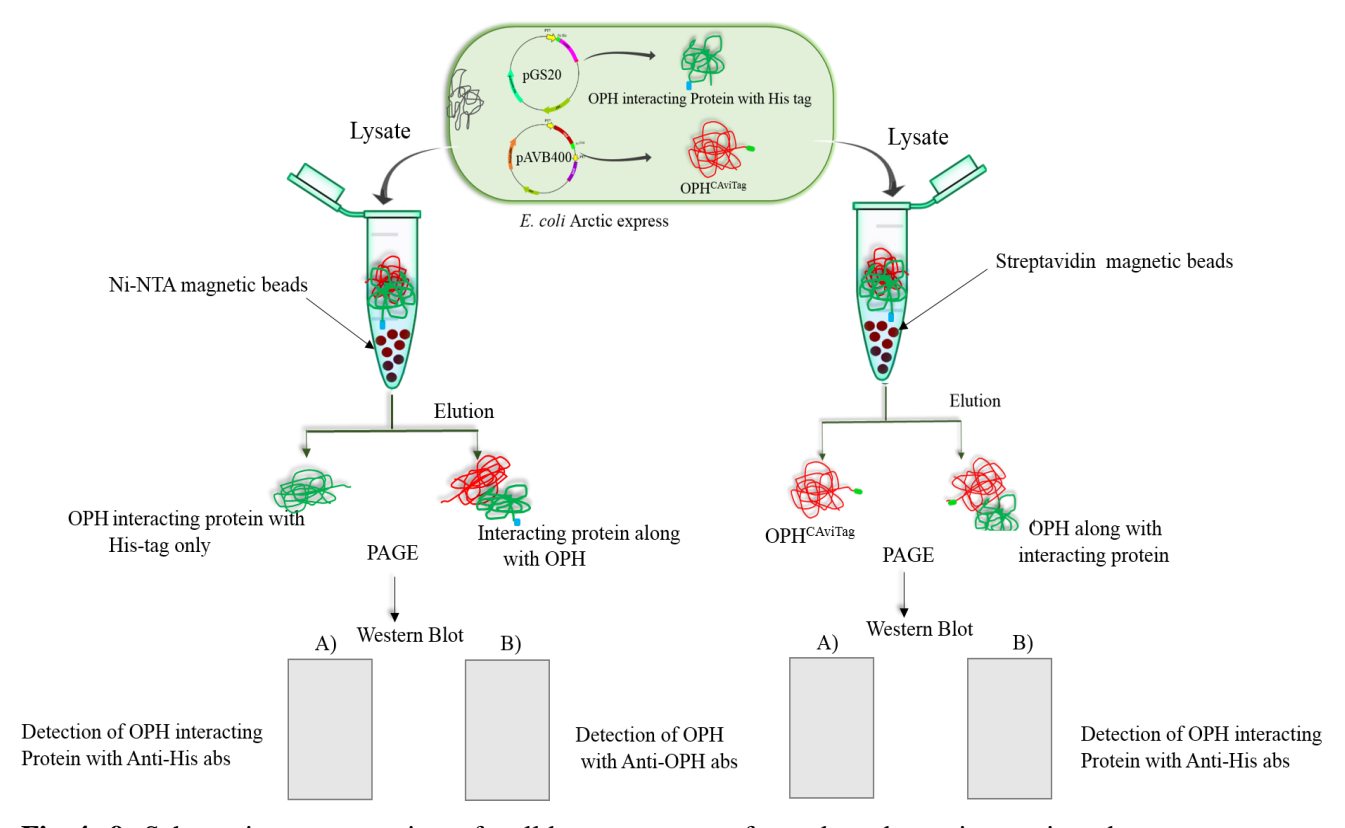


Fig 4. 9. Schematic representation of pulldown assays performed to detect interactions between OPH and TonB dependent transport components.

4.1.5. Analysis of protein-protein interaction with Bacterial two-hybrid system.

The proteins interacting with OPH were initially identified by performing reciprocal pulldown assays. The pulldown assays have clearly shown strong interactions between OPH-ExbD. These results were further confirmed by performing bacterial two hybrid system.

4.1.6. ExbD-OPH interactions

The energy transducing proton channel *exbD* of *Sphingobium fuliginis* was amplified by PCR using gene specific primers RG15 FP and RG15 RP. The amplified product was digested with XbaI and EcoRI and ligated to similarly digested pKT25 and pUT18 vectors. The ligation strategy places *exbD* in frame of the vector sequence coding T25 and T18 fragments. The resulting plasmids were named as pGS31 and pGS29. In similar *opd* gene was amplified from genomic DNA of *Sphingobium fuliginis* by using RG14 FP and RG14 RP. The amplified product was digested with PstI and BamHI and ligated to similarly digested pKT25 and pUT18 vectors. The ligation strategy places the *opd* gene in frame of vector sequence coding T25 and T18 fragments. The resulting plasmids were named as pGS28 and pGS26.

In order to test ExbD-OPH interactions, the BTH101 (pGS26+pGS31) coding OPH with C-terminal T18 fragment and ExbD with N-terminal T25 fragment and BTH101 (pGS28+pGS29), coding OPH with N-terminal T25 fragment and ExbD with C-terminal T18 fragment were induced and the interactions were measured by quantifying β-galactosidase activity (Miller, 1972). The BTH101 cells (pKT25+pGS26) expressing T25 fragment and OPH with C-terminal T18 fragment, and BTH101 (pKT25+pGS29) coding T25 fragment and ExbD with N-terminal T25 fragment served as control cultures. Both test and control cells were grown in 10ml LB media with 0.5mM IPTG till culture reached to mid log phase at 30°C with 180 rpm. The cells were harvested by centrifuging the culture at 6,500 rpm for 10 min. The cell pellet obtained was then washed with Z-buffer and performed β-galactosidase assay as mentioned in the general methods section.

4.1.7. TonB-OPH interactions

The *tonB* gene of *Sphingobium fuliginis* ATCC 27551 was amplified by PCR using gene specific primers RG22 FP, RG22 RP and RG23 FP, RG23 RP. The amplified products were digested with XbaI and KpnI and ligated similarly digested pKT25 and pUT18 vector.

The ligation strategy places *tonB* in frame of the vector sequence coding T25 fragment and T18 fragment. The resulting plasmids designated as pGS32 and pGS33.

BTH101 cells (pGS32+ pGS26) and (pGS28+pGS33) served as test cultures. The interactions between TonB and OPH were measured by quantifying β -galactosidase activity. The BTH101 (pKT25+pGS33) and (pKT25+pGS26) served as control cultures. Both test and control cells were used to perform β -galactosidase assay as mentioned in the materials and methods section.

4.1.8. ExbD-OPH interactions: in silico predictions

Homology Modelling of ExbD

Since X-ray/NMR/Cryo structure of ExbD of *Sphingobium fuliginis* has not yet been determined, resorted to build its 3D model by means of homology modelling. FUGUE (Shi *et al.*, 2001) was used to detect its structural homologue. Ten homology models were built using FUGUE alignment (Fig. 4. 10) as input to Modeller 9.19-1 (Webb & Sali 2017). Of the ten models the best model was selected based on molpdf score which was further examined for its stereo chemical quality and structure validation by means of PROCHECK (Laskowski *et al.*, 1993) and VERIFY-3D (Luthy *et al.*, 1992) respectively.

Fig. 4. 10. Alignment of templates to ExbD used for homology modelling of ExbD

Interacting residues between OPH and ExbD.

I-COMS server used (Iserte *et al.*, 2015) to identify coevolving residues between OPH and ExbD based on corrected mutual information algorithm (MI). I-COMS server performs PSI-

BLAST searches for query proteins on Uniprot-KB and retrieves all those sequences with an Evalue threshold of 1e-5 after 3 PSI-BLAST iterations. The sequences so retrieved were used to build multiple sequence alignments of homologues of OPH and ExbD. Mutual information (MI) method was used to calculate MI scores for all possible pairs of residue positions in OPH and ExbD. Of the co-evolving pairs we only chose top 100 scoring residues and calculated their solvent accessibility values in the OPH and ExbD using GETAREA tool (Fraczkiewicz & Braun 1998). Residues with more than 50% of their surfaces exposed to solvent were considered as surface residues.

Protein-Protein docking Studies on OPH and ExbD

Cluspro2.0 (Kozakov *et al.*, 2018) for protein-protein docking studies. C-terminal of ExbD (Res 241-358) was used as ligand and OPH homo dimer (PDB Id: 1EZ2) as receptor while performing targeted protein-protein docking using the list of solvent exposed coevolved residues in OPH as probable sites of interaction. Performed blind docking where whole protein surfaces were sampled for protein-protein docking. This was done to find whether the most preferred pose from targeted docking can also be found as one of the poses from blind docking. The different poses obtained were analysed for their binding energies, presence of polar interactions at interfaces, change in solvent accessibility of residues due to protein interactions and presence of coevolving residues at the interfaces. PPCheck tool used (Sukhwal & Sowdhamini 2013) to calculate binding energy and identify interactions at the interface.

4.1.9. Generation of OPH variants and validation of OPH/ExbD interactions

The *in silico* predictions indicated interactions of OPH with ExbD through the arginine residues found at positions 91 and 96. These two residues are shown to interact with valine and leucine residues of ExbD present at positions 112 and 83rd. In order to validate these interactions the OPH variants were generated by substituting these two residues with alanine, glycine and phenylalanine. The amino acid substitutions were introduced into OPH by performing site directed mutagenesis by using Q5 site directed mutagenesis kit (New England Bio Labs, USA) as described in general methods section.

a) Generation of expression plasmid coding OPH^{R91A/R96G}

The expression plasmid pUCOPH codes mature form of OPH from a constitutively expressed promoter. The purification of OPH is very well standardized in our laboratory. Therefore we have used pUCOPH as a template for performing site directed mutagenesis.

While generating OPH variant OPH^{R91A/R96G} pUCOPH was used as a template and RG17 FP and RG16 RP as forward and reverse primers. The primers contain the modified bases (Table 4. A) to introduce alanine in place of arginine found at 91 position and to introduce glycine in place of arginine found at 96 position. The resulting plasmid designated as pGS^{R91A/R96G} encodes OPH^{R91A/R96G}.

b) Generation of expression plasmid coding OPH^{R91F/R96G}

While generating OPH variant OPH^{R91F/R96G} pUCOPH was used as a template and RG17 FP and RG18 RP as forward and reverse primers. The primers contain the modified bases (Table 4. A) to introduce phenylalanine in place of arginine found at 91 position and introduce glycine in place of arginine found at 96 position. The resulting plasmid designated as pGS^{R91F/R96G} encodes OPH^{R91F/R96G}.

c) Generation of expression plasmid coding OPHR91A/R96F

While generating OPH variant OPH^{R91A/R96F} pUCOPH was used as a template and RG19 FP and RG16 RP as forward and reverse primers. The primers contain the modified bases (Table 4. A) to introduce alanine in place of arginine found at 91 position and introduce phenylalanine in place of arginine found at 96 position. The resulting plasmid designated as pGS^{R91A/R96F} encodes OPH^{R91A/R96F}.

d) Generation of expression plasmid coding OPH^{R91F/R96F}

While generating OPH variant OPH^{R91F/R96F} pUCOPH was used as a template and RG19 FP and RG18 RP as forward and reverse primers. The primers contain the modified bases (Table 4. A) to introduce phenylalanine in place of arginine found at 91 position and introduce phenylalanine in place of arginine found at 96 position. The resulting plasmid designated as pGS^{R91F/R96F} encodes OPH^{R91F/R96F}.

4.2. Expression and detection of OPH variants

After generating plasmids coding OPH variants they were independently transformed in to DH5 α cells and grown in 10ml LB at 30 for 12 h with shaking at 180 rpm. Cells harvested at 6500 rpm for 10 min and washed two times with wash buffer (PBS pH 7.4, 150mM NaCl and 5% glycerol). The cell pellet obtained after washing was resuspended in 1ml of lysis buffer (PBS pH 7.4, 150mM NaCl, 5% glycerol, 1mM PMSF) and proteinase cocktail (10 μ l) was added before lysing the cells by sonication for 10 minutes (10 sec ON and 40 sec OFF for 5). The cell lysate was then subjected to centrifugation for 20 minutes at 13,000 rpm to get clear cell lysate. The clear cell lysate was taken and estimated protein

concentration by using Bradford's reagent. The 40µg of protein was used for SDS-PAGE and followed by western blotting using anti-OPH antibodies. While determining activity to OPH variants, about 20µl of clear cell lysate was taken and OPH activity was determined by following standard methods (Chaudhry *et al.*, 1988).

Interactions between ExbDN6xHis and OPH variants.

The plasmids coding OPH variants, pGS^{R91A/R96G} and pGS^{R91F/R96G} were independently transformed into *E. coli* (pGS19) cells expressing ExbD^{N6xHis}. These cultures were used for pulldown assay by using Ni-NTA magnetic beads was described elsewhere

4.3. Results & discussion

4.3.1. Biotinylation of OPH

The OPH^{CAviTag} and BirA ligase coding plasmid pAVB400 was transformed into Arctic express and induced following standard protocols described elsewhere. Before proceeding to pulldown assays, the expression of OPH^{CAviTag} was observed at different induction time points by analyzing the cell lysate on SDS-PAGE followed by western blot probed using anti-OPH antibodies (Fig. 4. 11. Panel A). The western blot results clearly indicated the stability of OPH^{CAviTag}. Further the OPH activity was performed to rule out the addition of AviTag at the C-terminus of OPH has no influence on OPH activity. There was no significant difference between the activity of native OPH (85µM PNP/mg/min) and OPH^{CAviTag} (80µM PNP/mg/min) (Fig. 4. 11. Panel B). The data clearly indicate that the addition of AviTag has no significant influence on OPH activity.

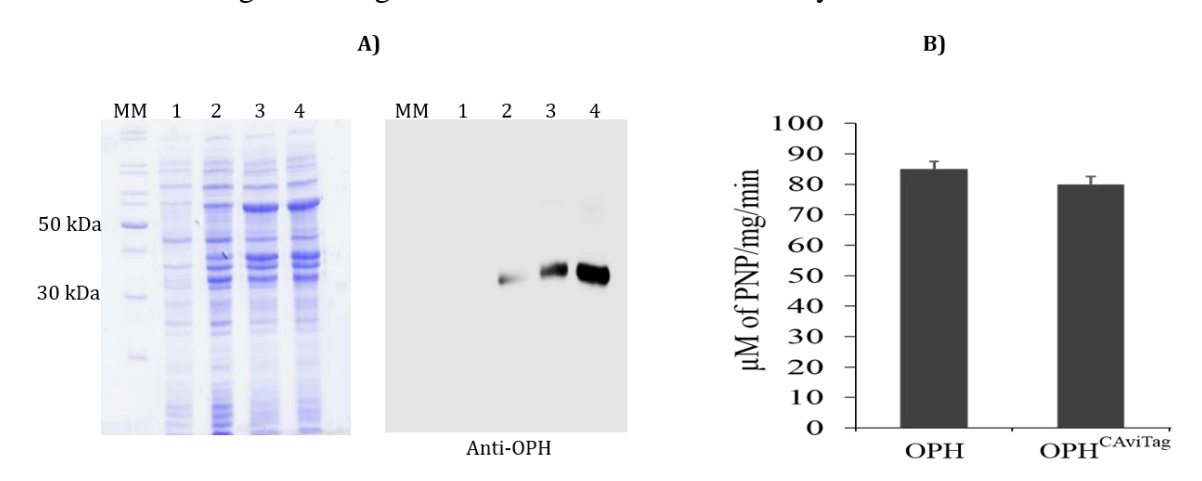


Fig. 4. 11. Panel A shows SDS-PAGE (12.5%) and corresponding western blot, performed using anti-OPH antibodies. Lane MM shows molecular weight marker. Lane 1 to 4 indicate protein extracts from uninduced and induced cells for 3h (lane 2), 6h (lane 3) and 12h (lane 4) respectively. The activity of OPH and OPH^{CAviTag} is shown in panel B.

Addition of biotin enhances production of biotinylated OPH.

Arctic express (pAVB400) cells co-express OPH^{CAviTag} and BirA ligase. However, synthesis of biotinylated OPH depends on ligation of biotin at the conserved lysine residue of AviTag. Therefore the expression of OPH^{CAviTag} and BirA ligase was done in presence of biotin (2μM). Induction of these two enzymes in presence of biotin significantly increased formation of biotinylated OPH. The OPH^{CAviTag} expressed in presence of biotin completely bound to the streptavidin magnetic beads. However a portion of OPH^{CAviTag} always remained in cell lysate if it is expressed in the absence of biotin (data not shown), indicating partial biotinylation of OPH^{CAviTag}. These results clearly indicated enhanced production of biotinylated OPH in presence of biotin.

The results discussed in the preceding chapter have clearly shown co-purification of TonBDT components with OPH. The TonBDT components are divided into two parts the inner membrane associated Ton complex comprising of TonB and ExbB/ExbD and an outer membrane receptor often referred as TonB dependent receptor. Since OPH is inner membrane associated protein initial experiments were performed to establish its interactions with Ton complex.

4.3.2. Expression of Ton complex in E. coli Arctic express with N-terminal His-tag

The genes coding Ton complex components of *Sphingobium fuliginis*, *tonB*, *exbB*, *exbD* and TonB dependent receptor *tonR*, were cloned in pGS2N. The details of the construction is mentioned in materials and methods section. The expression plasmids coding Ton complex pGS16 (TonB^{N6xHis}), pGS19 (ExbD^{N6xHis}), pGS17 (ExbB^{N6xHis}) and TonR^{N6xHis} (pGS20) were transformed independently into Arctic express and induced following standard protocols described elsewhere. Before proceeding to pulldown assays, the expression of TonBDT components was established by analyzing the respective cell lysates on SDS-PAGE followed by performing western blots using anti-His antibodies.

4.3.3. The TonB^{N6xHis} and ExbD^{N6xHis} are found in soluble fractions

The Arctic express cells expressing Ton complex components were induced and then expression profile of TonB^{N6xHis}, ExbB^{N6xHis} and ExbD^{N6xHis} were established. The Arctic express cells having expression plasmids pGS16 (TonB^{N6xHis}), pGS17 (ExbB^{N6xHis}) and pGS19 (ExbD^{N6xHis}) were induced and the clear lysate and particulate fractions were analysed by performing western blots using anti-His antibodies. Interestingly The TonB^{N6xHis} and ExbD^{N6xHis} were detected in soluble fraction (Fig. 4. 12. Panels A & B)

suggesting that these two proteins of Ton complex were successfully expressed in Arctic express cells. Therefore the corresponding expression plasmids were transformed into Arctic express cells (pAVB400) to perform reciprocal pulldown assays.

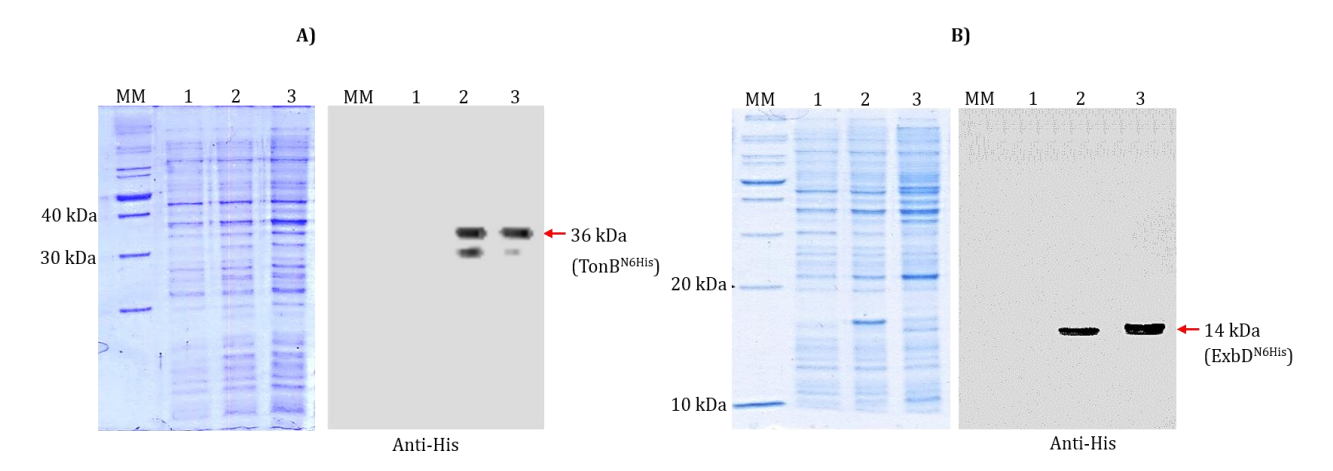


Fig. 4. 12. Panel A and B show expression and subsequent detection of TonB^{N6xHis}. The cell lysate of Arctic express (pGS16) were fractionated and the clear lysate (lane 2) and particulate fractions (lane 3) were analysed on 12. 5% SDS-PAGE along with total cell lysate prepared from uninduced culture (lane 1). The corresponding western blot performed using anti-His antibodies, indicates presence of TonB^{N6xHis} both in soluble and particulate fraction. Panel B shows expression and subsequent detection of ExbD^{N6xHis}. The cell lysate of Arctic express (pGS19) were fractionated and the clear lysate (lane 2), and particulate fractions (lane 3) were analysed on 15% SDS-PAGE along with total cell lysate prepared from uninduced culture (lane 1). The corresponding western blot performed using anti-His antibodies, indicates presence of ExbD^{N6xHis} both in soluble and particulate fraction.

4.3.4. The ExbB^{N6xHis} is not stable

Though TonB^{N6xHis} and ExbD^{N6xHis} were successfully expressed, no ExbB^{N6xHis} specific signal was detected in cell lysate, prepared from Arctic express (pGS17) cells (Fig. 4. 13. Panel B lane 2). These observation is agreement with published results which suggested that ExbB is not stable in the absence of ExbD (Held *et al.*, 2002). Since the ExbB is not stable in absence of ExbD, the ExbB and ExbD were co-expressed in Arctic express cells by cloning *exbBD* operon under the control of T7 promoter.

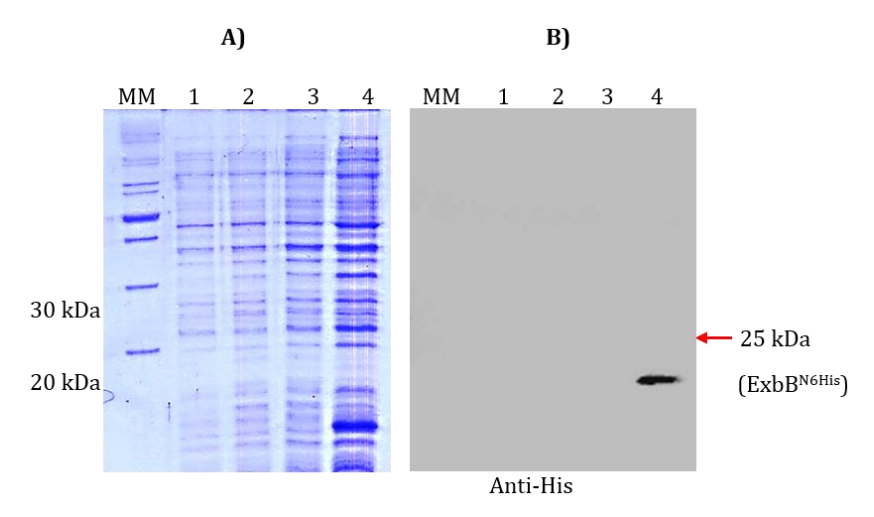


Fig. 4. 13. Panel A and B show expression and subsequent detection of ExbB^{N6xHis}. The cell lysate of Arctic express (pGS17) were fractionated and the clear lysate (lane 2), and particulate fractions (lane 3) were analysed on 12. 5% SDS-PAGE along with total cell lysate prepared from uninduced culture (lane 1). Panel B shows corresponding western blot performed using anti-His antibodies. Absence of ExbB^{N6xHis} signal both in soluble and particulate fraction is shown in panel B. *E. coli* cell lysate expressing GntR^{N6xHis} (12.5kDa) used as positive control was loaded in lane 4.

4.3.5. ExbB is stable in presence of ExbD

The *exbBD* operon coding ExbB and ExbD were amplified and cloned in pETDuet1 vector (vide materials & methods section). The recombinant plasmid, pGS23 codes ExbB^{NFLAG} and ExbD^{CMyc}. The induced Arctic express cells were fractionated and the expression of ExbB^{NFLAG} and ExbD^{CMyc} was analysed by performing SDS-PAGE, followed by western blot probed using anti-FLAG and anti-Myc antibodies (Fig. 4. 14. Panel B & C). The ExbB^{NFLAG} and ExbD^{CMyc} specific signals were observed both in particulate and soluble fractions indicating existence of considerable amounts of ExbB^{NFLAG} and ExbD^{CMyc} in soluble fraction. Therefore the expression plasmid pGS23 coding ExbB^{NFLAG} and ExbD^{CMyc} was used to transform Arctic express cells (pOPHV400) expressing biotinylated OPH^{CAviTag}.

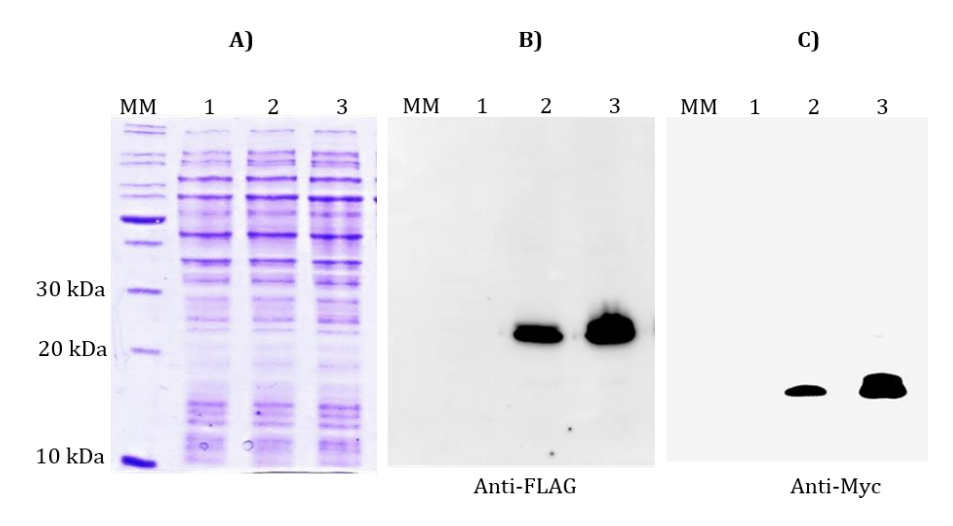


Fig. 4. 14. Shows expression and subsequent detection of ExbB^{NFLAG} and ExbD^{CMyc}. The cell lysate of Arctic express (pGS23) was fractionated and the soluble (lane 2) and particulate (lane 3) fractions were analysed on 12. 5% SDS-PAGE (Panel A) along with total cell lysate prepared from uninduced culture (lane 1). The corresponding western blot performed using anti-FLAG and anti-Myc antibodies, indicate presence of ExbB^{NFLAG} (Panel B) and ExbD^{CMyc} (Panel C) both in soluble and particulate fractions.

4.3.6. OPH interacts with TonB

Since the expression of TonB^{N6xHis}, ExbD^{N6xHis} and ExbB^{NFLAG}/ExbD^{CMyc} have successful the Arctic express (pAVB400) cells were transformed with the respective expression plasmid to co-express TonB^{N6xHis} and ExbD^{N6xHis} with biotinylated OPH. Similarly the Arctic express (pOPHV400) was transformed with expression plasmid to co-express $ExbB^{NFLAG}/ExbD^{CMyc}$ with biotinylated OPH. The cell lysate prepared from the Arctic express cells (pAVB400+pGS16) coding OPH^{CAviTag} and TonB^{N6xHis} were used to perform pulldown assays using streptavidin magnetic beads The cell lysate, flowthrough, wash and elution fractions were collected and analysed on SDS-PAGE. The western blots were probed with either anti-OPH or anti-His antibodies to detect OPH^{CAviTag} and TonB^{N6xHis} (Fig. 4. 15. Panel A). As expected the TonB^{N6xHis} and OPH^{CAviTag} were seen in cell lysate (Fig. 4. 15. Panel A lane 1). None of these proteins were detected in flowthrough (FT) and wash fractions (W) (Fig. 4. 15. Panel A lane 2 & 3). As expected in elution fraction OPH specific signal was observed as biotinylated OPH has affinity to the streptavidin magnetic beads (Fig. 4. 15. Panel A lane 4). Interestingly in the elution fraction the TonB^{N6xHis} specific signal was also observed (Fig. 4. 15. Panel A lane 4), suggesting that the TonB^{N6xHis} is copurified with biotinylated OPH. The elution fraction collected from the cells expressing only TonB^{N6xHis} didn't show any signal (Fig. 4. 15. Panel A lane 6) indicating that TonB^{N6xHis} has no affinity towards streptavidin magnetic beads. Reciprocal pulldown assays were performed in a similar manner by using Ni-NTA magnetic beads (vide materials and methods section). The elution fractions collected from Ni-NTA magnetic beads showed OPH specific signal in addition to TonB^{N6xHis} specific signal (Fig. 4. 15. Panel B lane 4) Elution fractions collected from the beads incubated with cell lysates expressing only OPH^{CAviTag} didn't bind to Ni-NTA magnetic beads (Fig. 4. 15. Panel B lane 5). This clearly represents possible interactions between OPH and TonB. Interestingly the western blots performed using anti-His antibodies clearly show two closely placed signals suggesting existence of two forms of TonB^{N6xHis}. TonB is a membrane associated protein. It contains signal peptide to facilitate membrane targeting and it will be cleaved after successful targeting to the membrane.

Removal of signal peptide results in reduction of size. The closely placed His-specific signals probably indicate precursor and mature form of TonB^{N6xHis}.

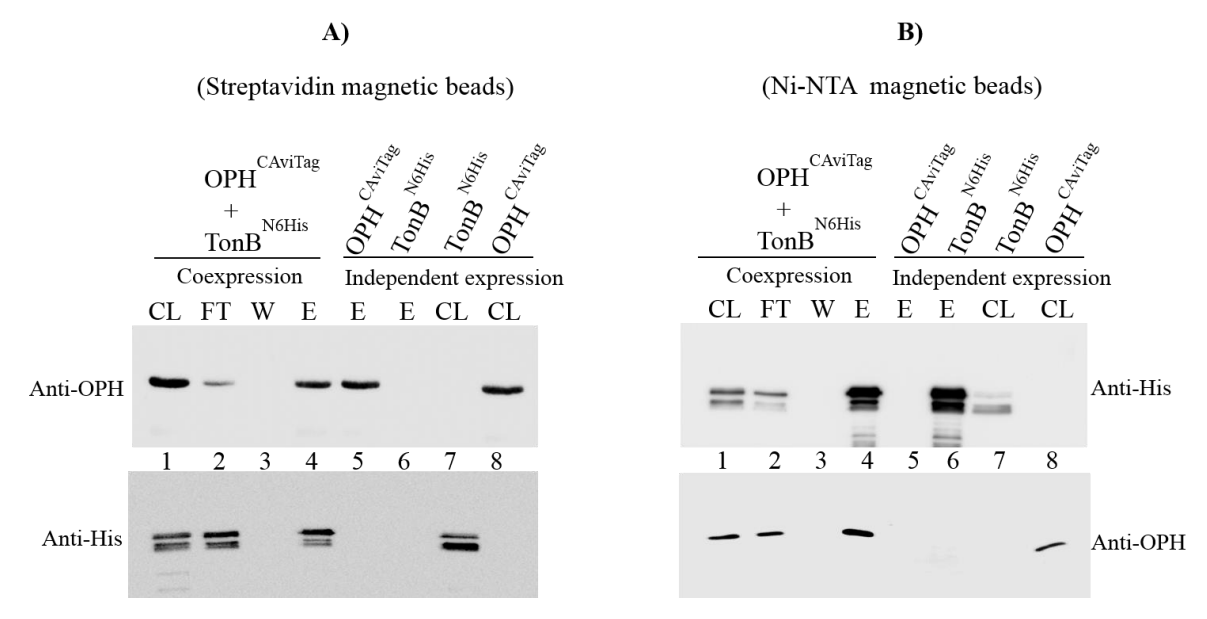


Fig. 4. 15. Pulldown assays performed using streptavidin and Ni-NTA magnetic beads are shown in panels A and B respectively. The cell lysates prepared from cells (pAVB400+pGS16) expressing OPH^{CAviTag} and TonB^{N6xHis} together (co-expression) and separately (Independent expression) were used to perform pulldown assays. CL represents cell lysate used as input. The FT, W and E indicate flowthrough, wash and elution fractions respectively.

The Bacterial two hybrid (BCTH) analysis reveals OPH interats with TonB.

In order to gain secondary evidence on TonB-OPH interactions, adenylate cyclase based bacterial two hybrid system (BCTH) was performed. The TonB and OPH were translationally fused to the T18 and T25 fragments of adenylate cyclase and the resulting plasmids pGS33 and pGS28 (vide meterias and methods section) were co-transformed into BTH101 cells. The interactions between OPH and TonB were assessed by measuring the βgalactosidase activity. The β-galactosidase activity of 2800 miller units was observed in cells expressing TonB-T18 (pGS33) together with T25-OPH (pGS28). However in control cultures expressing TonB-T18 (pGS33) together with T25 (pKT25) gave only 440 units of β-galactosidase activity (Fig. 4. 16). Reciprocally, the OPH and TonB fused to T18 and T25 fragment of adenylate cyclase, the resulting plasmids pGS26 and pGS32 (vide materias and methods section) were co-transformed into BTH101cells. The cultures expressing OPH-T18 (pGS26) together with T25-TonB (pGS32) gave 2600 units of β-galactosidase activity as against 460 units of β-galactosidase activity in control culture expressing TonB-T18 (pGS33) together with T25 (pKT25) (Fig. 4. 16). The higher β-galactosidase activity was observed only when adenylate cyclase fragments fused to TonB and OPH were

together present in cultures. Restoration of active adenylate cyclase activity results in enhanced production of β -galactosidase activity. Such restoration of adenylate cyclase is only possible if physical interactions, exists between TonB and OPH. In control cells expressing TonB-T18 (pGS33) together with T25 (pKT25) and OPH-T18 (pGS26) together with T25 (pKT25) no such interactions are possible therefore not much β -galactosidase activity was observed. These results clearly indicate existence of physical interactions between OPH and TonB. Bacterial two hybrid analysis as well as reciprocal pulldown assays clearly suggest OPH interacts with TonB.

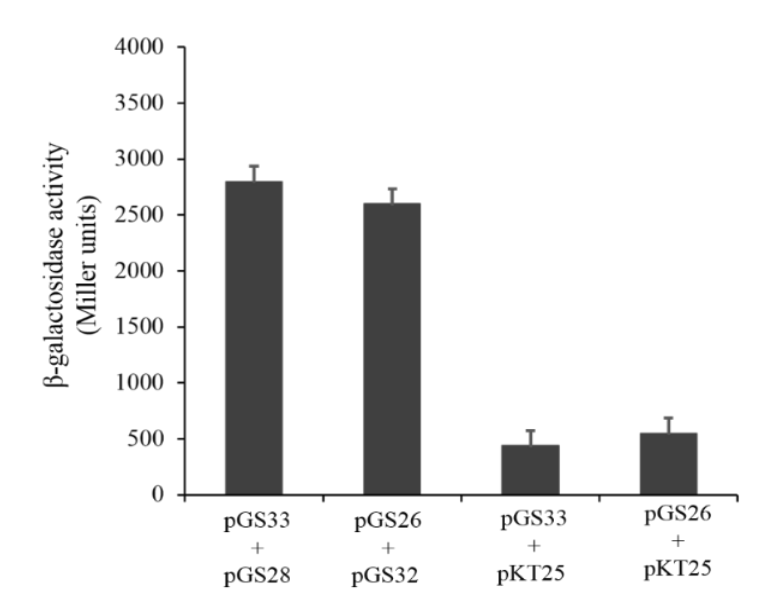


Fig. 4. 16. Bacterial two hybrid assay. Increased β-galactosidase activities were found in cultures having (pGS33+pGS28) and (pGS26+pGS32) due to restoration of adenylate cyclase activity. Similar activity was not found in control cultures having (pGS33+pKT25) and (pGS26+pKT25).

4.3.7. OPH interacts with ExbD

After establishing OPH-TonB interactions, reciprocal pulldowns and bacterial two hybrid assays were performed to assess interactions between ExbD and OPH. The cell lysate prepared from the Arctic express cells (pAVB400 and pGS19) induced for expression of OPH^{CAviTag} and ExbD^{N6xHis} was used to perform pulldown assay using streptavidin and Ni-NTA magnetic beads. The cell lysate, flowthrough, wash and elution fractions collected were analysed on SDS-PAGE. These gels were then used to perform western blot using either anti-OPH or anti-His antibodies (Fig. 4. 17). The ExbD^{N6xHis} and OPH^{CAviTag} specific signals were found in cell lysate indicating co-expression of these two proteins in Arctic express cells (pAVB400+pGS19) (Fig. 4.17. Panels A and B lane 1). None of them were detected in flowthrough and wash fractions (Fig. 4. 17. Panel A lane 2 and 3). As expected in fractions

eluted from streptavidin magnetic beads OPH specific signal was observed due to specific binding of biotinylated OPH to streptavidin magnetic beads (Fig. 4. 17. Panel A lane 4). Interestingly, the elution fraction has shown ExbD^{N6xHis} specific signal when probed with anti-His antibodies (Fig. 4. 17. Panel A lane 4). The elution fractions obtained from streptavidin magnetic beads incubated with cell lysate containing only ExbD^{N6xHis} didn't give any signal specific to ExbDN6xHis (Fig. 4. 17. Panel A lane 6). This clearly suggests that ExbD^{N6xHis} has no affinity to streptavidin magnetic beads and its co-elution from streptavidin magnetic beads is due to its interactions with OPH^{CAviTag}. Reciprocal pulldown assays performed using Ni-NTA magnetic beads gave similar results. The Ni-NTA magnetic beads specifically pull ExbD^{N6xHis} but not biotinylated OPH. Interestingly in elution fraction collected from the lysate containing both $OPH^{CAviTag}$ and $ExbD^{N6xHis}$ the $OPH^{CAviTag}$ specific signal was identified along with $ExbD^{N6xHis}$ (Fig. 4. 17. Panel B lane 4). This may be due to interaction between biotinylated OPH^{CAviTag} and ExbD^{N6xHis}. The elution fraction collected from Ni-NTA magnetic beads incubated with cell lysate containing only $OPH^{CAviTag}$ didn't give any signal suggesting that OPH^{CAviTag} has no affinity to Ni-NTA magnetic beads. The reciprocal pulldown assays, performed in the present study clearly show existence of strong physical interactions between OPH^{CAviTag} and ExbD^{N6xHis}.

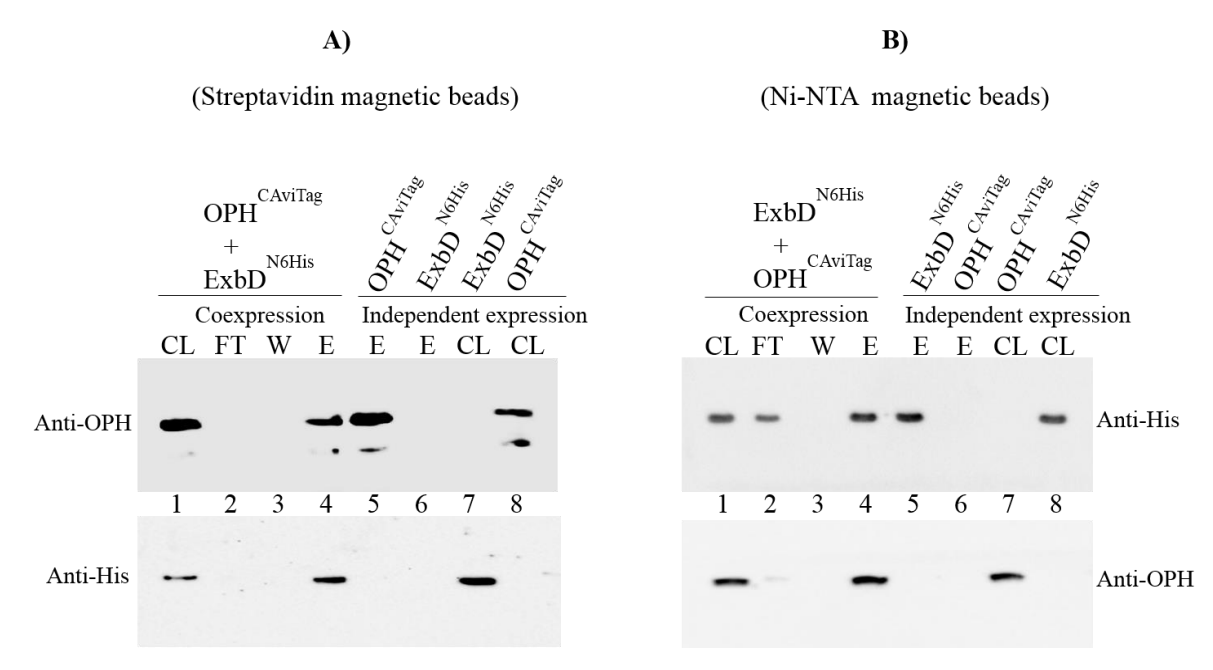


Fig. 4. 17. Pulldown assays performed using streptavidin and Ni-NTA magnetic beads are shown in panels A and B respectively. The cell lysates prepared from cells (pAVB400+pGS19) expressing OPH^{CAviTag} and ExbD^{N6xHis} together (co-expressing) and separately (Independent expression) were used to perform pulldown assays. CL represents cell lysate used as input. The FT, W and E indicate flowthrough, wash and elution fractions respectively.

The Bacterial two hybrid analysis reveals OPH interats with ExbD

The secondary evidence on ExbD-OPH interactions were obtained using adenylate cyclase based bacterial two hybrid system (BCTH). Plasmids were constructed to translationally fuse ExbD and OPH to the T18 and T25 fragments of adenylate cyclase. The resulting plasmids pGS29 and pGS28 were co-transformed into BTH101 cells. The BTH101 cells (pGS29+pGS28) were then used to assess interactions between ExbD and OPH by measuring the β-galactosidase activity. The cultures expressing ExbD-T18 (pGS29) together with T25-OPH (pGS28) gave 3800 units of β-galactosidase activity as against 480 units of β-galactosidase activity in control culture expressing ExbD-T18 (pGS29) together with T25 (pKT25) (Fig. 4. 18). Reciprocally, the OPH and ExbD were fused to T18 and T25 fragments of adenylate cyclase and the resulting plasmids pGS26 and pGS31 were cotransformed into BTH101 cells and performed β -galactosidase activity. The β -galactosidase activity of 3250 miller units was observed in cells expressing OPH-T18 (pGS26) together with T25-ExbD (pGS31) as against 550 of miller units in controls cultures expressing OPH-T18 (pGS26) together with T25 (pKT25) (Fig. 4. 18). The higher β-galactosidase activity observed in cells expressing ExbD-T18 (pGS29) together with T25-OPH (pGS28) may be due to OPH and TonB interactions, which restore adenylate cyclase activity. In control cells expressing ExbD-T18 (pGS29) together with T25 (pKT25) and OPH-T18 (pGS26) together with T25 (pKT25) containing either ExbD-T18 or OPH-T18 failed to activate adenylate cyclase. These results clearly indicates interactions between the OPH and TonB.

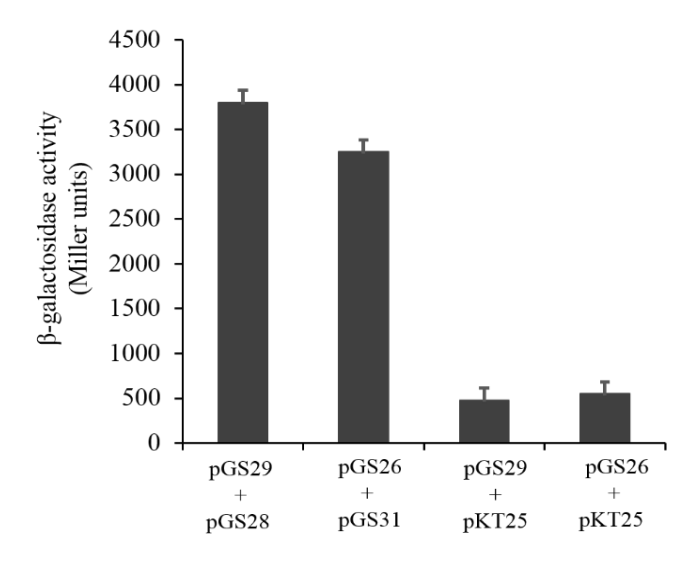


Fig. 4. 18. Bacterial two hybrid assay. Increased β-galactosidase activities were found only in cultures having pGS29+pGS28 and pGS26+pGS31 due to restoration of adenylate cyclase activity. Similar activity was not found in control cultures having pGS29+pKT25 and pGS26+pKT25.

4.3.8. ExbB/ExbD and OPH form complex

Formation of inner membrane associated ExbB/ExbD complex is known in Gramnegative bacteria (Braun et al., 1995). Since ExbB is unstable in the absence of ExbD, the ExbB expression was achieved by cloning the exbBD operon under the control of vector specific T7 promoter. Successful expression of ExbB^{NFLAG} and ExbD^{CMyc} is shown in Arctic express (pGS23) cells (Fig. 4. 14). After achieving the stability of ExbB, pulldown assays were performed to identify interactions between OPH and ExbB-ExbD complex. The Arctic express cells (pOPHV400) expressing biotinylated OPH was transformed with pGS23. The lysate prepared from these cells were then used to perform pulldown assays using streptavidin magnetic beads. As expected, the $OPH^{CAviTag}$, $ExbB^{NFLAG}$ and $ExbD^{CMyc}$ specific signals were seen in cell lysate (Fig. 4. 19. Lane 1). However, none of the proteins were detected in wash fractions (W) (Fig. 4. 19). The elution fraction (E) showed presence of OPH as biotinylated OPH shows affinity to the streptavidin magnetic beads (Fig. 4. 19). Interestingly the elution fraction has also shown presence of ExbBNFLAG and ExbDCMyc suggesting the ExbBNFLAG and ExbDCMyc complex is getting copurified along with biotinylated OPH^{CAviTag} (Fig. 4. 19. Lane 4). The cell lysates prepared from control cultures expressing only ExbBNFLAG and ExbDCMyc didn't show any signal in elution fraction and thus showed no affinity of ExbB^{NFLAG} ExbD^{CMyc} to streptavidin magnetic beads (Fig. 4. 19. Lane 6). The data clearly show interaction of OPH-ExbB/ExbD complex in Arctic express cells due to direct interactions of OPH with ExbD.

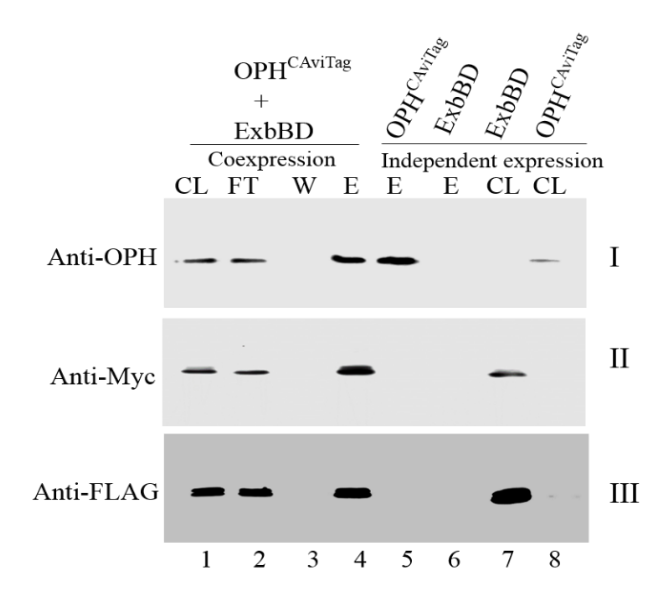


Fig. 4. 19. Interactions between OPH^{CAviTag} and ExbB^{NFLAG}/ExbD^{CMyc} complex. The cell lysate prepared from cultures expressing OPH^{CAviTag} and ExbB^{NFLAG}/ExbD^{CMyc} together (co-expression) and independently were used to perform pulldown assays using streptavidin magnetic beads Panels I, II and III show western blots performed using anti-OPH anti-Myc and anti-FLAG antibodies. CL

represents cell lysate used as input. The FT, W and E indicate flowthrough, wash and elution fractions respectively.

The pulldown assays show existence of physical interactions between OPH and ExbD. However, they don't provide structural details on these interactions. Therefore both *in silco* and *in vitro* approaches were employed to gain structural insights on OPH-ExbD interactions.

4.3.9. In silico predictions on OPH-ExbD interactions

Having establishing that OPH-ExbD physically interact with each other, *in silico* studies were performed to predict amino acid residues involved in the intermolecular interactions. Since complete 3D structure of ExbD is not yet available, its homology model was built using MODELLER (Webb & Sali 2017) based on the available *E.coli* ExbD structures (PDB ids: 5SV1 and 2PFU) (Fig. 4. 20) for alignments and for its stereo chemical quality and fold compatibility respectively (Fig. 4. 21).

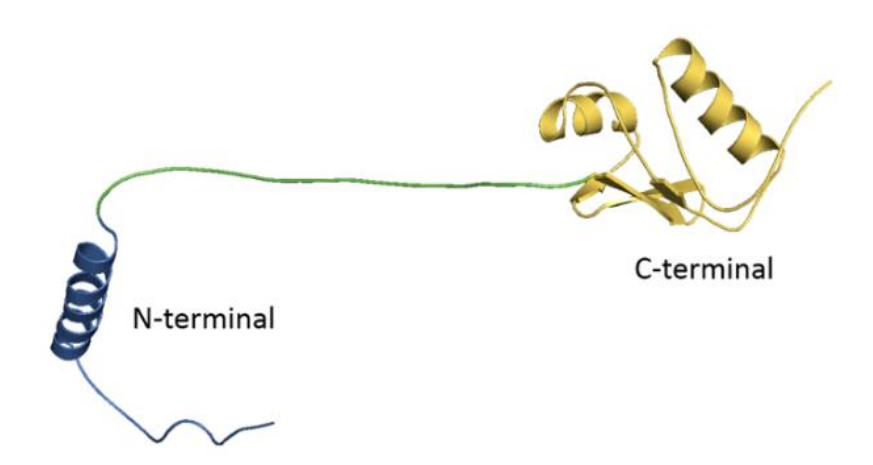


Fig. 4. 20. Homology model of ExbD representing N-terminal region and C-terminal region.

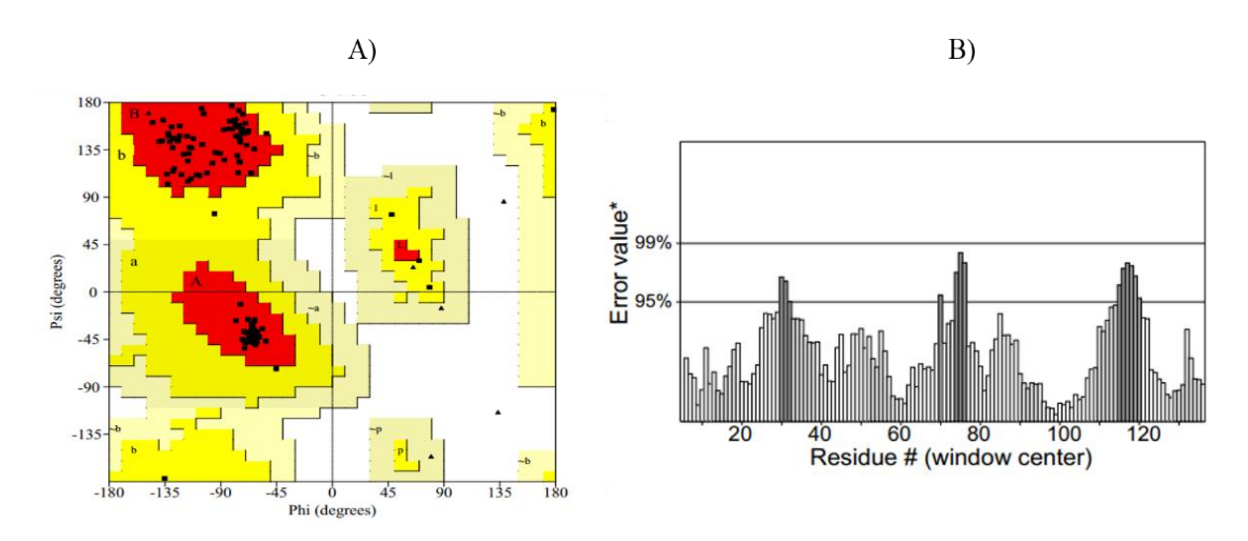


Fig. 4. 21. Panel A and B show Ramachandran plot and Errat plot for homology model of ExbD.

In order to find the amino acid residues that potentially facilitate physical interactions between OPH and ExbD a coevolution study was performed using I-COMS server (Iserte *et al.*, 2015). The study revealed several potentially co-evolving pairs of residues between the two proteins; of these top 100 pairs were based on their weights as coevolving residues (Fig. 4. 22). Among these pairs only those found on the protein surfaces were selected as potential interacting pairs. The ordered pairs of interacting residues between OPH and ExbD thus found are: (E81,Q87), (G291,E48), (G291,Y111), (G291,G133), (P334,S47), (P334,E48), (P334,Y111), (G340,S47), (G340,E48) and (G340,Y111). Using these coevolving surface residues of OPH and ExbD as reference and performed targeted protein-protein docking studies on the two proteins. Of the docking poses selected, the best pose was based on the criteria mentioned in methods section.

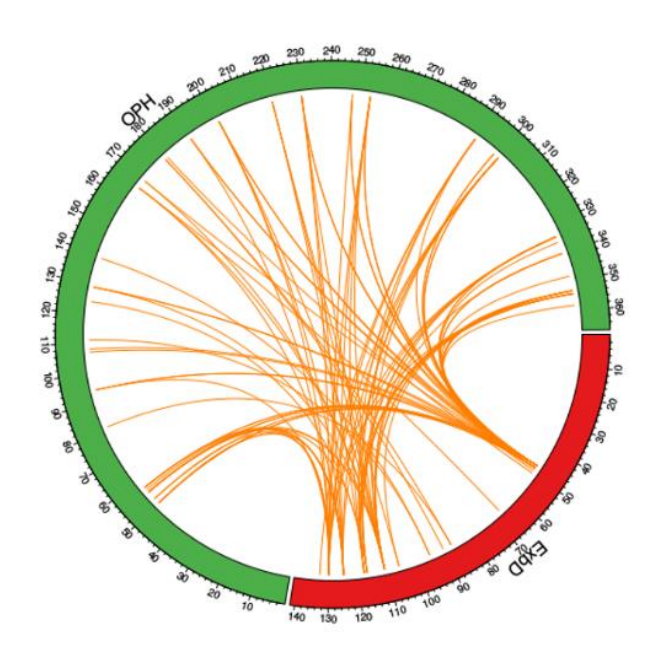


Fig. 4. 22. Circos plot representing top 100 coevolving residues of OPH and ExbD.

According to the best pose, the putative physical interaction between OPH and ExbD is stabilized by polar as well as apolar contacts as given in table 4. D. We also observed similar pose from blind docking studies. Of the interacting residues R96 and R91 of OPH and L83 And V112 of ExbD were predicted as "hotspot" residues by PPCHECK hotspot prediction Tool (Sukhwal & Sowdhamini 2013) (Fig. 4. 23).

Table 4. D: List of potential interactions between OPH and ExbD Interface residues.

	OPH OPH		ExbD	
S. No	Residue	Atom	Residue	Atom
I	Potential Salt Bridges			
1	E48	OE2	R86	NH1
2	E48	OE2	R86	NH2
3	R88	NH2	D81	OD1
4	R88	NH2	D81	OD2
5	R91	NH1	D81	OD1
6	R91	NH1	D81	OD2
7	R91	NH2	D81	OD1
8	R91	NH2	D81	OD2
9	R96	NH1	E116	OE1
10	R96	NH2	E116	OE1
11	R96	NH2	E116	OE2
12	R96	NH1	E120	OE1
13	R96	NH1	E120	OE2
14	R337	NH2	D115	OD1
15	E344	OE1	K122	NZ
16	E344	OE2	K122	NZ
II	Hydrophobic inter	ractions	,	,
1	92A	СВ	82L	СВ
2	93A	СВ	112V	СВ
3	122V	СВ	83L	СВ
4	330L	СВ	112V	СВ
5	333I	СВ	112V	СВ
6	347A	СВ	119A	СВ
7	351V	СВ	119A	СВ

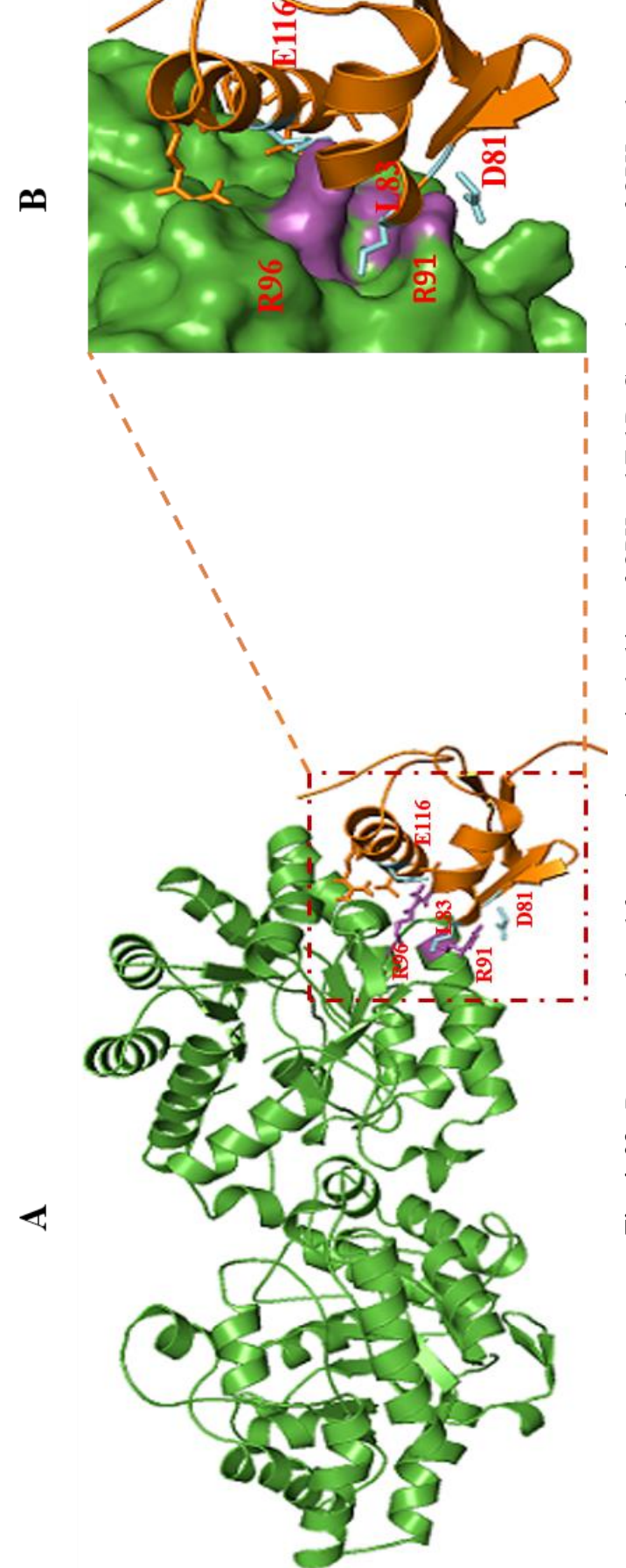


Fig. 4. 23. Best pose selected from protein-protein docking of OPH and ExbD. Complete view of OPH and ExbD proteins in cartoon model and sidechains of residues shown to form saltbridges at interphase are shown as sticks are shown in panel A. Panel B shows close view of interphase of OPH-ExbD. Arg96 forms Leu83. Interphase OPH residues are labelled with three letter code and ExbD residues are labelled with Single saltbridge with Glu116 and Arg91 forms saltbridge with Asp81 and both Arg96 and Arg91 interacts with letter codes shown in panel B.

4.4. OPH interacts with ExbD through 91 and 96 arginine residues

The *in silico* predictions suggested interactions of OPH with ExbD through surface exposed arginine residues found at 91 and 96 positions (Fig. 4. 23). While validating the *in silico* predictions, four OPH variants OPH^{R91A/R96G}, OPH^{R91F/R96G}, OPH^{R91A/R96F} and OPH^{R91F/R96F} and OPH^{R91F/R96F} variants coding plasmids (vide general materials & methods section) and these substitutions were verified by determining the sequence of the plasmids coding OPH variants. OPH^{R91A/R96G}, OPH^{R91A/R96G}, OPH^{R91A/R96F} and OPH^{R91F/R96F} the coding plasmids were designated as pGS^{R91A/R96G}, pGS^{R91F/R96G}, pGS^{R91A/R96F} and pGS^{R91F/R96F} respectively. (Fig. 4. 24).

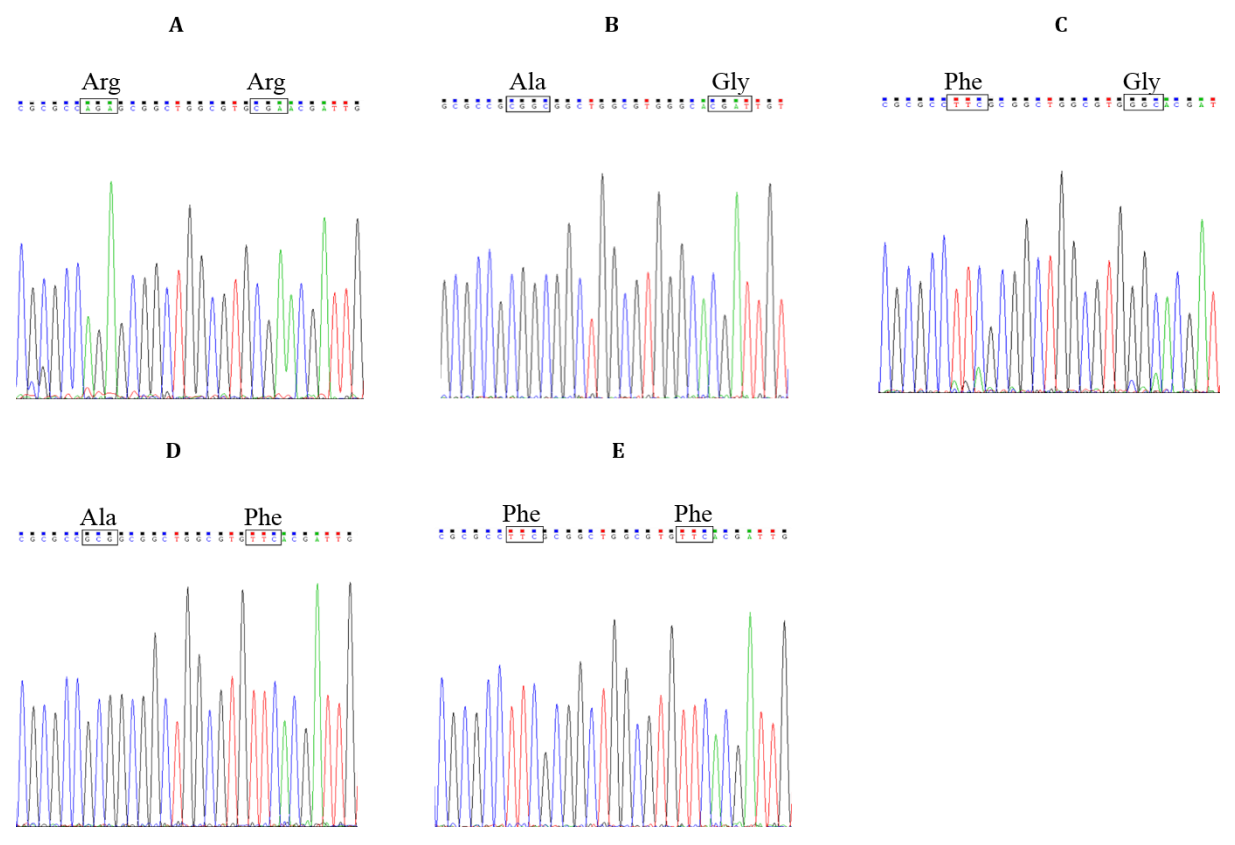


Fig 4. 24. Generation of OPH variants. Panel A shows chromatogram of the native OPH, the codons specify arginines residues are shown in open box. Substitution of these codons with alanine and glycine at positions 91 and 96 respectively are shown in panel B by showing them in open box. Panel C, D and E show substitutions of arginines with phenylalanine and glycine (panel C), alanine and phenylalanine (D) and phenylalanine and phenylalanine (panel E). Codons showing the substitution are shown with open box.

After confirming the generation of *opd* variants the expression and stability of OPH variants were determined by performing western blot and OPH activity. The plasmids pGS^{R91A/R96G}, pGS^{R91A/R96F} and pGS^{R91F/R96F} were independently transformed into *E. coli* cells and the cell lysate was used to perform SDS-PAGE as well as western blots using anti-OPH antibodies (Fig. 4. 25. Panel A). Further the activity was measured for all four of the OPH variants to verify if the OPH variants retained their triesterase its activity. Only two variants OPH^{R91A/R96G}, OPH^{R91F/R96G} have showed triesterase activity (Chaudhry *et al.*, 1988) which is comparable with the activity of native OPH. The remaining two variants, OPH^{R91A/R96F} and OPH^{R91F/R96F} didn't show any triesterase activity (Fig. 4. 25. Panel B) and hence not considered for performing further experiments.

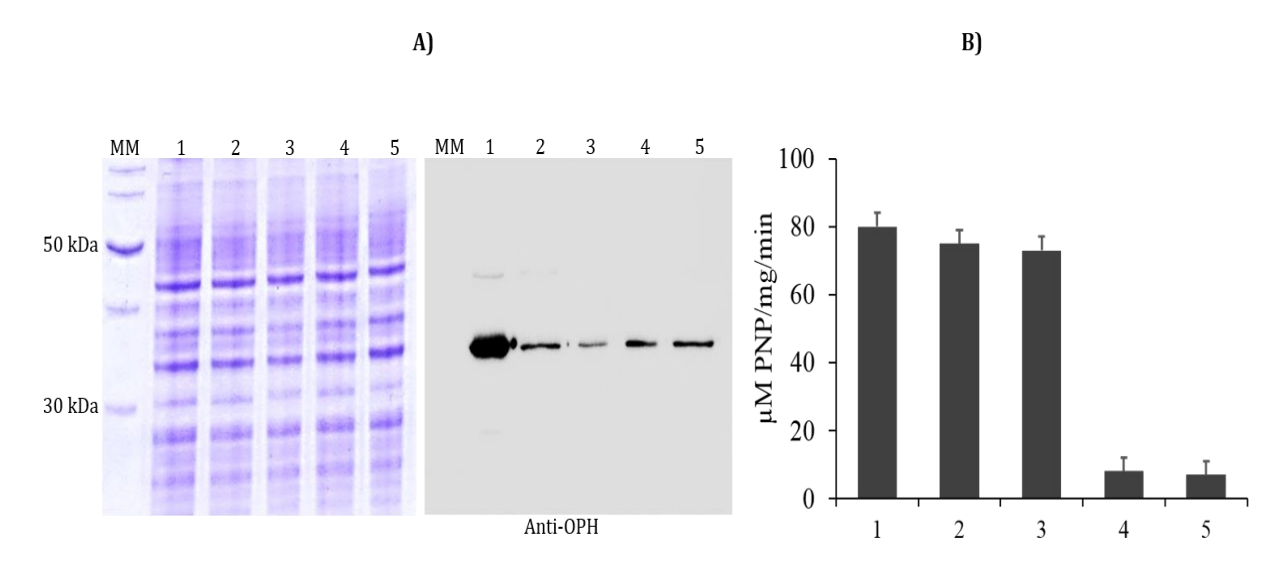


Fig. 4. 25. Stability and activity of OPH variants. Panel A shows (12.5%) SDS-PAGE and corresponding western blot probed using anti-OPH antibodies indicating expression, and stability of OPH (lane 1) and its variants OPH^{R91A/R96G} (lane 2), OPH^{R91F/R96G} (lane 3) OPH^{R91F/R96A} (lane 4) and OPH^{R91F/R96F} (lane 5). The activity of OPH (lane 1) and its variants OPH^{R91A/R96G} (lane 2), OPH^{R91F/R96G} (lane 3) OPH^{R91F/R96A} (lane 4) and OPH^{R91F/R96F} (lane 5) are shown in panel B.

The two plasmids pGS^{R91A/R96G} and pGS^{R91F/R96G} coding, OPH^{R91A/R96G}, OPH^{R91F/R96G} were transformed independently into Arctic express cells expressing ExbD^{N6xHis} (pGS19). The cell lysate prepared from these cells were then used to perform pulldown assays using Ni-NTA magnetic beads (vide materials and methods section). The cell lysate containing native OPH and ExbD^{N6xHis} treated in similar manner were used as positive control. Western blots were performed using either anti-OPH or anti-His antibodies to detect OPH and ExbD^{N6xHis} (Fig. 4. 26). Validating the *in silico* predictions which suggested OPH interactions with ExbD^{N6xHis} through arginine residues found at 91 and 96 positions of OPH,

none of the OPH variants interacted with ExbD^{N6xHis}. There was no OPH specific signal in elution fractions collected from cell lysate co-expressing ExbD^{N6xHis} and OPH^{R91A/R96G} and OPH^{R91F/R96G}. The OPH specific signal was seen only in cultures expressing native OPH (Fig. 4. 26). These results suggest that the OPH interaction with ExbD through surface exposed arginine residues found at 91 and 96 positions. Since ExbB and ExbD interactions are well established reactions between OPH-ExbD, OPH-TonB and ExbB and ExbD lead to formation of Ton complex in Arctic express cells.

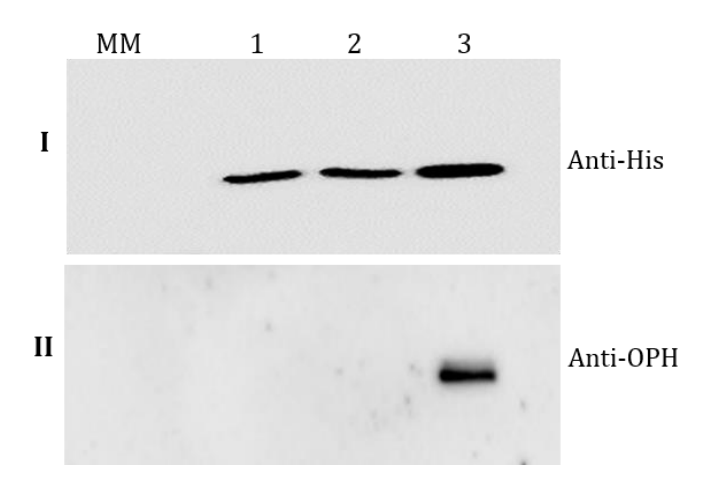


Fig. 4. 26. Interactions between OPH variants and ExbD^{N6xHis}. The lysate prepared from cells expressing ExbD^{N6xHis} in combination of OPH^{R91A/R96G}, OPH^{R91F/R96G} and native OPH were incubated with Ni-NTA magnetic beads and the elution fractions collected were loaded in lane 1, 2 and 3 respectively. Presence of ExbD^{N6xHis} (Panel I) and OPH (Panel II) and its interactions were determined by performing western blots using either anti-His or anti-OPH antibodies.

4.4.1. The TonR^{N6xHis} goes in to inclusion bodies

Cell lysate prepared from the induced similarly the Arctic express cells (pGS20) were lysed and the pellet and soluble fractions were analysed on SDS-PAGE to detect protein found in these fractions. The separated fractions were then probed using anti-His antibodies to detect TonR^{N6xHis}. As shown in fig 4. 27 most of the expressed TonR^{N6xHis} was found in particulate fraction. There was no signal in lane 2 of fig. 4. 27 loaded with clear lysate indicate that most of the expressed TonR^{N6xHis} has gone into inclusion bodies (Fig. 4. 27). The TonR^{N6xHis} couldn't obtained in soluble fraction further changing the expression conditions. Therefore no experiments were done to detect the TonR^{N6xHis} and OPH^{CAviTag} interactions.

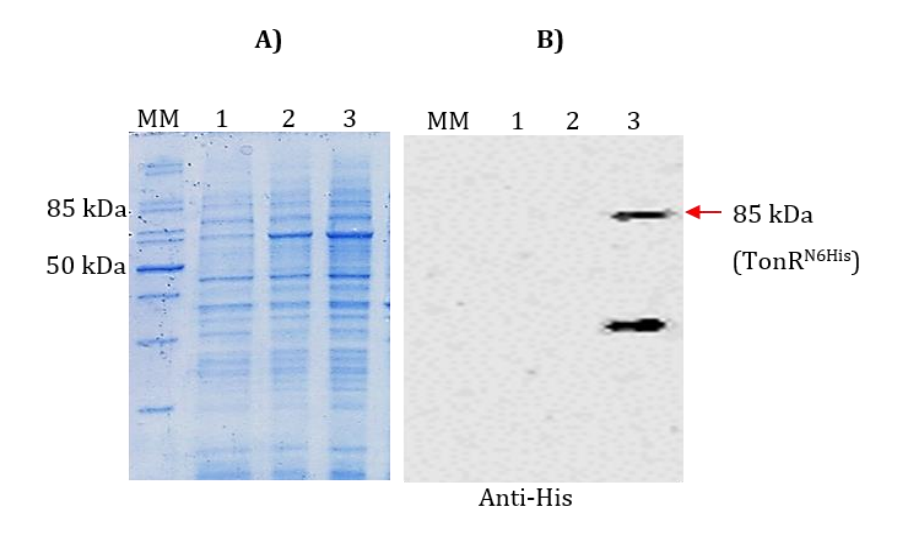


Fig. 4. 27. Shows expression and subsequent detection of TonR^{N6xHis}. The cell lysate of Arctic express (pGS20) cells were fractionated and the clear lysate (lane 2), and particulate fraction (lane 3) analysed on 12. 5% SDS-PAGE (Panel A). The lane 1 shows total cell lysate prepared from uninduced culture. The corresponding western blot performed using anti-His antibodies, indicates presence of TonR^{N6xHis} in particulate fraction (Panel B).

The co-purification of TonB dependent transport (TonBDT) components along with OPH came as a big surprise. Initially the lab colleagues including myself, were skeptical about these results. Therefore the experiments pertaining to purification of OPH was repeated by using the membrane fraction obtained from the *opd* negative mutant of *Sphingopyxis wildii*. The elution fraction didn't contain any proteins indicating that the proteins co-purified with OPH are truly associating with OPH. After gaining confidence that the proteins co-purified with OPH are associating with OPH, further experiments were planned to establish the interactions between OPH and the components of Ton complex.

The results discussed in this chapter clearly show OPH interactions with Ton complex. Both *in silico* and *in vitro* experiments have shown OPH direct interactions with ExbD and TonB. Existence of Ton complex is known in many gram negative bacteria (Ferguson *et al.*, 1998). The role of Ton complex in TonBDT system is known (Noinaj *et al.*, 2010). The Ton complex provides energy to the outer membrane receptor and facilitates active transport across the membrane which is deprived of energy. In gram negative bacteria known to date the Ton complex contains only three proteins TonB, ExbB and ExbD. The ExbB, which is unstable in absence of ExbD is an inner membrane component. About five copies of ExbB proteins exists in Ton complex (Higgs *et al.*, 2002). It contains three transmembrane spanning helices with a large cytoplasmic domain. About two copies of ExbD and one copy of TonB exists in Ton complex (Celia *et al.*, 2017). The ExbB/ExbD

complex generate energy via proton motive force. The generated energy is then transduced to TonB dependent receptor through TonB. TonB interacts with the outer membrane located TonB dependent receptor by establishing physical contact with a conserved sequence motif is known as "TonB-Box". The TonB-Box is located at the N-terminus of all TonB dependent transporters (Noinaj et al., 2010). Upon ligand binding to the TonR, the TonBbox gets exposed facilitating its interaction with TonB. Such interaction leads to conformational changes in TonR and facilitates the release of substrate into periplasmic space (Wiener, 2005). Initially the TonBDT system was identified with transport of B12. Subsequently its role is known in transport of ferric enterobactin, phage T1, nickel complexes, carbohydrates, natural antibiotics...etc (Braun 1999 & Schauer et al., 2008). A number of TonB dependent receptors are there in each gram negative bacteria. The number increases with the complexity of their habitat. Such increase points towards having greater me for TonBDT in survival of gram negative bacteria. Having known such voluminous information about TonBDT in gram negative bacteria, existence of OPH as part of TonBDT is a biggest puzzle. After obtaining undisputable evidence on OPH interactions with Ton complex. Our laboratory has revisited information an OPH and critically questioned its role in degradation of organophosphates. The results to be described in next chapter suggest a new role for OPH. The study thus opened up a door for conducting further study for the better understanding of OPH biology.

Reconstitution of Sf TonBDT system in GS027

5.1. Objective specific methodology

The experimental evidence gained in the preceding chapter clearly demonstrated interactions between OPH, ExbD and TonB. Such novel interactions suggests unusual and hitherto unknown physiological function to OPH. Therefore further experiments were conducted to validate physiological role of OPH. The strategy is to reconstitute TonBDT system of *Sphingobium fuliginis* in *E. coli*, therefore the TonBDT negative mutants were generated in Arctic express cells. After generating TonBDT negative mutants of Arctic express they were complemented with TonBDT system of *Sphingobium fuliginis* by expressing TonBDT components in TonBDT mutant of Arctic express in presence and absence of OPH.

Table 5. A: Primers used in this study

Primer Name	Sequence (5' → 3')	Description
RG9 FP	AAA <u>CATATG</u> ATGCGGAAGCTTGCCCTCGC	Forward primer used to amplify <i>tonB</i> from pGS24 plasmid. The <i>NdeI</i> site appended to facilitate cloning is underlined.
RG9 RP	AAA <u>CTCGAG</u> CTGACCCGAACCCGGACCGTA	Reverse primer used to amplify <i>tonB</i> from <i>S. fuliginis</i> . The <i>Xho</i> I site appended to facilitate cloning is underlined.
RG10 RP	CCTT <u>AGATCT</u> CTAGTTATTGCTCAGCGGTGGC	Vector specific reverse primer used to amplify <i>tonB</i> from pGS24. The <i>Bgl</i> II site appended to facilitate cloning is underlined
RG11 FP	AAA <u>CTGCAG</u> ATCCGGATATAGTTCCTCCTT	Forward primer used to amplify MCS of pET28a vector. The <i>PstI</i> site appended to facilitate cloning is underlined.
RG11 RP	AAA <u>CTGCAG</u> GATAGTCATGCCCCGCGCCCA	Reverse primer used to amplify MCS of pET28a. The <i>Pst</i> I site appended to facilitate cloning is underlined.
RG12 FP	AAA <u>CTGCAG</u> GTGCCTCACTGATTAAGCATT	Forward primer used to amplify <i>oriV</i> and kanamycin resistant gene of pACYC177. The <i>Pst</i> I site appended to facilitate cloning is underlined.
RG12 RP	AAA <u>CTGCAG</u> AGTGTTACAACCAATTAACC	Reverse primer used to amplify <i>oriV</i> and kanamycin resistant gene of pACYC177. The <i>PstI</i> site appended to facilitate cloning is underlined.

RG13 FP	AAA <u>CCATGG</u> AAATGGGTATGGGAAAGTTTGC	Forward primer used to amplify <i>tonR</i> from <i>S. fuliginis</i> . The <i>Nco</i> I site appended to facilitate cloning is underlined.
RG13 RP	AAA <u>CTCGAG</u> CCAGGCCTTTGAGACGGTG	Reverse primer used to amplify <i>tonR</i> from <i>S. fuliginis</i> . The <i>Xho</i> I site appended to facilitate cloning is underlined.
RG24 FP	AGGTATTGTTGCTGCAAAGCCGT	Primer used to amplify <i>exbD::kan</i> region from the genomic DNA of <i>E. coli</i> MG1655 to screen <i>exbD</i> knockout.
RG24 RP	GTGAACGCCTTATCCGGCCTACAA	Primer used to amplify <i>exbD::kan</i> region from the genomic DNA of <i>E. coli</i> MG1655 to screen <i>exbD</i> knockout.
RG26 FP	ACATTTTCACTGATCCTGATCGTCT	Primer used to amplify tonB::kan region from the genomic DNA of E. coli MG1655 to screen tonB knockout.
RG26 RP	ATTATTTAAGTATGTCGCGGTTG	Primer used to amplify tonB::kan region from the genomic DNA of E. coli MG1655 to screen tonB knockout.

Table 5. B: Plasmids used in this Study

Plasmid Name	Description	Reference or Source
pET23b	Amp ^r , The T7 promoter driven expression vector. Facilitates expression of cloned genes with C-terminal 6xHis-tag.	Novagen
pGS2C	Km ^r , low copy number, broad host range expression vector, generated by ligating MCS of pET28a and kanamycin resistant gene and <i>oriV</i> of pACYC177. When cloned it codes for a protein with C-terminal 6xHis-tag.	This Study
pGS5	Amp ^r , Expression plasmid. Codes for TonB ^{C6xHis} . The <i>tonB</i> amplified as NdeI and BglII fragment using pGS24 as template is cloned in pETDuet1.	This Study
pGS6	Amp ^r , Expression plasmid. Generated by cloning <i>exbBD</i> operon in pGS5 as EcoRI and SacI fragment. The <i>exbBD</i> operon is taken from pGS23. Codes for TonB ^{C6xHis} and ExbB ^{NFLAG} /ExbD ^{CMyc} .	This Study
pGS24	Amp ^r , Expression plasmid. Generated by cloning <i>tonB</i> gene in pET23b. The <i>tonB</i> was amplified from <i>Sphingobium fuliginis</i> ATCC 27551 by using RG9 FP and RG10 RP as forward and reverse primers. Codes for TonB ^{C6xHis} .	This Study
pGS25	Km ^r , The T7 promoter driven expression plasmid. Generated by cloning <i>tonR</i> in pGS2C. The <i>tonR</i> was amplified from <i>Sphingobium fuliginis</i> ATCC 27551 by using RG13 FP and RG13 RP as forward and reverse primers. Codes for TonR ^{C6xHis} .	This Study

Table 5. C: Strains used in the present study

Strains	Genotype or Phenotype	Reference or Source
E. coli K-12	Wild type strain,	
MG1655	$F, \lambda, rph 1$	Blattner et al. 1997
E. coli GS023	Gm ^r , Km ^r . Arctic express, exbD::km	This study
	Gm ^r , Δ <i>exbD</i> . Generated by deleting Km resistant	
E. coli GS024	cassette from exbD::Km	This study
E. coli GS026	Gm ^r , Km ^r . Generated by inserting Km cassette into <i>tonB</i> . Δ <i>exbD</i> , <i>tonB</i> ::Km	This study
	Gm ^r . Generated by deleting Km cassette from	
E. coli GS027	$tonB::Km$ of E. coli GS026. $\Delta exbD$, $\Delta tonB$.	This study

5.1.1 Reconstruction of *Sphingobium fuliginis* ATCC 27551 TonB dependent Signal Transduction system in *E. coli*

Reconstruction of TonB dependent transport system of Sphingobium fuliginis ATCC 27551 (sfTonBDT) in E. coli is necessary to validate the role of OPH in TonB dependent transport system. The role of TonB dependent transport system is well characterized in E. coli and other gram negative bacteria (Ferguson et al., 1998; Schauer et al., 2008). However in none of them OPH is shown as part of the system. If precise role of OPH in TonB dependent transport of Sphingobium fuliginis is to be established it is necessary to reconstruct energy coupled outer membrane transport and signal transduction system of S. fuliginis in E. coli. Further OPH is a known Tat substrate (Gorla et al., 2009). It can be expressed as an active protein in E. coli, but it remains as a cytoplasmic protein and never targets to the membrane (Gorla et al., 2009). Generally multi-protein complexes are Tat substrates (Berks et al., 2003; Parthasarathy et al, 2016). Since OPH interacts with TonB dependent transport system, if the system is reconstructed in E. coli there is a possibility for the OPH complex to target membrane. In order to test the aforementioned hypothesis it is necessary to express TonB dependent transport components of S. fuliginis in E. coli without disturbing their respective signal peptides. Therefore TonB dependent transport components are expressed in E. coli with detectable epitopes at the C-terminal end.

5.1.2. Generation of TonB dependent transport negative strains of *E. coli*.

The TonB transport system (TonBDT) of *E. coli* consists of four proteins. They are TonB dependent outer membrane receptor (TonR), the energy transducer, TonB and the

protonmotive force (PMF) generating component proteins ExbB/ExbD. The TonB, ExbB and ExbD complex is designated as energy transducing system or Ton complex (Noinaj *et al.*, 2010). The ExbB is unstable in the absence of ExbD (Held *et al.*, 2002). Similarly the TonB is essential for the TonBDT function as it transduces energy generated from inner membrane associated proton motive force pump components ExbB and ExbD to TonR located in outer membrane. Therefore these two genes are deleted to create TonBDT null mutants in *E. coli* Arctic express strain.

5.1.3. Generation of ExbD mutant

Initially the *E. coli exbD* keio mutant was obtained (generous gift from Dr. Manjula Reddy, CCMB, Hyderabad) and used to generate *exbD* mutant in Arctic express strain by following P1 Transduction method (Thomason *et al.*, 2007).

5.1.4. Transduction:

- a) Phage P1 lysate preparation: In order to create exbD mutant of $E.\ coli$ Arctic express, 0.3ml of overnight culture of donor $E\ coli$ K12 MG1655 $\Delta exbD$ strain having a mutation in exbD gene was mixed with 10µl of P1 phage (10 7 Pfu) and incubated at 37 $^\circ$ C without shaking to facilitate phage adsorption. About 10ml of LB broth and sterile CaCl₂ (5mM) was added to this infection mixture prior to its incubation with shaking at 37 $^\circ$ C for 4 to 6 h or till the complete lysis of cells. After observing the cell lysis, 200µl of chloroform was added to the phage lysate to prevent further growth of the cells. This preparation was centrifuged at 5500 rpm for 10 min to remove cell debris. The obtained supernatant containing transducing particles was stored at 4 $^\circ$ C until further use.
- b) Phage infection: To the 2ml of overnight culture of Arctic express cells, 5mM CaCl₂ and 100μl of phage preparation was added. After addition of phage lysate, the cells were incubated at 37°C for about 15 min to allow phage adsorption. Unabsorbed phage particles were removed by centrifuging at 5500 rpm for 10 min. Further 5ml of LB broth containing 10mM sodium citrate was added to the infected *E. coli* cells and allowed to incubate for 45 min at 37°C. Finally the cells were harvested and resuspended in 0.2ml of fresh LB broth and plated on LB agar plates containing 10mM sodium citrate and 30μg/ml of kanamycin. Finally the mutation in respective gene was confirmed by performing PCR amplification by using RG24 FP and RG24 RP which were designed 100bp upstream and downstream of the *exbD* gene of *E. coli*. The resulting strain named as *E. coli* GS023, acquires kanamycin resistance.

c) Elimination of the Kanamycin resistance cassette from E. coli GS023

After generating E. coli GS023, pCP20 plasmid was electroporated in to it by following standard protocol (Datsenko et al., 2000). The pCP20 plasmid confers ampicillin and chloramphenicol resistance. It has temperature sensitive origin of replication and encodes FLP recombinase. After electroporation, cells were plated on LB plates containing ampicillin (50µg/ml) or chloramphenicol (15µg/ml) and incubated at 30°C for 12 to 18h. Picked a single colony and inoculated in to 3ml LB media and incubated overnight at 42°C with shaking at 180 rpm to induce FLP recombinase and to eliminate kanamycin resistance cassette. Since pCP20 replicates using temperature sensitive replication origin growth of E. coli GS023 strain at 42⁰C results in loss of pCP20. After incubation, 100μl of overnight culture was taken and serially diluted before plating 50µl from 10⁻⁵ and 10⁻⁶ dilution on LB plates (without antibiotics) and incubated at 37°C for 12h. Next day 6 colonies were taken and streaked on LB+Amp, LB+Cm, LB+Km, LB plates and incubated at 37°C for overnight. Cells grown on LB plates but not on LB+Amp, LB+Km, LB+Cm this indicates loss of the pCP20 plasmid and eliminated kanamycin cassette from the strain. Few colonies were taken and screened for loss of kanamycin cassette by PCR using RG24 FP and RG24 RP. The resulting kanamycin sensitive E. coli exbD null mutant designated as E. coli GS024 and used for further experiments.

5.1.5. E. coli exbD, tonB double mutant

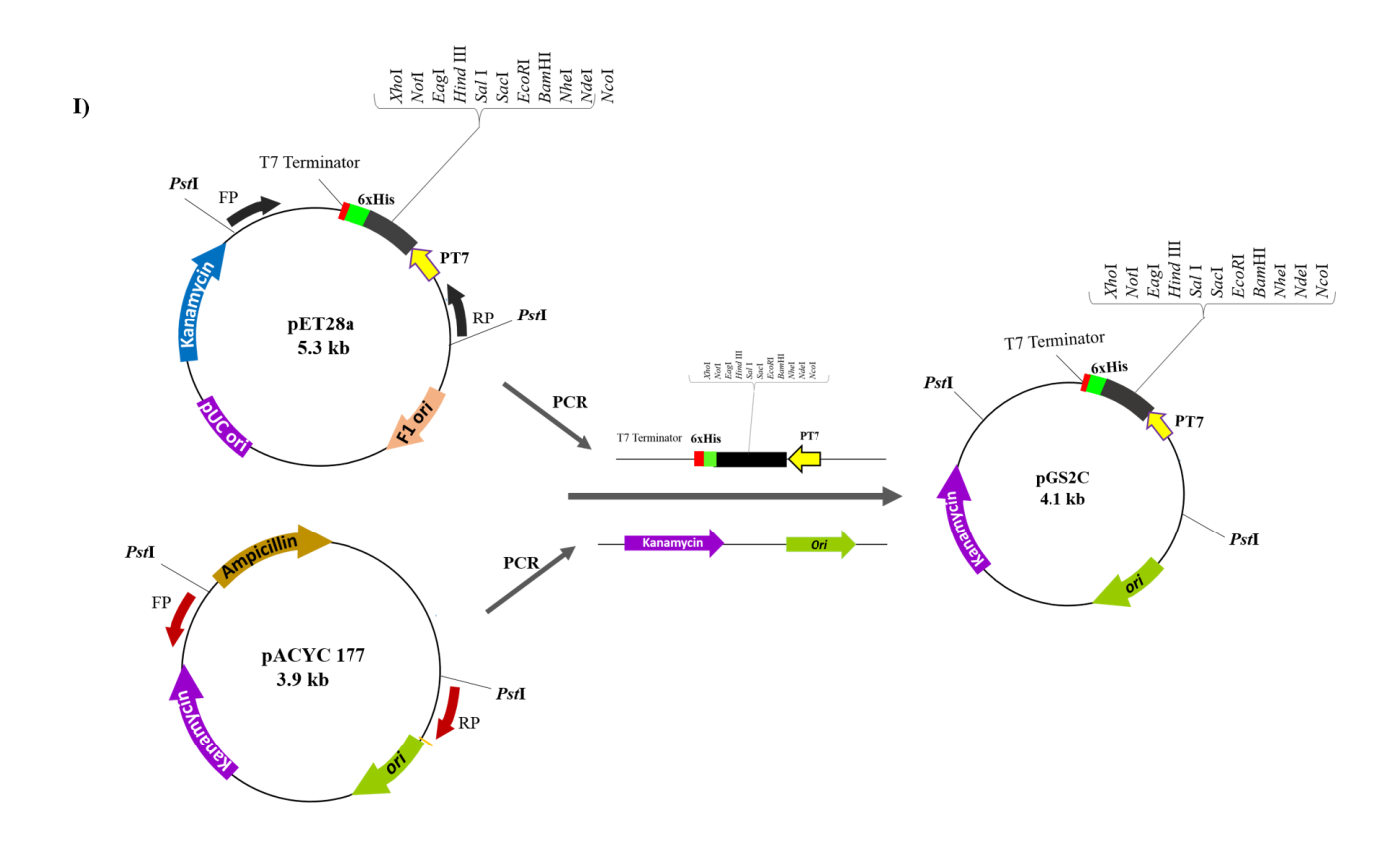
In order to generate *tonB* mutant in GS024, *E. coli* keio *tonB* null mutant used as donor and *E. coli* GS024 used a recipient. Followed the P1 phage transduction method described above to generate *tonB* mutant. The *tonB* mutant in *E. coli* GS024 strain was identified by performing colony PCR by using RG26 FP and RG26 RP which were designed taking sequence found 100bp upstream and downstream of the *tonB* gene of *E. coli*. The resulting strain named as *E. coli* GS026 it acquires kanamycin resistance due to insertion Km cassette in *tonB* (*tonB::Km*). Further, the kanamycin cassette was removed from the strain *E. coli* GS026 by using pCP20 plasmid by using standard protocol described above. The resulting strain named as *E. coli* GS027 strain is a deletion mutant of *exbD*, *tonB* and is kanamycin sensitive.

5.1.6. Construction of compatible expression systems to reconstitute s_f TonBDT in E. coli

Three expression vectors were used for expressing all components of TonBDT of *S fuliginis* ATCC 2755 in *E. coli*. One of them is pETDuet1 and it is used to express ExbB/ExbD and TonB. The second expression vector, compatible to pETDuet1, is pACYC177 derivative constructed in this study. The third expression plasmid is pMMB206 (Morales *et al.*, 1991) derivative and is used to express OPH^{CAviTag}.

5.1.7. Construction of expression vector with oriV of p15A incompatible group

The expression vector pGS2C was constructed by taking MCS of pET28a and replicative origin and kanamycin resistance gene from pACYC177. The corresponding regions from these two plasmids were amplified as PstI fragments using primers RG11 FP, RG11 RP and RG12 FP, RG 12 RP (Fig. 5. 1 Panel II- A). The generated amplicons were digested with PstI and ligated following standard protocols. The resulting expression vector is designated as pGS2C (Fig. 5. 1 Panel II- B). Since it contains pET28a MCS the cloned genes will be fused to the vector specific His-tag coding sequences and the recombinant protein coded by pGS2C derivatives will have C-terminal 6xHis-tag.



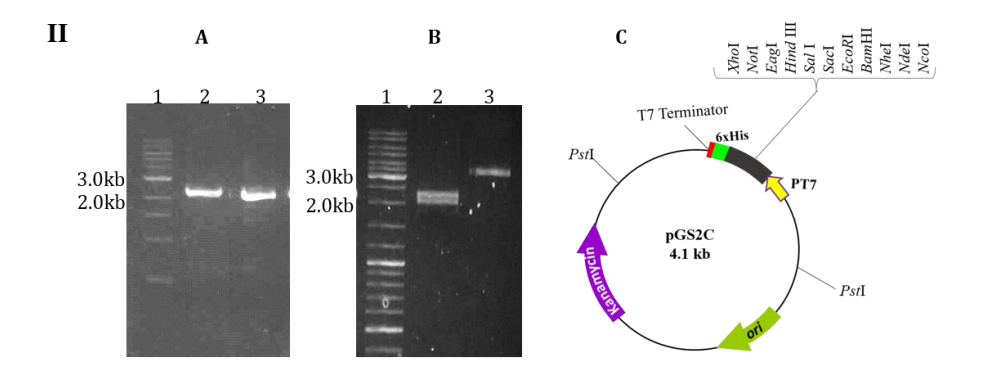


Fig. 5. 1. Construction of expression vector pGS2C. The schematic representation of pGS2C construction is shown in panel I. Panel II-A shows PCR amplification of *oriV* and kanamycin resistance gene (2.1kb) of pACYC177 (lane2) and PCR amplification of MCS and *Pt*7 region of pET28 vector (2kb) (lane3). The 1kb DNA ladder used as size marker is loaded in lane 1. Pst1 digested pGS2C is shown in panel B. Panel C shows diagrammatic representation of pGS2C.

5.1.8. Construction of pGS6

The *tonB* of gene was cloned in one of the MCS of pETDuet1. Before cloning in pETDuet1 the *tonB* gene was amplified from genomic DNA of *Sphingobium fuliginis* by using RG9 FP and RG9 RP appended with NdeI and XhoI restriction sites The PCR product was then digested with NdeI and XhoI and ligated to similarly digested pET23b vector. The resulting plasmid encodes TonB with C-terminal 6xHis-tag and is designated as pGS24 (Fig. 5. 2).

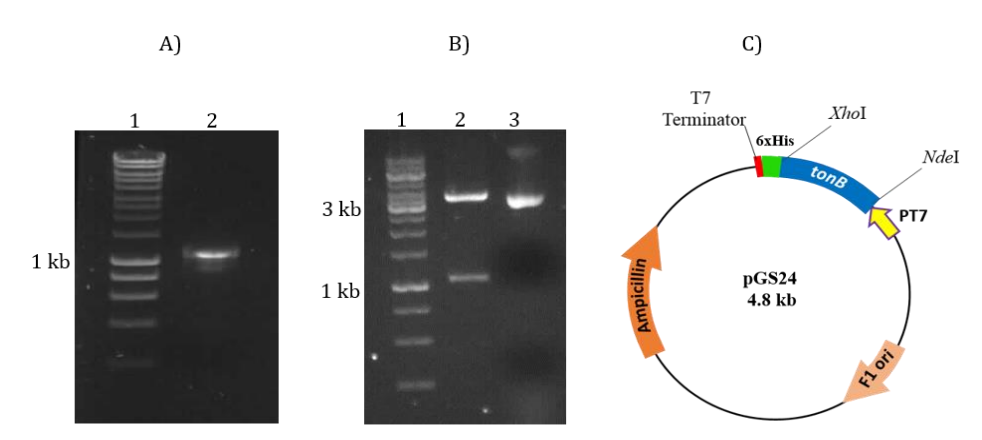


Fig. 5. 2. Construction of pGS24. Panel A shows PCR amplification of *tonB*. Lanes 1 & 2 show 1kb DNA ladder and PCR amplicon containing *tonB* (1.2kb). Panel B shows ligation of *tonB* in pET23b vector. Lanes 1 & 2 indicate 1kb DNA ladder and release of insert containing *tonB* from pGS24 upon digesting with NdeI and XhoI. The undigested plasmid pGS24, is loaded in lane 3. Panel C shows diagrammatic representation of pGS24 plasmid.

The plasmid pGS24 was then used as a template to amplify *tonB* gene RG9 FP and RG10 RP as forward and reverse primers respectively (Fig. 5. 3. Panel A). The PCR amplicon was then digested with NdeI and BglII and ligated at MCS2 of pETDuet1 digested with similar

enzymes. The resulting recombinant plasmid named as pGS5, encodes TonB with C-terminal 6xHis-tag (Fig. 5. 3. Panel B).

The *exbBD* operon was taken as an EcoRI and SacI fragment from pGS23 and ligated to similarly digested pGS5 (Fig. 5. 3. Panel C). The resulting recombinant plasmid, pGS6 encodes three components of TonB transport components, viz. ExbB^{NFLAG}, ExbD^{CMyc} and TonB^{C6xHis}. The remaining two proteins of *sf*TonBDT are TonB dependent receptor (TonR) and OPH. Out of these two *tonR* was cloned in pGS2C to express TonR^{C6xHis} and the expression plasmid pOPHV400 constructed in our previous study was used as source of plasmid coding biotinylated OPH, OPH^{CAviTag} (Parthasarathy *et al.*, 2016).

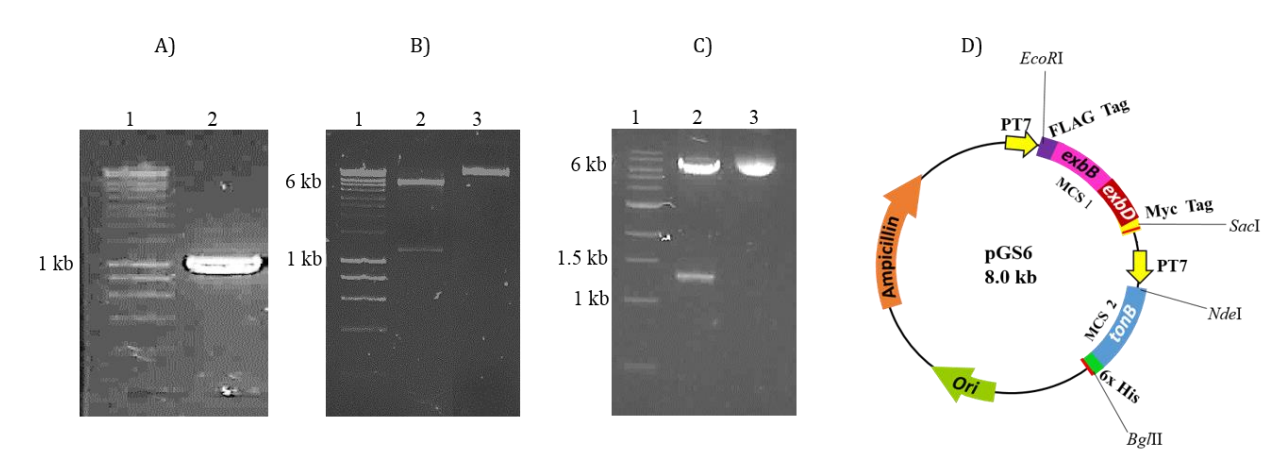


Fig. 5. 3. Construction of pGS6. Panel A shows PCR amplification of *tonB*. Lanes 1 & 2 show 1kb DNA ladder and PCR amplicon containing *tonB* (1.2kb). Panel B shows ligation of *tonB* at the MCS2 of pETDuet1 vector. Lanes 1 & 2 indicate 1kb DNA ladder and release of insert containing *tonB* from pGS5 upon NdeI and BgIII digestion. The undigested plasmid pGS5, is loaded in lane 3. Panel C shows ligation of *exbBD* operon at the MCS1 of pGS5. Lanes 1 & 2 indicate 1kb DNA ladder and release of insert containing *exbBD* operon from pGS6 upon digesting with EcoRI and SacI. Undigested pGS6 plasmid shown in lane 3. Panel D shows diagrammatic representation of pGS6 plasmid.

5.1.9. Construction of pGS25

TonB dependent receptor gene (*tonR*) was amplified using genomic DNA of *Sphingobium fuliginis* as template and RG13 FP and RG13 RP as forward and reverse primers (Fig. 5. 4. Panel A). The generated amplicons were digested with NcoI and XhoI ligated to similarly digested pGS2C (Fig. 5. 4. Panel B). The resulting plasmid, pGS25 encodes TonR^{C6xHis}.

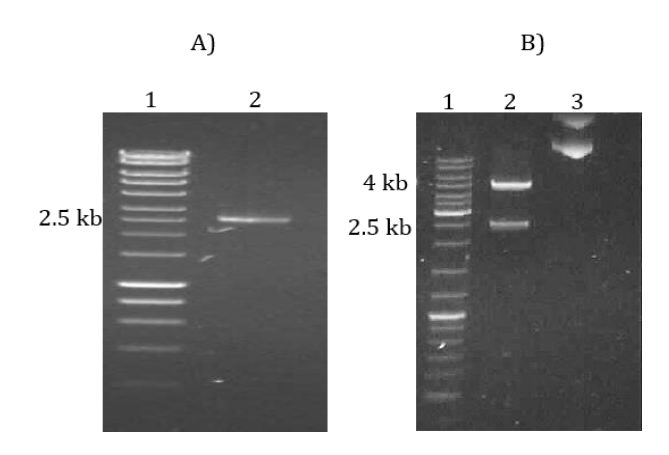


Fig. 5. 4. Construction of pGS25. Panel A shows PCR amplification of *tonR*. Lanes 1 & 2 show 1kb DNA ladder and PCR amplicon (2.5kb) containing *tonR*. Panel B shows ligation in pGS2C. Lanes 1 & 2 show 1kb DNA ladder and release of insert containing *tonR* from pGS25 upon digestion with NcoI and XhoI. The undigested pGS25 is loaded in lane 3.

5.2.0. Expression and subcellular localization of *sf*TonBDT components in *E. coli* GS027:

Before reconstituting *Sf*TonBDT components in *E. coli* their expression and subcellular localization was checked independently in *E. coli* GS027.

5.2.1. Expression and subcellular localization of TonR^{C6xHis}

The *E. coli* GS027 (pGS25) encoding TonR^{C6xHis} was induced following procedures described in general methods section. The subcellular fractionations of the induced culture was done by following procedures described elsewhere (Gorla *et al*, 2009). The cytoplasm and membrane fractions were analysed on SDS-PAGE and the existence of TonR^{C6xHis} was detected by performing western blot using anti-His antibodies.

5.2.2. Expression and subcellular localization of ExbBNFLAG/ExbDCMyc

The *E. coli* GS027 (pGS23) was induced as described in general methods section. The subcellular fractions were prepared following procedures optimized in our laboratory (Gorla *et al.*, 2009) and as described in general methods section. The presence of ExbB^{NFLAG} and ExbD^{CMyc} were detected by probing these fractions by using anti-FLAG and anti-Myc antibodies.

5.2.3. Expression and subcellular localization of TonB^{C6xHis}

The *E. coli* GS027 (pGS24) cells were induced following the method described in general methods section. Its expression and subcellular localization was described following procedures optimized in our laboratory (Gorla *et al.*, 2009). The cytoplasm and membrane

fractions were analysed on SDS-PAGE and the existence of TonB^{C6xHis} was detected by performing western blots using anti-His antibodies.

5.2.4. Expression and subcellular localization of OPH^{CAviTag}

The *E. coli* GS027 (pOPHV400) was induced following standard procedures described in general methods and the cells were fractionated (vide General methods) and the membrane purity was assessed by assaying marker enzymes. The presence of OPH^{CAviTag} in subcellular fractions was determined by performing western blots using anti-OPH antibodies.

5.2.5. Co-expression of $OPH^{CAviTag}$ and $TonB^{C6xHis}$ and subcellular localization of $OPH^{CAviTag}$

The *E. coli* GS027 (pOPHV400 + pGS24) was induced following standard procedures described in general methods and the cells were fractionated (vide General methods) and the membrane purity was assessed by assaying marker enzymes. The presence of TonB^{C6xHis} and OPH^{CAviTag} in subcellular fractions were detected by performing western blotting with anti-His and anti-OPH antibodies.

$5.2.6. \quad Co-expression \quad of \quad OPH^{CAviTag} \quad and \quad ExbB^{NFLAG}/ExbD^{CMyc} \quad and \quad subcellular \\ localization \quad of \quad OPH^{CAviTag}$

The *E. coli* GS027 (pOPHV400 + pGS23) was induced following standard procedures described in general methods and the cells were fractionated (vide General methods) and the membrane purity was assessed by assaying marker enzymes. The presence of ExbB^{NFLAG}, ExbD^{CMyc} and OPH^{CAviTag} in subcellular fraction was detected by performing western blots with anti-OPH, anti-FLAG, anti-Myc and anti-OPH antibodies.

5.2.7. Verification of *E. coli* GS027 for TonBDT null phenotype

The strain *E. coli* GS027 generated by deleting *exbD* and *tonB* was tested for TonBDT negative phenotype. The ExbD and TonB are prominent components of TonBDT system involved in iron acquisition. Therefore GS027 was tested if it can grow under iron limiting conditions.

5.2.8. Reconstitution of sfTonBDT without OPH in E. coli GS027.

E. coli GS027 strain was used as model system to reconstitute _{Sf}TonBDT components. *E. coli* GS027 (pGS6+pGS25) was induced to express TonB^{C6xHis}, ExbB^{NFLAG}/ExbD^{CMyc} and TonR^{C6xHis} following standard procedures described in general methods and the cells were fractionated (vide General methods) and the membrane purity was assessed by assaying marker enzymes. The presence of ExbB^{NFLAG} ExbD^{CMyc}, TonB^{C6xHis} and TonR^{C6xHis} in

subcellular fraction was detected by performing western blotting with anti-FLAG, anti-Myc and anti-His antibodies.

5.2.9. Reconstitution of SfTonBDT with OPH in E. coli GS027

E. coli GS027 (pGS6+pGS25) + (pOPHV400) was induced following standard procedures described in general methods and the cells were fractionated (vide General methods) and the membrane purity was assessed by assaying marker enzymes. The presence of ExbB^{NFLAG} ExbD^{CMyc}, TonB^{C6xHis}, TonR^{C6xHis} and OPH^{CAviTag} in subcellular fraction was detected by performing western blotting with anti-FLAG, anti-Myc, anti-His and anti-OPH antibodies.

5.3. Results & Discussion

5.3.1. Construction of TonB dependent transport deficient Arctic express cells (*E. coli* GS027).

As mentioned in earlier sections the TonBDT system is essential for transport of nutrients. The prominent components of TonBDT are TonB and ExbD. The TonB transduces energy generated by cytoplasmically located ExbB and ExbD through proton motive force to TonR located at the energy deprived outer membrane. The ExbB is unstable in the absence of ExbD (Held et al., 2002). The E. coli having deletion either tonB or exbD showed TonBDT negative phenotype (Skare & Postle 1991). Therefore TonBDT negative Arctic express cells were generated by deleting of both tonB and exbD. The transducing particles generated by infecting on keio mutant (exbD::km) strain have successfully transduced Arctic express cells and the exbD gene got successfully replaced by exbD::km. The kanamycin resistance colonies of Arctic express generated after transduction were screened for presence of exbD::km. The PCR amplicon clearly shown elimination of exbD with exbD::km. The increase size of *exbD::km* is clearly seen in kanamycin resistance colonies of Arctic express generated after transduction (Fig. 5. 5. Panel A). The exbD null mutants of Arctic express cells are kanamycin resistance. The strain needs to be used for reconstruction of SfTonBDT components. Therefore existence of kanamycin cassette is hindrance for transform kanamycin resistant expression plasmids coding TonBDT components. Therefore the kanamycin cassette is removed by transforming into kanamycin resistance exbD mutant of Arctic express with temperature sensitive FLP recombinase coding pCP20. The FLP recombinase removed kanamycin cassette from the exbD::km and the generated exbD null mutant without kanamycin cassette. The kanamycin sensitive colonies generated through

FLP recombinase clearly showed deletion of kanamycin gene from *exbD* null mutant of Arctic express (Fig. 5. 5. Panel B).

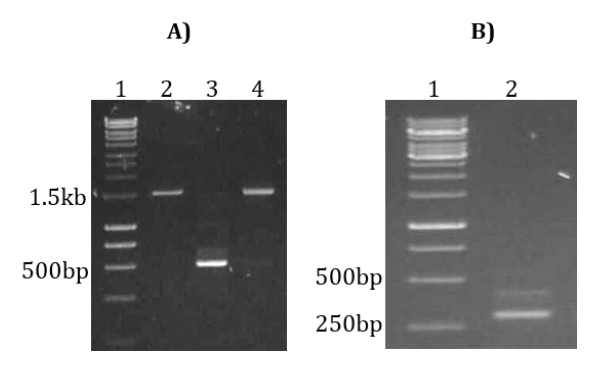


Fig. 5. 5. Generation of km sensitive *E. coli* ($\triangle exbD$). Panel A shows PCR amplification of *E. coli* (exbD::km) from Arctic express cells transduced with phage P1 particles obtained from keio exbD::km null mutants of *E. coli*. Lanes 1 & 2 show 1kb DNA ladder, PCR amplicon from Arctic express exbD::km (1.5kb) cells. Lanes 3 & 4 show PCR amplicon of exbD gene from wild type (500bp) and keio mutant (exbD::km) cells. Panel B shows deletion of km cassette from Arctic express (exbD::km) cells using FLP recombinase. Lanes 1 & 2 show 1kb DNA ladder and PCR amplification generated from Arctic express ($\triangle exbD$) cells after deleting km cassette from exbD::km region (220bp).

The kanamycin sensitive *exbD* mutant was then used to delete *tonB* by infecting transducing particles of phage P1 obtained after infecting *tonB::km* keio mutants of *E. coli*. The replacement of *tonB* from *exbD* null mutant of Arctic express with *tonB::km* is evident as PCR amplification done using *tonB* specific primers gave *tonB::km* amplification (Fig. 5. 6. Panel A). Subsequent removal of kanamycin cassette clearly showed deletion of kanamycin gene (Fig. 5. 6. Panel B). The *exbD* and *tonB* double mutant of Arctic express strain thus generated was designated as *E. coli* GS027 and is used for the reconstitution of *Sphingobium fuliginis* TonBDT components by expressing TonB dependent transporter TonR and Ton complex components TonB, ExbB and ExbD.

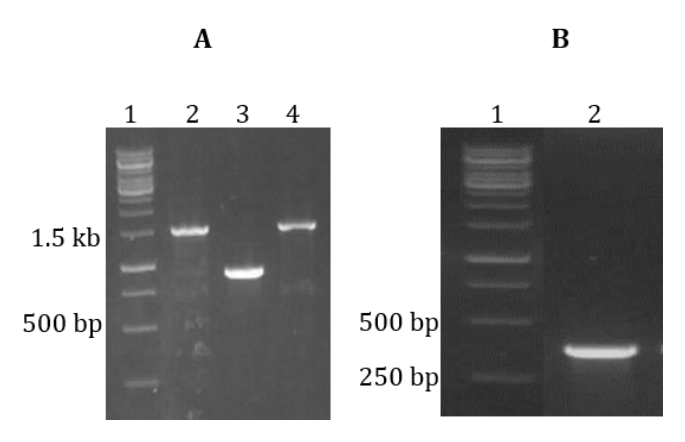


Fig. 5. 6. Generation of *E. coli* GS027. Panel A shows PCR amplification of tonB::km in km sensitive Arctic express ($\Delta exbD$) cells infected with transducing particles of phage P1 obtained from

tonB mutants of *E. coli* keio strain. The 1kb DNA ladder and *tonB::km* amplicon generated from Arctic express (Δ*exbD*) mutant cells generated after infecting with P1 transducing particles obtained from *tonB* keio mutant of *E. coli* are shown in lanes 1 and 2. Lanes 3 & 4 show PCR amplicon of *tonB* gene from wild type Arctic express strain (850bp) and keio mutant *tonB::km* used as a positive control. Panel B shows PCR amplification of DNA region of *tonB* after deleting km cassette from *E. coli* (Δ*exbD*) Arctic express cells (lane 2). 1kb DNA ladder loaded in lane 1.

5.3.2. The TonR^{C6xHis} is found in the membrane of GS027 cells.

After generating TonBDT negative mutant of Arctic express cells (*E. coli* GS027) they were transformed with expression plasmid (pGS25) coding TonR^{C6xHis} and the expression of TonR^{C6xHis} was induced for 12h by following protocols described in materials and methods section. The expression of TonR^{C6xHis} was only seen in cells induced for 3h. There was a slight increase in its expression in overnight induced cultures (Fig. 5. 7. Panel B)

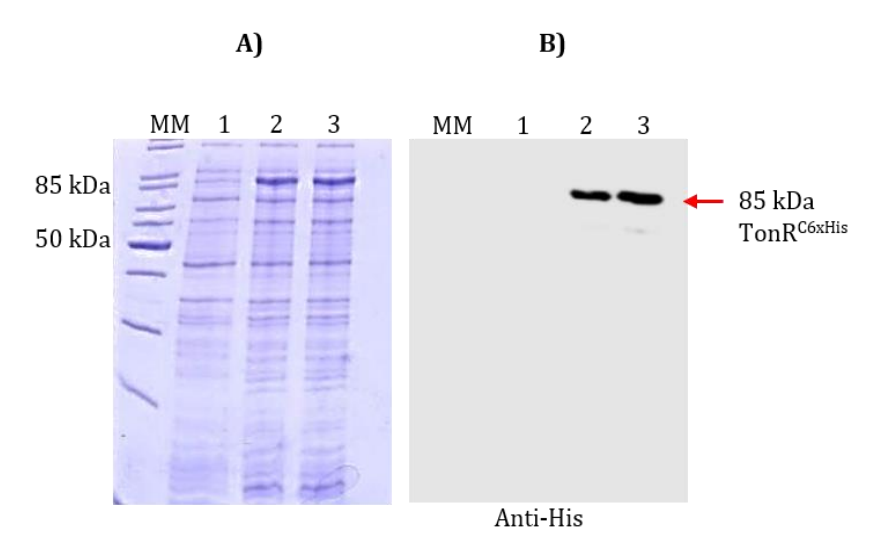


Fig. 5. 7. Expression of TonR^{C6xHis} in GS027 (pGS25) cells. The cell lysate collected from uninduced cells is loaded in lane 1. The cell lysate prepared from GS027 (pGS25) cells induced for 3h (lane 2) and 12h (lane 3) was analysed on 12.5% SDS-PAGE (Panel A). The corresponding western blot probed using anti-His antibodies is shown in panel B. Expression of TonR^{C6xHis} is shown with arrow.

After confirming TonR^{C6xHis} expression, the induced cultures were used for conducting further experiments. Initially the localization of expressed TonR^{C6xHis} was assessed in Arctic express GS027 cells. The membrane and cytoplasmic fraction collected from these cells were analysed and presence of TonR^{C6xHis} was determined by following western blot analysis using anti-His antibody. The TonR^{C6xHis} specific signal was found in both whole cell lysate and membrane fraction. In general the membrane proteins exists as precursor and mature forms. The mature form of protein will be generated after successful membrane targeting and subsequent removal of signal peptide. Therefore there should be a change in

the size of precursor form of protein and its mature version. The western blot gave TonR^{C6xHis} specific signal both in whole cell lysate and membrane fraction. The TonR^{C6xHis} found in whole cell lysate appears to be the precursor form. Its size should be more than the size of membrane associated TonR^{C6xHis}, as it the got to be mature version of TonR^{C6xHis}. Clear examination of western blot showed no such difference in size of TonR^{C6xHis} found in whole cell lysate and membrane fraction. There may be three reasons for such unusual observation one of them may be that TonR^{C6xHis} is not processed due to lack of cognate signal peptidase required for cleavage of signal peptide. Second reason could be the percentage of SDS-PAGE (12.5%). The 12. 5% SDS-PAGE may not be suitable for separation of precursor and mature form of 85kDa TonR^{C6xHis}. The third reason could be that the entire expressed TonR^{C6xHis} is processed and that what is seen in whole cell lysate is that of mature form of TonR^{C6xHis}, which upon segregation is found in membrane fraction. Surprisingly there was also second signal in the membrane fraction. It is just 30kDa in size. It might have generated due to degradation of TonR^{C6xHis} under physiological conditions where its expression has no physiological relevance. It appears to be specific and its signal is seen cytoplasmic fraction (Fig. 5. 8).

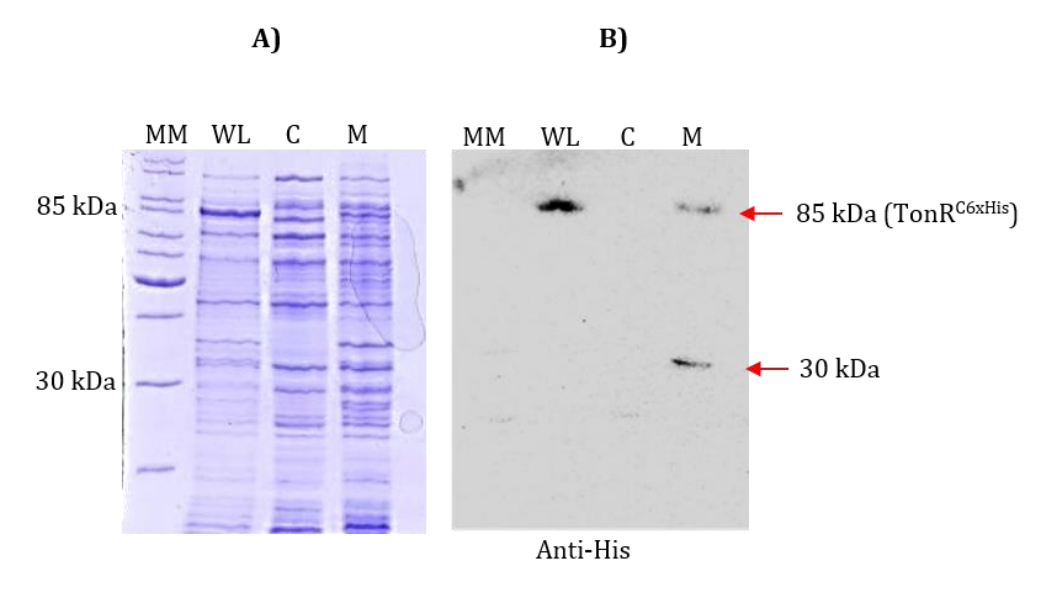


Fig. 5. 8. Membrane localization of TonR^{C6xHis} in GS027 cells. The subcellular fractions prepared from the GS027 (pGS25) cells induced for the expression of TonR^{C6xHis} were analysed on 12.5% SDS-PAGE. The corresponding western blot probed using anti-His antibodies is shown in panel B. MM represents molecular weight marker. CL, C and M indicate cell lysate, cytoplasmic and membrane fractions respectively. The TonR^{C6xHis} is shown with arrow.

5.3.3. The ExbB^{NFLAG} and ExbD^{CMyc} are found in the membrane

The expression of ExbBNFLAG, ExbDCMyc in Arctic express cells was determined (vide results section chapter 2). The Arctic express strain of E. coli GS027 cells transformed with expression plasmid (pGS23) coding ExbB^{NFLAG}, ExbD^{CMyc} were induced and fractionated to assess its localization. The membrane and cytoplasmic fraction collected from these cells were analysed for the presence of ExbB^{NFLAG}, ExbD^{CMyc} by performing western blot probed independently using anti-FLAG and anti-Myc antibodies. The ExbBNFLAG, ExbDCMyc specific signals were found in both whole cell lysate and membrane fraction. There was no signal in cytoplasmic fraction suggesting that the expressed proteins has successfully targeted to the membrane. The precursor and mature forms of ExbBNFLAG, ExbDCMyc were not observed on western blots. This may be due to lack of cognate signal peptidase required for the processes of heterologously expressed ExbB/ExbD (Kampfenkel et al., 1992). It may also possible that the entire expressed proteins are processed and that what is observed in whole cells lysate may be the mature version of ExbBNFLAG and ExbDCMyc which upon segregation found at the membrane. However, the results obtained in this study provide undisputable evidence on successfully membrane targeting of ExbB^{NFLAG}, ExbD^{CMyc} (5. 9. Panel B & C).

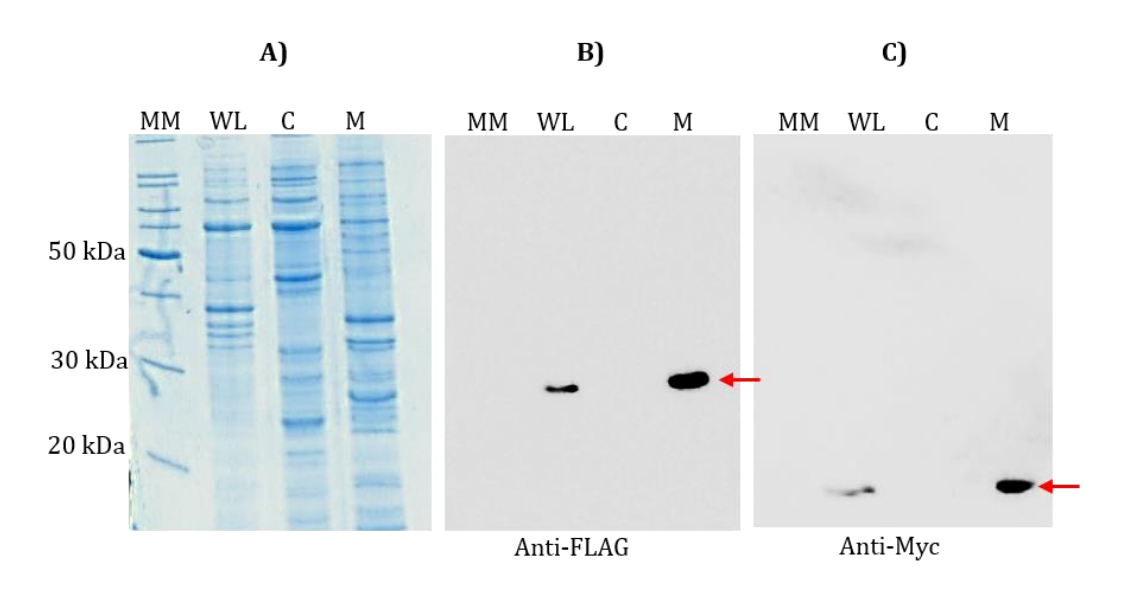


Fig. 5. 9. Membrane localization of ExbB^{NFLAG} and ExbD^{CMyc} in GS027 cells. The cytoplasmic and membrane fractions prepared from the GS027 (pGS23) cells induced for the expression of ExbB^{NFLAG} and ExbD^{CMyc} were analysed on 15% SDS-PAGE (Panel A), The corresponding western blots probed using anti-FLAG and anti-Myc antibodies to detect ExbB^{NFLAG} and ExbD^{CMyc} are shown in panel B and C respectively. MM represents molecular weight marker. CL, C and M indicate cell lysate, cytoplasmic and membrane fraction respectively.

5.3.4. TonB^{C6xHis} is found in the membrane.

The GS027 cells transformed with expression plasmid (pGS24) coding TonB^{C6xHis} were taken and the expression of TonB^{C6xHis} was induced for 3 and 12h by following protocols described in materials and methods section. The expression of TonB^{C6xHis} was only seen 3h after induction of its expression. There was an increase in its expression in overnight induced cultures (Fig. 5. 10. Panel B). The western blot gave signals around 25kDa and 15kDa. This might be due to degradation of heterologously expressed TonB^{C6xHis} in the absence of its interacting partners ExbB and ExbD.

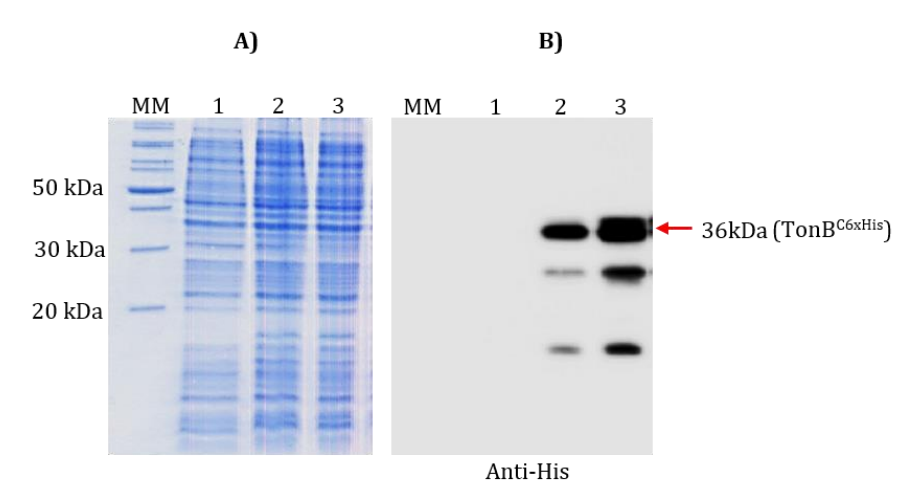


Fig. 5. 10. Expression of TonB^{C6xHis} in GS027 (pGS25) cells. The cell lysate collected from uninduced cells is loaded in lane 1. The cell lysate prepared from GS027 (pGS24) cells induced for 3h (lane 2) and 12h (lane 3) was analysed on 12.5% SDS-PAGE (Panel A). The corresponding western blot probed using anti-His antibodies is shown in panel B. The TonB^{C6xHis} specific signal corresponding to TonB^{C6xHis} is shown with arrow.

After confirming TonB^{C6xHis} expression, the induced cultures were used for assessing its localization in *E. coli* GS027. The membrane and cytoplasmic fractions collected from these cells were analysed in 12. 5% SDS PAGE and presence of TonB^{C6xHis} was determined by following western blot probed using anti-His antibodies. The TonB^{C6xHis} specific signals were found in both whole cell lysate and membrane fractions. There was no signal in cytoplasmic fraction. The precursor and mature forms of TonB^{C6xHis} signals were observed on western blot. The whole cell lysate clearly indicates more preTonB^{C6xHis} (Fig. 5. 11. Panel B). However in the membrane only mature form of TonB^{C6xHis} is seen. This is a clear indication to show successful expression and processing of expressed TonB^{C6xHis} in GS027 cells.

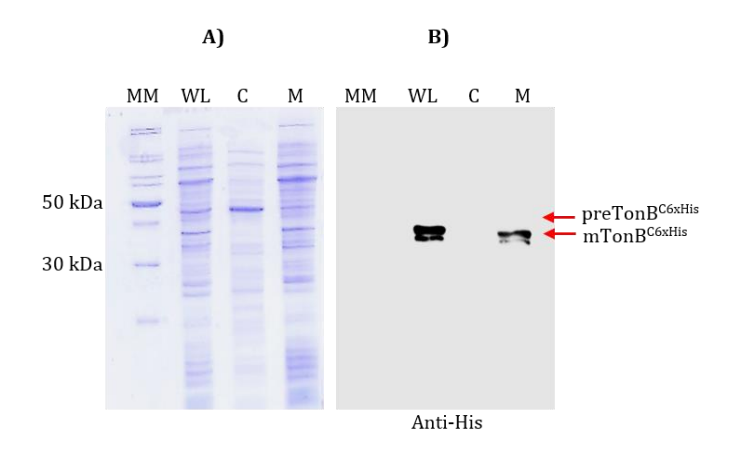


Fig. 5. 11. Membrane localization of TonB^{C6xHis} in GS027 cells. The subcellular fractions prepared from the GS027 (pGS24) cells induced for the expression of TonB^{C6xHis} were analysed on 12.5% SDS-PAGE. The corresponding western blot probed using anti-His antibodies is shown in panel B. The TonB^{C6xHis} specific signals are shown with arrow. The preTonB^{C6xHis} and mTonB^{C6xHis} indicate precursor and mature form of TonB^{C6xHis}. MM represents molecular weight marker. CL, C and M indicate cell lysate, cytoplasmic and membrane fraction respectively.

5.3.5. Expression and subcellular localization of Ton complex.

The inner membrane protein complex components ExbB, ExbD and TonB designated as Ton complex. Construction of expression plasmid pGS6 discussed in methods section codes for Ton complex (ExbB^{NFLAG}/ExbD^{CMyc} and TonB^{C6xHis}) from vector specific T7 promoters. The GS027 (pGS6) cells were induced and the expression of ExbB^{NFLAG}/ExbD^{CMyc} and TonB^{C6xHis} were detected by performing SDS-PAGE followed by western blot probed with anti-FLAG, anti-Myc and anti-His antibodies. (Fig. 5. 12). The cell lysate prepared from the GS027 (pGS6) cells gave ExbB^{NFLAG}/ExbD^{CMyc} and TonB^{C6xHis} specific signals indicating successful expression of these proteins in GS027cells (Fig. 5. 12. Panel B, C, and D).

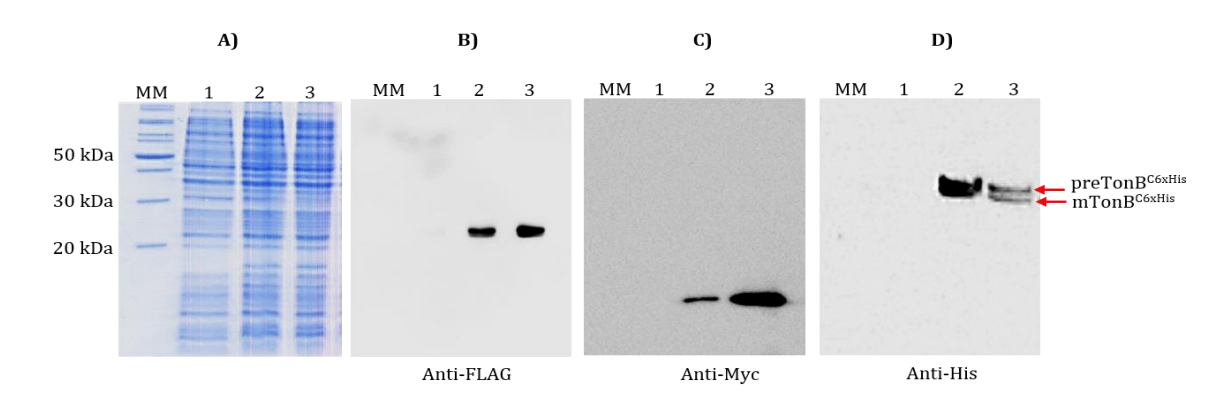


Fig. 5. 12. Expression of ExbB^{NFLAG}/ExbD^{CMyc} and TonB^{C6xHis} in GS027 cells. Panel A shows (15%) SDS-PAGE, lane MM indicates protein molecular weight marker, uninduced whole cell lysate was loaded in lane 1, the whole cell lysate prepared from GS027(pGS6) induced for 3h and 6h to express TonB^{C6xHis}, ExbB^{NFLAG} and ExbD^{CMyc} were loaded in lane 2 and lane 3 respectively.

Panels B, C and D show the corresponding western blots probed with anti-FLAG, anti-Myc and anti-His antibodies to detect ExbB^{NFLAG}, ExbD^{CMyc} and TonB^{C6xHis}.

After successful expression, the localization of Ton complex, ExbB^{NFLAG}/ExbD^{CMyc} and TonB^{C6xHis} were analysed by subcellular fractionation (vide General methods). The cytosolic and membrane fractions were independently probed with anti-FLAG, anti-Myc and anti-His specific antibodies. The specifc signals were only found in whole cell lysate and membrane fractions, and no signal was seen in cytosolic fraction (Fig. 5. 13. Panels 2, 3, and 4). Indicating that the expressed proteins have targeted membrane without leaving any traces in cytoplasmic fractions. As shown in earlier results the TonB is processed and mTonB^{C6xHis} was alone found in membrane fraction. Interestingly, in presence of ExbB^{NFLAG} and ExbD^{CMyc}, the TonB^{C6xHis} expressed in GS027 cells showed no signs of degradation, as was seen when it was expressed alone in GS027 cells (Fig. 5. 10).

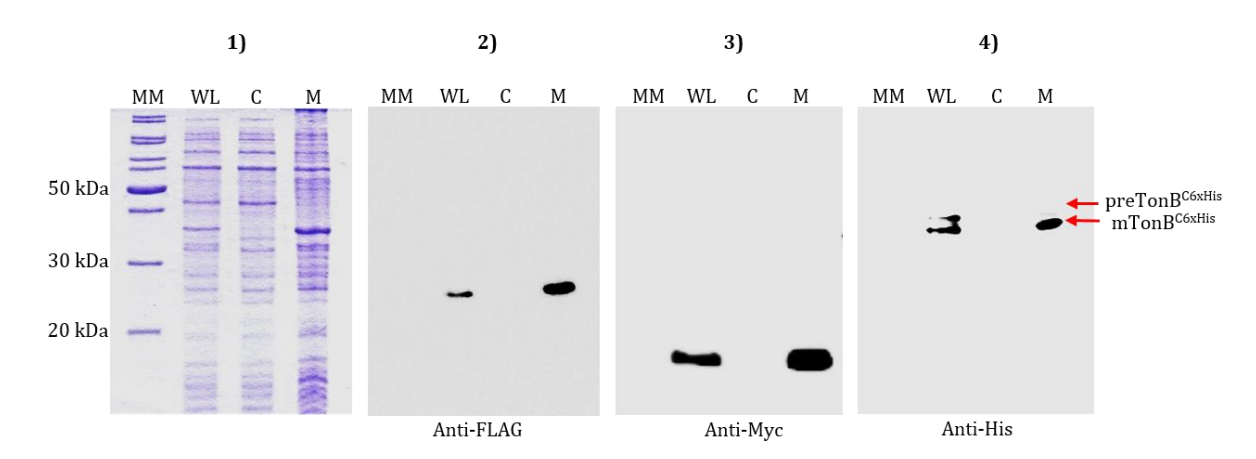


Fig. 5. 13. Subcellular localization of ExbB^{NFLAG}/ExbD^{CMyc} and TonB^{C6xHis}. Panel 1 shows the subcellular fractions of GS027 (pGS6) cells analysed on (15%) SDS-PAGE. The corresponding western blots probed using anti-FLAG, anti-Myc and anti-His antibodies to detect ExbB^{NFLAG}, ExbD^{CMyc} and TonB^{C6xHis} are shown in panels 2, 3 and 4. MM represents molecular weight marker. CL, C and M indicate cell lysate, cytoplasmic and membrane fractions respectively.

5.3.6. OPH targets membrane in presence of TonB, ExbB/ExbD

Previously we have performed several studies to understand membrane targeting of OPH using *E. coli* as model system. When precursor form of OPH (preOPH) was expressed in *E. coli* it remained in cytoplasm in its unprocessed form (Siddavattam *et al.*, 2003; Gorla *et al.*, 2009). Reconfirming the same observations, the preOPH^{CAviTag} expressed in *E. coli* remained unprocessed and accumulated in cytoplasm (Fig. 5. 14. Panel A). Multi protein complexes target membrane following Tat route (Berks *et al.*, 2003; Natale *et al.*, 2008). Since OPH^{CAviTag} interacting with energy transducing components TonB^{N6xHis}, and ExbB^{NFLAG}/ExbD^{CMyc} (vide results section in chapter 2), the subcellular

localization of OPH was examined in the presence of energy transducing components. Initially the TonB^{C6xHis} coding plasmid pGS24 transformed into GS027 cells. The second plasmid pOPHV400 coding OPH^{CAviTag} was then transformed into the GS027 (pGS24) cells. The GS027cells (pOPHV400+pGS24), expressing OPH^{CAviTag} and TonB^{C6xHis} were grown to mid log phase and expression of TonBC6xHis and OPHCAviTag were confirmed before fractionating into cytoplasm, membrane. The subcellular fractions were analysed on 12.5% SDS-PAGE. The localization of proteins were determined by western blot probed using anti-OPH and anti-His antibodies to detect OPH^{CAviTag} and TonB^{C6xHis}. As seen in fig. 5. 14 panel A the OPH remained in unprocessed and most of the protein remained in cytoplasm. The TonB^{C6xHis} as shown before has (Fig. 5. 13. Panel 4) successfully processed and the mature form of TonB^{C6xHis} was seen associating to the membrane (Fig. 5. 13. Panel 4). In cell lysate, two closely related TonB^{C6xHis} signals were obtained. One of this is specific to preTonB^{C6xHis} and the second one which is about 2kDa smaller in size corresponds to mature form of TonB^{C6xHis}. The western blot results have clearly seen that in cultures co-expressing both OPH^{CAviTag} and TonB^{C6xHis}, only TonB^{C6xHis} is targets to the membrane, but not OPH^{CAviTag} (Fig. 5. 14). Since OPH interaction with ExbD were established (vide results section chapter 2) further experiments were done to see if OPH targets membrane in presence of ExbB and ExbD.

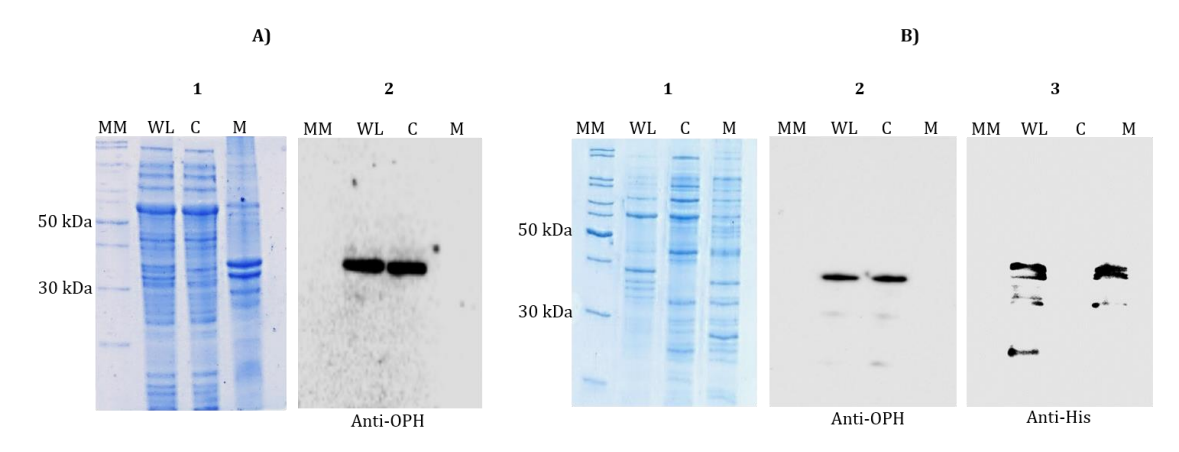


Fig. 5. 14. Subcellular localization of OPH^{CAviTag} in GS027 (pGS24) cells. Panel A shows the cytoplasmic localization of OPH^{CAviTag} in the absence of ExbB^{NFLAG}/ExbD^{CMyc} and TonB^{C6xHis}. Panel A-1 shows (12.5%) SDS-PAGE. The corresponding western blot probed using anti-OPH antibodies are shown in panel A-2. Panel B shows cytoplasmic localization of OPH^{CAviTag} in presence of TonB^{C6xHis}. Panel B-1 represents (12.5%) SDS-PAGE. The cytoplasmic localization of OPH^{CAviTag} (B-2), membrane localization of TonB^{C6xHis} (B-3) determined by probing with anti-OPH and anti-His antibodies are shown in panels B-2 and B-3.. MM represents molecular weight marker. CL, C and M indicate cell lysate, cytoplasmic and membrane fraction respectively.

The ExbB^{NFLAG}/ExbD^{CMyc} coding plasmid pGS23 transformed into GS027 (pOPHV400) cells expressing OPHCAviTag. The GS027 cells (pOPHV400+pGS23) co-expressing both OPH^{CAviTag} and ExbB^{NFLAG}/ExbD^{CMyc} were fractionated and their subcellular localizations were determining by performing western blots using anti-OPH, anti-Myc and anti-FLAG antibodies. Interestingly, preOPH^{CAviTag} got processed and successfully targeted to the membrane in presence of ExbB^{NFLAG}/ExbD^{CMyc} (Fig. 5. 15. Panel 2). After detection of OPH in membrane fraction the western blots were also performed to detect ExbBNFLAG and ExbD^{CMyc}. Both ExbB^{NFLAG} and ExbD^{CMyc} specific signals were seen in membrane (Fig. 5. 15. Panel 3 and 4). The ExbBNFLAG/ExbDCMyc when co-expressed in GS027 cells, both of them targeted to the membrane independent of OPH^{CAviTag} (Fig. 5. 9. Panel B and C). Only the OPH required presence of ExbBNFLAG/ExbDCMyc for translocation across the membrane. The OPH is the Tat substrate, it is not known from the present results to suggest if the OPH^{CAviTag} - ExbB^{NFLAG}/ExbD^{CMyc} complex formed in cytoplasm is targeted using Tat specific signal peptide found in the precursor form of OPH. Likewise, the ExbB/ExbD are inner membrane associated proteins and are widely distributed among gram-negative bacteria. They target inner membrane through their own signal peptide even in the absence of OPH (Kampfenkel & Braun 1992, 1993). The existing data doesn't clearly show so as to which of the components of ternary complex is responsible for taking it to the membrane.

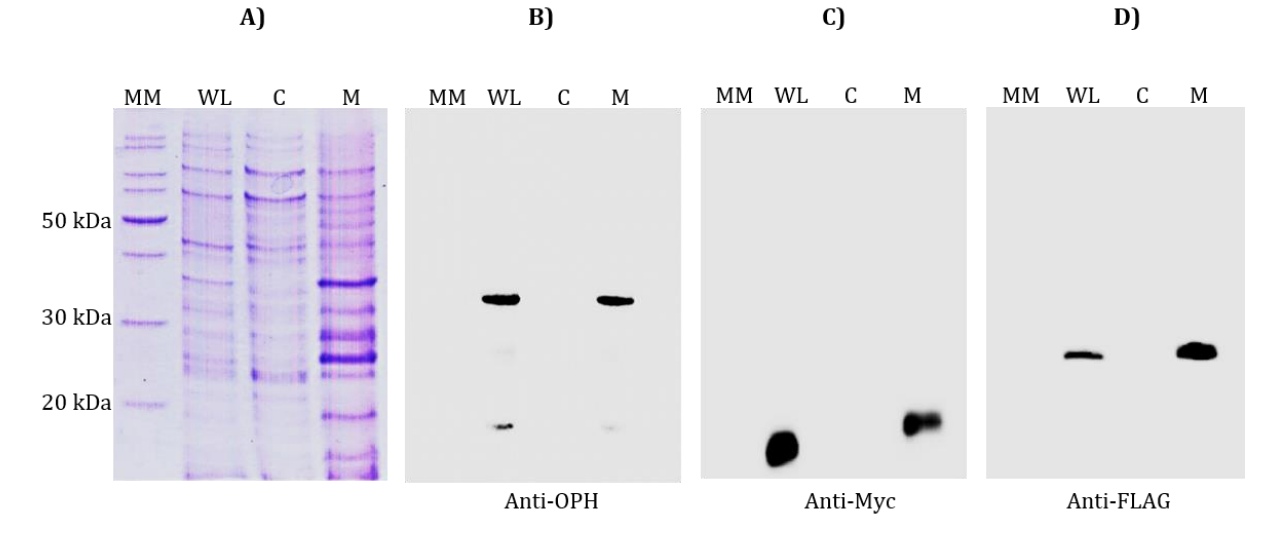


Fig. 5. 15. Membrane localization of OPH^{CAviTag} in GS027 (pGS23) cells. Panel A represents (12.5%) SDS-PAGE analysis of protein extracts from GS027 (pOPHV400+pGS23) cells. Membrane localization of OPH^{CAviTag} (B), ExbD^{CMyc} (C) and ExbB^{NFLAG} (D) determined by probing with anti-OPH, anti-Myc and anti-FLAG antibodies to detect OPH^{CAviTag}, ExbD^{CMyc} and ExbB^{NFLAG} are shown in panels B, C and D respectively. MM stands molecular weight marker. CL, C and M indicate cell lysate, cytoplasmic and membrane fraction respectively.

5.3.7. Reconstitution of SfTonBDT system in E. coli GS027.

The TonBDT system is well characterized in gram negative bacteria (Schauer *et al.*, 2008). It contains an outer membrane receptor, energy transducer and proton motive pump components (Noinaj *et al.*, 2010). Surprisingly, in *Sphingobium fuliginis*, the TonBDT system is associating with a triesterase. In order to understand the precise role of OPH with the *sf*TonBDT system was reconstituted in *E. coli* with and without OPH. Initially, the generated TonBDT negative strain of Arctic express strain GS027 generated by deleting both *exbD* and *tonB* was tested to know if it can grow under iron limiting condition. As expected, the GS027 cells failed to grown under iron limiting conditions (Fig. 5. 16).

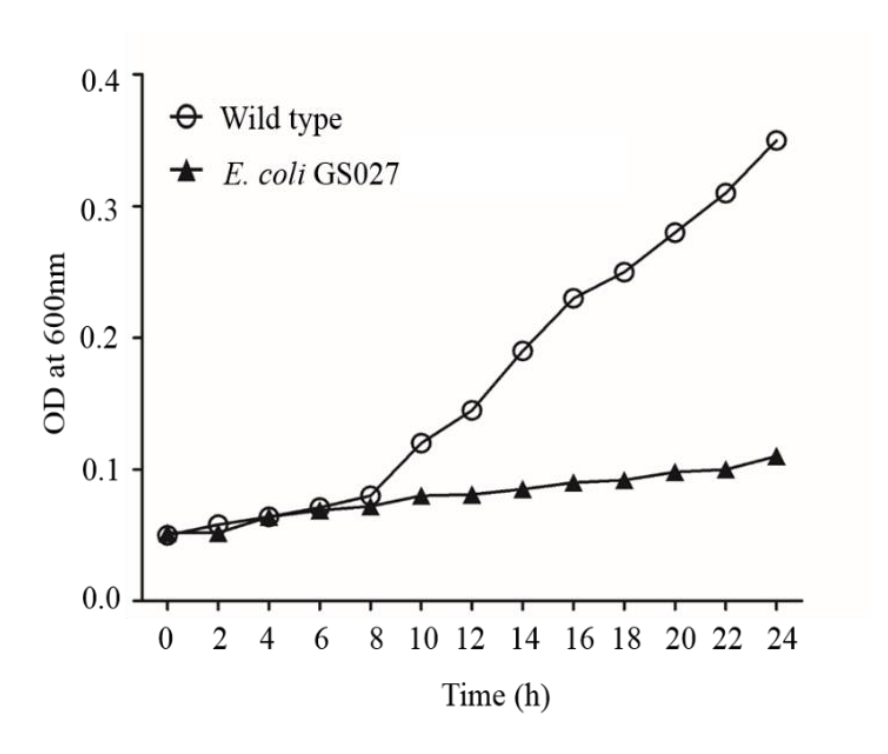


Fig. 5. 16. Shows growth of E. coli GS027 in iron limiting minimal media.

After establishing the growth phenotype of GS027 it was transformed with expression plasmids coding TonBDT components. Expression plasmid pGS6 codes for *sy*ExbB^{NFLAG}, *sy*ExbD^{CMyc}, *sy*TonB^{C6xHis} and their membrane localization was established in GS027 (pGS6) cells (Fig. 5. 13). The GS027 (pGS6) cells were transformed with expression plasmid pGS25 which codes for TonR^{C6xHis}.

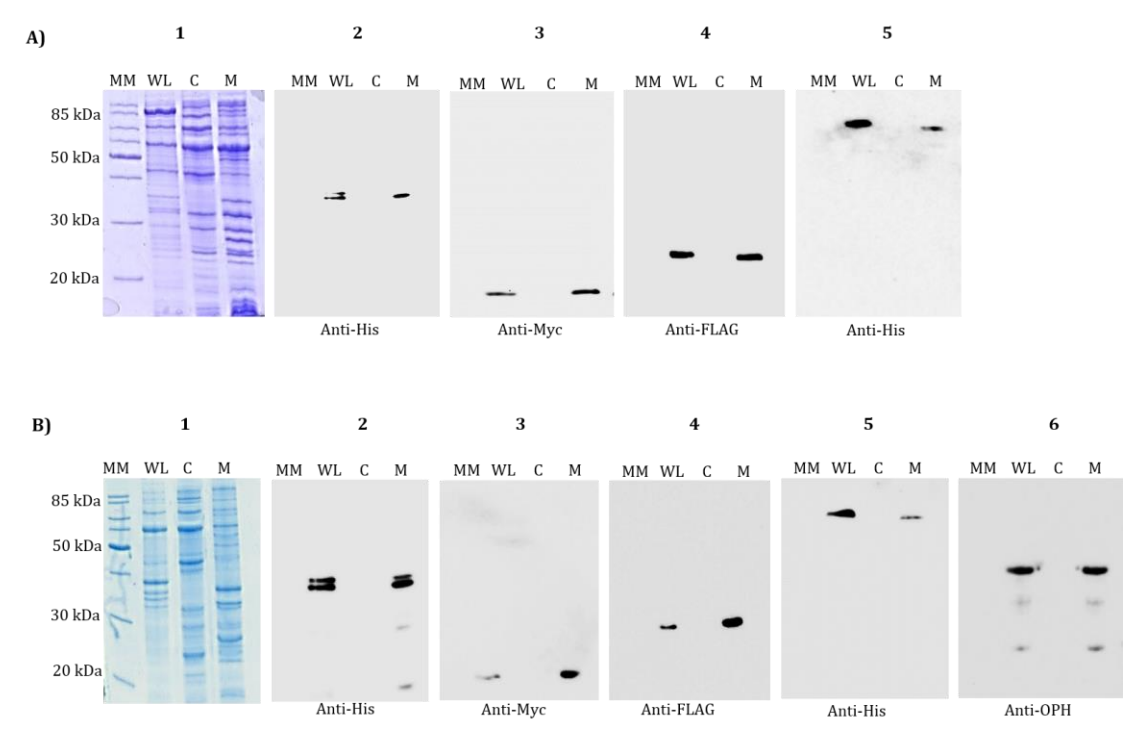


Fig. 5. 17. Reconstitution of *sy*TonBDT system in GS027 cells. Panel A shows reconstitution of *sy*TonBDT components without OPH^{CAviTag}. Panel A-1 represents (12.5%) SDS-PAGE. Membrane localization of TonB^{C6xHis} (A-2). ExbD^{CMyc} (A-3), ExbB^{NFLAG} (A-4), TonR^{C6xHis} (A-5) determined by probing with anti-His, anti-Myc, anti-FLAG and anti-His are shown in panels-A-2, 3, 4 and 5 respectively. Similar analysis done for the cells expressing *sy*TonBDT system with OPH is shown in panel B. Mebrane localization of OPH^{CAviTag} determined by probing with anti-OPH antibodies shown in panel B-6. MM represents molecular weight marker. CL, C and M indicate cell lysate, cytoplasmic and membrane fractions respectively.

The TonR, ExbB/ExbD are primary components of TonBDT. Ectopic expression of these components in GS027 cell amounts expression of sfTonBDT components in GS027 cells. All sfTonBDT components successfully targeted to the membrane in GS027 cells and hence were used to test for complementation of TonBDT negative phenotype. (Fig. 5. 17. Panel-A). After reconstitution TonBDT in GS027 cells without OPH, the GS027 (pGS6+pGS25) cells were transformed with expression plasmid (pOPHV400) coding OPH^{CAviTag}. The subcellular fractions and subsequent detection of TonBDT components and OPH successfully targeted membrane, indicating reconstitution of TonBDT with OPH. The GS027 cells expressing TonBDT with and without OPH, these strains were s then to test growth phenotype under iron limiting conditions and also for iron uptake studies.

Transport of nutrients across outer membrane of Gram negative bacteria is mediated by two independent mechanisms. The transport through outer membrane porins is a passive mechanism and it is limited to nutrients that are less than 600 Da in size. Passage of nutrients bigger than 600 Da through energy deprived outer membrane is a major

challenge and it depends on a special transport system called TonB dependent transport system (TonBDT). The TonBDT consists of ton complex and an outer membrane receptor called TonB dependent receptor (TonR). The unique structural features of TonR facilitates transport of nutrients such as vitamin B12, siderophores, heme, host iron binding proteins, maltodextrins, nickel etc across the outer membrane (Killmann et al., 1995; Braun 1999; Schauer et al., 2008 & Sheldon et al., 2015). The TonR contains a membrane-spanning barrel domain comprising 22 anti-parallel β-strands that is bigger than the barrel domain found in porins (Noinaj et al., 2010). The N-terminus of the TonR contains a plug domain that seals the barrel and prevents passage of solutes into periplasmic space. Substrate binding at plug domain induces conformational change and exposes the TonB box to facilitate interaction between TonR and inner membrane associated TonB. The energy derived from inner membrane associated Ton complex, comprising of TonB, ExbB and ExbD is transduced to TonR through TonB. The exact mechanism by which TonB transduces energy is TonR is still not known. Two independent models exists pertaining to transduction of energy from Ton complex to TonR. One of them is a shuttle model and it suggests exit of energized TonB from inner membrane and shuttles to TonR via periplasm to transduce energy to TonR (Larsen et al., 2003; Letain & Postle 1997). The second one is pulling model which proposes association of TonB to inner membrane and spans to periplasmic space to connect TonB-Box of TonR. The conformational changes of energized TonB pulls the plug domain into periplasmic space and the substrate bound to plug domain of TonR translocates to the periplasmic space (Schauer et al., 2008). Unlike cytoplasmic membrane (CM) transporters and transcription factors there exists no correlation between genome size and TonRs. Number of TonRs is not dependent on genome size, rather its dependent on organisms physiology and ecological niche (Schauer et al., 2008). The pathogenic E. coli contain twice the number of TonRs than non-pathogenic E coli. More number of TonRs means more efficient scavenging of nutrients either in densely populated microbial niches or in nutrient poor environments (Xu et al., 2003). The Ton complex components are rather conserved even in the genomes with many TonRs single copy genes code Ton complex components. In S. fuliginis there exists 87 TonRs coding sequences as against one copy of ExbB, 3 copies ExbD and four copies of TonB coding sequences. More number of TonRs indicate efficient and robust mechanisms to transport rare carbon sources and scarcely available nutrients.

As stated before despite of having structural diversity in TonRs, the energy transducing Ton complex of TonBDT is conserved. It is a ternary complex comprising of TonB, ExbB and ExbD in a 1:7:2 ratio (Higgs et al., 2002). Contrary to this established notion we have found quaternary complex in S. fuliginis. The OPH, which is found in addition to the ExbB, ExbD and TonB, is clearly contributing for better iron uptake process. Existence of enterobactin hydrolase activity as part of Ton complex helps in efficient transport and simultaneous release of iron into periplasmic space. This activity of OPH, which is associated due to existence of additional active site, is certainly advantageous to the organism. Previously we have shown OPH as a part of multiprotein complex in Sphingophyxis wildii and its requirement to acquire phosphate from OP insecticides (Parthasarathy et al., 2016). The peptide sequences generated through orbitrap analysis for OPH associated proteins have shown similarity to Tol complex components. In fact some of the peptide sequences of S. wildii have even shown identity to the Ton complex of S. fuliginis. The Tol and Ton complexes consists analogous components and are evolutionarily related to each other (Celia et al., 2016). Association of OPH with such TonBDT systems speaks of its versatile role in transport of nutrients across the energy deprived outer membrane. In the light of the current findings role of other phosphotriesterases (PTEs) coding sequences, such as mpd and opdA need to be revisited. Interestingly the mpd and opdA linked genes are associated with membrane transport. There seems to be PTE assisted membrane transport mechanism, hitherto unknown in Gram-negative bacteria.

Role of OPH in iron transport

6.1. Objective specific methodology

The primary goal of the present work is to determine the physiological role of OPH in soil bacteria. In the previous chapter the TonBDT was reconstituted with and without OPH. In fact expression of *sf*TonBDT in Arctic express cells was a significant mile stone in determining the function of OPH. After reconstituting the *sf*TonBDT we performed growth experiments under iron limiting conditions TonBDT plays a significant role in transport of iron.

6.1.1. Growth of reconstitution of E. coli GS027 (S_f TonBDT) under iron limiting conditions

The E. coli GS027 was transformed with the appropriate expression plasmids to generate SfTBDT components with OPH and without OPH (vide methods section of chapter 3). Prior to perform of experiments all the glassware were made iron free by following procedures described in general methods section. The GS027 (pGS6+pGS25+pOPHV400) cells express sfTonBDT components with OPH (ExbBNFLAG/ExbDCMyc TonBC6xHis TonRC6xHis and OPH^{CAviTag}). The GS027 (pGS6+pGS25) cells express sfTonBDT components without OPH (ExbB^{NFLAG}/ExbD^{CMyc}, TonB^{C6xHis} and TonR^{C6xHis}) upon induction. The overnight cultures of these cells were inoculated into LB broth containing appropriate antibiotics and grown at 37°C with vigorous shaking till the culture density reaches to 0.5. OD (A600nm) Expression of TBDT components was induced by adding 1mM IPTG these induced cultures were allowed to grow at 18°C with shaking at 180 rpm. The cells were harvested and washed two times with iron free minimal media. Finally the cells were resuspended in minimal media containing 0.02µg/ml of Fe (Iron limiting). The culture is supplemented with 0.5mM IPTG to keep the TonBDT components under induced condition and allowed to grow the cells for 12h at 18°C with shaking at 160 rpm and acclimatized to grow under iron limiting conditions. After acclimatization, the cells were harvested and resuspended (0.05 OD) in minimal media containing 0.02µg/ml of Fe (Iron limiting) and 0.5mM IPTG, the antibiotics were kept at low concentration (ampicillin 50µg, kanamycin 10µg and chloramphenicol 10µg) to facilitate the survival under iron limiting conditions. These cultures were allowed to grow at 30°C with shaking 160 rpm and growth was recorded every 2h at 600 nm. The wild type Arctic express treated in similar manner served as control.

6.2. Determination of OPH influence on transport of ferric enterobactin

6.2.1 Preparation of ⁵⁵Fe-enterobactin complex

The stock solution of enterobactin (Sigma-Aldrich, USA) was prepared by dissolving 1mg of enterobactin in 100µl of DMSO. While preparing ⁵⁵Fe-enterobactin 3µl of enterobactin stock solution was taken in a sterile eppendorf tube and 5µl of ⁵⁵Fe was added from 0. 2µmol of ⁵⁵Fe stock (American Radiolabeled Chemicals, MO, USA; specific activity of 10.18mCi/mg) and incubated at RT for 5min. The contents were made up to 50µl with HEPES buffer (pH 7.3) and the free ⁵⁵Fe was removed by passing it through Sephadex G-25 column. The ⁵⁵Fe-enterobactin eluted in the flow through was collected and the radioactivity determined by pipetting 2µl into 5ml of scintillation fluid [2, 5 - diphenyloxazole and 1, 4 - bis (5-phenyl-2-oxazolyl) benzene] and the the quantity of radioactivity was measured using scintillation counter (Perkin Elmer Tri-Carb 2910TR).

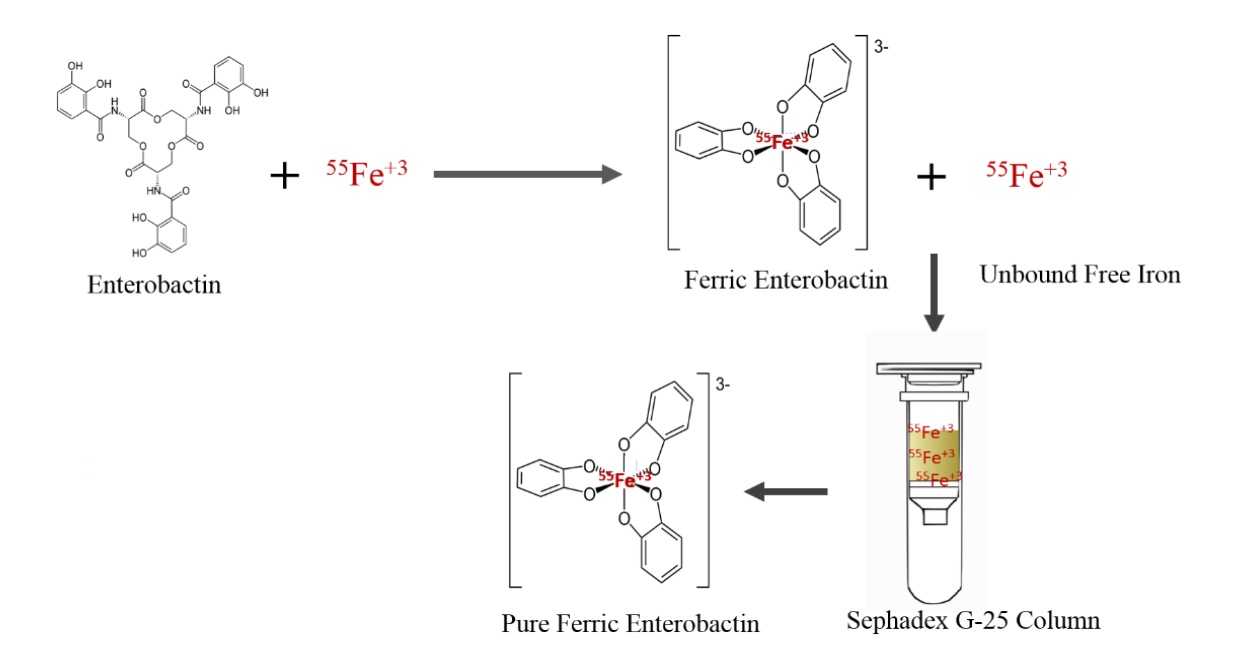


Fig. 6. 1. Schematic diagram showing labelling of enterobactin with ⁵⁵Fe⁺³ and purification of ⁵⁵Fe-enterobactin complex.

6.2.2. ⁵⁵Fe-enterobactin uptake assay

The null mutant of GS027 and sfTonBDT reconstituted strains without OPH GS027 (pGS6+pGS25) and with OPH GS027 (pGS6+pGS25+pOPHV400) were initially grown to mid log phase in LB broth and the expression of sfTonBDT components were induced with

ImM IPTG for six hours at 18°C. After induction, the cells were harvested and the cell pellet was washed twice with the iron free minimal salt medium. The cell pellet was then redissolved in equal volume of iron limiting medium. The cells were shifted to iron limiting minimal media and for continuing the expression of *sf*TonBDT components the cells were grown at 18°C and induced 12 hours by adding 1mM IPTG. After induction, cells were harvested and extensively washed and redissolved in iron free minimal media to obtain a cell density of 1.0 OD (A_{600nm}), which is equivalent to 8x10⁸ cells/ml. The cell suspension was then supplemented with ⁵⁵Fe-enterobactin (equivalent to 178μmol of ⁵⁵Fe) and incubated at 37°C for 2h with gentle shaking (150 rpm). After incubation the cells were harvested and the pellet was extensively washed with 0.1M LiCl₂ followed by twice with cold iron free minimal media. After washing, the cell pellet was dried by keeping the pellet in dry bath set at 60°C and the dried cells were transferred into 5ml of scintillation fluid and the amount of iron found in cell pellet was counted as mentioned above. The wild type Arctic express cells treated in similar manner served as controls.

6.3. Results & Discussion

6.3.1. OPH enhances the growth of GS027 (s_f TonBDT) cells under iron limiting conditions

The TonBDT system is well characterized in gram negative bacteria (Schauer *et al.*, 2008). It contains an outer membrane receptor, energy transducer and proton motive pump components (Noinaj *et al.*, 2010). Surprisingly, in *Sphingobium fuliginis*, the TonBDT system is associating with a triesterase. While establishing precise role of OPH in *sy*TonBDT system of *Sphingobium fuliginis* we have reconstituted *sy*TonBDT system in *E. coli* with and without OPH. Initially the TonBDT negative strain of *E. coli* Arctic express strain is generated by deleting both *exbD* and *tonB*. The *exbD* and *tonB* double mutant, designated as GS027, failed to grow under iron limiting condition (vide results section of chapter 3). After establishing the growth phenotype of GS027 it was transformed independently with expression plasmids coding Ton complex components. Expression plasmid pGS6 is a pETDuet1 derivative and codes for *sy*ExbB^{NFLAG}, *sy*ExbD^{CMyc}, *sy*TonB^{C6xHis}. The membrane fraction collected from GS027 (pGS6) was probed independently with anti-FLAG, anti-Myc and anti-His antibodies to know if these Ton complex components of *sy*TonBDT are targeting to the membrane. Interestingly all of them were found in the membrane fraction of GS027 strain (vide results section of chapter 3, fig. 5. 13). The TonR co-expressed with these TonBDT components by

transforming pGS25 into GS027 (pGS25) cells also targeted membrane suggesting successful reconstitution of SfTonBDT in E. coli without OPH. Finally the GS027 (pGS6+pGS25) cells were transformed with plasmid (pOPHV400) coding OPH^{CAviTag} and as shown before the expressed OPH^{CAviTag} got successfully targeted to the membrane in presence of SfTonBDT components (vide results section of chapter 3, fig 5. 15 panel B). The Arctic Express strains GS027 (pGS6+pGS25+pOPHV400) and GS027 (pGS6+pGS25) were used as strains with reconstituted sfTonBDT with and without OPH respectively (vide results section of chapter 3, fig. 5. 17). Since TonBDT are known to transport ferric enterobactin (Hollifield et al., 1978; Raymond et al., 2003), the TonBDT mutant GS027 and TonBDT reconstituted strains GS027 (pGS6+pGS25) and GS027 (pGS6+pGS25+pOPHV400) were grown under iron limiting conditions to check if sfTonBDT system restores growth of GS027 strain under iron limiting condition. Both GS027 (pGS6+pGS25) and GS027 (pGS6+pGS25+pOPHV400) strains have successfully grown under iron limiting condition. However, the GS027 (pGS6+pGS25+pOPHV400) strain having sfTonBDT with OPHCAviTag has shown better growth than its counterpart possessing sfTonBDT without OPH^{CAviTag} (Fig. 6. 2). There was a difference in growth of wild type and SfTonBDT reconstituted cells. The wild type cell have grown much faster in iron limiting conditions when compared to the cells complemented with SfTonBDT. This may be due to presence of antibiotics in the culture medium added to retain the expression plasmids in the GS027 cells. Further addition of IPTG to induce expression of TonBDT components impose physiological burden causing growth retardation.

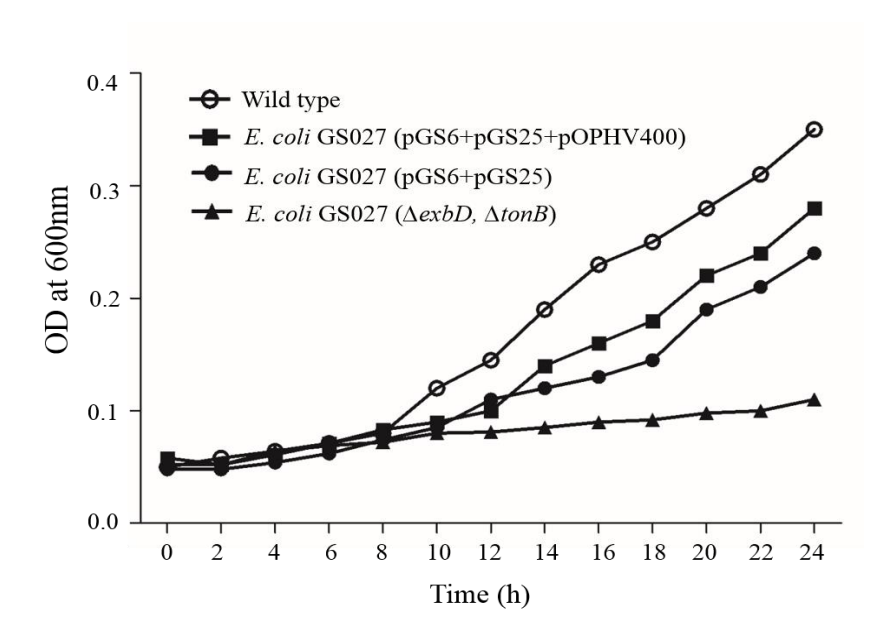


Fig. 6. 2. Growth of reconstitution of E. coli GS027 (sfTonBDT) under iron limiting conditions.

6.3.2. OPH dependent increase in iron uptake.

Following the observation that showed increased growth in GS027 cells with *sf*TonBDT and OPH^{CAviTag} we further probed if the increased growth recorded in these cells is due to increased iron uptake. We have performed iron uptake assay by incubating the equal number of cells acclimatized to the low iron containing medium for two hours with pure ⁵⁵Fe-enterobactin. As expected no ⁵⁵Fe was found in GS027 cells. Nearly 38,000 picomoles of iron was found in wild type cells. The GS027 cells (pGS6+pGS25) having *sf*TonBDT without OPH showed 26,000 picomoles of iron uptake. Interestingly, the cells having *sf*TonBDT system reconstituted with OPH showed accumulation of 48,000 picomoles of iron. There is two fold increase when compared to the iron uptake in cells have *sf*TonBDT without OPH (Fig. 6. 3) the results clearly indicate physiological role for OPH in iron uptake.

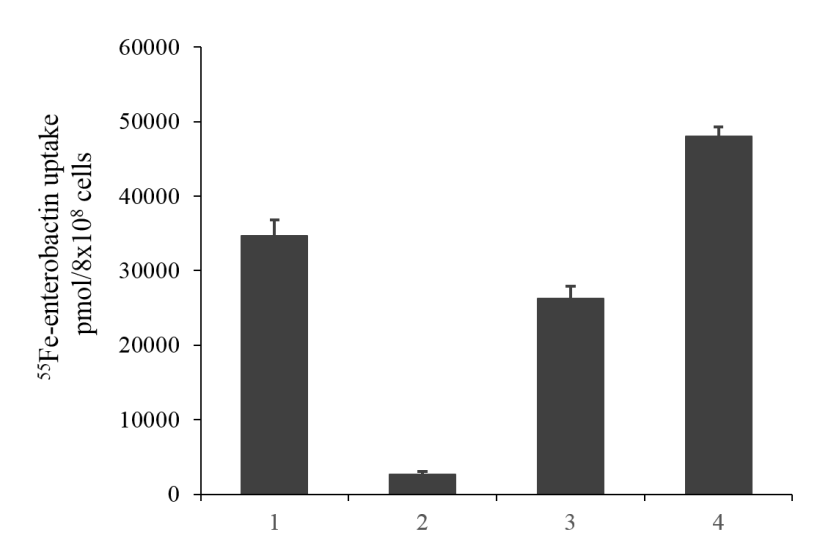


Fig. 6. 3. Shows uptake of ⁵⁵Fe by *E. coli* cells. Concentration of iron in 1) Wild type, (2) GS027, (3) GS027 (pGS6+pGS25) and (4) GS027 (pGS6+pGS25+pOPHV400).

The results obtained in the present study shows acceleration of iron uptake and better growth phenotype in GS027 cells having s_f TonBDT with OPH. These observations make to have a brainstorming in our laboratory on OPH biology. The TonBDT is known for transport of a variety of nutrients and toxins as well as natural antibiotics (Killmann *et al.*, 1995; Braun 1999; Schauer *et al.*, 2008 & Sheldon *et al.*, 2015). It is even shown to act as gateway for entry of phages like T1 in gram negative bacteria more particularly in *E. coli* (Cascales *et al.*, 2007). In none of them, OPH is shown as part of Ton complex. It is for only in the *Sphingobium fuliginis*. What advantage it can add to Ton complex of *Sphingobium*

fuliginis? These are some of the questions we discussed in our laboratory brainstorming meeting. The TonBDT system is an active transporter of outer membrane. The available literature shows that there is no substrate specificity for TonBDT system. The more important aspect is interaction of nutrient with outer membrane receptor, TonR. These interactions are independent of Ton complex. These interactions bring conformational changes in TonR and exposes "Ton box" of TonR and makes it available for the TonB. The critical issue is TonR nutrient interactions and existence of five amino acids long TonB box. Taking these two components into considerations the genome sequence of Sphingobium fuliginis was searched to identify TonR copies in S. fuliginis. It contains 87 copies of TonR in the genome of Sphingobium fuliginis. The sequence diversity of S. fuliginis TonR sequences indicate a significant role for TonBDT system in nutrients transport. Phosphate is a major nutrient. It is essential for survival of bacteria. The bacteria surviving in soil ecosystem, soil is the sole source of phosphate. Phosphate doesn't exist in soluble form in soils. It always interacts with organic and inorganic molecules and exists as complexes stabilized through diester and triester linkages. Unfortunately the cell has to derive the most needed inorganic phosphate from these complexes. The OPH, due to its triesterase activity can aid generation of inorganic phosphate pool. If this proposition is taken into consideration, together with its association with Ton complex, it is certainly advantageous to have OPH as part of Ton complex. If organic phosphate is transported through TonBDT, in periplasmic space it is quickly hydrolysed to generate inorganic phosphate pool required for survival of the cell.

The aforementioned hypothesis doesn't support accelerated iron uptake and OPH dependent enhanced growth property as the nutrient transported through TonBDT is not organic phosphate rather it is ferric enterobactin. How OPH is helping in transport of ferric enterobactin? Iron binds enterobactin strongly with dissociation constant of [3.03 E-05 K_D (M)]. Unless the trilactone ring of enterobactin is cleaved, then bound iron cannot be released. Is OPH hydrolysing enterobactin? On perusal of literature we found a paper that demonstrated lactonase activity for OPH (Afriat *et al.*, 2006). Is this lactonase activity of OPH contribute for hydrolysis of enterobactin and thus facilitate release of iron? Taking these things into consideration a model is proposed which suggests a role for OPH in TonBDT system. Further work is done by my colleagues to validate the proposed hypothesis.

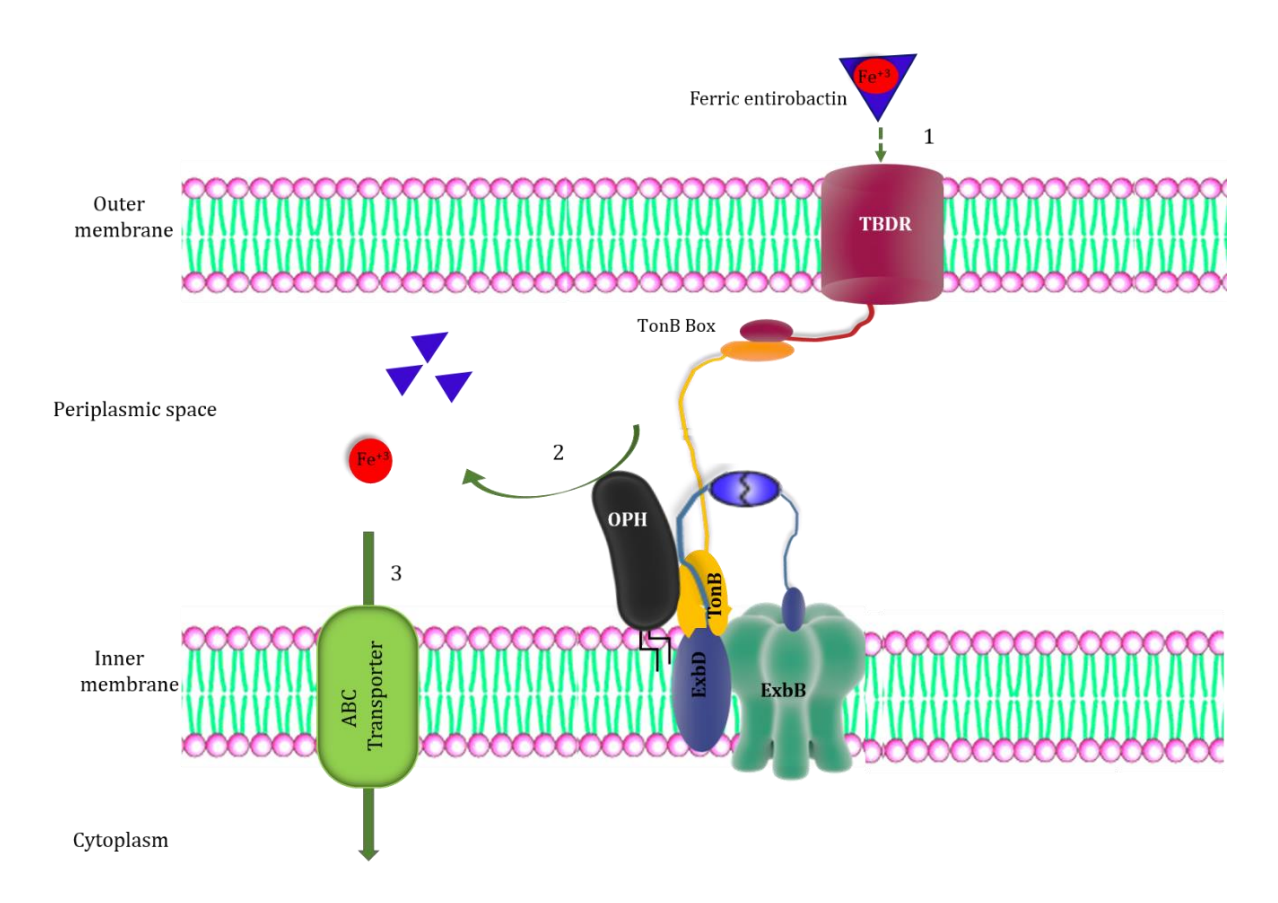


Fig. 6. 4. Proposed role of OPH as part of Ton complex. Stage 1 indicates translocation of ferric enterobactin into periplasmic space through TonR. The OPH mediated hydrolysis of enterobactin and subsequent release of iron from ferric enterobactin as shown in stage 2, entry of ferrous ions into cytoplasm through ABC transporter is shown in stage 3.



7. Conclusions

The research work clearly demonstrated co-purification of TonBDT components along with OPH. Further the result presented in the dissertation clearly demonstrated physical interactions between OPH and Ton complex components ExbD and TonB. The novel Ton complex of *Sphingobium fuliginis* consisting ExbB/ExbD/OPH and TonB play a significant role in acquisition of nutrients, especially phosphate and iron. The *Sf* TonBDT reconstituted in *E. coli* provided undisputable evidence to suggest a role for OPH in iron acquisition.

References

- 1. Afriat, L., Roodveldt, C., Manco, G., and Tawfik, D. S. (2006) The latent promiscuity of newly identified microbial lactonases is linked to a recently diverged phosphotriesterase. *Biochemistry*. **45**, 13677–86
- 2. Attaway, H., Nelson, J. O., Baya, A. M., Voll, M. J., White, W. E., Grimes, D. J., and Colwell, R. R. (1987) Bacterial detoxification of diisopropyl fluorophosphate. *Appl. Environ. Microbiol.* **53**, 1685–9
- 3. Baier, F., and Tokuriki, N. (2014) Connectivity between catalytic landscapes of the metallo-β-lactamase superfamily. *J. Mol. Biol.* **426**, 2442–56
- 4. Benning, M. M., Shim, H., Raushel, F. M., and Holden, H. M. (2001) High resolution X-ray structures of different metal-substituted forms of phosphotriesterase from Pseudomonas diminuta. *Biochemistry*. **40**, 2712–22
- 5. Berks, B. C. (1996) A common export pathway for proteins binding complex redox cofactors? *Mol. Microbiol.* **22**, 393–404
- 6. Berks, B. C., Palmer, T., and Sargent, F. (2003) The Tat protein translocation pathway and its role in microbial physiology. *Adv. Microb. Physiol.* 47, 187–254
- 7. Birnboim, H. C., and Doly, J. (1979) A rapid alkaline extraction procedure for screening recombinant plasmid DNA. *Nucleic Acids Res.* **7**, 1513–23
- 8. Blattner, F. R., Plunkett, G., Bloch, C. A., Perna, N. T., Burland, V., Riley, M., Collado-Vides, J., Glasner, J. D., Rode, C. K., Mayhew, G. F., Gregor, J., Davis, N. W., Kirkpatrick, H. A., Goeden, M. A., Rose, D. J., Mau, B., and Shao, Y. (1997) The complete genome sequence of Escherichia coli K-12. *Science*. 277, 1453–62
- 9. Boyer, H. W. & Roulland-Dussoix, D. A complementation analysis of the restriction and modification of DNA in Escherichia coli. *J. Mol. Biol.* **41**, 459–72 (1969).
- 10. Braun, V. (1999) Active transport of siderophore-mimicking antibacterials across the outer membrane. *Drug Resist. Updat.* **2**, 363–369
- 11. Cascales, E., Buchanan, S. K., Duche, D., Kleanthous, C., Lloubes, R., Postle, K., Riley, M., Slatin, S., and Cavard, D. (2007) Colicin Biology. *Microbiol. Mol. Biol. Rev.* 71, 158–229
- 12. Chang, A. C., and Cohen, S. N. (1978) Construction and characterization of amplifiable multicopy DNA cloning vehicles derived from the P15A cryptic miniplasmid. *J. Bacteriol.* **134**, 1141–56
- 13. Chaudhry, G. R., Ali, A. N., and Wheeler, W. B. (1988) Isolation of a methyl parathion-degrading Pseudomonas sp. that possesses DNA homologous to the opd gene from a Flavobacterium sp. *Appl. Environ. Microbiol.* **54**, 288–93

- 14. Cheng, T. C., Harvey, S. P., and Stroup, A. N. (1993) Purification and Properties of a Highly Active Organophosphorus Acid Anhydrolase from Alteromonas undina. *Appl. Environ. Microbiol.* **59**, 3138–40
- 15. Cheng, T., Liu, L., Wang, B., Wu, J., DeFrank, J. J., Anderson, D. M., Rastogi, V. K., and Hamilton, A. B. (1997) Nucleotide sequence of a gene encoding an organophosphorus nerve agent degrading enzyme from Alteromonas haloplanktis. *J. Ind. Microbiol. Biotechnol.* **18**, 49–55
- 16. Cherepanov, P. P. & Wackernagel, W. Gene disruption in Escherichia coli: TcR and KmR cassettes with the option of Flp-catalyzed excision of the antibiotic-resistance determinant. *Gene* **158**, 9–14 (1995).
- 17. Chou, M. M., and Kendall, D. A. (1990) Polymeric sequences reveal a functional interrelationship between hydrophobicity and length of signal peptides. *J. Biol. Chem.* **265**, 2873–80
- 18. Chu, X., Zhang, X., Chen, Y., Liu, H., and Song, D. (2003) [Study on the properties of methyl parathion hydrolase from Pseudomonas sp. WBC-3]. *Wei Sheng Wu Xue Bao.* 43, 453–9
- 19. Cooper, H. M., and Patterson, Y. (2008) Production of polyclonal antisera. *Curr. Protoc. Immunol.* Chapter 2, Unit 2.4.1-2.4.10
- 20. Cui, Z., Zhang, R., He, J., and Li, S. (2002) [Isolation and characterization of a p-nitrophenol degradation Pseudomonas sp. strain P3 and construction of a genetically engineered bacterium]. *Wei Sheng Wu Xue Bao.* 42, 19–26
- 21. Datsenko, K. A., and Wanner, B. L. (2000) One-step inactivation of chromosomal genes in Escherichia coli K-12 using PCR products. *Proc. Natl. Acad. Sci. U. S. A.* 97, 6640–5
- 22. De Leeuw, E., Porcelli, I., Sargent, F., Palmer, T., and Berks, B. C. (2001) Membrane interactions and self-association of the TatA and TatB components of the twinarginine translocation pathway. *FEBS Lett.* **506**, 143–8
- 23. DeFrank, J. J., and Cheng, T. C. (1991) Purification and properties of an organophosphorus acid anhydrase from a halophilic bacterial isolate. *J. Bacteriol*. 173, 1938–43
- 24. DeFrank, J. J., Beaudry, W. T., Cheng, T. C., Harvey, S. P., Stroup, A. N., and Szafraniec, L. L. (1993) Screening of halophilic bacteria and Alteromonas species for organophosphorus hydrolyzing enzyme activity. *Chem. Biol. Interact.* 87, 141–8
- 25. DeLisa, M. P., Samuelson, P., Palmer, T., and Georgiou, G. (2002) Genetic analysis of the twin arginine translocator secretion pathway in bacteria. *J. Biol. Chem.* 277, 29825–31

- 26. DeLisa, M. P., Tullman, D., and Georgiou, G. (2003) Folding quality control in the export of proteins by the bacterial twin-arginine translocation pathway. *Proc. Natl. Acad. Sci. U. S. A.* 100, 6115–20
- 27. Dong, Y.-J., Bartlam, M., Sun, L., Zhou, Y.-F., Zhang, Z.-P., Zhang, C.-G., Rao, Z., and Zhang, X.-E. (2005) Crystal structure of methyl parathion hydrolase from Pseudomonas sp. WBC-3. *J. Mol. Biol.* **353**, 655–63
- 28. Eijlander, R. T., Jongbloed, J. D. H., and Kuipers, O. P. (2009) Relaxed specificity of the Bacillus subtilis TatAdCd translocase in Tat-dependent protein secretion. *J. Bacteriol.* **191**, 196–202
- 29. Elias, M., and Tawfik, D. S. (2012) Divergence and convergence in enzyme evolution: parallel evolution of paraoxonases from quorum-quenching lactonases. *J. Biol. Chem.* **287**, 11–20
- 30. Elias, M., Dupuy, J., Merone, L., Mandrich, L., Porzio, E., Moniot, S., Rochu, D., Lecomte, C., Rossi, M., Masson, P., Manco, G., and Chabriere, E. (2008) Structural basis for natural lactonase and promiscuous phosphotriesterase activities. *J. Mol. Biol.* 379, 1017–28
- 31. Fekkes, P., and Driessen, A. J. (1999) Protein targeting to the bacterial cytoplasmic membrane. *Microbiol. Mol. Biol. Rev.* **63**, 161–73
- 32. Ferguson, A. D., Hofmann, E., Coulton, J. W., Diederichs, K., and Welte, W. (1998) Siderophore-mediated iron transport: crystal structure of FhuA with bound lipopolysaccharide. *Science*. **282**, 2215–20
- **33**. Fraczkiewicz, R., and Braun, W. (1998) Exact and efficient analytical calculation of the accessible surface areas and their gradients for macromolecules. *J. Comput. Chem.* **19**, 319–333
- 34. Frobel, J., Rose, P., and Muller, M. (2012) Twin-arginine-dependent translocation of folded proteins. *Philos. Trans. R. Soc. B Biol. Sci.* **367**, 1029–1046
- **35.** Ghanem, E., and Raushel, F. M. (2005) Detoxification of organophosphate nerve agents by bacterial phosphotriesterase. *Toxicol. Appl. Pharmacol.* **207**, 459–70
- 36. Gierasch, L. M. (1989) Signal sequences. *Biochemistry*. 28, 923–30
- 37. Gorla, P., Pandey, J. P., Parthasarathy, S., Merrick, M., and Siddavattam, D. (2009) Organophosphate hydrolase in Brevundimonas diminuta is targeted to the periplasmic face of the inner membrane by the twin arginine translocation pathway. *J. Bacteriol.* 191, 6292–9
- 38. Hanahan, D. (1983) Studies on transformation of Escherichia coli with plasmids. *J. Mol. Biol.* **166**, 557–80

- 39. Harper, L. L., McDaniel, C. S., Miller, C. E., and Wild, J. R. (1988) Dissimilar plasmids isolated from Pseudomonas diminuta MG and a Flavobacterium sp. (ATCC 27551) contain identical opd genes. *Appl. Environ. Microbiol.* **54**, 2586–9
- **40.** Held, K. G., and Postle, K. (2002) ExbB and ExbD do not function independently in TonB-dependent energy transduction. *J. Bacteriol.* **184**, 5170–3
- 41. Higgs, P. I., Larsen, R. A., and Postle, K. (2002) Quantification of known components of the Escherichia coli TonB energy transduction system: TonB, ExbB, ExbD and FepA. *Mol. Microbiol.* 44, 271–81
- 42. Hollifield, W. C., and Neilands, J. B. (1978) Ferric enterobactin transport system in Escherichia coli K-12. Extraction, assay, and specificity of the outer membrane receptor. *Biochemistry*. 17, 1922–8
- 43. Horne, I., Sutherland, T. D., Harcourt, R. L., Russell, R. J., and Oakeshott, J. G. (2002) Identification of an opd (organophosphate degradation) gene in an Agrobacterium isolate. *Appl. Environ. Microbiol.* **68**, 3371–6
- 44. Hoskin, F. C., and Roush, A. H. (1982) Hydrolysis of nerve gas by squid-type diisopropyl phosphorofluoridate hydrolyzing enzyme on agarose resin. *Science*. **215**, 1255–7
- 45. Hu, Y., Zhao, E., Li, H., Xia, B., and Jin, C. (2010) Solution NMR structure of the TatA component of the twin-arginine protein transport system from gram-positive bacterium Bacillus subtilis. *J. Am. Chem. Soc.* 132, 15942–4
- 46. Iserte, J., Simonetti, F. L., Zea, D. J., Teppa, E., and Marino-Buslje, C. (2015) I-COMS: Interprotein-COrrelated Mutations Server. *Nucleic Acids Res.* 43, W320-5
- 47. Jack, R. L., Sargent, F., Berks, B. C., Sawers, G., and Palmer, T. (2001) Constitutive expression of Escherichia coli tat genes indicates an important role for the twin-arginine translocase during aerobic and anaerobic growth. *J. Bacteriol.* **183**, 1801–4
- **48.** Kampfenkel, K., and Braun, V. (1993) Topology of the ExbB protein in the cytoplasmic membrane of Escherichia coli. *J. Biol. Chem.* **268**, 6050–7
- 49. Karimova, G., Pidoux, J., Ullmann, A., and Ladant, D. (1998) A bacterial two-hybrid system based on a reconstituted signal transduction pathway. *Proc. Natl. Acad. Sci. U. S. A.* 95, 5752–6
- 50. Kawahara, K., Tanaka, A., Yoon, J., and Yokota, A. (2010) Reclassification of a parathione-degrading Flavobacterium sp. ATCC 27551 as Sphingobium fuliginis. *J. Gen. Appl. Microbiol.* **56**, 249–55
- 51. Keenan, R. J., Freymann, D. M., Stroud, R. M., and Walter, P. (2001) The signal recognition particle. *Annu. Rev. Biochem.* **70**, 755–75

- 52. Killmann, H., Videnov, G., Jung, G., Schwarz, H., and Braun, V. (1995) Identification of receptor binding sites by competitive peptide mapping: phages T1, T5, and phi 80 and colicin M bind to the gating loop of FhuA. *J. Bacteriol.* 177, 694–8
- 53. Kolakowski, J. E., Defrank, J. J., Harvey, S. P., Szafraniec, L. L., Beaudry, W. T., Lai, K., and Wild, J. R. (1997) Enzymatic Hydrolysis of the Chemical Warfare Agent VX and its Neurotoxic Analogues by Organophosphorus Hydrolase. *Biocatal. Biotransformation.* 15, 297–312
- 54. Kozakov, D., Hall, D. R., Xia, B., Porter, K. A., Padhorny, D., Yueh, C., Beglov, D., and Vajda, S. (2017) The ClusPro web server for protein-protein docking. *Nat. Protoc.* 12, 255–278
- 55. Krewulak, K. D., and Vogel, H. J. (2008) Structural biology of bacterial iron uptake. *Biochim. Biophys. Acta.* 1778, 1781–804
- 56. Laemmli, U. K. (1970) Cleavage of structural proteins during the assembly of the head of bacteriophage T4. *Nature*. **227**, 680–5
- 57. Lai, K., Stolowich, N. J., and Wild, J. R. (1995) Characterization of P-S bond hydrolysis in organophosphorothioate pesticides by organophosphorus hydrolase. *Arch. Biochem. Biophys.* **318**, 59–64
- 58. Landis, W. G., Haley, D. M., Haley, M. V, Johnson, D. W., Durst, H. D., and Savage, R. E. (1987) Discovery of multiple organofluorophosphate hydrolyzing activities in the protozoan Tetrahymena thermophila. *J. Appl. Toxicol.* **7**, 35–41
- 59. Larsen, R. A., Letain, T. E., and Postle, K. (2003) In vivo evidence of TonB shuttling between the cytoplasmic and outer membrane in Escherichia coli. *Mol. Microbiol.* 49, 211–8
- 60. Laskowski, R. A., MacArthur, M. W., Moss, D. S., and Thornton, J. M. (1993) PROCHECK: a program to check the stereochemical quality of protein structures. *J. Appl. Crystallogr.* **26**, 283–291
- **61.** Lee, P. A., Tullman-Ercek, D., and Georgiou, G. (2006) The bacterial twin-arginine translocation pathway. *Annu. Rev. Microbiol.* **60**, 373–95
- 62. Letain, T. E., and Postle, K. (1997) TonB protein appears to transduce energy by shuttling between the cytoplasmic membrane and the outer membrane in Escherichia coli. *Mol. Microbiol.* **24**, 271–83
- 63. Liu, Y.-H., Liu, Y., Chen, Z.-S., Lian, J., Huang, X., and Chung, Y.-C. (2004) Purification and characterization of a novel organophosphorus pesticide hydrolase from Penicillium lilacinum BP303. *Enzyme Microb. Technol.* **34**, 297–303
- 64. Lüthy, R., Bowie, J. U., and Eisenberg, D. (1992) Assessment of protein models with three-dimensional profiles. *Nature*. **356**, 83–5

- 65. McDaniel, C. S., Harper, L. L., and Wild, J. R. (1988) Cloning and sequencing of a plasmid-borne gene (opd) encoding a phosphotriesterase. *J. Bacteriol.* **170**, 2306–11
- **66.** Morales, V. M., Bäckman, A., and Bagdasarian, M. (1991) A series of wide-host-range low-copy-number vectors that allow direct screening for recombinants. *Gene.* **97**, 39–47
- 67. Mulbry, W. W., and Karns, J. S. (1989) Parathion hydrolase specified by the Flavobacterium opd gene: relationship between the gene and protein. *J. Bacteriol.* 171, 6740–6
- **68.** Mulbry, W. W., Karns, J. S., Kearney, P. C., Nelson, J. O., McDaniel, C. S., and Wild, J. R. (1986) Identification of a plasmid-borne parathion hydrolase gene from Flavobacterium sp. by southern hybridization with opd from Pseudomonas diminuta. *Appl. Environ. Microbiol.* **51**, 926–30
- **69.** Natale, P., Brüser, T., and Driessen, A. J. M. (2008) Sec- and Tat-mediated protein secretion across the bacterial cytoplasmic membrane--distinct translocases and mechanisms. *Biochim. Biophys. Acta.* **1778**, 1735–56
- 70. Ng, T.-K., Gahan, L. R., Schenk, G., and Ollis, D. L. (2015) Altering the substrate specificity of methyl parathion hydrolase with directed evolution. *Arch. Biochem. Biophys.* **573**, 59–68
- 71. Nikaido, H. (2003) Molecular basis of bacterial outer membrane permeability revisited. *Microbiol. Mol. Biol. Rev.* **67**, 593–656
- 72. Noinaj, N., Guillier, M., Barnard, T. J., and Buchanan, S. K. (2010) TonB-dependent transporters: regulation, structure, and function. *Annu. Rev. Microbiol.* **64**, 43–60
- 73. Omburo, G. A., Kuo, J. M., Mullins, L. S., and Raushel, F. M. (1992) Characterization of the zinc binding site of bacterial phosphotriesterase. *J. Biol. Chem.* **267**, 13278–83
- 74. Orriss, G. L., Tarry, M. J., Ize, B., Sargent, F., Lea, S. M., Palmer, T., and Berks, B. C. (2007) TatBC, TatB, and TatC form structurally autonomous units within the twin arginine protein transport system of Escherichia coli. *FEBS Lett.* **581**, 4091–7
- 75. Palmer, T., Sargent, F., and Berks, B. C. (2005) Export of complex cofactor-containing proteins by the bacterial Tat pathway. *Trends Microbiol.* **13**, 175–80
- 76. Parthasarathy, S., Parapatla, H., and Siddavattam, D. (2017) Topological analysis of the lipoprotein organophosphate hydrolase from Sphingopyxis wildii reveals a periplasmic localisation. *FEMS Microbiol. Lett.* 10.1093/femsle/fnx187
- 77. Parthasarathy, S., Parapatla, H., Nandavaram, A., Palmer, T., and Siddavattam, D. (2016) Organophosphate Hydrolase Is a Lipoprotein and Interacts with Pi-specific Transport System to Facilitate Growth of Brevundimonas diminuta Using OP Insecticide as Source of Phosphate. *J. Biol. Chem.* **291**, 7774–85

- 78. Poelarends, G. J., Serrano, H., Johnson, W. H., and Whitman, C. P. (2005) Inactivation of malonate semialdehyde decarboxylase by 3-halopropiolates: evidence for hydratase activity. *Biochemistry*. 44, 9375–81
- 79. Punginelli, C., Maldonado, B., Grahl, S., Jack, R., Alami, M., Schröder, J., Berks, B. C., and Palmer, T. (2007) Cysteine scanning mutagenesis and topological mapping of the Escherichia coli twin-arginine translocase TatC Component. *J. Bacteriol.* **189**, 5482–94
- 80. Rapoport, T. A. (1992) Transport of proteins across the endoplasmic reticulum membrane. *Science*. **258**, 931–6
- 81. Rastogi, V. K., DeFrank, J. J., Cheng, T. C., and Wild, J. R. (1997) Enzymatic hydrolysis of Russian-VX by organophosphorus hydrolase. *Biochem. Biophys. Res. Commun.* 241, 294–6
- 82. Raymond, K. N., Dertz, E. A., and Kim, S. S. (2003) Enterobactin: an archetype for microbial iron transport. *Proc. Natl. Acad. Sci. U. S. A.* 100, 3584–8
- 83. Roodveldt, C., and Tawfik, D. S. (2005) Shared promiscuous activities and evolutionary features in various members of the amidohydrolase superfamily. *Biochemistry.* 44, 12728–36
- 84. Sargent, F., Bogsch, E. G., Stanley, N. R., Wexler, M., Robinson, C., Berks, B. C., and Palmer, T. (1998) Overlapping functions of components of a bacterial Secindependent protein export pathway. *EMBO J.* 17, 3640–50
- 85. Sargent, F., Gohlke, U., De Leeuw, E., Stanley, N. R., Palmer, T., Saibil, H. R., and Berks, B. C. (2001) Purified components of the Escherichia coli Tat protein transport system form a double-layered ring structure. *Eur. J. Biochem.* **268**, 3361–7
- 86. Schägger, H. (2001) Blue-native gels to isolate protein complexes from mitochondria. *Methods Cell Biol.* 65, 231–44
- 87. Schägger, H. (2006) Tricine-SDS-PAGE. Nat. Protoc. 1, 16–22
- 88. Schägger, H., and von Jagow, G. (1991) Blue native electrophoresis for isolation of membrane protein complexes in enzymatically active form. *Anal. Biochem.* **199**, 223–31
- 89. Schägger, H., Cramer, W. A., and von Jagow, G. (1994) Analysis of molecular masses and oligomeric states of protein complexes by blue native electrophoresis and isolation of membrane protein complexes by two-dimensional native electrophoresis. *Anal. Biochem.* 217, 220–30
- 90. Schauer, K., Rodionov, D. A., and de Reuse, H. (2008) New substrates for TonB-dependent transport: do we only see the "tip of the iceberg"? *Trends Biochem. Sci.* 33, 330–8

- **91.** Sethunathan, N., and Yoshida, T. (1973) A Flavobacterium sp. that degrades diazinon and parathion. *Can. J. Microbiol.* **19**, 873–5
- 92. Shi, J., Blundell, T. L., and Mizuguchi, K. (2001) FUGUE: sequence-structure homology recognition using environment-specific substitution tables and structure-dependent gap penalties. *J. Mol. Biol.* 310, 243–57
- 93. Showe, M. K., and DeMoss, J. A. (1968) Localization and regulation of synthesis of nitrate reductase in Escherichia coli. *J. Bacteriol.* 95, 1305–13
- 94. Siddavattam, D., Khajamohiddin, S., Manavathi, B., Pakala, S. B., and Merrick, M. (2003) Transposon-like organization of the plasmid-borne organophosphate degradation (opd) gene cluster found in Flavobacterium sp. *Appl. Environ. Microbiol.* **69**, 2533–9
- 95. Singh, B. K. (2009) Organophosphorus-degrading bacteria: ecology and industrial applications. *Nat. Rev. Microbiol.* **7**, 156–64
- **96.** Singh, B. K., and Walker, A. (2006) Microbial degradation of organophosphorus compounds. *FEMS Microbiol. Rev.* **30**, 428–71
- 97. Skare, J. T., and Postle, K. (1991) Evidence for a TonB-dependent energy transduction complex in Escherichia coli. *Mol. Microbiol.* **5**, 2883–90
- 98. Sogorb, M. A., and Vilanova, E. (2002) Enzymes involved in the detoxification of organophosphorus, carbamate and pyrethroid insecticides through hydrolysis. *Toxicol. Lett.* 128, 215–28
- 99. Somara, S., and Siddavattam, D. (1995) Plasmid mediated organophosphate pesticide degradation by Flavobacterium balustinum. *Biochem. Mol. Biol. Int.* **36**, 627–31
- 100. Strauch, E.-M., and Georgiou, G. (2007) Escherichia coli tatC mutations that suppress defective twin-arginine transporter signal peptides. *J. Mol. Biol.* **374**, 283–91
- 101. Sukhwal, A., and Sowdhamini, R. (2013) Oligomerisation status and evolutionary conservation of interfaces of protein structural domain superfamilies. *Mol. Biosyst.* 9, 1652–61
- 102. Sutherland, B. W., Toews, J., and Kast, J. (2008) Utility of formaldehyde cross-linking and mass spectrometry in the study of protein-protein interactions. *J. Mass Spectrom.* **43**, 699–715
- 103. Tawfik, D. S. (2006) Biochemistry. Loop grafting and the origins of enzyme species. *Science*. **311**, 475–6
- 104. Thomason, L. C., Costantino, N., and Court, D. L. (2007) E. coli genome manipulation by P1 transduction. *Curr. Protoc. Mol. Biol.* Chapter 1, Unit 1.17
- 105. Tian, J., Guo, X., Chu, X., Wu, N., Guo, J., and Yao, B. (2008) Predicting the protein family of methyl parathion hydrolase. *Int. J. Bioinform. Res. Appl.* **4**, 201–10

- 106. Timmis, K. N., and Pieper, D. H. (1999) Bacteria designed for bioremediation. Trends Biotechnol. 17, 200–4
- 107. Vanhooke, J. L., Benning, M. M., Raushel, F. M., and Holden, H. M. (1996) Three-dimensional structure of the zinc-containing phosphotriesterase with the bound substrate analog diethyl 4 methylbenzylphosphonate. Biochemistry. 35, 6020–5
- 108. Von Heijne, G. (1990) The signal peptide. *J. Membr. Biol.* 115, 195–201 Webb, B., and Sali, A. (2017) Protein Structure Modeling with MODELLER. Methods Mol. Biol.1654, 39–54
- 109. Weiner, J. H., Bilous, P. T., Shaw, G. M., Lubitz, S. P., Frost, L., Thomas, G. H., Cole, J. A., and Turner, R. J. (1998) A novel and ubiquitous system for membrane targeting and secretion o cofactor-containing proteins. Cell. 93, 93–101
- 110. Wiener, M. C. (2005) TonB-dependent outer membrane transport: going for Baroque? Curr. Opin. Struct. Biol. 15, 394–400
- 111.Xu, J., Bjursell, M. K., Himrod, J., Deng, S., Carmichael, L. K., Chiang, H. C., Hooper L. V, and Gordon, J. I. (2003) A genomic view of the human-Bacteroides thetaiotaomicron symbiosis. Science. 299, 2074–6
- 112. Yair, S., Ofer, B., Arik, E., Shai, S., Yossi, R., Tzvika, D., and Amir, K. (2008) Organophosphate degrading microorganisms and enzymes as biocatalysts in environmental and personal decontamination applications. Crit. Rev. Biotechnol. 28, 265–75
- 113. Yang, W., Zhou, Y.-F., Dai, H.-P., Bi, L.-J., Zhang, Z.-P., Zhang, X.-H., Leng, Y., and Zhang, X.- E. (2008) Application of methyl parathion hydrolase (MPH) as a labeling enzyme. Anal. Bioanal.Chem. **390**, 2133–40
- 114. Yew, W. S., Akana, J., Wise, E. L., Rayment, I., and Gerlt, J. A. (2005) Evolution of Enzymatic Activities in the Orotidine 5'-Monophosphate Decarboxylase Suprafamily: Enhancing the Promiscuous <scp>d</scp> arabino -Hex-3-ulose 6-Phosphate Synthase Reaction Catalyzed by 3-Keto- <scp>l</scp> -gulonate 6-Phosphate Decar. Biochemistry. 44, 1807–1815
- 115. Zhang, Z., Hong, Q., Xu, J., Zhang, X., and Li, S. (2006) Isolation of fenitrothion-degrading strain Burkholderia sp. FDS-1 and cloning of mpd gene. *Biodegradation*. 17, 275–83
- 116. Zheng, J., Constantine, C. A., Zhao, L., Rastogi, V. K., Cheng, T.-C., Defrank, J. J., and Leblanc, R. M. Molecular interaction between organophosphorus acid anhydrolase diisopropyl fluorophosphate. *Biomacromolecules*. 6, 1555
- 117. Zhongli, C., Shunpeng, L., and Guoping, F. (2001) Isolation of methyl parathion-degrading strain M6 and cloning of the methyl parathion hydrolase gene. *Appl. Environ. Microbiol.* **67**, 4922–5





The Organophosphate Degradation (opd) Island-borne Esterase-induced Metabolic Diversion in Escherichia coli and Its Influence on p-Nitrophenol Degradation*

Received for publication, May 2, 2015, and in revised form, September 24, 2015 Published, JBC Papers in Press, October 9, 2015, DOI 10.1074/jbc.M115.661249

Deviprasanna Chakka¹, Ramurthy Gudla¹, Ashok Kumar Madikonda¹, Emmanuel Vijay Paul Pandeeti, Sunil Parthasarathy, Aparna Nandavaram, and Dayananda Siddavattam²

From the Department of Animal Biology, School of Life Sciences, University of Hyderabad, Hyderabad 500 046, India

Background: Because of the mobile nature of the *opd* island, identical *opd* and *orf306* sequences are found among soil bacteria.

Results: In *E. coli*, Orf306 suppresses glycolysis and the TCA cycle and promotes up-regulation of alternate carbon catabolic operons.

Conclusion: The up-regulated *hca* and *mhp* operons contribute to PNP-dependent growth of *E. coli*. **Significance:** Together with *opd*, *orf*306 contributes to the complete mineralization of OP residues.

In previous studies of the organophosphate degradation gene cluster, we showed that expression of an open reading frame (orf306) present within the cluster in Escherichia coli allowed growth on p-nitrophenol (PNP) as sole carbon source. We have now shown that expression of orf306 in E. coli causes a dramatic up-regulation in genes coding for alternative carbon catabolism. The propionate, glyoxylate, and methylcitrate cycle pathwayspecific enzymes are up-regulated along with hca (phenylpropionate) and *mhp* (hydroxyphenylpropionate) degradation operons. These hca and mhp operons play a key role in degradation of PNP, enabling E. coli to grow using it as sole carbon source. Supporting growth experiments, PNP degradation products entered central metabolic pathways and were incorporated into the carbon backbone. The protein and RNA samples isolated from E. coli (pSDP10) cells grown in 14C-labeled PNP indicated incorporation of 14C carbon, suggesting Orf306-dependent assimilation of PNP in E. coli cells.

Bacterial phosphotriesterases (PTEs)³ are a group of structurally unrelated enzymes that cleave the triester linkage found in both organophosphate (OP) insecticides and OP nerve agents (1). Because of their broad substrate range and high catalytic efficiency, they have been exploited for detection and decontamination of OP compounds (2). The PTEs have been

classified into three main groups: (i) the organophosphate hydrolases (OPHs), (ii) methyl parathion hydrolases (MPHs), and (iii) organophosphate acid anhydrases. Among the PTEs, only the organophosphate acid anhydrases have known physiological substrates: they have been shown to be dipeptidases that cleave dipeptides with a prolyl residue at the carboxyl terminus and hence are described as prolidases (3). The OP hydrolyzing activity of prolidases is considered to be an ancillary activity due to the structural similarity of OP compounds to their usual substrates (3).

The physiological substrates for OPH and MPH enzymes are unknown. These enzymes are believed to have evolved in soil bacteria to counter the toxic effects of OP insecticide residues released into agricultural soils (4, 5). Bacterial OPH enzymes, besides showing high structural similarities with the quorum-quenching lactonases, possess weak lactonase activity (6, 7). Consequently the quorum-quenching lactonases are considered to be the possible progenitors of the bacterial OPH enzymes (7). Unlike the OPH enzymes, the MPHs have no structural similarity with quorum-quenching lactonases but instead are highly similar to β -lactamases (8). The structurally diverse PTEs are therefore assumed to have evolved independently in response to OP residues accumulated in agricultural soils (9, 10).

The genetics of organophosphate degradation has attracted considerable attention among soil microbiologists. Both the OPH-encoding organophosphate degradation (opd) genes and the MPH-encoding methyl parathion degradation (mpd) genes have been shown to be part of mobile genetic elements (11–13). The lateral transfer of opd and mpd genes is evidenced by the existence of identical opd and mpd genes among taxonomically unrelated soil bacteria (14, 15). Even dissimilar indigenous plasmids found in bacteria collected from diverse geographical regions contained identical opd gene clusters (14). There are four indigenous plasmids in OP-degrading Sphingobium fuliginis ATCC 27551. Of these four plasmids, the opd containing pPDL2 has been shown to be a mobilizable plasmid within which the opd region has unique organizational features (11).

^{*} This work was supported by Indian Council of Medical Research and Council for Scientific and Industrial Research (CSIR) research fellowships (to D. C., R. G., and A. K. M.). The authors declare that they have no conflicts of interest with the contents of this article.

¹ These authors contributed equally to this work.

² To whom correspondence should be addressed: Dept. of Animal Biology, School of Life Sciences, University of Hyderabad, Prof. C. R. Rao Rd., Gachibowli, Hyderabad 500 046, India. Tel.: 91-40-23134578; Fax: 91-40-23010120/145; E-mail: sdsl@uohyd.ernet.in.

³ The abbreviations used are: PTE, phosphotriesterase; PNP, p-nitrophenol; OP, organophosphate; orf306, open reading frame 306; OPH, organophosphate hydrolase; MPH, methyl parathion hydrolase; opd, organophosphate degradation gene; mpd, methyl parathion degradation gene; TCA, tricarboxylic acid; IPTG, isopropyl 1-thio-β-D-galactopyranoside; qPCR, quantitative PCR; PP, phenylpropionate; HPP, hydroxyphenylpropionate; Tn, transposon; IS, insertion element.

Genome-Guided Insights Reveal Organophosphate-Degrading *Brevundimonas diminuta* as *Sphingopyxis wildii* and Define Its Versatile Metabolic Capabilities and Environmental Adaptations

Sunil Parthasarathy^{1,†}, Sarwar Azam^{2,†}, Annapoorni Lakshman Sagar¹, Veera Narasimha Rao², Ramurthy Gudla¹, Hari Parapatla¹, Harshita Yakkala¹, Sujana Ghanta Vemuri¹, and Dayananda Siddavattam^{1,*}

Accepted: November 5, 2016

Abstract

The complete genome sequence of *Brevundimonas diminuta* represented a chromosome (~4.15 Mb) and two plasmids (pCMS1 and pCMS2) with sizes of 65,908 and 30,654 bp, respectively. The sequence of the genome showed no significant similarity with the known bacterial genome sequences, instead showed weak similarity with the members of different genera of family, Sphingomonadaceae. Contradicting existing taxonomic position, the core genome-guided phylogenetic tree placed *B. diminuta* in the genus Sphingopyxis and showed sufficient genome-to-genome distance warranting a new species name. Reflecting the strains ability to grow in harsh environments, the genome-contained genetic repertoire required for mineralization of several recalcitrant man-made aromatic compounds.

Key words: biodegradation, aromatic compound degradation, biotransformation, Sphingomonadales.

Introduction

The safe disposal of neurotoxic organophosphate (OP) residues has attracted the attention of several microbiologists. Bacterial strains possessing organophosphate hydrolase (OPH) activity have been isolated from sewage and soil samples (Munnecke and Hsieh 1974). Using conventional taxonomic tools, the isolated OP-degrading bacterial strains have been placed in the genus, Pseudomonas (Munnecke and Hsieh 1974). However, when the genus *Pseudomonas* was reclassified, bacterial strains that were previously named as Pseudomonas diminuta and Pseudomonas vesicularis were moved to a separate genus known as Brevundimonas. Accordingly, the P. diminuta MG was renamed Brevundimonas diminuta MG (Segers et al. 1994). In this study, we generated the complete genome sequence of B. diminuta MG and report several interesting features pertaining to its taxonomy, evolution, and degradation potential.

Results and Discussion

A total of 6.8 Gbp data was generated to assemble the complete genome of B. diminuta. The scaffold level assembly contained 28 scaffolds with N50 of 1,786,567 bp. These scaffolds were further merged to obtain three super scaffolds using data generated from a mate-pair library. The super scaffolds were circularized by manually generating sequence for the DNA, amplified using primers specific to the right and left flanks of the assembled scaffold sequences. The largest super scaffold with a length of 4,147,822 bp is regarded as the chromosome sequence of B. diminuta (fig. 1A). The other two scaffolds gave circular DNA molecules with a size of 65,908 bp (fig. 1B) and 30,654 bp (fig. 1C), respectively. The 65,908 bp circular sequence matched perfectly with the physical map and partial sequence of pCMS1, a previously reported indigenous plasmid of B. diminuta (Pandeeti et al. 2011). However, the second circular DNA showed no complete similarity to any other

This is an Open Access article distributed under the terms of the Creative Commons Attribution Non-Commercial License (http://creativecommons.org/licenses/by-nc/4.0/), which permits non-commercial re-use, distribution, and reproduction in any medium, provided the original work is properly cited. For commercial re-use, please contact journals.permissions@oup.com

¹Department of Animal Biology, School of Life Sciences, University of Hyderabad, Hyderabad, India

²National Institute of Animal Biotechnology, Hyderabad, India

[†]These authors contributed equally to this work.

^{*}Corresponding authors: E-mails: sdsl@uohyd.ernet.in; siddavattam@gmail.com.

[©] The Author(s) 2016. Published by Oxford University Press on behalf of the Society for Molecular Biology and Evolution.

Review Article

Evolution of Phosphotriesterases (PTEs): How Bacteria Can Acquire New Degradative Functions?

SUNIL PARTHASARATHY, RAMURTHY GUDLA and DAYANANDA SIDDAVATTAM*

Dept. of Animal Biology, School of Life Sciences, University of Hyderabad, Hyderabad 500 046, India

(Received on 12 August 2017; Revised on 22 August 2017; Accepted on 23 August 2017)

The promiscuity of enzymes has often been considered a vestige activity based on the broad substrate spectrum of their progenitors. As such, divergent enzymes can be used as a fingerprint to track their evolutionary history. In the presence of structural mimics of active site or binding site ligands, and assisted by mutations in the associated binding site, this promiscuity contributes to acquisition of new catalytic functions. This phenomenon is often referred to as substrate-assisted gain-of-function and helps soil microbes to thrive on re-calcitrant xenobiotic molecules, hitherto unfamiliar to the microbial world. This review describes the evolution of organophosphorous hydrolases, which potentially and originally functioned as quorum-sensing 'quenching' lactonases and highlights their remarkable horizontal mobility within diverse bacterial species.

Keywords: Phosphotriesterase; Organophosphates; Evolution

Introduction

There is a growing worldwide concern over the steady accumulation of xenobiotic materials, which have been produced or used in industrial/agricultural processes over the past several decades. These compounds include various organic solvents, heavy metals, neurotoxic pesticides, halogenated aromatic compounds, explosives and carcinogenic industrial chemicals. Although the introduction of xenobiotics into the environment is lamentable, and the effects they have on the environment can be devastating, many different types of microbial systems rapidly acquired the ability to thrive on these compounds, using them as sources of carbon, phosphate, nitrogen, etc. There are a number of excellent reviews describing the complex metabolic pathways involved in the conversion of these otherwise recalcitrant and toxic chemicals into central metabolic intermediates. The well-structured genetic information and finely-tuned regulatory mechanisms of these degradative enzymes/ pathways indicate that these traits evolved specifically to enable microbes to use these re-calcitrant compounds, generated through anthropogenic

activities, as a nutrient source (Allpress and Gowland, 1998; Janssen *et al.*, 2005; Khajamohiddin *et al.*, 2006; Juhas *et al.*, 2009; Carmona *et al.*, 2009). Understanding the biology of these metabolic traits is relevant to our general understanding of remarkably rapid evolution and acquisition of these degradative genes.

Chemistry of Organophosphates

Organophosphates (OP) are esters or thiols derived from phosphoric, phosphonic or phosphoramidic acid (Sogorb and Vilanova, 2002). Gerhard Schradera, a German chemist working at the Bayer Company (IG Farben), developed the insecticide "Schraden" in 1941. Schraden was eventually not used as an insecticide owing to its extreme toxicity to mammals; rather it was principally synthesized for military purposes. However, this discovery led to the synthesis of the first OP insecticide tetraethyl pyrophosphate (TEPP) and that of an extensively used OP compound, parathion (O, O-dimethyl-O-*p*-nitrophenyl phosphorothioate). Since then, thousands of OP compounds have been synthesized for use as

^{*}Author for Correspondence: E-mail: sdsl@uohyd.ernet.in/siddavattam@gmail.com

Anti-plagiarism Certificate

Functional analysis of membrane associated organophopsphate hydrolase (OPH) complex in Sphingobium fuliginis ATCC 27551.

by Ramurthy Gudla

Submission date: 24-Sep-2018 03:24PM (UTC+0530)

Submission ID: 1007324117 File name: 12laph02.pdf (9.6M)

Word count: 28761

Character count: 152569

Functional analysis of membrane associated organophopsphate hydrolase (OPH) complex in Sphingobium fuliginis ATCC 27551.

rung	IIIIS AT CC 27551.	
ORIGINA	ALITY REPORT	
SIMILA	5% 11% 11% 6% RITY INDEX INTERNET SOURCES PUBLICATIONS STUDEN	IT PAPERS
PRIMAR	Y SOURCES	
1	Submitted to University of Hyderabad, Hyderabad Student Paper	2%
2	www.jbc.org Internet Source	1%
3	Emmanuel Vijay Paul Pandeeti. "Purification and Characterization of Catechol 1,2-Dioxygenase from Acinetobacter sp. DS002 and Cloning, Sequencing of Partial catA Gene", Indian Journal of Microbiology, 03/08/2011 Publication	<1%
4	neuroviisas.med.uni-rostock.de Internet Source	<1%
5	mmbr.highwire.org Internet Source	<1%
6	Submitted to Mahidol University Student Paper	<1%

7	onlinelibrary.wiley.com Internet Source	<1%
8	d-nb.info Internet Source	<1%
9	Kristine Schauer, Dmitry A. Rodionov, Hilde de Reuse. "New substrates for TonB-dependent transport: do we only see the 'tip of the iceberg'?", Trends in Biochemical Sciences, 2008 Publication	<1%
10	Submitted to Jawaharlal Nehru Technological University Student Paper	<1%
11	shodhganga.inflibnet.ac.in Internet Source	<1%
12	"Transcriptional Regulation", Springer Nature America, Inc, 2012 Publication	<1%
13	www.ukessays.com Internet Source	<1%
14	core.ac.uk Internet Source	<1%
15	Handbook of Hydrocarbon and Lipid Microbiology, 2010. Publication	<1%